Polymeric Ionic Liquids (PILs): Synthetic Approaches and Gas Permeation Studies with an Emphasis on CO$_2$ Separation

Thesis Submitted to AcSIR

For the Award of the Degree of

DOCTOR OF PHILOSOPHY

In

CHEMISTRY

By

Rupesh Sudhakar Bhavsar
(Registration Number: 10CC11J26106)

Under the guidance of
Dr. Ulhas K. Kharul

Polymer Science and Engineering Division
CSIR-National Chemical Laboratory
Pune - 411008, India.

August 2014

Certificate of the Guide

Certified that the work incorporated in the thesis entitled "**Polymeric Ionic Liquids (PILs): Synthetic Approaches and Gas Permeation Studies with an Emphasis on CO_2 Separation**" submitted by Rupesh Sudhakar Bhavsar was carried out under my supervision. All the materials obtained from other sources have been duly acknowledged in the thesis.

August, 2014

CSIR-National Chemical Laboratory

Pune - 411 008.

Dr. U. K. Kharul

(Research Guide)

Declaration by the Candidate

I declare that the thesis entitled "**Polymeric Ionic Liquids (PILs): Synthetic Approaches and Gas Permeation Studies with an Emphasis on CO$_2$ Separation**" is my own work conducted under the supervision of Dr. U. K. Kharul, at Polymer Science and Engineering Division, CSIR-National Chemical Laboratory, Pune, India. I further declare that to the best of my knowledge, this thesis does not contain any part of work, which has been submitted for the award of any degree either of this University or any other University without proper citation.

Rupesh Sudhakar Bhavsar
(Research Student)

Dedicated to my Parents

Acknowledgements

I am thankful to my research supervisor, Dr. Ulhas K. Kharul for providing me an opportunity to pursue my carrier as a Ph.D. student and offering valuable suggestions and encouragement in more stressful times. He taught me useful skills for research work as well as technical writing during the course of work. I consider myself to be fortunate that I got an opportunity to work under his guidance.

I am grateful to Dr. Saurav Pal, Director, NCL, Dr. Vivek Ranade, Deputy Director, NCL and Dr. A. J. Varma, Head, Polymer Science and Engineering Division for the opportunity I got to work in this prestigious institute and help during various stages of my stay at NCL. I would also like to thank Dr. C. G. Suresh, for his help, support, suggestions during the course of this study. I duly acknowledged CSIR, New Delhi for valuable support in the form of a Senior Research Fellowship.

It gives me great pleasure to thanks my DAC committee members, Dr. P. P. Wadgaonkar, Dr. A. K. Lele, Dr. C. P. Vinod and Dr. Prashant Kulkarni, for timely evaluation of my work and their important suggestions. I would like to thank Mr. K. V. Pandare, Dr. C. Ramesh, Dr. Tambe, Dr. Rajmohan, Dr. Neelima Bulakh, Mrs. Dhoble, Mrs. Sangita, Mrs. Purvi, Mr. Saroj for their valuable suggestions and allowing me to use facilities. I would like to thanks Mohan, Yogesh, Kalyani, Sandeep and many others for their help for material characterization. I would also like to acknowledge valuable support of Mr. Vivek Borkar and Swapnil. I am thankful to NMR facility, Elemental Analysis Group, Glass Blowing and Workshop groups for their technical support. I also wish to thank the Library, Administrative and other supporting staff at NCL.

I wish to place on record my sincere thanks to Dr. Sandeep Kothawade, Dr. Santosh Kumbharkar, Dr. Yogesh Chendake and Dr. Harshada Lohkare for their constant support and encouragement. They have placed a major influence on me during the period of my thesis. I would like to thanks Mrs. Kanchan Nehate and Dr. Niranjan who suggested me a career path as a researcher at NCL.

I owe special thanks to my lab mates Anita, Sayali, Anand, Harshal for their constant encouragement & always being with me in all sorts of situations during my stay in NCL. I truly enjoyed the valuable discussions with them. At this stage I can not forget my all other lab members, Rahul, Bhavana, Vinaya, Soumya, Manisha, Deepti, Sneha D., Nikita, Smita, Kiran,

Contents

List of Schemes

List of Figures

List of Tables

Chapter 1

Introduction and Literature survey

1.1 Gas separation

An economical separation of gases is crucial in many applications of industrial and societal relevance. These include O_2/N_2 air enrichment, H_2 and N_2 separation from ammonia purge gas, H_2 separation from hydrocarbons, He recovery, CO separation in petrochemicals, CO_2 separation in natural gas processing, flue gas, enhanced oil recovery, landfill gas upgradation, etc. [Abedini (2010)]. Among these, techno-economically viable separation of CO_2 has a special relevance in view of its detrimental effects on environment. This is largely associated with the rising concentration of anthropogenic CO_2, leading to global warming. It is arguably one of the most important environmental issues that our world faces today [Tome (2013a)].

1.2 Sources of CO_2 emission and need for its separation

As a result of increase in the combustion of fossil fuels such as petroleum, natural gas and coal, approximately 29 Gt of carbon are emitted to the earth's atmosphere each year [Li (2012)]. Over the last half-century, the CO_2 concentration in atmosphere has increased from about 310 ppm in 1960 to over 390 ppm in 2010 [Liu (2012)]. A large portion of this carbon is in the form of gaseous CO_2. Approximately 30% of this CO_2 is emitted from fossil fuel based power plants. In addition to rising levels of atmospheric CO_2, the earth's temperature is increasing. In the absence of climate change policies, global temperatures are projected to rise between 1.4 - 5.8 °C by 2100 [Powel (2006)]. This increase in global temperatures is likely to cause a number of negative effects; including rising sea levels, changes in ecosystems, loss of biodiversity and reduction in crop yields [Powel (2006)]. Carbon capture and storage (CCS) from large point sources such as power plants is one of the options for reducing anthropogenic CO_2 emissions [D'Alessandro (2010)]. It is estimated that CO_2 emissions to the atmosphere could be reduced by 80–90% by using power plant equipped with carbon capture and storage technology [Metz (2005), D'Alessandro (2010)].

In addition to CO_2 capture from the flue gas, CO_2 separation is required in various other applications such as natural gas production, enhanced oil recovery, water gas shift reaction,

landfill gas upgradation, etc. Each application involves different gases, separation of which imposes distinct requirements and constraints. Usually low CO_2 concentration as well as pressure and high volume stream are mainly responsible for this. Natural gas reserves (esp. CH_4) are typically contaminated with over 40% CO_2 and N_2. Utilization of such gas fields is acceptable if this CO_2 is separated and sequestered at the source of production. This application requires an efficient separation of CO_2 from the natural gas components at high pressures. CO_2 separation from other fuel gases (e.g., output from gasification, water-gas shift reactors, etc.) also occurs under high pressure and temperatures (250–450 °C) [D'Alessandro (2010)], with the relevant precombustion separation being CO_2/H_2. Currently, CO_2 separation is performed by cryogenic distillation, adsorption, absorption and membrane based processes [Aron (2005), Li (2011)], as discussed below.

1.3   Technologies for CO_2 separation

1.3.1   Absorption

Absorption is a process that relies on a solvent's chemical affinity to dissolve one species preferably over the another. The process of CO_2 absorption by a liquid solvent or solid matrix is currently being investigated for scrubbing of CO_2 from flue gas streams [Aron (2005)]. Presently, the process to remove CO_2 from natural gas and power plant flue gas involves a monoethanolamine as chemical absorbent [Sanders (2013)]. When an amine is reacted with CO_2, carbamic acid is formed [Sanders (2013)]. This is a rather unstable product which would decompose to the original amine and carbon dioxide at modest temperatures (>100 °C) [Sanders (2013)]. Thus, amines can be used to capture CO_2 at ambient temperatures and these amines can be regenerated, wherein CO_2 is collected at higher temperatures. This process has been proposed for the collection of CO_2 for sequestration from power plant flue gas [Sanders (2013)]. Inorganic solvents such as aqueous potassium and sodium carbonate as well as aqueous ammonia solutions have also been considered for chemical absorption [D'Alessandro (2010)]. While monoethanolamine is one of the preferred amines used in this process, other similar amines such as diethanolamine, methyl diethanolamine and triethanolamine, which can also remove H_2S from natural gas streams, have been employed [Sanders (2013)]. Currently the most utilized technology for CO_2 capture is the amine based sorption system [Li (2012)]. However, the use of aqueous solution of amine has serious inherent drawbacks, including solvent loss and

degradation in the regeneration step, corrosion and high energy demand for regeneration of solvents [Wang (2010, 2011)].

1.3.2 Adsorption

This process involves physisorption (van der Waals) or chemisorption (covalent bonding) between the gas molecules and the surface of a material [D'Alessandro (2010)]. Many solids have the capability to selectively adsorb CO_2 into small cracks, pores or just their external surfaces under specific temperature and pressure conditions [Aron (2005)]. The two main methods for adsorption are pressure swing adsorption (PSA) and temperature swing adsorption (TSA). In either case, adsorption rate depends on temperature, partial pressures of CO_2, surface forces (interaction energy between sorbent and CO_2) and pore size or available surface area of the sorbent [Aron (2005)]. Possible mechanisms of adsorptive separation include: (i) the molecular sieving effect, which is based upon size/shape exclusion of certain components of a gas mixture, (ii) the thermodynamic equilibrium effect due to preferential adsorbate-surface or adsorbate packing interactions and (iii) the kinetic effect due to differences in the diffusion rates of different components of a gas mixture [D'Alessandro (2010)]. It has been established that PSA is superior to TSA due to its lower energy demand and higher regeneration rate. Adsorption can be performed using naturally occurring substances such as coal or more complex sorbents such as activated carbon, molecular sieves, zeolites, metal oxides, etc. [Aron (2005), D'Alessandro (2010)]. There are two significant drawbacks that make adsorption currently unfavorable as a stand-alone process. The first is that the system cannot easily handle large concentrations of CO_2, usually between 0.04 % and 1.5 %, while most power plants have much higher concentrations of CO_2 in flue gases, approximately 15 %. The second is that available sorbents are not selective enough for CO_2 separation from flue gases [Aron (2005)].

1.3.3 Cryogenic distillation

Cryogenic separation of gas mixtures uses the difference in boiling points of various gas species to separate them. The critical temperature and triple point of CO_2 are 31.6 °C and -56.8 °C respectively. Between these temperatures, CO_2 can be liquefied by compression and cooling [Plasynski (2000)]. The major disadvantage of cryogenic method is the high-energy consumption and costs associated with the gas compression and cooling. Since the concentration of CO_2 in

flue gas is about 15 %, the energy used to compress the rest 85% of flue gas is substantial. A simple calculation for the energy requirement for liquefying CO_2 by isothermally compressing the flue gas near the critical temperature to 74 bar would spend about 30 % of total power plant output in compressing 85% of the remaining gases. This is about 50 % more than MEA-absorption process [Plasynski (2000)]. Thus, the main disadvantage of cryogenic separation is that the process is highly energy intensive for regeneration and can significantly decrease the overall power plant efficiency. Moreover, tendency for blockage of process equipment is high [Shimekit (2012)].

1.3.4   Membrane separation

A membrane is a selective barrier that allows the passage of certain constituents and retains other [Mulder (1998)]. For most of the large scale applications, they are predominately based on polymeric materials. Membrane technology is an attractive and competitive alternative to conventional technology owing to its several advantages. Membrane systems are skid mounted, therefore, scope, cost and time taken for site preparation is minimal. Membrane units do not require additional gadgets, e.g. solvent storage, water treatment, etc. [Dortmundt (1999)]. Hence their installation costs are significantly lower. The only major cost is for membrane replacement, which is significantly lower than the solvent replacement and energy costs associated with traditional technologies. The only equipment necessary for membrane separation is the membrane and compressor. There are almost no moving parts and the construction is fairly simple. This makes membrane processes operationally simple and highly reliable. Due to the compact nature of membrane devices, they are usually less voluminous [Li (2005)]. This space efficiency is especially important for offshore operations where energy and space management gains prime importance. This makes membranes more attractive for remote locations. The modularity of membrane modules makes the design simple and easy to be scaled up linearly [Li (2005)]. The membrane process is easily adaptable for various feed CO_2 concentration [Dortmundt (1999)]. Since membrane processes rely on physical separation, they do not involve handling of solvents or other chemicals for separation. Thus, they are environment friendly. Despite all the advantages of membranes and the large number of polymeric materials investigated and developed for gas separation applications, the number of polymers used in commercial system is still limited. The main polymers employed for gas separation membranes

are poly(dimethylsiloxane), cellulose acetate, polycarbonates, polyimides, poly(phenylene oxide) and polysulfone [Bernardo (2009)]. A limitation can be found in the permeability-selectivity tradeoff relation, wherein more permeable membrane materials are generally less selective and vice-versa [Aron (2005), Bernardo (2009), Salleh (2011), Tome (2013b)]. It was also reported that polymeric membranes are not suitable to be applied in harsh environments, e.g., those prone to corrosion and high temperatures [Salleh (2011)]. Plasticization of the polymer membrane by CO_2, partial pressure and temperature is well known. This phenomenon decreases membrane's separation ability and may also adversely affect the gas flux [Bernardo (2013)]. Thus, long term stability and performance of the polymeric membranes at elevated temperatures and pressure are necessary to maintain the robustness of the membrane-based systems [Shao (2009)].

1.4   Gas separation membranes: Theoretical considerations

Gas-transport mechanisms in membrane separation are mainly viscous flow, Knudsen diffusion, molecular sieving and solution-diffusion [Mulder (1991), Koros (1993, 2000), George (2001), Scholes (2008), Shao (2009)], as given schematically in Figure 1.1.
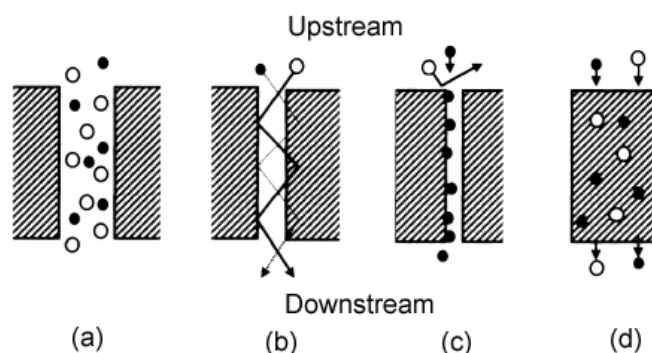
Figure 1.1. Mechanism of gas transport through the membrane, a) viscous flow, b) knudson diffusion, c) moleculer sieving and d) solution-diffusion [George (2001)].

Depending on the properties of the targeted gases as well as the morphology, material and functionality of the membrane type, one or a combination of these transport mechanisms may be applicable [Shao (2009)]. In porous membranes, gas separation is governed by viscous flow, Knudsen diffusion and molecular sieving mechanism. In viscous flow mechanism, the flow is inversely proportional to the viscosity of fluid. In Knudson diffusion, flow is inversely proportional to the square root of the molecular mass of diffusing species [George (2001)]. This mechanism is often predominant in macroporous and mesoporous membranes [Javaid (2005)].

For the molecular sieving, the smaller molecules readily permeate through the membrane while the passage of the larger molecules is hindered. Separation based on molecular sieving typically utilizes the higher diffusion rate of the smaller gas molecule [Shao (2009)]. However, the molecular-sieving mechanism may not be effective for the separation of similar-size penetrants (e.g. O_2 and N_2) because of competitive sorption and the difficulties in precisely controlling the pore size and its distribution.

The solution-diffusion mechanism is a most widely applicable model for gas transport across a dense polymeric membrane [Shao (2009)]. According to this mechanism, solution equilibrium is assumed to be established between the gas in contact with the membrane interfaces and the gas dissolved in the membrane at these interfaces. This is followed by diffusion of the penetrant gas molecules in the membrane matrix [Stern (1994)]. This mechanism comprises three main steps: (i) sorption of the gaseous penetrants at the upstream side of membrane, (ii) activated diffusion of the penetrants across the membrane and (iii) desorption of the penetrants at the downstream [Shao (2009)]. The diffusion of gas through the membrane can be expressed by Fick's first law [George (2001), Javaid (2005), Shao (2009)], as given below.

$$J = -D\left(\frac{dC}{dx}\right) \tag{1.1}$$

where, J is the flux of the gas through the membrane, D is the diffusion coefficient, and dC/dx is the concentration gradient of the gas across the membrane. At steady state, the flux is a constant. If D is assumed to be constant, Eq. (1.1) can be integrated as

$$J = D\left(\frac{C_0 - C_1}{l}\right) \tag{1.2}$$

where C_0 and C_1 are the concentration of the gas on the upstream and downstream ends, respectively, and l is the thickness of the membrane. At low pressures, Henry's law is often adequate to express the concentration of the gas in the membrane:

$$C = S.p \tag{1.3}$$

where, S is the Henry's solubility constant and p is the gas pressure. By substituting Eq. (1.3) into Eq. (1.2) we get:

$$J = D.S\frac{(p_0 - p_1)}{l} = P\frac{(p_0 - p_1)}{l} \tag{1.4}$$

where, P is permeability of the gas and according to Eq. (1.4) can be defined as:

$$P = D.S \tag{1.5}$$

Both, P and D (and thus S) can be determined in a single experiment by measuring the "time lag" for pressure increase on the low pressure side of the membrane as described in Section 1.4.1. In the real systems, the diffusion coefficient (D) and the solubility coefficient (S) may both be the function of concentration. In gas separation with membranes, selectivity is defined as the ratio of the individual gas permeabilities. Based on single gas permeabilities of species "A" and "B" we may write an ideal selectivity as:

$$\alpha(A/B) = \frac{P_A}{P_B} = \frac{D_A.S_A}{D_B.S_B} \tag{1.6}$$

The selectivity can therefore be viewed as a function of differences in both the diffusivity and solubility coefficients of the two gases [Javaid (2005)].

1.4.1   Methods for determining gas permeability

a)   Time-lag or variable pressure method

This method usually requires that both sides of the membrane be initially evacuated. A constant gas pressure is then applied on one side of the membrane and the increase in the pressure of the permeating gas is measured on the opposite side [Stern (1963)]. The downstream pressure initially increases nonlinearly and then linearly as a function of time, as shown in Figure 1.2 for a typical experiment. The linear increase of the downstream pressure is usually attributable to steady-state concentration profile in the membrane [Hu (2006)]. Slope of the linear part of the curve can be used to calculate the permeation coefficient.
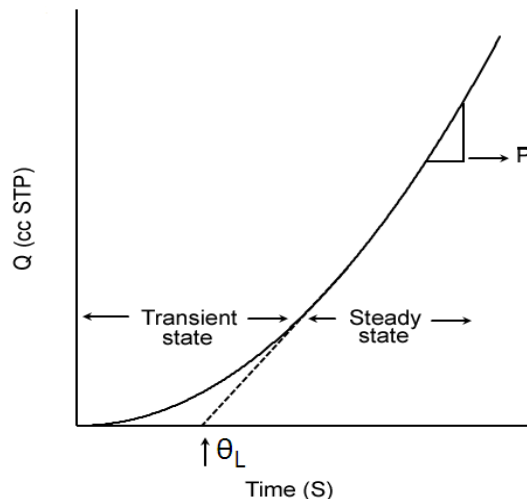
Figure 1.2. Time-lag measurement of gas permeation.

For each experiment of this kind, one can calculate the permeability as follows [Hu (2006)];

$$P = \frac{V.l}{A.T.p_2}\left(\frac{dp_1}{dt}\right) \tag{1.7}$$

where P is the gas permeability coefficient of the membrane to a gas with an unit in Barrer (1 Barrer is $10^{-10}cm^3(STP)cm/cm^2.s.cmHg$), V is the volume of the downstream chamber (cm^3), l is the thickness of the membrane (cm), A refers to the effective area of the film (cm^2), T is the experimental temperature (K), p_2 is the upstream pressure (psi), p_1 is the downstream pressure (psi), and t is the time taken for the pressure (p_1) buildup.

The diffusivity (D) can be found by extrapolating the slope of the steady-state flux back to the time axis (Figure 1.2). This intercept is the 'time lag' (θ) of the gas through the membrane and is related to D by eq. 1.8 as;

$$\theta = \frac{l^2}{6.D} \tag{1.8}$$

Determination of P and D allows for the estimation of solubility (S) following Eq. 1.5.

b)   Variable volume method

According to this method, a high gas pressure is applied on one side of the membrane and the permeated gas is allowed to expand on the opposite side against some low constant pressure, usually atmospheric. The change in the volume of the permeate is then measured as a function of time by measuring the displacement of a short column of liquid or mercury in a capillary [Stern (1963)]. The gas permeation of the membrane by this method can be calculated as;

$$P = \frac{J.l}{(p_1 - p_2)} \tag{1.9}$$

where J is the steady-state rate of gas permeation through unit membrane area when the constant gas pressures p_1 and p_2 are maintained at the membrane interfaces ($p_1 > p_2$) and l is the membrane thickness. Permeability is dependent on the nature of the penetrant and of the membrane, temperature and in the most general case, on both p_1 and p_2.

1.5   Membrane materials for gas separation

The choice of a membrane material for a gas separation application is based on specific physical and chemical properties, since these materials should be tailored in an advanced way to separate particular gas mixtures. Moreover, robust (i.e., long-term and stable) materials are

required to be applied in a membrane gas separation process. The gas separation properties of membranes depend upon the material (permeability, separation factors), the membrane structure and thickness (permeance), the membrane configuration (e.g., flat, hollow fiber), the membrane module and system design [Bernardo (2009)].

Both inorganic and polymeric membranes can be designed to achieve solubility-based gas separations. Both materials have certain advantages and disadvantages and presently research effort is concentrating on designing membranes that provide high throughput as well as selectivity [Javaid (2005)].

The development of inorganic membranes (e.g., silica, zeolites, etc.) and carbon-based molecular sieves is particularly interesting because they can withstand aggressive chemicals as well as high temperatures. These materials present drawbacks, viz.; high cost, modest reproducibility, brittleness, low membrane area to module volume ratio, low permeability in the case of highly selective dense membranes (e.g., metal oxides at temperatures below 400 °C) and difficult sealing at high temperatures [Bernardo (2009)].

The use of polymer membranes has generated an ever increasing interest in the field of gas separation [Javaid (2005)]. Polymers are available in a wide array of chemistries that can be used to suit a particular application. As with inorganic membranes, one would like to form the polymer layer with minimum possible thickness. Polymeric membranes are therefore cast on supports to form integrally skinned membranes. Phase inversion is one of the commonly used processes to form integrally skinned polymeric membranes. In this process a sol is inverted to form a porous three-dimensional macromolecular network. For gas separation, the most desirable polymers are those that provide both high permeability and selectivity.

The two types of polymeric membranes that are commercially available for gas separations are glassy and rubbery membranes. Glassy membranes are rigid and glass-like and operate below their glass transition temperatures. On the other hand, rubbery membranes are flexible, soft and operate above their glass transition temperatures. Mostly, rubbery polymers show a high permeability, but a low selectivity; whereas, glassy polymers exhibit a low permeability but a high selectivity. Glassy polymeric membranes dominate industrial membrane separations because of their high gas selectivities, along with good mechanical properties [Shekhawat (2006)].

1.5.1   Gas transport in rubbery polymers

Important characteristic of rubbery polymers is segmental mobility. Hence, easy diffusion of small molecules through rubbery polymers is usually observed [George (2001)]. At low pressures, gas sorption in rubbery polymers is linear with pressure and can be described by Henry's law [Barbari (1994)], as given below;

$$C = k_D.P \qquad (1.10)$$

where, C is the concentration of gas in the polymer, k_D is a Henry's law constant and P is the gas pressure. The units most often used for C and P in the gas sorption literature are $cm^3(STP)/cm^3$ of polymer and atm, respectively. Deviations from Henry's law are observed for rubbery polymers in the presence of high activity gases or vapors. The Henry's law constant, k_D, appearing in eq. 1.10 can be related to the Lennard-Jone's force constant, that provides a measure of the ease of condensation of the gas [Michaels (1961)]. Alternatively, critical point or boiling point of the gas can also be chosen as a correlating parameter, with equally good results [Stern (1969)]. Diffusion coefficient for gases in rubber can be described by eq. 1.11 [Barrer (1939), Stern (1980), Shao (2009)],

$$D = D_0.exp(-E/RT) \qquad (1.11)$$

The activation energy (E) is an energy that must be concentrated in the polymer adjacent to diffusing molecule to open a passage of enough free volume, to allow the penetrant to execute diffusional jump, D_0 is pre-exponential factors, R is gas constant and T is temperature. The concept of "free-volume" or "empty" volume used to describe the transport of gases and liquids in polymers is well reviewed [Stern (1980), Shao (2009)].

1.5.2   Gas transport in glassy polymers

Glassy polymers are characterized by restricted chain mobility [George (2001)]. Thus, the process of gaseous diffusion in glassy polymers is known to be more complex than that of rubbery polymers. A glassy polymeric membrane structure is composed of two components: microvoids (frozen free volume or free volume holes) and the matrix phase. Transport properties, viz., sorption (S), diffusion (D) and permeation (P) can be explained by a detailed elucidation of transport phenomena through glassy polymeric membranes. Different levels of interactions between the glassy polymeric membrane and the penetrant species affect gas transport [Tsujita (2003)]. The reason lies in the inhomogeneity in the polymer matrix due to intersegmental

packing defects (free volume) frozen into the structure, when the temperature drops below T_g [Kesting (1993)].

A number of statistical models have been developed to explain the transport mechanism in glassy polymers and estimate the parameters P, D and S [Stern (1994)]. The most widely used model to correlate gas sorption in glassy polymers at low to moderate pressures is the dual mode sorption model [Barbari (1994)]. This model assumes that two distinct populations of penetrant molecules exist within the glassy polymer. The one in which molecules are sorbed by an ordinary dissolution mechanism (the dissolved or Henry's law population) and another, in which molecules reside in pre-existing gaps frozen into the glassy polymer (the hole or Langmuir population) [Barbari (1994)] as shown in Figure 1.3 [Tsujita (2003)].

▨ : Henry sorption into matrix phase
○ : Langmuir sorption into micro void
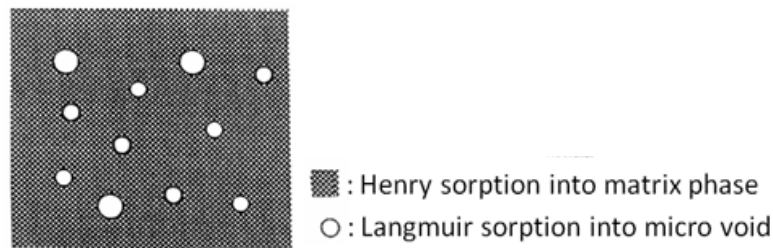
Figure 1.3 Schematic representation of polymeric glassy state depicting the matrix and the microvoids [Tsujita (2003)].

Local equilibrium exists between molecules in Henry and Langmuir sites. The description of gas sorption and diffusion through glassy polymers utilizing two different sites is known as the 'dual-mode sorption theory'. The dual-mode sorption is normally described by the sum of these two contributions as follows (Figure 1.4) [Tsujita (2003)]:
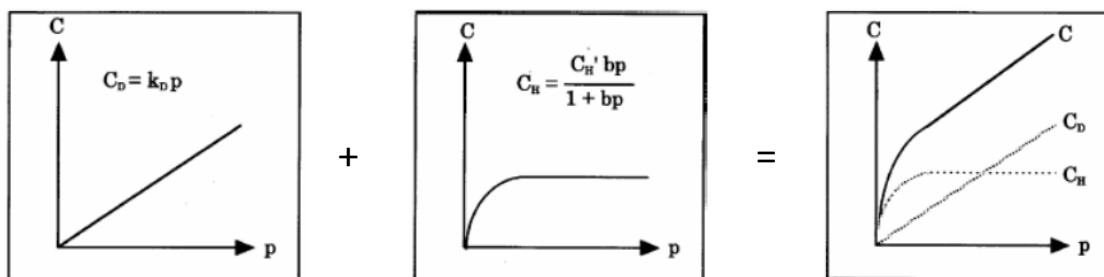
Figure 1.4 Schematic representation of dual-mode sorption, Henry sorption and Langmuir sorption [Tsujita (2003)].

$$C = C_D + C_H = k_D.P \frac{C'_H.b.p}{(1+b.p)} \qquad (1.12)$$

where, C is the total sorption amount in glassy polymeric membrane, C_D is Henry mode sorption, C_H is Langmuir sorption amount, P is applied gas pressure, k_D is Henry's solubility coefficient, C'_H is Langmuir saturation constant and b is Langmuir affinity constant.

The dual-mode sorption equation (1.12) provides a linear relationship with pressure in the high pressure region [Tsujita (2003)]. The linear slope in the high pressure region corresponds to the Henry's solubility coefficient and the intercept of the extrapolated line to the C axis is the Langmuir saturation constant (Figure 1.4). Based on the gas sorption isotherm obtained experimentally, one can determine the three dual-mode sorption parameters, k_D, C'_H, and b, by curve fitting using a nonlinear least squares method. C'_H is related to the unrelaxed volume (eq. 1.13), which is a measure of the departure from equilibrium in the glassy state, i.e. the difference between the specific volume of glassy state and liquid states ($V_g - V_l$).

$$C'_H = \left(\frac{V_g - V_l}{V_g}\right)\frac{22400}{V_p} \qquad (1.13$$

where, V_p is the molar volume of sorbant gas, evaluated from the experimentally determined sorption isotherm. If a gas is polar in nature and condensable, gas sorption may exhibit an anomalous isotherm. For example, some glassy polymers can be plasticized to rubbery state by CO_2 owing to their interactions [Wang (1996)]. Thus, a linear relationship in the high pressure region does not occur over a wide pressure range, due to the subtle effects of plasticization at high pressure by sorbant gas or vapor.

1.6   Factors affecting gas separation performance

Various polymer properties, experimental conditions, processing history of membrane affect the gas permeation properties. It is well established that chemical structures coupled with the physical properties of a membrane material influence the permeability and selectivity. The response of a polymeric material to the permeation is strongly influenced by polarity and steric characteristics of the polymer as well as the permeating component. Size and shape of the bulky groups in the main chain as well as the side chain determine certain fundamental properties like packing density and rigidity, which in turn influence its accessibility [Sridhar (2007)]. These factors are briefly described in following sections.

1.6.1 Physical properties of polymer

a) Chain packing density

Chain packing density is one of the most important variables affecting the permeability [Stern (1989)]. Both, *d*-spacing (d_{sp}, average intersegmental distance) and fractional free volume (v_f or FFV) are used as indices of the degree of openness of the polymer matrix [Hellums (1989)]. Effects of decreasing packing density of a polymer matrix on increasing diffusivity and permeability has been shown in several types of polymers [Stern (1989), McHattie (1991), Stern (1994), Karadkar (2007), Li (2013)]. The penetrant diffusivity depends strongly on the polymer fractional free volume present in glassy polymer. Gas diffusion coefficients are typically related to free volume and can be expressed by following equation [Ghosal (1994)];

$$D = D_0 . \exp\left(\frac{-B}{V_f}\right) \tag{1.14}$$

where, Do and B are constants characteristic of the polymer-penetrant system.

A commonly used method to determine fractional free volume (v_f) is based on semiempirical calculation using experimentally determined density of the polymer and van der Waals volume (V_w) by group additivity [Bondi (1964)]. The positron annihilation lifetime spectroscopy, photochromic and fluorescence technique are also used for determining the free volume [Victor (1987)]. Fractional free volume (V_f) can be estimated by the following eq. 1.15 [Hu (2003)];

$$V_f = \frac{V - V_0}{V} \tag{1.15}$$

where V is the polymer specific volume, calculated from bulk polymer density values, and V_0 is the occupied volume. V_0 may be calculated from the correlation, $V_0 = 1.3V_w$, where V_w is the van der Waals volume, which is often estimated using Bondi's group contribution method [Bondi (1964)].

It was noted that substitutions on the polymer chain inhibits chain packing and increases permeability [Hellums (1989), McHattie (1992), Stern (1994)]. Chain packing in polymers is also strongly affected by interchain interactions [Stern (1994)]. Generally, increase in the gas permeability with increasing v_f has been reported for many polymer families, viz., polycarbonate [Hellums (1989)], polyimide [Coleman (1990), Li (2013)], polyarylate [Pixton (1995a)], polysulfone [McHattie (1991)], etc.

b)   Chain and subgroup mobility

Chain and subgroup mobility has direct relationship with the penetrant permeability and inverse relationship with the selectivity. Structural alterations which inhibit chain packing while simultaneously inhibiting rotational motion about flexible linkages on polymer backbone tend to increase permeability while maintaining or increasing selectivity [Coleman (1990)]. The introduction of a flexible linkages such as -O- and -CH₂-, which have low energetic barriers to intrasegmental bond rotation into the polymer backbone increases torsional mobility and in turn gas diffusion coefficients [Ghosal (1994)]. Introduction of rigid linkages such as aromatic group decrease the torsional mobility and reduce penetrant mobility [Ghosal (1994)]. Inhibition of the segmental and sub-segmental mobility can be judged by increase in glass transition (T_g) or sub-T_g temperatures.

c)   Molecular weight

In low molecular weight polymers, a large contribution to segmental mobility comes from chain ends, which are less constrained by chain connectivity requirements and are, therefore, more mobile [Freeman (1990), Ghosal (1994)]. As polymer molecular weight increases, the concentration of chain ends decreases and in turn, the polymer free volume decreases. As a combined result, penetrant diffusivity decreases with increasing molecular weight. At higher molecular weights, when the concentration of chain ends is low, diffusivity is relatively independent of molecular weight [Ghosal (1994)].

d)   Polarity

Due to unevenness in electron distribution, the polarity is described by group properties such as charge density, dipole moment, hydrogen-bonding capacity and bulk properties like dielectric constant and surface tension [Sridhar (2007)]. Polarity strongly influences solubility, esp. of polar gases and subsequently their permeability [Sridhar (2007)]. Therefore, it is possible that selectivity for a polar gas in the feed gas stream may be improved with membrane polarity. For gases such as CO_2, which has a quadrupole moment, are in general, more soluble in polar polymers [Hirayama (1999)]. Presence of polar groups like bromo, chloro, nitro, sulfonic/carboxylic acid group and their salts, etc. generally lead to a decrease in permeability

and increase in selectivity. This was observed for various types of polymers such as poly(phenylene oxide) [Bhole (2007)], polysulfone [Ghosal (1992, 1995)], etc.

e)   *Crystallinity*

The diffusion of gases takes place primarily through amorphous region, where as the crystalline region acts as barrier to gases [Zhao (2008)]. Crystalline regions in polymers typically preclude penetrant solubility. Impermeable crystallites act to increase the tortuosity of the path taken by penetrant molecules through a polymer. They may also restrict segmental mobility in the non-crystalline regions of the polymer. Both these effects tend to reduce gas diffusivity. Since crystalline regions reduce both, the penetrant solubility and diffusivity, thereby reducing permeability [Ghosal (1994)]. When the crystallinity is low, diffusion resistance is quite low and consequently, the effect of crystallinity on the permeation rate is often very small. Various techniques have been employed to assess the relative and absolute degree of crystallinity, including X-ray diffraction, density methods, thermal analysis, nuclear magnetic resonance (NMR) and infrared (IR) spectroscopy [He (2000)]. Mcgonigle et al. (2004), reported that additional constraints resulting from increased crystallinity improved gas barrier performance of the polyester. Poly(phenylene oxide) (PPO), which can be prepared by melt processing as an amorphous thick film typically tends to crystallize when formed in solvent-nonsolvent induced asymmetric form. While PPO has good separation properties in the amorphous dense film form, the complications with crystallization of casting dopes for this material has prevented its large scale practical applications [Sridhar (2007)].

f)   *Crosslinking*

Cross-linking offers the potential to improve the mechanical and thermal properties of a polymeric membrane. It was suggested that cross-linking can be used to increase the membrane stability in presence of aggressive feed gases and to simultaneously reduce plasticization of the membrane [Powel (2006)]. One of the reasons to cross-link a polymer is to decrease the plasticization of a polymer in order to derive a good selectivity [Sridhar (2007)]. The gas permeability and solubility are known to be decreased with increasing crosslink density, since crosslinking reduces polymer segmental mobility [Ghosal (1994)]. There are various ways to crosslink a polymer matrix such as photochemical, thermal or chemical crosslinking.

Photochemical cross-linking by UV irradiation [McCaig (1999), Liu (1999), Dudley (2001)] and thermal cross-linking at elevated temperatures [Dudley (2001), Ismail (2002), Chung (2003)] were used to enhance polymers anti-plasticization properties.

1.6.2   Properties of gas

a)   *Size and shape of the gas*

The diffusion coefficient depends on penetrant size, as characterized by the Van der Waals volume or kinetic diameter of the penetrant. A decrease in the diffusivity with an increase in the size of penetrant has been reported [George (2001), Sadeghi (2009)]. Diffusion coefficients in polymers are also sensitive to penetrant shape [Ghosal (1994)]. The van der Waals volume can be calculated by geometrical method, provided the covalent radius and the van der Waals radius of each atom in the compound are available. However, the van der Waals volume does not account for the shape of the penetrant. The diffusivity of linear or oblong penetrant molecules such as CO_2 is higher than the diffusivities of spherical molecules of equivalent molecular volume. The Van der Waals volumes of CO_2 and CH_4 are estimated to be 17.5 and 17.2 cm^3/mole. These molecular volumes yield equivalent spherical diameters of 3.33 and 3.31Å for CO_2 and CH_4 respectively. Thus, the kinetic diameter is frequently used to characterize the penetrant size [Ghosal (1994)].

b)   *Gas condensability*

Gas solubility in the polymer matrix generally increases with increasing gas condensability [Pixton (1995b), Kanehashi (2005), Lin (2005)]. Gas critical temperature, T_c, normal boiling point, T_b or Lennard-Jones force constant represent gas condensability and correlate well with the solubility coefficients of a range of penetrants in a polymer [Ghosal (1994), Kanehashi (2005), Sanders (2013)]. For example, in most polymers, CO_2 ($T_c = 31$ °C) is more soluble than CH_4 ($T_c = -82.1$°C) and O_2 ($T_c = -118.4$ °C) than N_2 ($T_c = -147$ °C) [Ghosal (1994)].

1.6.3   Effect of operating parameters

a)   *Temperature*

Gas diffusion coefficients typically increase appreciably with increasing temperature, when the polymer does not undergo thermally induced morphological rearrangement such as

16

crystallization over the temperature range of interest [Ghosal (1994)]. In general, gas solubility decreases with increasing temperature, while diffusivity coefficients tend to increase with the temperature [Sridhar (2007)]. However, an increased diffusivity offsets the solubility decrease. The temperature dependence of gas permeation in various glassy polymers is well reported in the literature [Kim (1989), Costello (1994), Gülmüs (2007), Sales (2008)], where increase in permeability with increase in temperature was observed. The solubility coefficient for a given penetrant generally decreases with temperature; however, this decrease is overcome by the substantial increase in the diffusion coefficients, producing a net increase in the permeability coefficient. The permselectivity generally decreases with increase in temperature. Dependence of the permselectivity on temperature is larger for gas pairs with high difference in activation energies of gas pairs [Sales (2008)].

b)   *Pressure*

The driving force in gas separation is the partial pressure gradient across the membrane [Sridhar (2007)]. Diffusivity, solubility and in turn, permeability may vary appreciably as the pressure of penetrant in contact with the polymer changes. Low sorbing penetrants such as He, H_2, N_2, O_2 and other permanent gases in either rubbery or glassy polymers show small decrease in permeability with an increase in pressure [Ghosal (1994)]. On the other hand, for penetrants which have considerably high sorption in polymers (such as CO_2) generally show monotonic decrease in permeability with increasing pressure [Ghosal (1994), Lin (2001)]. This phenomenon of pressure dependence on permeability is consistent with the dual-mode transport model used to describe gas transport behavior of glassy polymers (represented as the sum of the Henry mode and the Langmuir mode). In general, the Langmuir mode, which is associated with the "excess" free volume formed in the glassy state, makes a large contribution to the pressure dependence on the permeability in glassy polymers. The permeability of a rubbery polymer to an organic vapor shows a monotonic increase in permeability and is related to increase in penetrant solubility and diffusivity with increasing pressure [Stern (1983), Ghosal (1994)]. A combination of these two behaviors is typical of the isotherm characterizing the permeability of a glassy polymer to a plasticizing penetrant such as an organic vapor [Chern (1991)]. The polymer permeation properties in such cases exhibit dual-mode behavior at low pressures and penetrant-induced

plasticization at high pressures. At high pressure, dual-mode behavior diminishes due to onset of the segmental motions after plasticization of polymer chains.

c)   Membrane preparation parameters

Owing to non-equilibrium character of glassy polymers, processing conditions employed to make membranes are important while considering the gas transport properties. The membrane morphology and the selectivity performance depends upon properties of the solvents used in preparing polymer solutions, solution concentration, surface (glass, steel, teflon, etc.) on which the membrane is cast, casting techniques (drop casting, blade casting), casting temperature and annealing temperature [Hacarlioglu (2003)]. Majority of the dense membranes used for evaluation of gas permeation properties are prepared by solution casting technique and the solvent used for making the polymer solution can affect permeation properties. Khulbe et al. (1997), used different solvents for preparing PPO membranes and observed that the permeability increased and the selectivity (O_2/N_2 and CO_2/CH_4) decreased with the increase in the boiling points of the solvents. Small amount of solvent in glassy polymer functions as the plasticizer to increase the chain mobility [Hacarlioglu (2003)]. It was reported that the permeability of poly(1-trimethyl-1-silypropyne) to helium may vary almost five fold, depending on the solvent used to cast the membrane [Ghosal (1994)]. In another example, a melt-extruded polysulfone film was approximately 20% less permeable to CO_2 than a solvent cast film [Ghosal (1994)].

The membrane surface morphology and the gas permeation through the membrane can also be affected by temperature used for solvent evaporation [Khulbe (2004)]. The permeation of CO_2, CH_4, O_2 and N_2 decreases as the evaporation temperature increases [Khulbe (2004)]. However, no significant change was observed on the permeability ratio for gas pairs CO_2/CH_4 and O_2/N_2. A sub-Tg, thermal annealing can be used to reduce free volume of glassy polymers, which decreases gas solubility, diffusivity and in turn, permeability. The annealing temperature and duration of the annealing step controls the amount of excess volume relaxation and, in turn, decreases gas solubility and diffusivity [Ghosal (1994)].

1.7   Challenges in membrane materials

A need for membrane material possessing high permeability as well as selectivity would remain as a steady demand in order to meet the rising economical changes of the separation

techniques. In addition to these, following are the typical "polymer-material' challenges that need to be addressed for better economical CO_2 separation using polymeric membranes.

a)   Permeability-selectivity tradeoff relationship

Several key factors in membrane transport performance include flux, permeability and selectivity [Sanders (2013)]. In general, polymer membrane research focuses on identifying materials with high combinations of permeability and permselectivity [Robeson (2014)]. It is well known that the membrane material performance shows tradeoff between selectivity and permeability, i.e., highly selective membrane are not very permeable an vice-versa [Aron (2005), Salleh (2011)]. Specifically, polymers offering the best combinations of selectivity and permeability are generally glassy and have rigid structures that exhibit poor chain packing [Sanders (2013)]. In essence, these polymers offer the size distribution of free volume elements required for approaching molecular sieving characteristics.

A concept emerged in the literature called the "upper bound" where log-log plots of selectivity versus permeability of the more permeable gas demonstrated that virtually all the data points were below a well-defined line [Robeson (1991, 2008)]. In recent publications, it was noted that the upper bound shifts with temperature and the Freeman theory was utilized to predict the shift for a number of gas pairs of interest [Sanders (2013)].

b)   Physical aging

The physical aging of membrane is a significant material challenge for their industrial viability [Sanders (2013)]. Many polymers used in gas separations are glassy in nature. They are non-equilibrium materials having excess free volume that is created due to the kinetic constraints on the polymer segmental motions. Physical aging slows over time for two reasons: (i) as the excess free volume gradually decreases, the driving force for the physical aging is diminished and (ii) as free volume is reduced, polymer chain mobility decreases. The decrease in permeability with time usually is accompanied by an increase in selectivity [Sanders (2013)].

c)   Plasticization

As the concentration of gas inside a polymer increases, the polymer may swell, which increases free volume and chain motion. This increases gas diffusion coefficient and decreases

diffusion selectivity. This phenomenon is known as plasticization [Sanders (2013)]. One common signature of plasticization is an increase in permeability of a gas as the upstream partial pressure of that gas increases. However, increase in permeability can be due to increase in solubility, increases in diffusivity or both [Sanders (2013)]. Another common symptom of plasticization is a loss in selectivity as upstream total pressure (or partial pressure of one or more components) increases. Among various gases of importance in gas separation applications, CO_2 is often among the more soluble gases. The plasticization by CO_2 is widely known and studied in relation to CO_2 removal from natural gas [Sanders (2013)].

1.8   Ionic liquids (ILs) and polymeric ionic liquids (PILs) for CO_2 separation

For a membrane to be useful for CO_2 separation, it should posses high permeability, higher CO_2 selectivity over other gases, thermally and chemically robustness, resistant to plasticization, resistant to aging, cost effectiveness and be able to be cheaply manufactured into different membrane forms [Powel (2006), Brunetti (2010)]. The development in polymeric membranes for this purpose is widely reviewed [Sridhar (2007), Schole (2008), Bernardo (2009, 2013), Sanders (2013)]. Ionic liquids (ILs) and polymeric ionic liquids (PILs) are emerging as promising materials for CO_2 separation, owing to their attractive CO_2 sorption properties. It would be worth to look at their various peculiarities, which would be useful in new material design.

1.8.1   Ionic liquids (ILs)

Ionic liquids (ILs) are salts composed of ions and generally are liquids below 100 °C [Petkovic (2011), Mecerreyes (2011), Yaun (2013)]. If melting point is below room temperature, the IL is called as room-temperature ionic liquid (RTIL) [Thomas (1999)]. Ionic liquids, which have been widely promoted as "green solvents", are attracting much attention for applications in many fields of chemistry and industry due to their chemical stability, thermal stability, low vapor pressure, high ionic conductivity, etc. [Lu (2009), Petkovic (2011), MacFarlane (2014)]. Their potential is further emphasized by the fact that their physical and chemical properties may be finely tuned by varying both the cation and the anion.

The RTILs for CO_2 capture have been analyzed since 1999, after it was reported first that CO_2 is highly soluble in 1-butyl-3-methyl-imidazolium hexafluorophosphate ([bmim][PF_6]),

reaching a 0.72 mole fraction of CO_2 at 40 °C and 93 bar [Zhang (2012)]. Unlike organic solvents, both the solubility and the selectivity of CO_2 in RTILs can be readily "tuned" by tailoring the structures of the cation and/or anion [Bara (2009a)]. Imidazolium-based RTILs have dominate the literature of CO_2 sorption in RTILs [Blanchard (1999), Bates (2002), Cadena (2004), Scovazo (2004), Anderson (2007), Bara (2007a, 2009a), Zhang (2012)]. Other classes of RTILs (phosphonium, ammonium, pyridinium etc.) also have received attention in CO_2 separations [Bara (2009), Zhang (2012)]. The CO_2 sorption of ILs while varying anion (chloride, bromide, dicyanamide, acetate, trifluoroacetate, lactate, carboxylates, dicarboxylate, methane sulphonate, trifluoromethane sulphonate, nitrate, perchlorate, chloroaluminate, tetrafluoroborate, hexafluorophosphate, bis(trifluoromethyl sulfonyl)imide, amino acid based anion, phenolate, etc.) were demonstrated [Anthony (2002, 2005), Cadena (2004), Muldoon (2007), Yokozeki (2008), Bara (2007a, 2009a), Raeissi (2009), Shiflet (2008, 2009, 2010), Gurkan (2010), Karadas (2010), Zhang (2006, 2009, 2012), Blath (2012), Goodrich (2011a, 2011b), Wang (2010, 2011, 2012), Tome (2013a) etc.]. Aki et al. (2004), found that CO_2 solubility in *1-n*-butyl-*3*-methylimidazolium, [BMIM]$^+$ based ILs increased with following order of anion variation; [NO_3] < [DCA] < [BF_4] < [PF_6] < [TfO] < [Tf_2N] < [methide].

The large structural variation on cation and anion for improving CO_2 sorption of ILs were reported. It was observed that the CO_2 solubility of imidazolium based ILs was increased with the increasing side alkyl chain length of the ILs [Zhang (2012)]. It was reported that anions of ionic liquids have a much stronger influence on the solubility of CO_2 than the cations of ionic liquids and it was observed that the CO_2 molecules have a greater affinity for anion versus cation associations [Anthony (2005)].

It is noted in that the task-specific ionic liquids (TSIL, also called functionalized ionic liquids) can improve the CO_2 absorption capacity by introducing suitable moieties (like amine) in the conventional ionic liquids. Bates et al. (2002), synthesized the [NH_2p-bim][BF_4] IL consisting of an imidazolium ion to which a primary amine moiety is covalently tethered to the cation and proposed the reaction mechanism between the TSIL and CO_2, which is similar to the reaction between an organic amine and CO_2. Due to the low volatility, TSILs can be regenerated easily by heating (80–100 °C) for several hours under vacuum, which can reduce the cost of energy [Zhang (2012)]. A new type of anion-tethered TSIL, tetrabutylphosphonium amino acid [$P(C_4)_4$][AA], was synthesized for CO_2 capture by the reaction of tetrabutylphosphonium

hydroxide $[P(C_4)_4][OH]$ with amino acids, including glycine, L-alanine, L-b-alanine, L-serine, and Lysine, and obtained a similar CO_2 capacity to $[NH_2p\text{-}bim][BF_4]$ [Zhang (2006, 2012)]. Thereafter, Goodrich et al. (2011a, 2011b), developed number of ILs with amine-functionalized anion. This IL exhibited 1:1 CO_2 sorption mechanism. However, the chemical absorption of CO_2 by these ILs dramatically increased the viscosity of the ionic liquid [Goodrich (2011b)].

In order to improve the CO_2 absorption capacity, dual amino functionalized phosphonium ionic liquids ($[aP4443][AA]$) were also developed [Zhang (2009)]. Wang et al. (2012), studied CO_2 absorption of ILs based on phosphonium cation with various basic anion. It was observed that the CO_2 absorption capacity increased with the basicity of anion. The similar results of higher CO_2 sorption in ILs possessing basic anion was observed by Blath et al. (2012), Tome et al. (2013a), etc.

Shiflet et al. (2009), studied the phase behavior of CO_2 in ILs (possessing acetate and trifluoroacetate anion). It was observed that the high CO_2 solubility in the [emim][Ac] is dramatically reduced when the methyl group of acetate anion (CH_3COO) is replaced with a fluorinated methyl group (CF_3COO). Shiflet et al. (2010), compared the energy requirement and economic investment of a commercial MEA based CO_2 capture facility with a new process designed to use ionic liquid viz., [bmim][Ac]. Based on the cost estimation, the total project investments for the MEA and ionic liquid processes are $18.1 and 15.8 million, respectively. Thus, the ionic liquid process can reduce the energy losses by 16% compared to the MEA-based process. The investment will be 11% lower than a MEA-based process and provide a 12% reduction in equipment footprint. Although a real industrial plant with ionic liquid as the capture solvent has not been installed yet, this work provided useful information on this new technology and a comparison with the MEA method [Shiflet (2010), Zhang (2012)].

1.8.2   *Supported ionic liquid membranes (SILMs) for CO₂ separation*

There has also been a great interest in using RTILs as the selective component in membranes. A straight forward approach to use RTILs in a membrane configuration is to employ supported ionic liquid membranes. In general, SILMs are composed of a IL immobilized within pores of a polymer or inorganic support. SILMs typically provide larger gas permeabilities than conventional polymer membranes, as gas diffusion through a dense liquid film is often much more rapid than that through a rubbery or glassy polymer.

Number of studies was published on the potential of SILMs in CO_2 separations [Scovazzo (2004), Hern´andez-Fern´andez (2007), Bara (2009a), Bara (2010), Santos (2014)]. Evaluation of several RTILs revealed that SILMs possessed permeability and selectivity properties for CO_2/N_2 that were superior to most conventional polymer membranes when viewed in the context of a "Robeson Plot". The CO_2/CH_4 separation appeared to be a less promising application for SILMs when analyzed via an analogous "Robeson Plot" for that gas pair [Bara (2010)].

Nevertheless, their industrial application is still limited, mainly due to concerns about SILM stability and long-term performance [Hern´andez-Fern´andez (2007), Bara (2009a)]. Typically, SILMs reported in the literature are quite thick, perhaps 150 μm or more. High-throughput industrial applications will require selective layers of less than 1 μm. One another limitation of SILMs (and SLMs in general) is that the liquid component is subject to "blow out" through the pores of the support should the pressure drop across the membrane exceed the capillary forces stabilizing the liquid within the matrix [Bara (2010)]. Thus, the transmembrane pressure differential that can be applied is limited to perhaps only a few atmospheres. Natural gas processing with membranes is performed at high pressures (30-60 bar), which current SILM configurations are certainly not capable of withstanding [Bara (2009a)]. CO_2 capture from flue gas occurs at atmospheric pressure and is perhaps a more realistic target separation for SILMs. To overcome these limitations, polymeric counterpart of IL could be a promising option.

1.8.3 *Polymeric ionic liquids (PILs)*

PILs are polyelectrolytes, whose repeating unit bear an electrolyte group (cation or anion). PILs can be classified as polycations bearing a cation in the backbone's part of the monomer unit, polyanions bearing an anion or polyzwitterions having both anion and cation. Furthermore, different types of copolymers (random, alternating, block) and macromolecular architectures such as branched, dendritic or ramified structures are potentially possible [Mecerreyes (2011)].

1.8.3.1 *Synthesis of PILs*

a)   Polymerization of ionic liquid monomer

Synthesis of PILs by polymerization of vinyl monomers containing pendant ionic liquid moiety has been the most popular route [Green (2009), Mecerreyes (2011), Yaun (2011, 2013)].

This route involving the polymerization of IL monomers enables the preparation of homopolymers as well as copolymers. However this method involves a number of organic synthesis and purification steps at the monomer level, as well as the need of controlling polymerization conditions of each individual monomer [Mecerreyes (2011)].

Most of these polymers have been synthesized using conventional radical polymerization [Mecerreyes (2011)]. However, examples of PILs synthesized by atom transfer radical polymerization (ATRP) [Cardiano (2008)], reversible addition-fragmentation transfer polymerization (RAFT) [Vijayakrishna (2008), Mori (2009)], ring-opening polymerization and ring-opening metathisis polymerization processes [Vygodskii (2008)] have also been reported. In addition to linear homopolymers, cross-linked PIL networks have been synthesized by radical polymerization methods. For this purpose, bi- or trifunctional acrylic or styrenic IL monomers were purposely prepared. Cross-linking was carried out by thermal or UV radical curing leading to PIL networks [Bara (2007b, 2008a, 2008b), Li (2011), Mecerreyes (2011), Yaun (2013)].

b)   *Anion exchange*

PILs having nonhalide anions can be alternatively prepared by an anion exchange reaction with pre-synthesized PILs having halide anions [Marcilla (2004), Green (2009), Mecerreyes (2011), Yaun (2011, 2013)]. Marcilla et al. (2004), demonstrated that the solubility characteristics of the polymers can be tuned by anion exchange of halide containing PILs by nonhalide anions (BF_4^-, PF_6^-, $CF_3SO_3^-$, $(CF_3SO_2)_2N^-$, $(CF_3CF_2SO_2)_2N^-$, ClO_4^-). The variations of morphology, thermal properties, electrochemical properties, hydrophobic-hydrophilic characteristics, gas separation performances, etc., by just replacing the anion of PILs were reviewed [Green (2009), Mecerreyes (2011), Yaun (2011, 2013)].

c)   *Condensation polymerization*

PILs incorporating imidazolium group in the main chain can be obtained by condensation polymerization [Xiong (2012)]. The most direct method includes the synthesis of PILs by direct quaternization of a dihalide or dihydroxide with a dimidazole or a dipyridine molecule, subsequent anion exchange step leaded to the corresponding PIL [Suzuki (2004), Li (2007), Amarasekara (2011), Mecerreyes (2011)]. The step-growth polymerization method based on the acyclic diene methatesis polymerization (ADMET) process led to ionic polyolefins [Aitken

(2010), Mecerreyes (2011)]. Another type of PILs was synthesized by the hydroboration polymerization of diallylimidazolium IL derivatives [Matsumi (2006)]. Recently IL based copolyimide with different proportion of IL content was developed by this methodology [Li (2010, 2013)].

The chemical structures of PILs investigated and their gas sorption and permeation, especially for CO_2 are summarized in Appendix I-III. It can be seen that, most of the PILs possess aliphatic backbone (except for few PIL-copolymers based on condensation polymers), serving mostly as a polymeric cation. The positively charged ammonium, pyridinium or imidazolium groups are either anchored to a polymeric backbone or sometimes are part of main chain backbone. PILs with anionic moieties in the polymer backbone and mobile counter-cations were also synthesized but number has been much smaller than the cationic based PILs [Mecerreyes (2011)]. This is probably due to the more difficult task of synthesizing anionic type monomeric ILs.

1.8.3.2 *Applications of PILs*

Applications of PILs as the new generation polyelectrolyte materials in energy devices (lithium ion batteries, dye sensitized solar cells, PEMFC, supercapacitors, light-emitting electrochemical cells, field effect transistors), biosensors, anion sensitive materials, electromagnetically active polymers, nanocomposites and many others are emerging fast [Green (2009), Mecerreyes (2011), Yaun (2011, 2013)]. PILs as CO_2 separation membrane material look promising due to their high CO_2 sorption, high absorption-desorption rates and appreciable thermal stability [Green (2009), Mecerreyes (2011), Yaun (2011, 2013)]. The CO_2 separation performance is briefly described in following sections.

1.8.3.3 *CO$_2$ separation performance of PILs*

a) *CO_2 sorption in PILs*

In order to overcome drawbacks associated with SILMs, incorporating the IL character in the polymer chains offering 'polymeric ionic liquid' (PIL) is emerging as a promising option. Tang et al. (2005a, 2005b, 2005c, 2005d, 2005e), first observed that several PILs unexpectedly exhibited significantly higher CO_2 absorption capacities than the corresponding ILs. Most importantly, CO_2 absorption and desorption of PILs are much faster and are completely

reversible than for the ionic liquids. Similar comparison was demonstrated for newly developed PILs and their monomeric ILs [Supasitmongkol (2010), Mecerreyes (2011), Xiong (2012), Yaun (2011, 2013), Privalova (2013)]. Yaun et al. (2013), noted that effects of the anion, cation and backbone of a PIL on its CO_2 sorption capacity were much different than those of room temperature ILs. While keeping anion same, PIL containing polystyrene backbone exhibited higher CO_2 absorption capacity than those containing a poly(meth)acrylate backbone [Bara (2007b)]. Long alkyl substituent on the cation is reported to decrease CO_2 absorption capacity [Bara (2007b)]. Tang et al. (2009), showed that cross-linking decreases CO_2 sorption capacity. The CO_2 solubility was increased by about 30% when switching from the non-polar alkyl chain to the polar PEG-based chain in the main backbone [Bara (2008a)]. Tang et al. (2009), investigated that CO_2 sorption capacities of the PILs decreased in the order of cation variation as ammonium > pyridinium > phosphonium > imidazolium. Similarly, PILs with different anions decreased CO_2 sorption in the order: $BF_4^- > PF_6^- > Tf_2N^-$ [Tang (2009)]. In another study, CO_2 sorption increased in the order of anion variation as $NTf_2^- < OTf^- < Br^- < BF_4^- < PF_6^-$ [Privalova (2013)]. A tetraalkylammonium-based PIL can absorb up to 77 wt% of CO_2 with higher CO_2/N_2 selectivity (70:1) [Supasitmongkol (2010)]. Modifications in PIL structure have also been investigated with an aim to increase CO_2 uptake. Various functional groups have been introduced and their effects on increasing the CO_2 affinities of PILs have been investigated [Yaun (2013)]. A mesoporous PIL was also reported, which exhibited faster CO_2 absorption rate with enhanced CO_2 capacity than their IL monomer and the bulk PIL [Wilke (2012)]. The CO_2 sorption data of reported PILs is summarized in Appendix-II.

b) *Gas permeation studies of PILs*

Separation of CO_2 from light gases, such as nitrogen or CH_4, is a challenging task of significant importance in both industry and scientific communities. Such a separation process requires a PIL membrane to possess high CO_2 flux, selectivity and stability at elevated temperatures and pressures. Investigations of PILs as a gas separation membrane material began soon after reporting the enhanced CO_2 uptake [Tang (2005a, 2005b, 2005c, 2005d, 2005e), Hu (2006)]. The major hurdle of the demonstrated PILs remained unsolved was their brittle nature and thus could not be used at higher pressure [Tang (2005e), Hu (2006), Bara (2007b, Bara 2008a), Li (2011)]. To overcome this hurdle, many studies have been aimed at understanding

and improving mechanical strength of PIL-membrane and their permeability, while maintaining the superior selectivity. It was said that this can be achieved by studying the effects of systematically changing structural parameters in PIL backbones, cations and anions [Yaun (2013)]. The alternative methodologies for making membrane, such as, copolymerization [Hu (2006), Li (2010, 2013), Chi (2013)], crosslinking [Bara (2007b, 2008a, 2008b, 2010), Carlisle (2010, 2013), Li (2011, 2012)] or polymerization on porous polymer support [Bara (2007b, 2008a, 2008b, 2010), Hudono (2011), Li (2011), Carlisle (2012)] were demonstrated for their effective testing in a flat film form. The gas permeation of these PILs at higher pressure yielded only little success.

Hu et al. (2006), developed a mechanically stable membrane by grafting polyethylene glycol (PEG) on to PILs. These copolymers possessed good separation performances at 40 psi upstream for the CO_2/N_2 gas pair. The good performance of poly(RTIL)-co-PEG copolymer is attributed to PEG, since PEG itself has strong interactions with CO_2 [Li (2011)]. In addition, higher amount of PEG was required for formation of mechanically strong film, which limits the RTIL concentration in the copolymer. Nobel's group developed styrene and acrylate containing imidazolium-based PILs with varying *N*-alkyl substituents by polymerization of IL monomer in presence of crosslinker on porous polymer support [Bara (2007b)]. They noted that the gas permeability (CO_2, N_2 and CH_4) of PILs was increased with increasing length of the *N*-alkyl substituent [Bara (2007b)]. In further study, they developed PILs based on cross-linked gemini room temperature ionic liquid monomer on porous polymer support. It was observed that diffusion of gases through these highly cross-linked poly(GRTIL) membranes is quite restricted and hence these membranes exhibited low gas permeability [Bara (2008a). They also demonstrated that PILs containing oligo(ethylene glycol) or nitrile-terminated alkyl polar substituents have excellent CO_2/N_2 separation and surpass the Robeson upper bound [Bara (2008b)]. The main-chain imidazolium polymer membranes possessing two different anions (Br^- and Tf_2N^-) were developed wherein, the PIL containing bulky anion (Tf_2N^-) exhibited higher gas permeability than the other one [Carlisle (2010)]. Li et al. (2011), have developed a vinyl imidazolium based PIL by adding crosslinker, which posses high CO_2 permeability of 101.4 Barrer. The gas permeation of this PIL membrane was also analyzed at 10 atm upstream pressure, indicating good mechanical stability. However, the high gas permeability of this PILs could be because of its rubbery nature ($T_g = -39\ °C$). The same group has reported gas

permeability of imidazolium based PILs by following same strategy as used earlier with increasing side alkyl chain length and DCA as an anion [Li (2012)]. It was observed that gas permeability in these PILs was increased with increasing the side alkyl chain length. Carlisle et al. (2013), have investigated several vinyl imidazolium based PIL membranes by UV polymerization on porous polymer support and their gas permeation was reported at 2 atm. The CO_2 permeability of these PILs was achieved upto 130 Barrer, with the loss of CO_2/N_2 and CO_2/CH_4 selectivity (14 and 8.7, respectively). The gas permeation of a free standing PIL, P[DADMA][Tf_2N] was reported at 1 atm [Tome (2013b)], which did not use crosslinker, copolymerization or polymer support. The IL based copolyimides were also reported with the different proportion of IL monomer [Li (2010, 2013)]. The gas permeation of these copolyimide (IL content upto 25 mol%) was recorded at 10 atm upstream pressure, while the copolyimide with 100 % IL monomer was unable to form film. Authors noted that increasing IL content in copolyimide exhibited gradual decrease in gas permeability, solubility as well as diffusivity. The reduction in free volume was said to be responsible for the decrease in gas permeation properties. The PVC-grafted PIL was also investigated and the gas permeation was reported with maximum 65 wt % of IL moiety [Chi (2013)]. The advantage PVC-g-PIL graft copolymer system was said to be good mechanical properties than reported earlier. The CO_2 permeability and selectivity over N_2 and CH_4 of reported PILs is summarized in Appendix-III.

c)   PIL-IL blend membranes

For improvement in CO_2 permeation of PILs, blend membrane of IL and PILs were demonstrated by several researchers [Bara (2008c, 2008d, 2009b, 2010), Hudino (2011), Li (2011, 2012), Carlisle (2010, 2012, 2013)]. These blend or composite membranes have been studied in order to combine the better mechanical properties of polymeric materials and the good CO_2 sorption properties of ionic liquids [Li (2011)]. Incorporation of ILs in the PILs decreased T_g, increased FFV, gas solubility, diffusivity and permeability [Li (2011), Carlisle (2013)]. Afterword For further improvement in gas permeability, three component mixed matrix membrane based on PIL, IL and zeolite or ZIF were also demonstrated [Hudino (2011), Hao (2013)].

In spite of many incremental improvements, the challenges regarding PIL-membrane permeability and stability at elevated pressure and temperature are not completely resolved. This

suggests that considerable research is still required for a complete understanding of the relationship between molecular composition, macromolecular structure and gas permeation properties [Tome (2013b)]. The knowledge gained from these studies, particularly with regard to structure–property relationships is a necessary step for developing improved PIL based membranes [Yaun (2013)].

1.9   Objectives

The overall aim of this work was to enhance an understanding towards physical and gas permeation properties of polymeric ionic liquids (PILs). Toward this goal, effects of anion variation (while keeping aliphatic polycation the same) on physical and gas sorption properties became the prime objective. Blend membrane formation was set as the next objective of obtaining film forming PILs.

As more and more literature on aliphatic type of backbone conveying their drawbacks (especially, film formation inability) became available, moving away from aliphatic cationic backbone to aromatic was aimed, specifically for achieving film forming ability. We have proposed, for the first time, that fully aromatic backbone may render film formation ability to PILs. Structural architecture of polybenzimidazoles through monomer and *N*-sustitution variations was set as the next objective to obtain PILs with rigid backbone. Although this altogether different methodology of obtaining PILs was introduced recently in our group, it needed further validation by varying anion and performing further structural architecture. These objectives were addressed by following methodology as given below.

a) Investigating effects of anion variation

A commercially available PIL precursor, viz., P[DADMA][Cl] was chosen in order to establish a metathesis protocol using salts of promising anions of three different categories, viz., carboxylates, sulfonates and inorganic anions. Investigations of physical and gas sorption properties of resulting PILs were planned in order to gain an understanding towards specificity of anions in governing these properties.

b) Blend membrane formation

In view of known film forming inability of PILs possessing aliphatic backbone, a promising methodology of obtaining film could be their blending with an appropriate film

forming polymer. In view of absence of literature information on this aspect, one of the promising PILs from above work was chosen for blending with a well known gas separation membrane material, PEBAX.

c) **Investigations on film forming PILs based on rigid PBI backbone**

The objective of this part of the work was to synthesize film forming PILs by *N*-quaternization of chosen polybenzimidazoles, initially by a primary substituent, methyl group. Developing a family of PILs by anion variation of *N*-quaternized PBI and investigating effects of anion variation on physical and gas permeation properties would lead to a crucial understanding of this new family of materials. Shifting from aliphatic backbone to fully aromatic one could be worth investigating towards not only film forming ability, but also on effects of anion variation on physical and gas permeation properties of resulting PILs.

d) **Investigating effects of bulky group for the *N*-substituent of PBI**

The objective of this work was to elevate gas permeation in PBI based PILs by *N*-quaternization using bulky alkyl halides. Two PBIs were chosen in order to evaluate effects of this methodology on physical and gas permeation properties of resulting PILs.

1.10   Organization of thesis

The work carried out towards detailed investigation of new family materials viz., PILs for gas separation (esp. CO_2) is presented in following chapters.

Chapter 1: This chapter reviewed the gas separation requirements and the need of CO_2 separation in current scenario. Current technologies used for CO_2 separations followed by advantages of the membrane based separation over the conventional processes are described. Theoretical aspects of gas permeation and factors affecting gas permeation properties in polymeric membranes are briefly described. The positioning of IL and PILs as membrane materials for CO_2 separation is described. This chapter ends with objectives of the work followed by organization of the thesis.

Chapter 2: This chapter presents investigation of family of PILs based on poly(diallyldimethylammonium chloride), P[DADMA][Cl] by varying anions categorized into carboxylates, sulfonates and inorganic types. Variation in anion was found to have a large effect of physical properties of obtained PILs. The obtained gas sorption properties are correlated with physical properties.

Chapter 3: In view of observed high CO_2 sorption and its selectivity in case of P[DADMA][Ac] as given earlier, this chapter specifically aims at evaluating effects of structural variation in carboxylate anion. For convenience, the cationic backbone, viz., P[DADMA] was retained the same. Effects of variation in alkyl chain length of carboxylated anion and substitution on aromatic ring of the carboxylate anions on physical and gas sorption properties of resulting PILs are presented.

Chapter 4: This chapter deals with, the blend membrane formation of one of the promising PIL from above study, viz., (P[DADMA][Ac]) exhibiting high CO_2 sorption and CO_2 based sorption selectivity with PEBAX (known for high gas permeability) with an aim of evaluating blends as a new methodology to overcome brittleness of aliphatic PILs.

Chapter 5: This chapter deals with the formation of PILs following an altogether different approach (that is not known in the literature), i.e., *N*-quaternization of rigid aromatic backbone, polybenzimidazoles, followed by anion exchange with promising anions. The synthetic aspects of PILs and detailed characterizations, viz., NMR, FTIR, degree of quaternization and anion exchange, solvent solubility, water sorption and contact angle, polyelectrolyte nature, film forming ability and mechanical property, density, WAXD, thermal stability are presented.

Chapter 6: This chapter deals with the enhancement in gas permeation properties of PBI based PILs by using bulky alkyl groups (*tert*-butylbenzyl bromide and *n*-butyl iodide) for the *N*-quaternization of PBI. PILs based on two structurally different PBIs (PBI-I and PBI-BuI) are evaluated. The synthetic aspects, physical properties, gas sorption and permeation properties revealing promises of PIL are presented.

***Chapter 7*:** This chapter deals with the synthesis of PILs with the flexible linkage in the backbone, with an aim of improving permeation properties esp. gas diffusion. For this, PILs were prepared by *N*-quaternization of PBI based on suberic acid, using *tert*-butylbenzyl bromide as a reagent. The anion exchange was performed with BF_4^- and Tf_2N^- anions. The obtained physical and gas sorption properties of PILs are presented.

***Chapter 8*:** This chapter summarizes the conclusions of various approaches studied towards applicability of PILs as a gas separation membrane material, esp. for CO_2; while investigating crucial physical and permeation properties.

Chapter 2

Polymeric ionic liquids (PILs): Effect of anion variation on their CO$_2$ sorption

2.1   Introduction

PILs possess unique combination of properties arising from IL character and polymeric nature. Their properties can be tuned by pairing a variety of polymeric cations with a wide range of either inorganic or organic anions. They can be synthesized either by polymerization of ionic liquid monomers, anion exchange of a precursor polymer or by condensation polymerization [Blasig (2007), Tang (2005a, 2009), Bara (2007b), Green (2009), Mecerreyes (2011), Yaun (2011, 2013), Xiong (2012), Li (2010, 2013), Chi (2013)].

It would be worth to investigate CO$_2$ sorption in PILs possessing different anions of varying structure and bulk, while keeping the polycation same. It would provide insights towards concurrent effects of polymeric nature, IL character and bulk of the anion in governing gas sorption properties in PILs. Present work deals with PIL synthesis and investigation of their physical and gas sorption (CO$_2$, N$_2$ and H$_2$) properties. PILs obtained from poly(diallyldimethyl ammonium chloride), P[DADMA][Cl] and various anions were investigated. The precursor P[DADMA][Cl] was chosen since it is known that tetra-alkyl ammonium based PILs have high CO$_2$ sorption than that of imidazolium based PILs [Tang (2005a), Mecerreyes (2011), Yaun (2011, 2013)]. It is cheaper and widely used in flocculation, dewatering, coagulation and separation processes [Wandrey (1999)]. For the conversion of precursor P[DADMA][Cl] to a particular PIL, we adopted altogether different methodology of using silver salt of an anion for the anion exchange reactions. In couple of cases, where use of Ag salt was not possible, Li or Na salt was used. PILs based on poly(vinylbenzyltrimethylammonium), P[VBTMA] as a cation and two selected anions (acetate and tetrafluoroborate) were investigated.

2.2   Experimental

2.2.1   Materials

Aqueous solution of poly(diallyldimethylammonium chloride), P[DADMA][Cl] (20 wt. % , average mol. wt. 100,000 - 200,000), silver acetate (99%), silver trifluroacetate (98%), silver

methanesulfonate, silver trifluromethanesulfonate (>99%), silver *p*-toluenesulfonate (97%), silver heptaflurobutyrate (97%), silver benzoate (99%), silver nitrate (99.99%), lithium bis(trifluoromethylsulfonyl)imide (99.95%) and sodium tetrafluoroborate (98%) were procured from Aldrich Chemicals. Poly(vinylbenzyltrimethylammonium chloride) (P[VBTMA][Cl]) was procured from Scientific Polymer Products Inc. as a dry powder (approx. mol. wt. 400,000). Solvents used (AR grade) in this investigation were purchased from S.D. Fine Chemicals. All these chemicals were used without further purification. Pure H_2 (min. purity: 99.9%) was procured from Vadilal Chemicals Ltd., N_2 (min. purity: 99.9%) was procured from Six Sigma Gases India. Pvt. Ltd., while CO_2 with purity of 99.995% was procured from Air Liquide.

2.2.2 Synthesis of polymeric ionic liquids (PILs)

2.2.2.1 PILs based on P[DADMA][Cl]

A 20% aqueous solution of P[DADMA][Cl] was diluted to 8 % in order to lower the solution viscosity and ease the anion replacement. Commercially available Ag salts of acetate (Ac), trifluroacetate (TFAc), methanesulfonate (MS), trifluromethanesulfonate (TFMS), *p*-toluenesulfonate (PTS), heptaflurobutyrate (HFB), benzoate (Bz) and nitrate (NO_3); while Li salt of bis(trifluoromethylsulfonyl)imide (Tf_2N) and sodium salt of tetrafluoroborate (BF_4) were used for anion exchange. To a 8 % solution of P[DADMA][Cl], equimolar quantity of Ag salt of desired anion was added while stirring at the ambient. As replacement of Cl^- with an anion progressed, AgCl precipitated out. In view of polymeric nature of cation, stirring was continued for 24h to ensure maximum possible exchange. The mixture was centrifuged at 16000 rpm for 30 min to separate AgCl. Supernatant solution was poured on to a flat teflon surface, dried at 60 °C in vacuum oven for 7 days. Obtained PILs were designated based on their anion (Scheme 2.1).

Use of $AgBF_4$ led to the precipitation of polymer along with AgCl. Thus, instead of $AgBF_4$, $NaBF_4$ was used for the anion exchange. In another case where Ag salt of Tf_2N anion was not available, anion exchange was performed using $LiTf_2N$. This led to the precipitation of PIL in water, while leaving by-product salt (NaCl or LiCl) dissolved in the water. The precipitated PIL was recovered by centrifugation and washed repeatedly with water in order to remove dissolved salt. The abbreviation used for different PILs is based on the nomenclature of their cation and anion, as given in Scheme 2.1. PIL based on BF_4 as the anion formed brittle

film, while exchange with Tf_2N led to a powder. Obtained polymer was dried in a vacuum oven at 60 °C for 7 days and stored in the desiccator until further use.

P[DADMA][Cl] → (1 eq. MX, Water) → P[DADMA][X]

Where,

$M = Ag^+, Li^+$ or Na^+

$X = $

$CH_3-\overset{O}{\underset{\|}{C}}-O^{\ominus}$, (Ac)

$CF_3-\overset{O}{\underset{\|}{C}}-O^{\ominus}$, (TFAc)

$CH_3-\overset{O}{\underset{\|}{\underset{O}{S}}}-O^{\ominus}$, (MS)

$CF_3-\overset{O}{\underset{\|}{\underset{O}{S}}}-O^{\ominus}$, (TFMS)

$CH_3-\langle\text{benzene}\rangle-\overset{O}{\underset{\|}{\underset{O}{S}}}-O^{\ominus}$, (PTS)

$C_3F_7-\overset{O}{\underset{\|}{C}}-O^{\ominus}$, (HFB)

$\langle\text{benzene}\rangle-\overset{O}{\underset{\|}{C}}-O^{\ominus}$, (Bz)

NO_3^- (NO₃),

$CF_3-\overset{O}{\underset{\|}{\underset{O}{S}}}-N^{\ominus}-\overset{O}{\underset{\|}{\underset{O}{S}}}-CF_3$ (Tf₂N),

BF_4^- (BF₄)
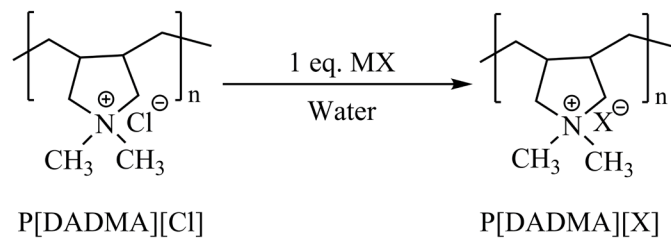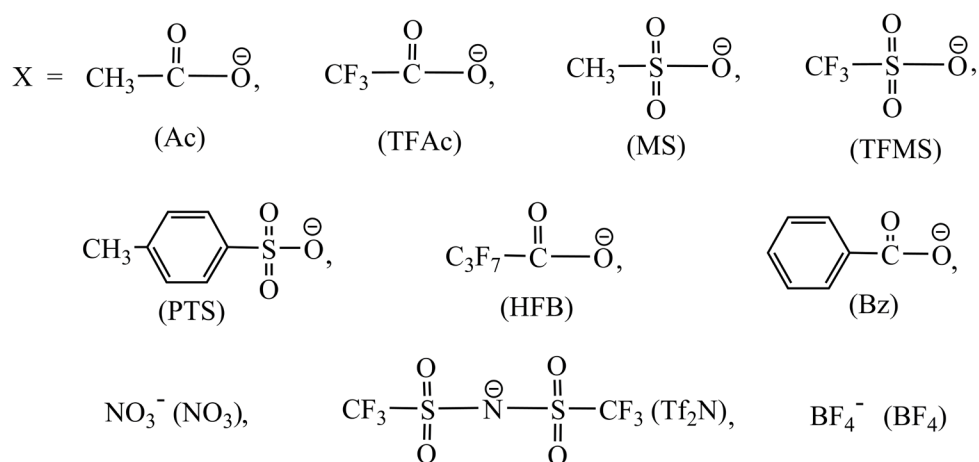
Scheme 2.1 Synthesis of PILs based on P[DADMA][Cl].
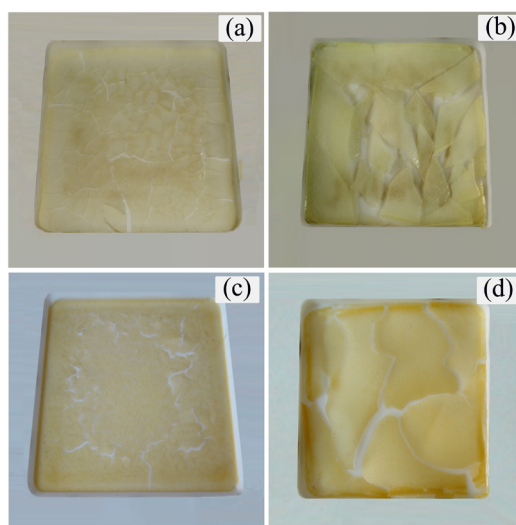
Figure 2.1 Photographs of PIL; (a) [PDADMA][TFMS], (b) [PDADMA][PTS], (c) [PDADMA][HFB] and (d) [PDADMA][NO₃].

2.2.2.2 PILs based on P[VBTMA][Cl]

To 8 % aqueous solution of P[VBTMA][Cl], equimolar quantity of silver acetate was added and stirred for 24 h at the ambient. The mixture was then centrifuged at 16000 rpm for 30 min. The supernatant polymer solution was poured on to a flat teflon surface, dried at 60 °C for 24 h and finally in vacuum oven at 60 °C for 7 days.
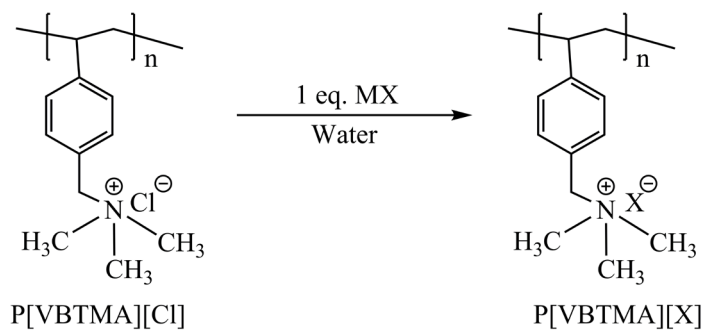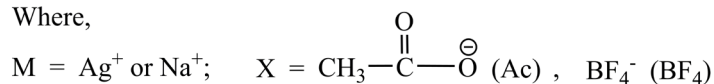
Scheme 2.2 Synthesis of PILs based on P[VBTMA][Cl].

In order to obtain PIL based on BF_4 as an anion, P[VBTMA][Cl] (15 g) was dispersed in 250 ml of acetonitrile : DMF (1:1); added 5 molar excess of $NaBF_4$ and stirred for 72 h at ambient. As replacement of Cl^- by BF_4^- progressed, polymer remained dissolved into the solvent, while NaCl precipitated out. The mixture was centrifuged to separate NaCl and the supernatant polymer solution was precipitated in chloroform. The obtained polymer was washed with an excess of $CHCl_3$ and then dried at 60 °C for 12 h. The dried polymer was washed with cold water (4 °C) thrice in order to remove salts ($NaBF_4$, NaCl), if any. Obtained PILs are designated based on their respective cation and anion (Scheme 2.2).

2.2.3 Characterizations

The quantitative analysis of water soluble PILs for residual Cl^- was performed by Inductively Coupled Plasma Optical Emission Spectrometry (ICPOES). The amount of Cl^- exchanged and the yield of obtained PIL are given in Table 2.1. The density (ρ) measurement of dry PILs was performed using specific gravity bottle. For this purpose, organic solvent, decalin having adequate density and negligible sorption in PILs were selected. The maximum sorption of decalin in PILs was ≤ 2 wt % for the exposure of 2 h at 35 °C. Five samples of each PILs were

analyzed and variation in the density was found to be $\pm$ 0.006 g/cm^3. FT-IR spectra of PILs were recorded in diffusive reflectance mode using Spectrum-1 spectrophotometer. Thin slurry of PIL in the dry methanol was coated on KBr crystal, followed by evaporation under IR lamp. The thermogravimetric analysis (TGA) using polymer was performed on Perkin Elmer TGA-7 under N$_2$ atmosphere with a heating rate of 10 °C/min. The glass transition temperature (T$_g$) was determined by differential scanning calorimetry on Thermal Instruments DSC-Q10 under N$_2$ atmosphere at a heating rate of 10 °C/min. Wide-angle X-ray diffraction (WAXD) spectra of all PILs were performed using Rigaku X-ray diffractometer (D-max 2500) with Cu-K$_\alpha$ radiation in 2θ range of 5-40°. The d-spacing (d$_{sp}$) of major amorphous hollow was calculated by Bragg's equation. Physical properties of PILs thus determined are summarized in Table 2.1. Solvent solubility was determined by dissolving 0.1 g of dried polymer in 5 ml of solvent at ambient for 8 h. In case of insolubility, it was heated at 60 °C for further 8 h and results are summarized in Table 2.2.

2.2.4 *Gas sorption*

Pure gases (H$_2$, N$_2$ and CO$_2$) were used for the analysis of gas sorption in PILs at 35 °C and at incremental pressures up to 20 atm. The gas sorption equipment consisted of dual-volume single-transducer set up based on the pressure decay method [Koros (1976), Karadkar (2007)]. The schematic of sorption equipment is given in Figure 2.2, while the photograph is given in Figure 2.3. The design of the sorption cell, specifications, material of construction, etc. is discussed elsewhere [Kumbharkar (2007)].
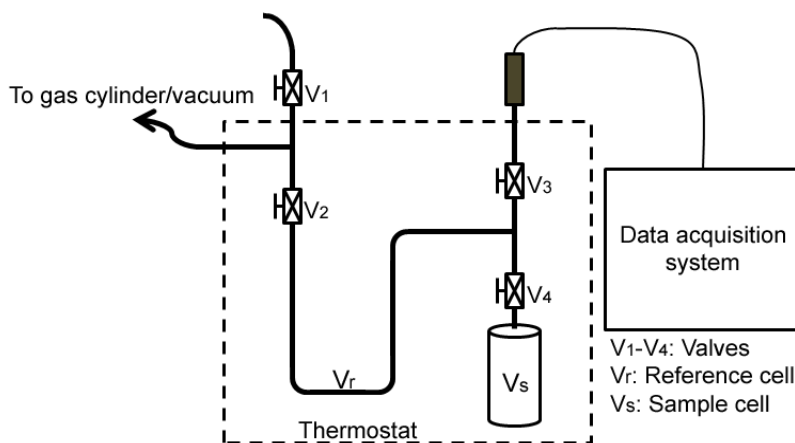
Figure 2.2 Schamatic of gas sorption equipment.

Figure 2.3 Photograph of gas sorption equipment.

The polymer sample in film form was placed in the sorption cell, evacuated and flushed with gas several times. The system was then evacuated to 0.00001 mbar using oil diffusion pump. The gas was introduced rapidly and initial pressure recorded. As the sorption proceeds, the pressure starts decreasing and ultimately remains constant after the equilibrium is established. Incremental raise in pressure of the equilibrated system until about 20 atm was attained. The amount of gas sorbed in the sample at each equilibrium pressure was determined from the initial and final pressure.

The gas solubility coefficient (S), for a gas in these glassy polymers is described by the dual-mode model [Vieth (1976)];

$$S_A = \frac{C}{p} = k_D + \frac{C'_H \, b}{(1 + bp)}$$

where, C is gas concentration in polymer, p the applied gas pressure, k_D is the Henry's solubility coefficient, C_H is the Langmuir saturation constant and b is the Langmuir affinity constant, i.e. the ratio of rate constants of sorption and desorption process [Vieth (1976)]. These constants were obtained by the nonlinear regression analysis of experimentally determined gas sorption by genetic algorithm, an optimization technique capable of searching global optima [Kumbharkar (2006)]. These parameters are given in Table 2.3. Gas solubility coefficient for CO_2 at 20 atm and solubility selectivity of different gas pairs at this pressure are given in Table 2.4.

2.3   Results and Discussion

2.3.1   *Preparation of PILs*

PILs were prepared by anion exchange method in an aqueous medium using commercially available polyelectrolyte precursors, viz., P[DADMA][Cl] and P[VBTMA][Cl]. The P[DADMA][Cl] contains quaternary ammonium group in a five-membered cyclic ring and is a part of polymer chain backbone (Scheme 2.1). On the other hand, P[VBTMA][Cl] contains quaternary ammonium group attached as a side chain functionality to a benzylic carbon (Scheme. 2.2).

For the anion exchange, Ag salt of an anion was used based on commercial availability. The advantage of using silver salt is that during anion exchange reaction to form a PIL, precipitation of silver chloride occurs in an aqueous solution. This has an advantage that the anion exchange reaction proceeds unidirectionally, leading to a quantitative exchange of anion. Moreover, an equivalent quantity of the Ag salt can be used. Moreover, separation of the formed AgCl can be done by simple centrifugation. The amount of chloride anion exchanged in this single step is given in Table 2.1, which was $\geq$ 96 %. Thus, adopted methodology of using silver salt led to appreciable anion exchange in a single step. The exchange was not precisely quantitative (100%), which could be due to the presence of impurities. Another possible reason could be the polymeric nature of cations, where some of the cationic sites remained shielded and thus unexchanged.

In the case of anion exchange using $AgBF_4$, anion exchanged polymer was also precipitated along with AgCl. Thus, $NaBF_4$ needed to be used for the anion exchange; where formed PIL precipitated out leaving behind NaCl in the solution. In order to obtain P[DADMA][Tf_2N], Li salt of Tf_2N needed to be used, due to unavailability of its Ag salt. Formed PIL precipitated out leaving behind the by-product (LiCl) dissolved in solution. In both these cases, analysis of Cl^- by ICPOES could not be performed, due to insolubility of polymers in water. The yield of PILs was high enough ($\geq$ 90%), as given in Table 2.1. In view of the lower molecular mass of repeat unit of precursor P[DADMA][Cl], this high yield could be regarded as an indirect evidence of almost quantitative anion replacement. Owing to this, no further efforts were attempted to analyze residual chloride.

Table 2.1 Physical properties of PILs based on P[DADMA][Cl] and P[VBTMA][Cl].

PILs	Chloride exchange[a] (mol %)	Yield (%)	ρ^b (g/cm^3)	$d_{sp}{}^c$ (Å)	$T_g{}^d$ (°C)	IDT[e] (°C)	pKa of conjugate acid[f]
P[DADMA][Cl]	0.0	–	1.232	–	204	320	-3.0
P[DADMA][Ac]	97.2	95.9	1.137	3.91	NO	190	4.8
P[DADMA][TFAc]	98.4	97.2	1.303	5.06	114	180	0.0
P[DADMA][MS]	98.9	90.9	1.316	–	112	315	-2.0
P[DADMA][TFMS]	96.5	90.9	1.342	–	112	372	-13.0
P[DADMA][PTS]	100.0	97.8	1.164	4.76	117	321	-2.8
P[DADMA][HFB]	100.0	90.0	1.330	5.39	103	160	0.4
P[DADMA][Bz]	98.6	93.1	1.170	4.34	90	180	4.2
P[DADMA][NO$_3$]	96.1	98.0	1.268	–	197	270	-1.5
P[DADMA][Tf$_2$N]	ND	95.6	1.437	–	NO	325	-4.0
P[DADMA][BF$_4$]	ND	95.2	1.376	–	NO	353	-0.44
P[VBTMA][Cl]	0.0	–	1.325	4.03	NO	237	-3.0
P[VBTMA][Ac]	100.0	92.4	1.213	4.12	NO	215	4.8
P[VBTMA][BF$_4$]	ND	90.0	1.406	4.63	216	340	-0.44

[a]: Determined by ICPOES; [b]: Density measured at 35 °C; [c]: *d*-spacing obtained from wide angle X-ray diffraction spectrum; [d]: Glass transition temperature; [e]: Initial decomposition temperature by TGA; [f]: Ref: [MacFarlane (2006), Cabusas (1998), Hollingsworth (2002)]; ND : Could not be detected due to insolubility in water; NO : Not detectable in the DSC scan even after repeated heating and cooling.

2.3.2   *Solubility, spectral characterizations and density of PILs*

The solvent solubility of PILs is summarized in Table 2.2. Except P[DADMA][Tf$_2$N], P[DADMA][BF$_4$] and P[VBTMA][BF$_4$], all of them were soluble in water. P[DADMA][Tf$_2$N] was soluble only in DMF, while P[DADMA][BF$_4$] was insoluble in all the solvents examined. P[VBTMA][Cl] and P[VBTMA][BF$_4$] were soluble in acetonitrile and DMF. Other PILs either swell or partially dissolve in acetonitrile, DMF and alcohols. All of them were insoluble in other common solvents, viz.; CHCl$_3$ and *1,4*-dioxane.

Table 2.2 Solubility of PILs in common solvents.

PILs	Water	Methanol	*n*-Propanol	Acetonitrile	DMF
P[DADMA][Cl]	+	+	−	−	±
P[DADMA][Ac]	+	±	±	±	±
P[DADMA][TFAc]	+	±	±	−	±
P[DADMA][MS]	+	±	±	−	±
P[DADMA][TFMS]	+	±	−	±	±
P[DADMA][PTS]	+	±	±	±	±
P[DADMA][HFB]	+	±	±	±	±
P[DADMA][Bz]	+	±	±	±	±
P[DADMA][NO$_3$]	+	±	±	±	−
P[DADMA][Tf$_2$N]	−	−	−	±	+
P[DADMA][BF$_4$]	−	−	−	−	−
P[VBTMA][Cl]	+	−	−	+	+
P[VBTMA][Ac]	+	±	±	±	±
P[VBTMA][BF$_4$]	±	−	−	+	+

+ : Soluble at ambient temperature, ± : partially soluble or swelling after heating at 60 °C for 8 h, − : insoluble after heating

FT-IR spectra of these PILs (Figure 2.4) indicated characteristics of the exchanged anion as that of precursor. Characteristic bands due to C-H stretching at ~1470 cm^{-1}, bending at ~2960 cm^{-1} and C-N stretching at ~1180 cm^{-1} were seen in the spectra of P[DADMA][Cl] as well as PILs derived from P[DADMA] as a cation. All of them showed a wide band at ~ 3400-3430 cm^{-1}, attributable to the absorbed water.

P[DADMA][Ac] showed C=O stretching (belonging to the ester group) at 1681 cm^{-1}. In the case of P[DADMA][TFAc], C=O stretching at 1694 cm^{-1} and C-F stretching at 1176 cm^{-1} were seen [Silverstein (1981)]. P[DADMA][MS] exhibited characteristic bands due to sulfonate group at 1060 cm^{-1} and 1162 cm^{-1} [Golding (2002)]. Similar bands in the case of P[DADMA][TFMS] were observed at 1032 cm^{-1} and 1160 cm^{-1}. P[DADMA][PTS] showed characteristic bands due to sulfonate group at 1020 cm^{-1} and 1030 cm^{-1}. P[DADMA][HFB]

exhibited carbonyl frequency of ester at 1691 cm^{-1}; while bands due to C-F stretching were seen at 1115 cm^{-1}. P[DADMA][NO$_3$] showed bands at 1650 cm^{-1} and 837 cm^{-1} corresponding to N=O and N-O stretching, respectively [Silverstein (1981)].
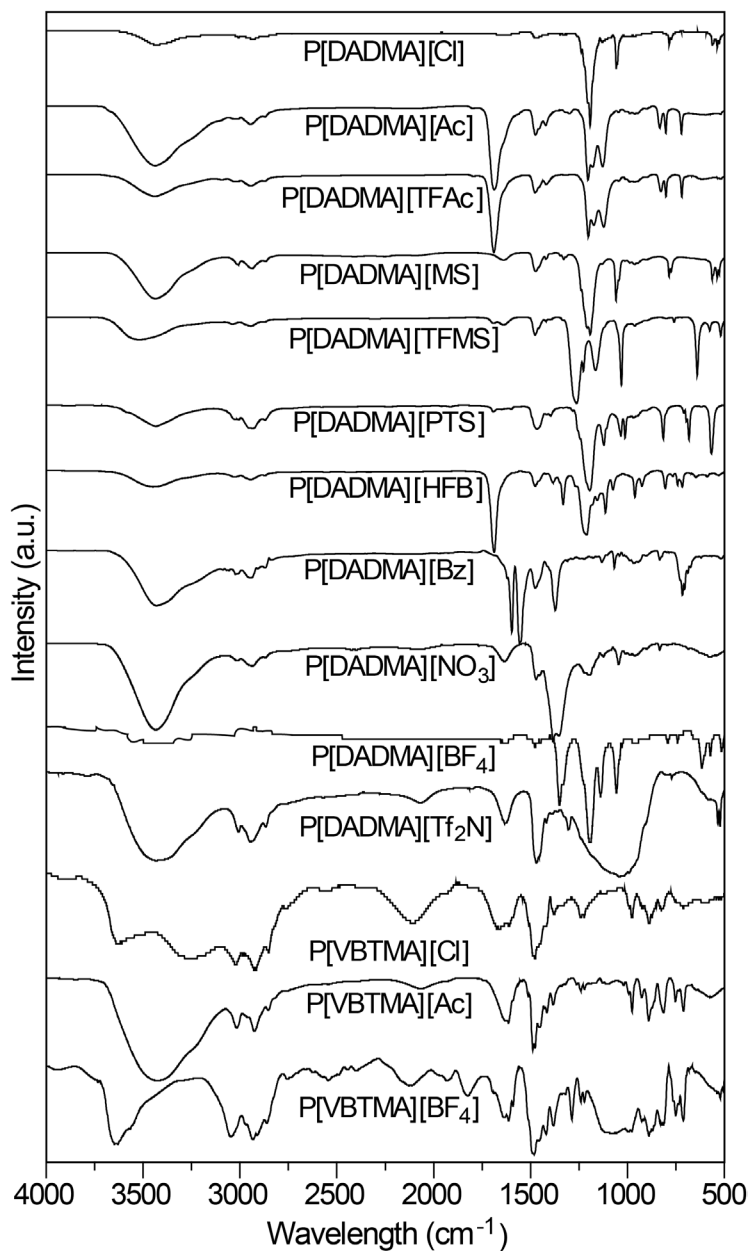
Figure 2.4 FT-IR spectra of PILs.

P[DADMA][Tf$_2$N] showed bands at 1353 cm^{-1}, 1171 cm^{-1} and 1060 cm^{-1} corresponding to the C-F, S=O and S-N stretching, respectively [Marcilla (2005), Rey (1998)]. P[DADMA][BF$_4$] exhibited a band at 1062 cm^{-1} corresponding to B-F stretching [Suarez

(1996)]. The spectra of P[VBTMA][Cl] showed bands at 1490 cm^{-1} (scissoring of methyl groups), 893 cm^{-1} (out of plane bending of the aromatic C–H) [Kumar (2006)] and at 1409 cm^{-1} (stretching vibration of the C–N of tertiary ammonium group). P[VBTMA][Ac] showed C=O stretching belonging to the ester group at 1577 cm^{-1}. P[VBTMA][BF$_4$] exhibited characteristic band due to B-F stretching at 1036 cm^{-1} [Suarez (1996)].
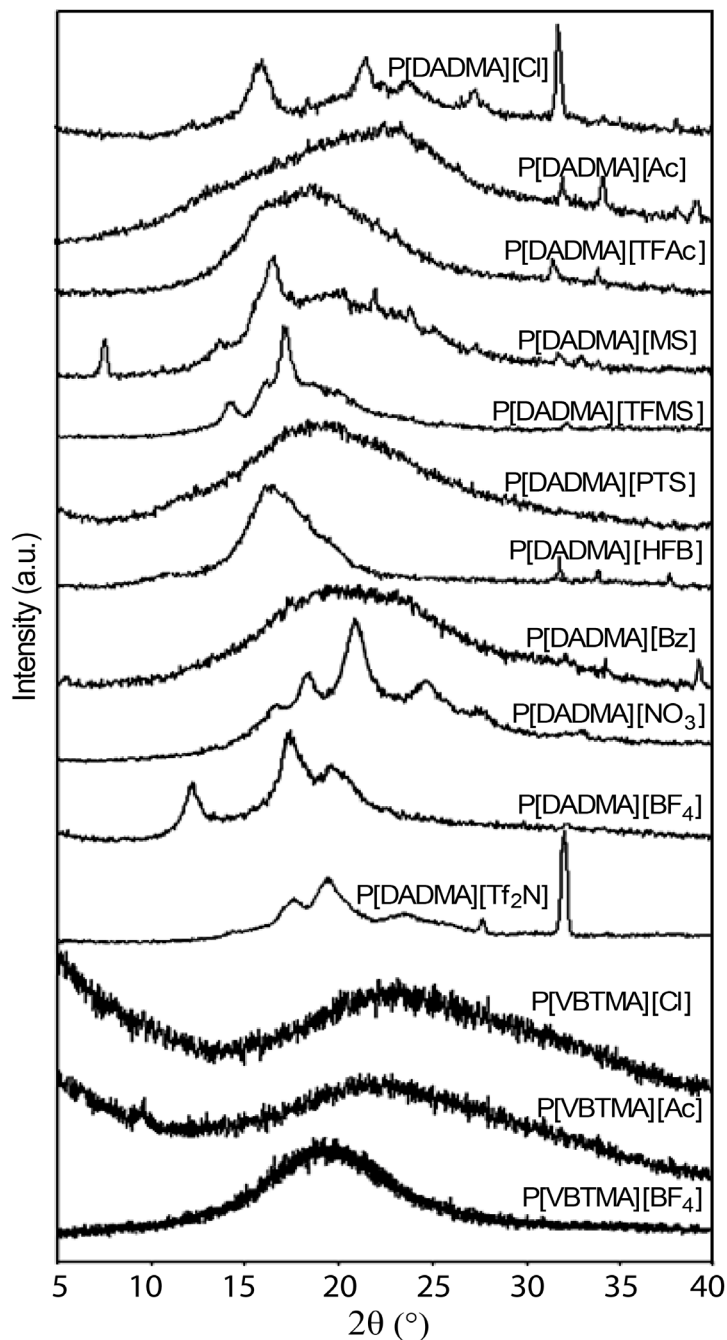
Figure 2.5 WAXD spectra of PILs.

Wide angle X-ay diffraction (WAXD) pattern of these PILs is shown in Figure 2.5. Those with [Ac], [TFAc], [PTS], [HFB] and [Bz] anion exhibited amorphous hollow. Fluorinated PILs (P[DADMA][TFAc] and P[DADMA][HFB]) showed higher d_{sp} in the series (Table 2.1). The d_{sp} of P[DADMA][TFAc] was higher than that of P[DADMA][Ac]. This conveyed that fluorinated PILs exhibit higher d_{sp} than their non-fluorinated analogue; as also observed in other common polymers like polycarbonate [Hellums (1989)].

In the case of PILs based on P[DADMA] as a cation and non-fluorinated anions, viz.; P[DADMA][Ac], P[DADMA][Bz] and P[DADMA][PTS]; it was found that d_{sp} increased in the order of increasing molar mass (thus size) of the anion (i.e. [Ac] < [Bz] < [PTS]). The d_{sp} of PILs with P[VBTMA] as a common cation also varied following the order of increasing molar mass of their anion as: [Cl] < [Ac] < [BF$_4$]. These observations suggest that in a series of PIL with a common cation, chain packing can be loosened by either fluorinated anion or by the one with higher molar mass. This could be useful in designing PILs for gas sorption / separation materials. For PILs based on P[DADMA] with [Cl], [MS], [TFMS], [NO$_3$], [Tf$_2$N] and [BF$_4$] as a anion; d_{sp} could not be calculated since well defined amorphous hollow was absent in their WAXD spectra.

PILs with fluorinated anion exhibited generally higher density in the series. This is in accordance with higher density of fluorinated polymers (polysulphone, polycarbonate, etc.), than their non–fluorinated analogue [Hellums (1989), McHattie (1992)]. The density of PILs varied with the change of anion as [Tf$_2$N] > [BF$_4$] > [TFMS] > [HFB] $\geq$ [MS] > [TFAc] > [NO$_3$] > [Cl] > [Bz] > [PTS] > [Ac]. The density of P[VBTMA] based PILs also varied with the variation of anion in an order, [BF$_4$] > [Cl] > [Ac]. The lowering in density with acetate as an anion in both PIL families is noteworthy.

2.3.3 *Thermal properties of PILs*

Initial decomposition temperature (IDT) of present PILs is given in Table 2.1. In a series with P[DADMA] as a common cation, the IDT varied from 160 - 372 °C. IDT of PILs based on [TFMS], [PTS], [BF$_4$] and [Tf$_2$N] as anions were higher than that of the precursor possessing chloride as an anion, indicating improved thermal stability. On the other hand, thermal stability of PILs with [Ac], [TFAc], [MS], [HFB], [Bz] and [NO$_3$] anions decreased. This indicated that the nature of anion plays a key role in governing thermal stability of a PIL. In case of PILs

derived from P[VBTMA][Cl], thermal stability increased with [BF$_4$] as an anion, while it decreased in case of [Ac] as an anion, than that of the precursor. Similar behavior is known for the room temperature ionic liquids, where thermal stability varied with the variation of their anion [Ngo (2000), Wang (2011)]. The glass transition temperature (T$_g$) of P[DADMA][Ac], P[DADMA][Tf$_2$N], P[DADMA][BF$_4$], P[VBTMA][Cl] and P[VBTMA][Ac] could not be detected even after repeated cooling and heating cycles during their DSC scan. The T$_g$ of remaining PILs as given in Table 2.1 conveyed that they are glassy in nature, but exhibit considerably lower T$_g$ than that of the precursor. The T$_g$ of precursor P[DADMA][Cl] was found to be 204 °C. The T$_g$ of P[DADMA][NO$_3$] containing inorganic anion reduced slightly to 197 °C. For other PILs with organic anion, the T$_g$ was considerably reduced to 90 − 117 °C. This lowering in T$_g$ after the exchange of Cl$^-$ by a particular anion could be attributed to the larger size of the anion in resulting PIL. The increased anion size may not render as efficient chain packing as in the precursor P[DADMA][Cl] having Cl$^-$ anion of smaller size. This would lead to lowering of interchain interactions in the formed PIL than those in the case of precursor polymer, P[DADMA][Cl]. This ultimately results in lowering of the glass transition temperature. Similar reduction in T$_g$ of PIL than that of precursor was also observed by Tang et al. [Tang (2005b)]. It was said that anions in poly(ionic liquid), such as tetrafluoroborate have a strong plasticizing effect and might improve flexibility of polymer chains, facilitate the segmental motion, and consequently reduce T$_g$ of the polymer.

2.3.4 Gas sorption properties

PILs were vacuum dried at 100 °C for 2 days prior to the sorption analysis. The sample after vacuum drying were immediately placed in a sorption cell and degassed further for 12 h prior to the gas charging. Equilibrium gas sorption isotherms (H$_2$, N$_2$, and CO$_2$) for these PILs obtained at 35 °C exhibited a typical dual-mode nature (Figure 2.6), as commonly observed for glassy polymers [McHattie (1992), Karadkar (2007), Li (2013)]. Similarly, extent of the sorption of different gases in most of the present PILs was found to be N$_2 \leq$ H$_2 \ll$ CO$_2$, as observed for most of the glassy polymers.

Dual-mode sorption parameters (k$_D$, C'$_H$ and b) for PILs are given in Table 2.3. The Henry's solubility constant, k$_D$ is known to be a function of both, gas–polymer and polymer–

polymer interactions and is more significant for rubbery polymers [Barbari (1988), Karadkar (2007)]. Owing to the glassy nature of present PILs, this coefficient was low for all gases.
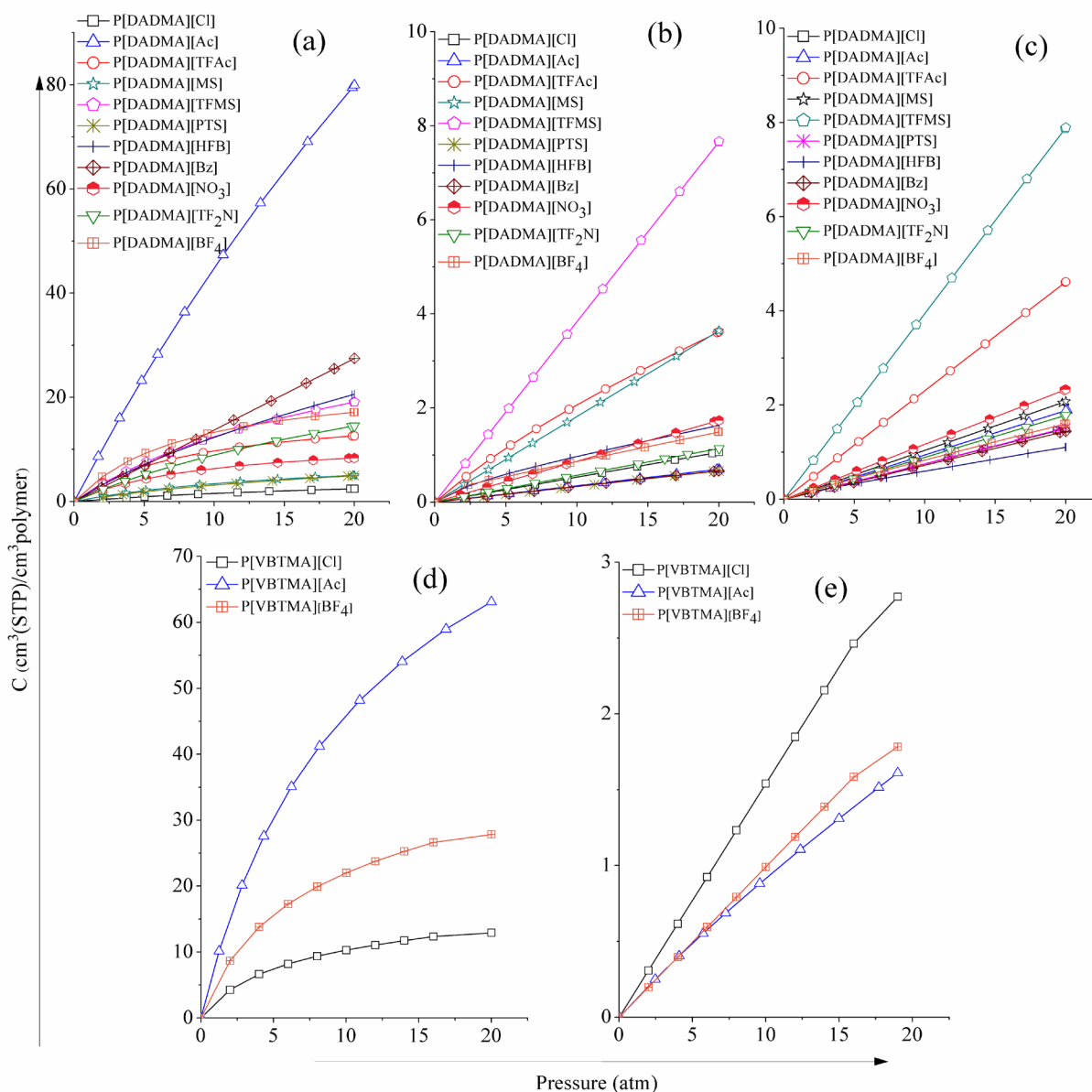
Figure 2.6 Sorption of (a) CO_2, (b) H_2 and (c) N_2 in PILs based on P[DADMA][Cl] and (d) CO_2, (e) N_2 in PILs based on P[VBTMA][Cl].

The Langmuir saturation constant C'_H was higher for CO_2 in every PIL than that for either H_2 or N_2, indicating favorable interactions of PIL with CO_2. This is also in accordance with the behavior of common glassy polymers [McHattie (1992), Karadkar (2007)]. A higher C'_H (for CO_2) in case of some of the PILs, e.g.; P[DADMA][Ac]: 197.75, P[DADMA][TFMS]:

29.90, P[DADMA][Bz]: 45.39 and P[VBTMA][Ac]: 80.00 is noteworthy. These values are significantly higher than those for several glassy polymers. For example, Barbari et al. (1989) have given C'_H values in bisphenol-A based polymers as; PSF (polysulphone): 16.63, PH (polyhydroxyether): 8.89, PEI (polyetherimide): 23.38 and PA (polyarylate): 20.54. Similarly lower values are reported for PC, PSF and PEI [Hu (2003)]. Even for polyimides based on 6FDA, these values are ~ 40 [Wang (2002)]. This behavior of PILs indicated that even in polymeric form, they retain basic property of ionic liquids of possessing high CO_2 sorption. Though d_{sp} for all the PILs could not be deduced from WAXD spectra, available data indicates that it is unlikely that PILs would possess high frozen free volume (higher than even 6FDA based polymers). Thus, observed high values of C'_H in present PILs needs further investigation.

Table 2.3 Dual-mode sorption parameters[a] for PILs.

PILs	k_D			C'_H			b		
	H_2	N_2	CO_2	H_2	N_2	CO_2	H_2	N_2	CO_2
P[DADMA][Cl]	0.075	0.053	0.023	1.21	1.44	3.9	5.3×10^{-6}	2.3×10^{-5}	0.05
P[DADMA][Ac]	0.094	0.035	1.111	3.09	1.00	197.7	1.9×10^{-5}	1.6×10^{-4}	0.02
P[DADMA][TFAc]	0.231	0.113	0.017	0.59	2.45	17.0	2.4×10^{-8}	3.4×10^{-6}	0.13
P[DADMA][MS]	0.104	0.182	0.012	1.39	1.02	8.7	5.8×10^{-6}	6.9×10^{-6}	0.06
P[DADMA][TFMS]	0.395	0.383	0.157	0.12	0.36	29.9	2.1×10^{-4}	1.9×10^{-4}	0.06
P[DADMA][PTS]	0.076	0.033	0.061	0.15	1.38	6.9	1.4×10^{-6}	9.7×10^{-6}	0.06
P[DADMA][HFB]	0.050	0.061	0.565	0.12	0.49	15.3	3.5×10^{-4}	6.5×10^{-5}	0.09
P[DADMA][Bz]	0.072	0.033	1.373	2.90	2.59	45.4	1.2×10^{-5}	2.6×10^{-5}	2.1×10^{-5}
P[DADMA][NO$_3$]	0.117	0.087	5.4×10^{-20}	1.03	0.64	12.2	1.5×10^{-5}	3.2×10^{-8}	0.11
P[DADMA][Tf$_2$N]	0.089	0.057	0.180	2.52	1.46	23.0	4.3×10^{-6}	8.6×10^{-6}	0.05
P[DADMA][BF$_4$]	0.076	0.063	1.6×10^{-4}	0.09	0.24	24.1	3.3×10^{-7}	4.6×10^{-5}	0.12
P[VBTMA][Cl]	–	0.150	0.160	–	0.41	12.4	–	8×10^{-4}	0.23
P[VBTMA][Ac]	–	0.060	0.414	–	0.88	80.0	–	0.05	0.11
P[VBTMA][BF$_4$]	–	0.010	0.310	–	0.95	28.5	–	0.001	0.19

[a]: k_D is expressed in cm^3 (STP)/cm^3 polymer.atm, C'_H is expressed in cm^3 (STP)/cm^3 polymer, while b is expressed in atm^{-1}.

2.3.4.1 Effect of variation in anion on CO$_2$ sorption

The CO$_2$ solubility coefficient (S_{CO_2}) and solubility selectivity for these PILs at 20 atm are tabulated in Table 2.4. Among all the PILs, P[DADMA][Ac] exhibited highest CO$_2$ solubility coefficient as well as solubility selectivity over H$_2$ and N$_2$. The S_{CO_2}/S_{H_2} of 42.6 and S_{CO_2}/S_{N_2} of 114.3 are highly attractive for P[DADMA][Ac]. These values are higher than that of common PILs as well as polymeric materials. This aspect is discussed in Section 3.4.3.

Table 2.4 Solubility coefficient (S)[a] and solubility selectivity (S$_A$/S$_B$) at 20 atm.

PILs	Solubility coefficient			Solubility selectivity		
	S_{H_2}	S_{N_2}	S_{CO_2}	S_{CO_2}/S_{H_2}	S_{CO_2}/S_{N_2}	S_{H_2}/S_{N_2}
P[DADMA][Cl]	0.075	0.053	0.12	1.6	2.3	1.4
P[DADMA][Ac]	0.094	0.035	4.00	42.6	114.3	2.7
P[DADMA][TFAc]	0.231	0.181	0.63	2.7	3.5	1.3
P[DADMA][MS]	0.104	0.182	0.25	2.4	1.4	0.6
P[DADMA][TFMS]	0.395	0.383	0.96	2.4	2.5	1.0
P[DADMA][PTS]	0.076	0.033	0.25	3.3	7.6	2.3
P[DADMA][HFB]	0.055	0.087	1.03	18.7	11.8	0.6
P[DADMA][Bz]	0.072	0.033	1.37	19.0	41.5	2.2
P[DADMA][NO$_3$]	0.117	0.087	0.42	3.6	4.8	1.3
P[DADMA][Tf$_2$N]	0.089	0.057	0.73	8.2	12.8	1.6
P[DADMA][BF$_4$]	0.080	0.075	0.86	10.8	11.5	1.1
P[VBTMA][Cl]	–	0.150	0.67	–	4.5	–
P[VBTMA][Ac]	–	0.084	3.16	–	37.6	–
P[VBTMA][BF$_4$]	–	0.099	1.45	–	14.6	–

[a]: Expressed in cm^3 (STP)/cm^3 polymer.atm

As could be seen from Table 2.1, this PIL is based on anion with highest basicity. This behavior of possessing high S_{CO_2}, S_{CO_2}/S_{H_2} and S_{CO_2}/S_{N_2} was followed by P[DADMA][Bz], which is based on anion with basicity next to [Ac]. In order to investigate the effect of anion, comparison of CO_2 sorption in a series of PILs based on P[DADMA] as the common cation is done below.

It could be anticipated that changing the basicity of an anion could affect its interaction with CO_2. This change in acid-base interaction would in turn influence the CO_2 sorption in PILs. Figure 2.7a shows that pKa of conjugate acid (a measure of basicity) of anion has a significant role in governing S_{CO_2}. The CO_2 sorption rapidly increased after pKa of ~ 0. For other two gases, sorption was much lower and no correlation was found with pKa. Similar behavior was seen in case of solubility selectivity. Figure 2.7b shows that S_{CO_2}/S_{H_2} and S_{CO_2}/S_{N_2} increased with increasing pKa of conjugate acid of anion. The selectivity of non-interacting gases (S_{H_2}/S_{N_2}) was significantly low (Table 2.4) and was not affected by the variation in pKa. Wang et al. (2011), showed that the CO_2 sorption in room temperature ionic liquids vary with pKa of conjugate acid of anion.
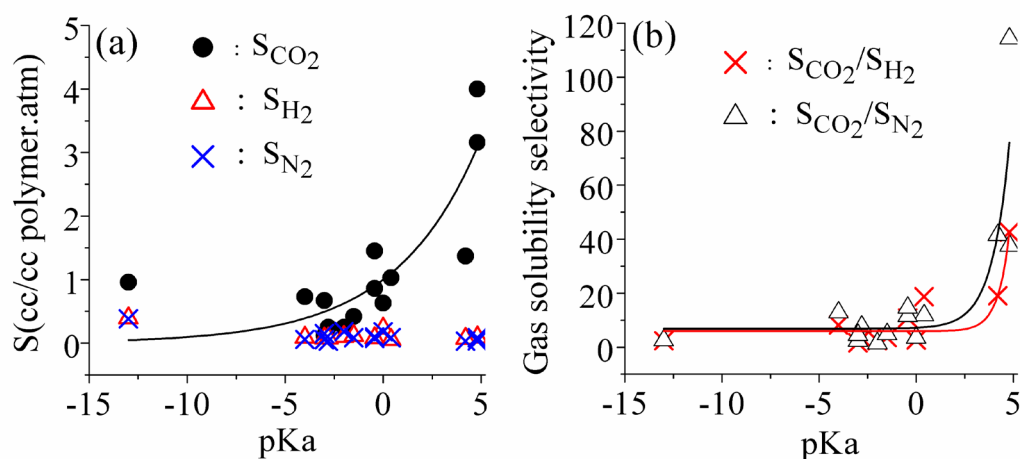
Figure 2.7 Variation of (a) gas solubility and (b) solubility selectivity with pKa.

Different types of counter ions such as organic anions, viz.; carboxylates (Ac, TFAc, HFB, Bz), sulfonates (MS, TFMS, PTS), sulfonamide (Tf_2N) and inorganic anions (BF_4, NO_3 and Cl) had a typical effect on governing CO_2 sorption properties of PILs. CO_2 sorption

coefficient (S_{CO_2}) in various carboxylate based PILs was increased in the order of variation of anion as: [TFAc] < [HFB] < [Bz] < [Ac], following the order of increasing their basicity (pKa of conjugate acids: [TFAc] = 0.0 < [HFB] = 0.4 < [Bz] = 4.2 < [Ac] = 4.8) [Cabusas (1998), Hollingsworth (2002), MacFarlene (2006)]. CO_2 based selectivities as given in Table 2.4 also varied in the same order. This behavior of PILs is similar to ionic liquids, where increasing basicity of anion is known to increase CO_2 sorption [Wang (2011)].

In case of PILs with sulfonated anions, S_{CO_2} followed the order of variation in anion as, [TFMS] > [PTS] ≈ [MS] (pKa of conjugate acids: [TFMS] = −13, [PTS] = −2.8, [MS] = −2.0) [MacFarlane (2006)]. In these cases, variation in CO_2 based solubility selectivity was only marginal (Table 2.4) in comparison to the variation observed in PILs based on carboxylate anions. Thus, basicity of anion may not be solely responsible for increasing the CO_2 sorption in PILs. Besides basicity, other polymer properties such as fractional free volume (FFV) in the polymer matrix may also compete for governing the CO_2 sorption. In various polymer families (polybenzimidazole [Kumbharkar (2013)], polycarbonate [Hellums (1992)], polyarylates [Karadkar (2007)] etc.); it is well known that the CO_2 solubility coefficient is also a function of fractional free volume. A variation of solubility coefficient with the density is shown in Figure 2.8a.
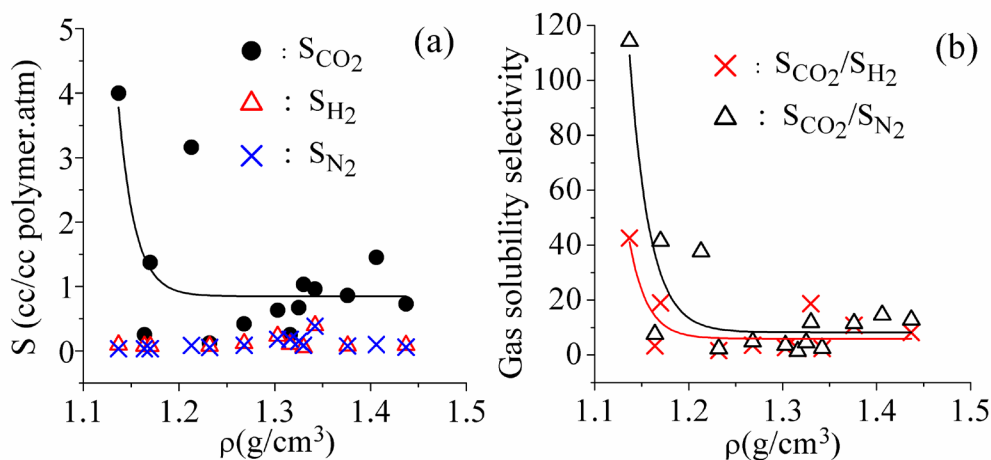
Figure 2.8 Variation of (a) gas solubility and (b) solubility selectivity with density.

The density can be taken as an indirect indication of available free volume in the polymer matrix. Though S_{H_2} and S_{N_2} were too low and no correlation with density could be observed,

S_{CO_2} was sharply reduced with the increase in density and then remained unaffected. Similar behavior was observed for S_{CO_2}/S_{H_2} and S_{CO_2}/S_{N_2} (Figure 2.8b), where both selectivities were initially high for lowest density PIL, P[DADMA][Ac], reduced sharply with increase in density and remain unaffected for PILs possessing higher density. Thus, unlike low molecular weight ILs, besides the CO_2 interaction, available free volume in the polymer matrix of PIL could also play a role in governing CO_2 sorption in them. This is justified in view of PILs' polymeric nature. In other words, not only properties related to ionic liquid nature, but also properties related to their polymeric nature are likely to govern CO_2 sorption in PILs. The influence of these properties may vary from case to case.

In case of PILs containing inorganic anion (Cl, NO_3 or BF_4), S_{CO_2} as well as S_{CO_2}/S_{H_2} and S_{CO_2}/S_{N_2} increased with increasing molar mass of the anion. This parameter of molar mass was not applicable in case of PILs possessing carboxylated or sulfonated anions.

2.3.4.2 *Effect of presence of fluorine in the anion*

Presence of fluorine group (especially in the form of hexafluoroisopropylidene linkage, i.e. $F_3C-C-CF_3$) in various polymer families as polysulfone [McHattie (1992)], polycarbonate [Hellums (1989)], polybenzimidazole [Kumbharkar (2006)], etc. is well known for improving their gas permeation properties. By incorporation of fluorine, gas diffusivity as well as solubility are known to be affected by virtue of increasing fractional free volume [Hellums (1989), McHattie (1992), Coleman (1994)]. Thus, it would be worth to investigate effect of fluorine in the anion of PILs on CO_2 sorption of resulting PILs. For this purpose, four cases of PILs possessing [MS], [TFMS], [Ac] and [TFAc] as anion were considered. As could be seen from Table 2.4, S_{CO_2} in case of P[DADMA][Ac] was highest among the series (4.0 cm^3(STP)/cm^3 polymer.atm). It was dramatically reduced to 0.63 cm^3 (STP)/cm^3 polymer.atm, by merely a small replacement of methyl (–CH_3) group by trifluoromethyl (–CF_3) in the anion of P[DADMA][TFAc]. Similar observation was reported in the case of ionic liquid, where high solubility of CO_2 in [emim][Ac] is dramatically reduced when the methyl group of acetate anion (CH_3COO^-) was replaced with a trifluomethyl group (CF_3COO^-) [Shiflet (2009)]. It is said that the CF_3 group withdraws electron density reducing the Lewis basicity of the anion and thus reducing the chemical complex formation and CO_2 solubility. An opposite effect is seen in case

of PILs based on sulfonated anions. S_{CO_2} in the case of P[DADMA][TFMS] containing fluorine in the anion is 3.8 times higher than that of its non-fluorinated counterpart, P[DADMA][MS]. Thus, in the former case of pairs with carboxylate anion, PIL with fluorinated anion exhibited lower CO_2 sorption capacity; while reverse is true in the later case of PIL pair with sulfonated anions. Though fluorine lowered pKa of carboxylate based anions and led to lowering in CO_2 sorption (which was initially high), improvement in initial lower sorption in sulfonated anion could be due to change in physical properties of polymer such as free volume (which is well known in common polymers like PBI [Kumbharkar (2006)], PSF [McHattie (1992)], PC [Hellums (1989)], etc.). These opposing effects of fluorine could be useful in further tuning of PIL properties.

2.3.4.3 Concurrent behavior of PILs as ionic liquid and polymer

Figure 2.9a shows that CO_2 solubility coefficient decreased with increasing pressure due to dual mode nature exhibited by gas sorption isotherms in these PILs.
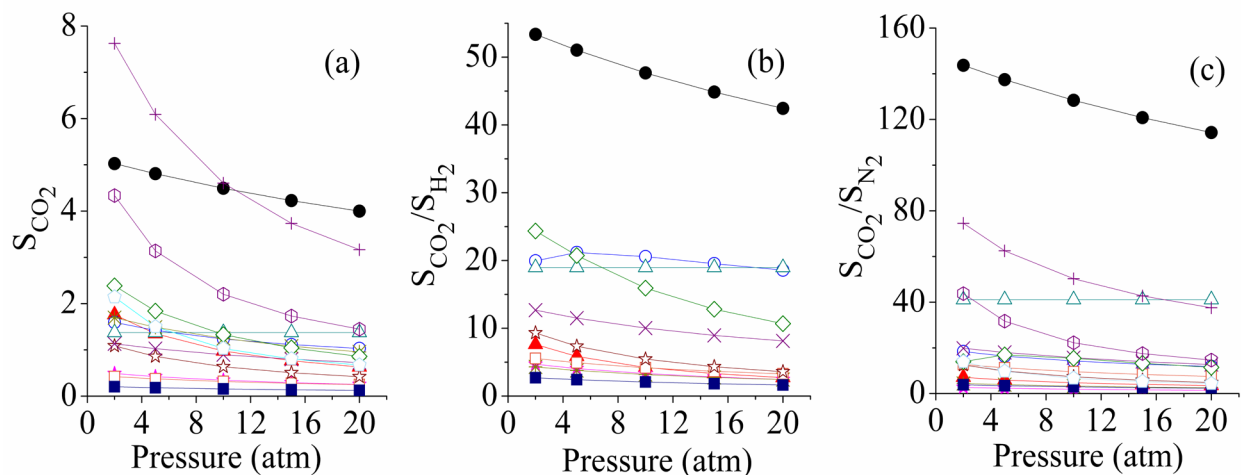
Figure 2.9 (a) CO_2 solubility coefficient, (b) CO_2/H_2 and (c) CO_2/N_2 selectivity with pressure in PILs (—■—: P[DADMA][Cl], —●—: P[DADMA][Ac], —▲—: P[DADMA][TFAc], —★—: P[DADMA][MS], —✳—: P[DADMA][TFMS], —□—: P[DADMA][PTS], —○—: P[DADMA][HFB], —△—: P[DADMA][Bz], —☆—: P[DADMA][NO$_3$], —×—: P[DADMA][Tf$_2$N], —◇—: P[DADMA][BF$_4$], —○—: P[VBTMA][Cl], —+—: P[VBTMA][Ac], —⊕—: P[VBTMA][BF$_4$]).

Figure 2.9b and 2.9c shows that S_{CO_2}/S_{H_2} and S_{CO_2}/S_{N_2} decreased with increasing pressure. Even at high pressure of ~ 20 atm, they remained high for P[DADMA][Ac] in comparison to common polymers as well as ionic liquids. As an example, S_{CO_2}/S_{N_2} for polyimides 6FDA-DAF and 6FDA-IPDA is 7.4 and 8.5, respectively [Kim (1989)]; while for PSF, it is 10.8 [Ghosal (1996)] at 10 atm. On the other hand, ionic liquids with [C_2mim] as a cation and [BF_4], [DCA] (dicyanamide), [OTf] (triflate) and [Tf_2N] as a anion showed S_{CO_2}/S_{N_2} as 38.0, 51.0, 37.0 and 24.0 at 40 °C, respectively [Bara (2009a)]. In the present series, S_{CO_2}/S_{N_2} of P[DADMA][Ac], P[DADMA][Bz] and P[VBTMA][Ac] is 114.3, 41.5 and 37.6, respectively at 20 atm. Other PILs based on [HFB], [Tf_2N] and [BF_4] also exhibited comparatively good S_{CO_2}/S_{N_2} selectivity (> 11) than that of above PI and PSF. Figure 2.7b showed variation of gas solubility selectivity with pKa, while Figure 2.8b showed variation of gas solubility selectivity with the density of PILs. It is found that, selectivities for both cases, i.e. S_{CO_2}/S_{H_2} and S_{CO_2}/S_{N_2} increased with increasing pKa and lowering the density. Both the selectivities were higher for PIL with [Ac] as an anion, indicating strong interaction of this PIL with CO_2. It means that in the case of PIL, both higher basicity of anion and lower density of PIL help to improve CO_2 solubility as well as its selectivity over H_2 and N_2. It may thus be possible that PILs possessing low density (and thus high free volume) and their anion possessing higher basicity may exhibit high CO_2 sorption. This indicates that in PILs, CO_2 solubility may not be solely controlled by any single parameter and the properties originating from IL nature as well as polymeric nature together govern the CO_2 sorption. More work is required to understand effects of physical properties of PILs on their sorption properties. Based on the results of PILs based on [Ac] and [Bz] as anion, it may be worth to investigate properties of PILs with wide structural variation in carboxylate anions.

2.3.4.4 *Effect of variation in cation on CO₂ sorption*

PILs based on P[VBTMA][Cl] as a precursor, viz., P[VBTMA][Ac] and P[VBTMA][BF_4] were investigated in order to examine the effect of [Ac] as an anion and effect of variation in cation. The CO_2 sorption in these PILs varied with the variation of anion as [Ac] > [BF_4] > [Cl]; similar to the behavior observed for P[DADMA][Cl] based PILs. Even though

the cation is changed from P[DADMA] to P[VBTMA], peculiarity of [Ac] anion in possessing high CO_2 sorption as well as high S_{CO_2}/S_{N_2} selectivity as that of PILs based on other anions in the series is still retained. In case of PILs with [Cl] and [BF_4] as an anion, S_{CO_2} and S_{CO_2}/S_{N_2} was higher when the cation was P[VBTMA] than it was with P[DADMA] as a cation. Effect of variation in cation is reported in the literature. Tang et.al. [Tang (2009)] reported hindered interaction between CO_2 and the cation due to steric effects caused by long alkyl groups on the cation. Plasticization of these polymers led to low microvoid volume fraction. Both of these effects reduced the CO_2 sorption in the PILs [Tang (2009)]. Cadena et. al. (2004), stated that it is the anion that governs the overall solubility of CO_2 in imidazolium-based ionic liquids, while the nature of the cation played a secondary role. In present cases also with [Ac] / [BF_4] as a anion and variation of cation (either P[DADMA] or P[VBTMA]) depicted that anions play a key role in determining CO_2 sorption.

All present PILs were brittle in nature and could not be transformed to good films that would withstand pressure in a permeation cell. To obtain a film (membrane), other methodologies such as blending, crosslinking or copolymerization [Hu (2006), Hudino (2011), Li (2011, 2012), Bara (2007b, 2008a), Chi (2013), Carlisle (2013)] could be practiced. Higher CO_2 sorption capacity as well as its higher solubility selectivity over H_2 and N_2 in some of the PILs can make them promising candidate for making blend membrane with another polymer or ionic liquids for CO_2 separation and need further investigations.

2.4   Conclusions

Polymeric ionic liquids (PILs) based on poly(diallyldimethylammonium chloride), P[DADMA][Cl] and poly(vinylbenzyltrimethylammonium chloride), P[VBTMA][Cl] as a precursor were prepared by a simple anion exchange method. Ag salt of required anion was used to prepare water soluble PILs with ≥ 96 % anion exchange in a single step, while Li or Na salts were used to obtain water insoluble PILs. PILs with fluorinated anion showed higher d_{sp} and density than that of non-fluorinated ones. Though thermal stability of PILs either increased or decreased as that of precursor P[DADMA][Cl] depending on the counter-anion present, T_g of PILs was decreased. This lowering was attributed to the decreased interchain interactions caused by increased size of the anion in comparison to [Cl].

PILs with carboxylate anions generally possessed a combination of high CO_2 sorption and high selectivity over H_2 and N_2. CO_2 sorption in PILs with inorganic anion increased with increasing order of their molar mass. P[DADMA][Ac] and P[DADMA][Bz] exhibited appreciable S_{CO_2}, coupled with excellent CO_2 based selectivities (S_{CO_2}/S_{N_2} of 114.3 and 41.5, respectively). This ability of PIL containing [Ac] as an anion was validated by observing similarly high CO_2 sorption properties based on another cation P[VBTMA]. CO_2 sorption in a series of PILs with varying anion was increased by increasing anion-basicity and decreasing PIL density. CO_2 based selectivities of some of the PILs were considerably higher than that of common polymers as well as ionic liquids. This indicated their promises as the next generation CO_2 sorbent materials.

Chapter 3

Effect on structural variations in carboxylates as anion on gas sorption properties of PILs

3.1   Introduction

During earlier investigations on PILs with same backbone and varying anions, it was observed that the physical and gas separation properties largely varied with the variation of anion [Chapter 2]. In all PILs, CO_2 sorption was majorly governed by the anion, while cation played a secondary role. PILs possessing carboxylate anion (esp. acetate and benzoate anion) exhibited higher CO_2 sorption as well as high CO_2/H_2 and CO_2/N_2 sorption selectivity than that of PILs with other anions. P[DADMA][Ac] exhibited highly attractive S_{CO_2} (4.0 $cm^3(STP)/cm^3polymer.atm$), S_{CO_2}/S_{H_2} (42.6) and S_{CO_2}/S_{N_2} (114.3) at elevated pressure of 20 atm. Privalova et al. (2013), also found the similar higher CO_2 sorption of acetate based PILs than PILs based on other anions. Not only PILs, but ILs possessing carboxylated anions also exhibited good CO_2 sorption [Privalova (2013), Tome (2013a), Blath (2012), Wang (2011)]. Blath et al. (2011), have said that ILs containing a carboxylic anion can be a promising alternative to common amine scrubbing processes. Commonly observed higher CO_2 sorption for carboxylate anion containing ILs and PILs became the motive to generate more understanding on physical and CO_2 sorption properties of PILs containing carboxylated anions.

It was thought to investigate effect of structural variations in carboxylate anion on physical and CO_2 sorption properties of resulting PILs. To investigate effect of various carboxylate anions, aliphatic carboxylates with increasing alkyl chain and aromatic substituted carboxyaltes were chosen for the anion exchange reaction. It was thought that the basic nature and the bulkier structure (due to increase aliphatic chain and substituted aromatic group) of these carboxylate anions would enhance CO_2 sorption of the formed PILs. For synthesis of PILs, P[DADMA][Cl] as a precursor was specifically chosen, based on higher CO_2 sorption observed in PILs possessing P[DADMA] backbone than that of PILs possessing P[VBTMA] backbone [Chapter 2]. The anion exchange of P[DADMA][Cl] was performed with sodium salt of carboxylates. Their requisite physical properties and pure gas sorption (CO_2, H_2 and N_2) were investigated and presented here.

3.2   Experimental

3.2.1   Materials

Aqueous solution of poly(diallyldimethylammonium chloride), P[DADMA][Cl] (20 wt. %, average mol. wt. 100,000 - 200,000), propionic acid (PrA, 99.5%), butyric acid (BuA, 99%), hexanoic acid (HeA, 99.5%), octanoic acid (OcA, 98%), decanoic acid (DeA, 98%), *3,5*-dimethoxy benzoic acid (DMBA, 97%), *2,4*-dihydroxy benzoic acid (DHBA, 97%), *4*-nitrobenzoic acid (NBA, 98%), *3,5*-dinitrobenzoic acid (DNBA, 99%), diphenyl acetic acid (DPA, 99%), benzilic acid (BLA, 99%), *2*-naphthoic acid (NAA, 98%) were procured from Aldrich Chemicals. Sodium hydroxide (97.5%) was procured from Thomas Baker. Solvents used in this investigation, methanol (99%), chloroform (99.4%), ethanol (99.9%), *n*-propanol (99%), *1*-methyl-*2*-pyrrolidone (99%), *N,N*-dimethylformamide (99.5%), dimethyl sulfoxide (99.5%) were procured from Merck. All these chemicals were used without further purification. Dialysis bag (M_w cut of 10,000) was procured from Aldrich Chemicals. Pure gases, viz., H_2, N_2 and CO_2 were procured as per details given in Chapter 2.

3.2.2   Synthesis

3.2.2.1 Synthesis of sodium carboxylates

A 10 g of carboxylic acid was taken in a 100 ml conical flask. Equimolar quantity of 2.5 N NaOH solution was added while stirring at ambient for 5 h. Water evaporated at 60 °C and obtained Na-salt of carboxylic acid was dried in a vacuum oven at 60 °C.

3.2.2.2 Synthesis of polymeric ionic liquids (PILs)

A 20% aqueous solution of P[DADMA][Cl] was diluted to 8 % in order to lower the solution viscosity and ease the anion replacement. To a 8 % solution of P[DADMA][Cl], 5 molar equivalents of Na salt of a carboxylic acid as prepared above was added while stirring for 24 h at ambient temperature. The formed PIL and byproduct salt (NaCl) remained soluble in water. The solution was poured in the dialysis bag and kept in a beaker containing deionised water. For efficient dialysis, water from the beaker was replaced 4-5 times in a day. The dialysis was continued till conductivity of the water reached to 1 µs/cm. The PIL solution from dialysis bag was concentrated using rotavapor at 60 °C. Such solution was poured on to a teflon plate and dried at 60 °C for 2 day, followed by vacuum drying at 60 °C for 3 days. Obtained PILs are

designated based on their cation and respective anion, as shown in Scheme 3.1. The PILs based on Pr¯, Bu¯, He¯, Oc¯ and De¯ anions offered brittle film, while those based on DMB¯, DHB¯, NB¯, DNB¯, DPA¯, BL¯ and NA¯ anions offered flakes. No self standing film could be obtained with any of the cases.
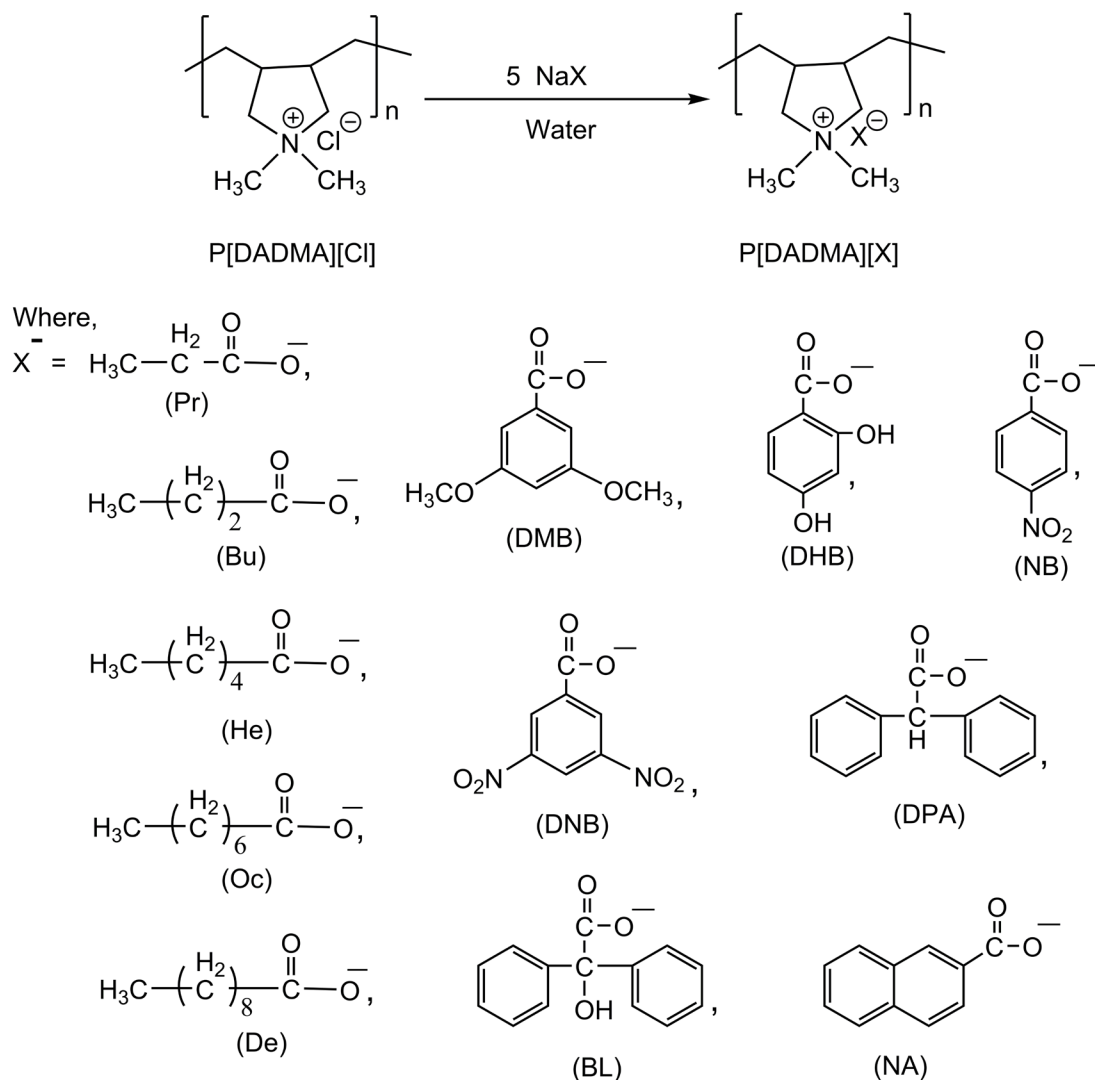
Scheme 3.1 Synthesis of PILs based on P[DADMA][Cl].

3.2.3 *Characterizations*

The quantitative analysis of chloride exchanged in a PIL was performed by conductometric titration with 0.01M AgNO$_3$. FT-IR spectra of PILs were recorded in diffusive reflectance mode using Spectrum-1 spectrophotometer. Thin slurry of PIL in dry methanol was

coated on KBr crystal, followed by evaporation under IR lamp. The solubility of PILs in common organic solvents was determined by stirring 0.1 g of PIL in 10 ml of a solvent at the ambient for 24 h. In case of insolubility, heating at 60 °C (or near boiling point, in case of the low boiling solvents) for 24 h was employed. The wide angle X-ray diffraction (WAXD) pattern of PILs was recorded using Rigaku X-ray diffractometer (D-max 2500) with Cu-K$_\alpha$ radiation. The average intersegmental *d*-spacing (d$_{sp}$) for the amorphous peak maxima was calculated using Bragg's equation (nλ = 2dsinθ). The density (ρ) of PILs was measured at 35 °C by using specific gravity bottle and decalin as the solvent that exhibited negligible sorption in PILs (< 1.5 %). This measurement was repeated with five samples and the deviation from the average value was $\leq$ 0.006 g/cm^3. The thermogravimetric analysis (TGA) was performed using Perkin Elmer TGA-7 in N$_2$ atmosphere with a heating rate of 10 °C/min. The glass transition temperature (T$_g$) was determined using DSC Q-10 (TA instruments, USA) under N$_2$ atmosphere with a heating rate of 10 °C/min.

3.2.4 *Gas sorption*

The pure gas sorption isotherms using H$_2$, N$_2$ and CO$_2$ were obtained at 35 °C using equipment that consisted of the dual-volume, single-transducer set up based on pressure decay method. The sorption parameters (k$_D$, C'$_H$ and b) were determined as given in Chapter 2 (Section 2.2.4).

3.3   Results and Discussion

3.3.1 *Synthesis of PILs*

PILs were synthesized by anion exchange method in an aqueous medium using commercially available polyelectrolyte precursors, P[DADMA][Cl]. It was observed that PILs based on P[DADMA] as a polycation and possessing Ac⁻ anion (P[DADMA][Ac]) exhibited higher CO$_2$ sorption and CO$_2$ based sorption selectivity (CO$_2$/H$_2$ and CO$_2$/N$_2$) than that of P[VBTMA] based PILs [Chapter 2]. The CO$_2$ sorption and selectivity of this PILs was higher than most of the reported PILs. Hence, it was worth to compare the gas sorption and physical properties of present PILs containing variety of carboxylate anions, but the same polycation, P[DADMA].

For chloride exchange of P[DADMA][Cl], Na salt of requisite anion was used, due to commercial unavailability of silver salt of carboxylic acids. Na salt of acids was prepared by using equimolar quantity of aqueous NaOH. For anion exchange reaction, 5 molar equivalents of Na salts of requisite anions were used in order to obtain maximum possible exchange of chloride anion. This higher quantity of Na salt was required since formed PIL and byproduct (NaCl) were in dissolved state. They would be form an equilibrium, which can restrict the maximum possible anion exchange. It was observed that in case of P[VBTMA][BF_4], the higher amount of $NaBF_4$ was needed in order to maximum possible anion exchange [Chapter 2].

Table 3.1 Physical properties of PILs

PILs	Chloride exchange[a] (mol %)	Yield (%)	ρ^b (g/cm³)	$d_{sp}{}^c$ (Å)	IDT[d] (°C)	pKa[e]
P[DADMA][Cl][f]	0	-	1.232	-	320	-0.8
P[DADMA][Pr]	87.2	79.3	1.144	4.76	177	4.87
P[DADMA][Bu]	90.2	75.7	1.158	4.79	166	4.82
P[DADMA][He]	93.9	66.9	1.147	4.50	156	4.88
P[DADMA][Oc]	95.6	69.9	1.086	4.83	160	4.89
P[DADMA][De]	94.7	83.4	0.971	4.61	210	4.9
P[DADMA][DMB]	97.7	84.7	1.166	4.05	202	3.96
P[DADMA][DHB]	97.9	78.1	1.164	3.70	223	-
P[DADMA][NB]	97.2	73.6	1.130	3.88	250	3.43
P[DADMA][DNB]	91.4	64.7	1.183	3.86	202	-
P[DADMA][DPA]	94.8	87.1	1.024	3.94	154	3.9
P[DADMA][BL]	94.2	64.9	1.126	3.85	160	
P[DADMA][NA]	91.6	68.5	0.994	3.73	245	4.17

[a]: Chloride exchange determined by conductometric titration; [b]: density measured at 35 °C; [c]: *d*-spacing obtained from wide angle X-ray diffraction spectrum; [d]: initial decomposition temperature by TGA; [e]: [Ref: MacFarlane (2006), Hollingsworth (2002), Wade (2003)], [f]: [Chapter 2].

Formed PILs and byproduct (NaCl) were separated by using dialysis bag. The dialysis bag is known to pass small molecules through the pores in the direction of decreasing concentration. Larger molecules that have dimensions significantly greater than the pore diameter are retained inside the dialysis bag. Complete separation of the byproduct (NaCl) from the formed PIL was thus possible and this was confirmed by conductivity analysis of water in which the dialysis bag was kept. When the conductivity of the water remained constant at ~ 1µs/cm for 24 h, it indicated almost complete separation of byproduct (NaCl) from the PIL. After drying, these PILs were used for further analysis.

Anion exchange of precursor PILs showed appreciable anion exchange, which was > 87 % as summarized in Table 3.1. The exchange was not precisely quantitative, which could be due to the formed PIL and byproduct (NaCl) were in dissolved state and could form equilibrium and hence the reversible reaction. Another possible reason could be the polymeric nature of cations, where some of the cationic sites remained shielded and thus unexchanged.

3.3.2   FT-IR analysis

FT-IR spectra of all these PILs showed in Figure 3.1. Characteristic bands due to C-H stretching at ~1470 cm^{-1}, bending at ~2960 cm^{-1} and C-N stretching at ~1180 cm^{-1} were seen in all the PILs, which corresponds to the polycation (P[DADMA]). All of them showed a wide band at ~ 3100-3600 cm^{-1}, attributable to the absorbed water. These bands were also observed during earlier investigation for P[DADMA] based PILs. These PILs showed characteristic C=O stretching (belonging to the ester group) in the range 1570-1610 cm^{-1} [Silverstein (1981)]. PILs with aliphatic carboxylate anions showed the band at 2800-3000 cm^{-1}, which could be ascribed to the C-H vibrations in methylene groups of the carboxylate anion. It was seen that intensity of this band was increased with increasing the chain length of alkyl group of the anion.

The spectra of P[DADMA][DMB] exhibited characteristic bands due to the ether group at ~1274 cm^{-1}. It is known that the asymmetric stretching band for C-O-C in alkyl aryl ether appear at 1275-1200 cm^{-1} [Silverstain (1981)]. The P[DADMA][DHB] exhibited bands due to O-H stretching at 3580 cm^{-1} and bending at 642 cm^{-1} [Coates (2006)]. The P[DADMA][NB] and P[DADMA][DNB] showed bands at 1522 cm^{-1} and 1538 cm^{-1} due to asymmetric stretching of NO$_2$ group and symmetric stretching at 1350 cm^{-1} and 1353 cm^{-1} for N-O linkage, respectively [Silverstein (1981)]. In the spectra of P[DADMA][DPA] and P[DADMA][BL], bending

vibrations between 600-900 cm^{-1} are usually associated to the presence of benzene rings. The similar bands were also seen in the spectra of benzilic acid [Vimala (2011)]. In the spectra of P[DADMA][NA], band appeared at ~ 780 cm^{-1} is due to the out of plane C-H blending [Silverstein (1981)]. Appearance of these bands in FT-IR spectra qualitatively confirmed the formation of PILs with requisite anion.
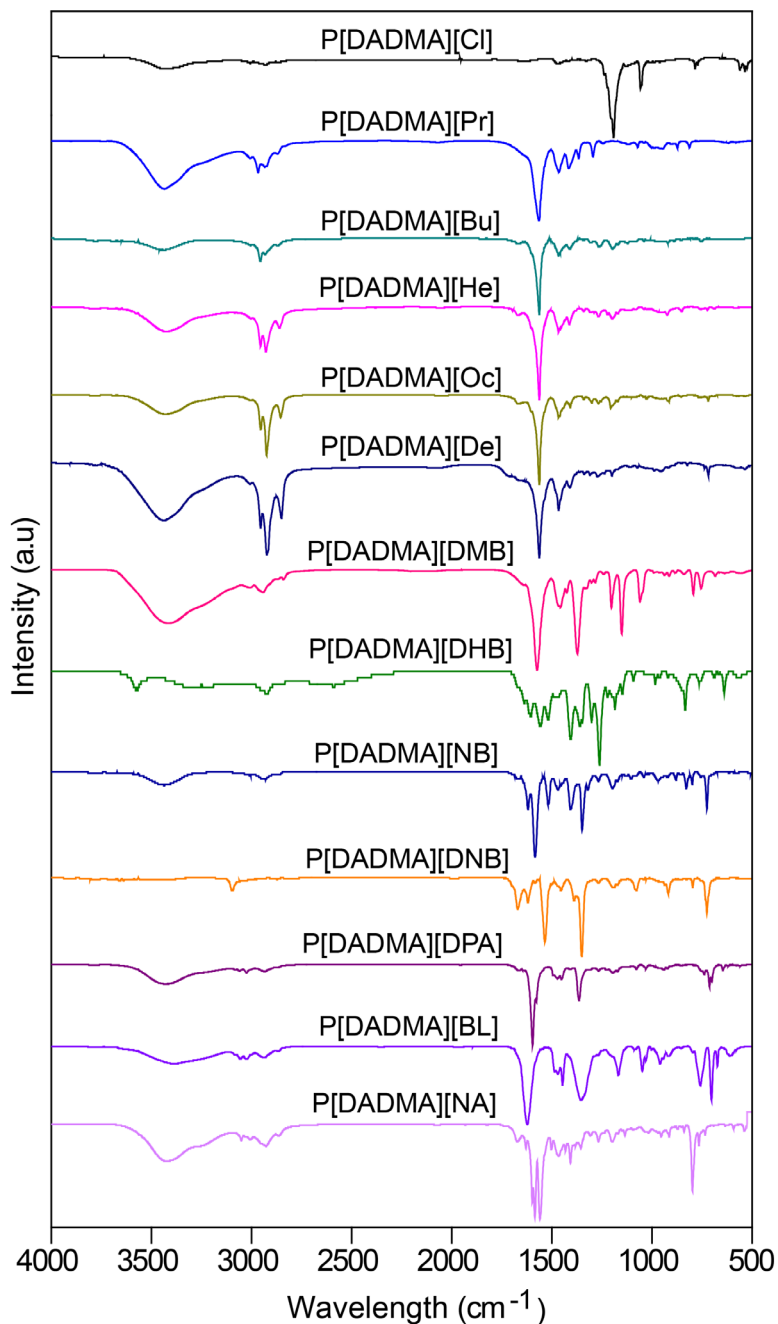
Figure 3.1 FTIR spectra of PILs.

3.3.3   **Physical properties**

3.3.3.1 Solvent solubility

All present PILs were soluble in water, while they were insoluble in NMP (Table 3.2). PILs with Pr¯, Bu¯, He¯, Oc¯, De¯, DMB¯, DHB¯ and DPA¯ as an anion were soluble in common alcohols, viz., methanol, ethanol and *n*-propanol. PILs with NB¯, DNB¯, BL¯ and NA¯ as anion were partially soluble in these alcohols. PILs based on DMB and DHB anions were soluble in DMF and were partially soluble in CHCl$_3$. These PILs also showed good solubility in DMSO, except those based on Cl¯ and Ac¯ anion. This study indicated, the solvent solubility of PILs can be tuned by the variation of anion, as also was observed earlier [Marcilla (2004)].

Table 3.2 Solvent solubility of PILs.

PILs	Water	Methanol	Ethanol	*1*-Propanol	Chloroform	DMF	DMSO	NMP
P[DADMA][Cl] [a]	+	+	+	−	−	±	±	±
P[DADMA][Pr]	+	+	+	+	−	−	+	−
P[DADMA][Bu]	+	+	+	+	−	−	+	−
P[DADMA][He]	+	+	+	+	−	−	+	−
P[DADMA][Oc]	+	+	+	+	−	−	+	−
P[DADMA][De]	+	+	+	+	−	−	+	−
P[DADMA][DMB]	+	+	+	+	±	+	+	−
P[DADMA][DHB]	+	+	+	+	±	+	+	−
P[DADMA][NB]	+	+	±	±	−	−	+	−
P[DADMA][DNB]	+	±	±	±	−	−	+	−
P[DADMA][DPA]	+	+	+	+	−	−	+	−
P[DADMA][BL]	+	±	±	±	−	−	+	−
P[DADMA][NA]	+	±	±	±	−	−	+	−

+: Soluble at ambient temperature, ± : partially soluble or swelling after heating at 60 °C for 8 h, − : insoluble after heating, [a]: [Chapter 2].

3.3.3.2 Packing density parameter: WAXD and density analysis

Wide angle X-ay diffraction (WAXD) spectra of PILs are shown in Figure 3.2. PILs possessing other than Cl⁻, Pr⁻ and Oc⁻ anion exhibited well defined amorphous hollow. The d-spacing (d_{sp}) of these PILs is given in Table 3.1.
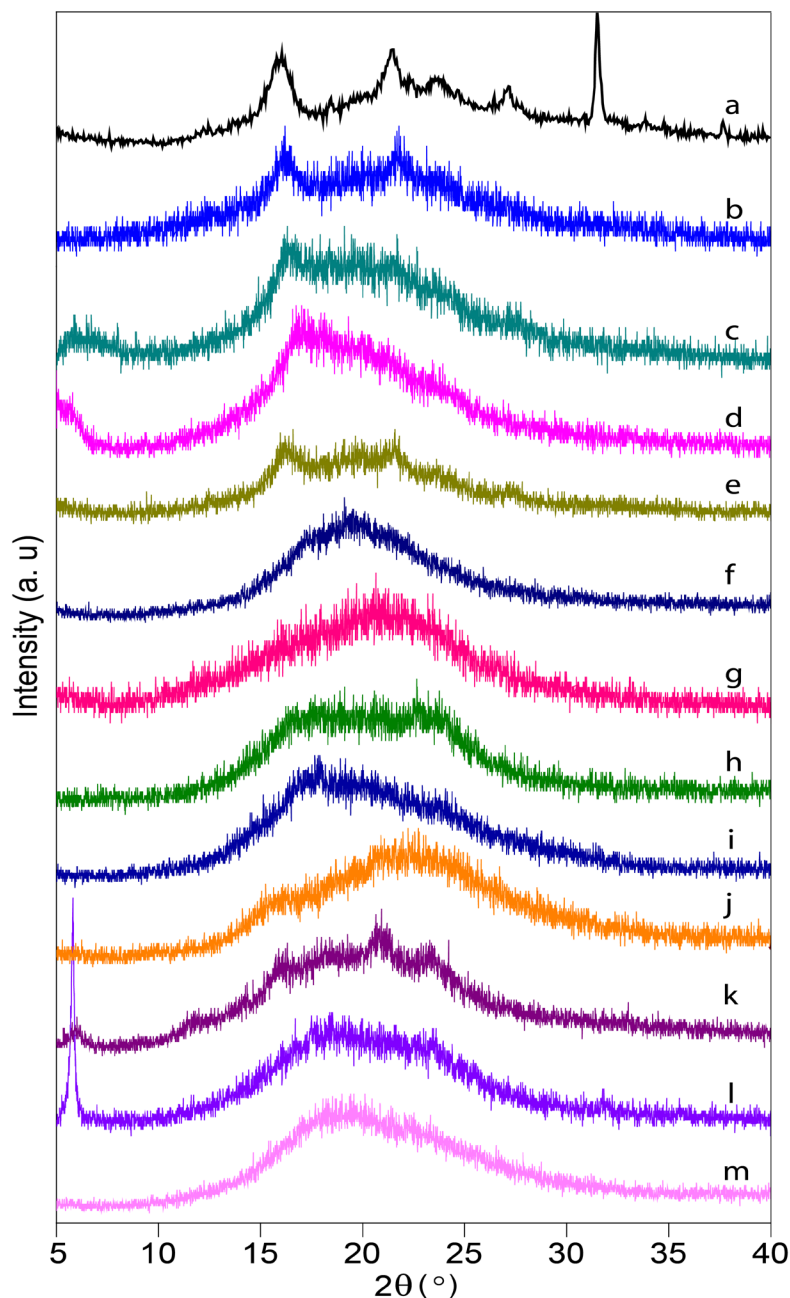
Figure 3.2 WAXD spectra of PILs. (a: P[DADMA][Cl], b: P[DADMA][Pr], c: [DADMA][Bu], d: P[DADMA][He], e: P[DADMA][Oc], f: P[DADMA][De], g: P[DADMA][DMB], h: P[DADMA][DHB], i: P[DADMA][NB], j: P[DADMA][DNB], k: P[DADMA][DPA], l: P[DADMA][BL], m: P[DADMA][NA]).

It was found that d_{sp} (Table 3.1) increased in the order of $De^- < DHB^- < NA^- < BL^- < DNB^- < NB^- < DPA^- < DMB^- < He^- < Pr^- < Bu^- < Oc^-$. PILs with aliphatic carboxylate anions showed higher d_{sp} than that of PILs with aromatic carboxylates as the anion. This could be informative while designing PILs for their applicability.

A large variation in the density of PILs was observed with the variation in their anion (Table 3.1). In these PILs, P[DADMA][Cl] showed highest density (1.232 g/cm^3), while P[DADMA][De] showed lowest density (0.971 g/cm^3). This could be due to, the smaller size of Cl^- anion could allow close chain packing, while the bulkier structure of De^- anion inhibits the efficient packing and form a less denser matrix and led to lowering in the density. The density of PILs varied with the variation of anion as $Cl^- > DNB^- > DMB^- > DHB^- > Bu^- > He^- > Pr^- > NB^- > BL^- > Oc^- > DPA^- > NA^- > De^-$. It was interesting to note that in cases of PILs containing aliphatic carboxylate anion, as the number of alkyl groups in the anion increased till butyl group, the density of formed PILs increased up to 1.158 g/cm^3. This indicated denser chain packing arrangement. As the alkyl chain length increased further, the density of PILs falls down upto 0.971 g/cm^3. This indicated looser chain packing arrangement. Bara et al. (2007b), also observed the similar trend for the variation in density of alkyl group substituted PILs. These results indicated that the anion could affect the chain packing arrangement.

3.3.3.3 Thermal properties of PILs

Initial decomposition temperature (IDT) of present PILs is given in Table 3.1. The IDT of PILs varied from 154 - 320 °C. It could be seen that PILs with carboxylate anions exhibited lower thermal stability than their parent PIL possessing chloride as an anion. This lowering in thermal stability, after the Cl^- exchange by a particular anion could be due to the thermal susceptibility of alkyl group containing anions. Another reason of the lower IDT of all these PILs could be the basic nature of anions. In case of ILs, it is reported that the thermal stability decreased with increasing pKa of the anion [Wang (2011)]. It was also observed that PILs possessing carboxylated anions generally exhibited lower thermal stability than that of sulfonated and inorganic anions [Chapter 2]. Variation in thermal stability of PILs with the variation of anions is well known [Mecerreyes (2011)]. The glass transition temperature (T_g) of PILs could not be detected even after repeated heating and cooling cycles during their DSC scan.

3.3.4 Gas sorption

The pure gas sorption isotherms (H_2, N_2 and CO_2) for these PILs obtained at 35 °C exhibited a typical dual-mode nature (Figure 3.3), as commonly observed for glassy polymers [Kumbharkar (2006), Karadkar (2007), McHattie (1992)]. The sorption of different gases in present PILs is increased in the order: $H_2 \approx N_2 << CO_2$, as observed for most of the glassy polymers. Figure 3.3 shows the large variation on gas sorption with the variation of anion of PILs. It would be worth to discuss their dual mode sorption parameters, as elaborated in the following section.
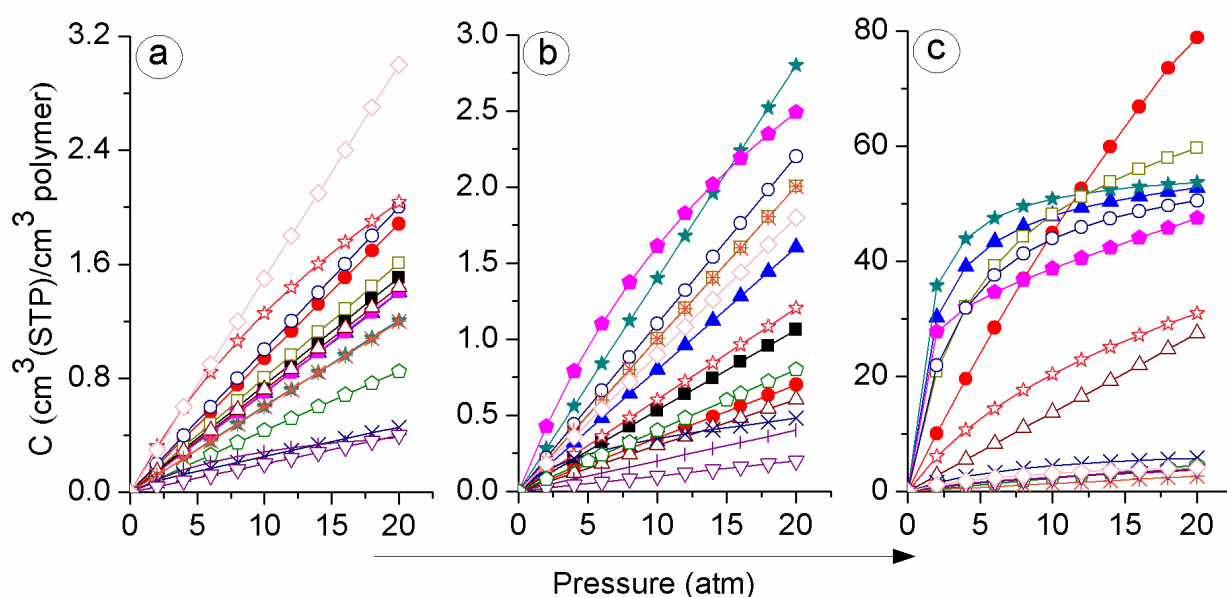
Figure 3.3 Sorption of (a) H_2, (b) N_2 and (c) CO_2 in PILs (■: P[DADMA][Cl], ●: P[DADMA][Ac], ▲: P[DADMA][Pr], ★: P[DADMA][Bu], ⬠: P[DADMA][He], □: P[DADMA][Oc], ○: P[DADMA][De], △: P[DADMA][Bz], ☆: P[DADMA][DMB], ○: P[DADMA][DHB], ✳: P[DADMA][NB], ✳: P[DADMA][DNB], +: P[DADMA][DPA], ▽: P[DADMA][BL], ◇: P[DADMA][NA]).

3.3.4.1 Gas sorption parameters

The dual-mode sorption parameters (k_D, C'_H and b) were estimated by the non-linear regression analysis [Karadkar (2007)] of experimentally determined gas sorption data at varying pressures up to 20 atm. These parameters are given in Table 3.3. The Henry's solubility coefficient k_D, related to the gas dissolution in rubbery state was low for all gases in these PILs.

This could be because of glassy nature of these PILs. The Langmuir affinity constant 'b' is the ratio of rate constants of sorption and desorption processes and characterizes the sorption affinity for particular gas-polymer system [Pixton (1995b)]. This parameter is negligible for H_2 and N_2 than that for CO_2. Due to close packed and dense structure of PILs, the dual-mode sorption parameters, especially K_D and b were too small to show any trend with respect to the nature of gas.

Table 3.3 Dual-mode sorption parameters[a].

PILs	k_D			C'_H			b		
	H_2	N_2	CO_2	H_2	N_2	CO_2	H_2	N_2	CO_2
P[DADMA][Cl][b]	0.08	0.05	0.02	1.21	1.44	4.0	5.3×10^{-6}	2.3×10^{-5}	0.05
P[DADMA][Ac][b]	0.09	0.04	1.11	3.09	1.00	197.8	1.9×10^{-5}	1.6×10^{-4}	0.02
P[DADMA][Pr]	0.07	0.08	0.15	1.19	2.16	53.7	3.5×10^{-5}	4.7×10^{-5}	0.63
P[DADMA][Bu]	0.06	0.14	1×10^{-4}	0.86	2.19	56.8	3.7×10^{-4}	1.2×10^{-5}	0.85
P[DADMA][He]	0.07	0.01	0.81	1.28	4.73	31.9	1.4×10^{-4}	4.7×10^{-2}	2.21
P[DADMA][Oc]	0.08	0.10	0.36	1.11	3.51	63.8	2.5×10^{-4}	5.5×10^{-5}	0.23
P[DADMA][De]	0.10	0.11	0.04	2.18	2.27	58.0	1.8×10^{-5}	4.6×10^{-5}	0.3
P[DADMA][Bz][b]	0.07	0.03	1.37	2.90	2.59	45.4	1.2×10^{-5}	2.6×10^{-5}	2.1×10^{-5}
P[DADMA][DMB]	0.03	0.06	0.57	2.87	3.34	29.3	0.05	6.4×10^{-5}	0.10
P[DADMA][DHB]	0.03	0.04	0.23	1.48	1.07	2.5	0.01	4.3×10^{-5}	2.4×10^{-7}
P[DADMA][NB]	0.02	0.01	4.9×10^{-17}	0.06	0.33	8.4	0.99	0.29	0.11
P[DADMA][DNB]	0.06	0.10	0.12	1.24	0.70	1.8	2.8×10^{-6}	1.1×10^{-4}	8×10^{-3}
P[DADMA][DPA]	1.8×10^{-11}	0.02	0.10	0.60	0.63	2.1	0.09	1.7×10^{-4}	0.21
P[DADMA][BL]	0.02	0.01	0.06	0.24	0.26	4.9	1.1×10^{-4}	6.7×10^{-9}	0.06
P[DADMA][NA]	0.15	0.09	0.02	0.39	0.16	5.3	4.2×10^{-5}	3.5×10^{-5}	0.12

[a]: k_D is expressed in cm^3 (STP)/cm^3 polymer.atm, C'_H is expressed in cm^3 (STP)/cm^3 polymer, while b is expressed in atm^{-1}, [b]: [Chapter 2].

The Langmuir saturation constant (C'_H) is much larger than k_D and b owing to glassy nature of all these PILs. This is also in accordance with the behavior of common glassy polymers

[McHattie (1992), Hu (2003), Kumbharkar (2006), Karadkar (2007)]. Sorption in glassy polymer is majorly dominated by C'_H. It is considered as the hole-filling constant, which represents maximum amount of the penetrant sorbed into 'microvoids' or the unrelaxed volume of the polymer matrix [Barbari (1988), Kanehashi (2005)]. It was interesting to note that PILs possessing aliphatic carboxylate anion exhibited a higher C'_H for CO_2 (e.g. P[DADMA][Pr]: 53.7, P[DADMA][Bu]: 56.8, P[DADMA][He]: 31.9 and P[DADMA][Oc]: 63.8, P[DADMA][De]: 58.0) than that of aromatic caroboxylate anions (Table 3.3). This behavior could be attributed to the higher d_{sp} of PILs based on aliphatic carboxylates than those based on aromatic ones (Table 3.1). The d_{sp} can be used as indices of the degree of openness of the polymer matrix [Hellums (1989)]. The high d_{sp} of PILs possessing aliphatic carboxylate anions could be responsible for their higher C'_H. These values are also considerably higher than other common glassy polymers such as polysulfone, polyetherimide and polyarylate [Barbari (1989), Hu (2003)]. This suggested that the type and structures of anion is also responsible for governing the CO_2 sorption, which is elaborated below.

3.3.4.2 Effect of aliphatic carboxylate anion on gas sorption

Gas solubility coefficient and solubility selectivity for various gas pairs at 2 and 20 atm is given in Table 3.4 and 3.5, respectively. It was observed that S_{CO_2} of all these PILs was higher than P[DADMA[Cl]. It could be seen from Table 3.4 that at 2 atm, P[DADMA][Bu] exhibited highest CO_2 solubility coefficient (S_{CO_2}: 17.88) coupled with higher CO_2 selectivity over H_2 and N_2 (S_{CO_2}/S_{H_2} = 296.5 and S_{CO_2}/S_{N_2} = 127.7). This behavior of significant enhancement in CO_2 solubility coefficient and CO_2 based selectivity than those for the precursor P[DADMA][Cl] was also seen in other aliphatic craboxylate anion based PILs. These PILs showed 51-88 folds increase in CO_2 solubility with 39-110 folds increase in CO_2/H_2 selectivity and 17-37 folds increase in CO_2/N_2 selectivity than compared to the precursor PILs. It is known that gas sorption in polymer is a function of gas-polymer interaction as well as available free volume in the polymer matrix [Li (2011)]. In the case of present PILs, the basic nature (pKa of aliphatic carboxylate anion = 4.76 to 4.9, Table 3.1) of all these anion could be responsible for higher observed CO_2 solubility coefficient as well as CO_2 sorption selectivity over H_2 and N_2. It is

known that in cases of ILs [Wang (2011)], CO_2 sorption was increased with an increase in pka of the anion.

Table 3.4 Solubility coefficient (S)[a] and solubility selectivity (S_A/S_B) at 2 atm.

PILs	Solubility coefficient			Solubility selectivity		
	S_{H_2}	S_{N_2}	S_{CO_2}	S_{CO_2}/S_{H_2}	S_{CO_2}/S_{N_2}	S_{H_2}/S_{N_2}
P[DADMA][Cl][b]	0.075	0.053	0.20	2.7	3.8	1.4
P[DADMA][Ac][b]	0.094	0.035	5.03	53.4	143.7	2.7
P[DADMA][Pr]	0.070	0.080	15.12	215.9	188.8	0.9
P[DADMA][Bu]	0.060	0.140	17.88	296.5	127.7	0.4
P[DADMA][He]	0.070	0.213	13.85	196.5	65.0	0.3
P[DADMA][Oc]	0.080	0.100	10.41	129.7	103.9	0.8
P[DADMA][De]	0.100	0.110	10.92	109.1	99.1	0.9
P[DADMA][Bz][b]	0.072	0.033	1.37	19.1	41.6	2.2
P[DADMA][DMB]	0.160	0.060	3.01	18.8	50.0	2.7
P[DADMA][DHB]	0.045	0.040	0.23	5.2	5.7	1.1
P[DADMA][NB]	0.040	0.071	0.76	19.0	10.7	0.6
P[DADMA][DNB]	0.060	0.100	0.13	2.2	1.3	0.6
P[DADMA][DPA]	0.046	0.020	0.41	9.0	20.4	2.3
P[DADMA][BL]	0.020	0.010	0.32	16.1	32.2	2.0
P[DADMA][NA]	0.150	0.090	0.53	3.6	5.9	1.7

[a]: Expressed in cm^3 (STP)/cm^3 polymer.atm, [b]: [Chapter 2].

It could be seen from Table 3.5 that CO_2 solubility coefficient of PILs at 20 atm increase in the order of anion as $Cl^- < DNB^- < DPA^- < BL^- < NA^- < DHB^- < NB^- < Bz^- < DMB^- < He^- < De^- < Pr^- < Bu^- < Oc^- < Ac^-$. Figure 3.4a shows that CO_2 solubility coefficient decreased with increasing pressure, which is due to dual mode nature exhibited by gas sorption isotherms in these PILs. This is an obvious behavior of glassy polymer. Figure 3.4b and 3.4c shows that S_{CO_2}/S_{H_2} and S_{CO_2}/S_{N_2} decreased with increasing pressure. At 20 atm pressure,

P[DADMA][Ac] showed higher S_{CO_2} than compared to other aliphatic carboxylate anion. This could be because of the effect of higher alkyl chain length of anion, where effect of chain packing could be nullifying at higher pressure and CO_2 sorption is governed by the PIL-CO_2 interaction. It is known that at higher pressure, the polymer get plasticize. Tang et al., (2009) noted that in PIL, plasticization led to low microvoid volume fraction, which reduced the CO_2 sorption. The increased anion size (due to increased alkyl chain length), reduced the IL density in the polymer matrix than compared to P[DADMA][Ac]. Hence higher CO_2 sorption in P[DADMA][Ac] could be because of higher interaction of PIL with CO_2 due to high IL density, than in case of other aliphatic carboxylate based PILs.

Table 3.5 Solubility coefficient (S)[a] and solubility selectivity (S_A/S_B) at 20 atm.

PILs	Solubility coefficient			Solubility selectivity		
	S_{H_2}	S_{N_2}	S_{CO_2}	S_{CO_2}/S_{H_2}	S_{CO_2}/S_{N_2}	S_{H_2}/S_{N_2}
P[DADMA][Cl][b]	0.075	0.053	0.12	1.6	2.3	1.4
P[DADMA][Ac][b]	0.094	0.035	4.00	42.4	114.3	2.7
P[DADMA][Pr]	0.070	0.080	2.64	37.7	32.9	0.9
P[DADMA][Bu]	0.060	0.140	2.68	44.5	19.2	0.4
P[DADMA][He]	0.070	0.125	2.37	33.7	19.1	0.6
P[DADMA][Oc]	0.080	0.100	2.98	37.1	29.7	0.8
P[DADMA][De]	0.100	0.110	2.53	25.2	22.9	0.9
P[DADMA][Bz][b]	0.072	0.033	1.37	19.1	41.6	2.2
P[DADMA][DMB]	0.102	0.060	1.55	15.2	25.7	1.7
P[DADMA][DHB]	0.042	0.040	0.23	5.4	5.7	1.1
P[DADMA][NB]	0.023	0.024	0.29	12.6	12.0	0.9
P[DADMA][DNB]	0.060	0.100	0.13	2.2	1.3	0.6
P[DADMA][DPA]	0.019	0.020	0.18	9.6	9.2	1.0
P[DADMA][BL]	0.020	0.010	0.19	9.7	19.4	2.0
P[DADMA][NA]	0.150	0.090	0.21	1.4	2.3	1.7

[a]: Expressed in cm^3 (STP)/cm^3 polymer.atm, [b]: [Chapter 2].
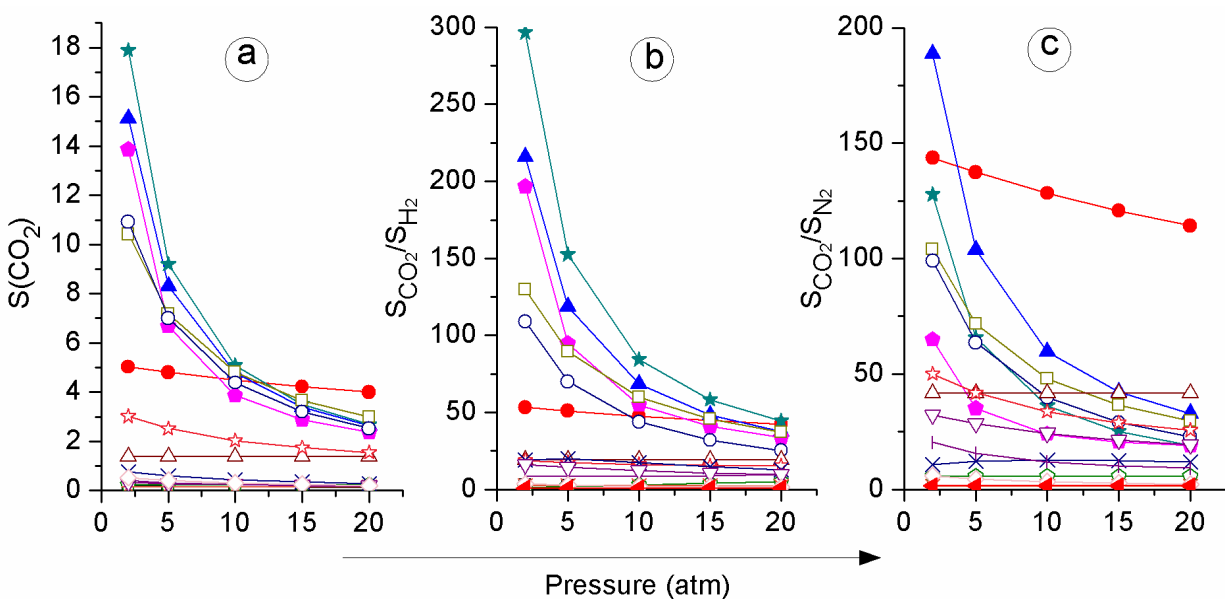
Figure 3.4 (a) S_{CO_2}, (b) S_{CO_2}/S_{H_2} and (c) S_{CO_2}/S_{N_2} in PILs (——■——: P[DADMA][Cl], ——●——: P[DADMA][Ac], ——▲——: P[DADMA][Pr], ——★——: P[DADMA][Bu], ——◆——: P[DADMA][He], ——□——: P[DADMA][Oc], ——○——: P[DADMA][De], ——△——: P[DADMA][Bz], ——✩——: P[DADMA][DMB], ——○——: P[DADMA][DHB], ——✳——: P[DADMA][NB], ——✳——: P[DADMA][DNB], ——+——: P[DADMA][DPA], ——▽——: P[DADMA][BL], ——◇——: P[DADMA][NA]).

3.3.4.3 Effect of alkyl group in aliphatic carboxylate anion

The effect of alkyl group in aliphatic carboxylate anion on CO_2 sorption could be more clearly seen by Figure 3.5. It can be seen that at 2 and 5 atm, initially the S_{CO_2} increased upto P[DADMA][Bu], which again starts falling down as the number of alkyl groups increased further up to the P[DADMA][De] case. This higher S_{CO_2} for P[DADMA][Bu] at 2 and 5 atm could be because of proper balance between IL density and the increased free volume. It was observed that in case of ILs, the solubility of CO_2 into [N2224][mono-carboxylate]-nH_2O samples grows with the increasing length of the alkyl chain in the anion [Wang (2012)]. Authors have noted that the volume between ions increase if the alkyl chain in the anion is enlarged [Wang (2012)]. At higher pressure the S_{CO_2} in PILs possessing aliphatic carboxylate anions varied in a narrower range. Even at 20 atm, the increase in S_{CO_2} was upto 25 folds than compared to the precursor P[DADMA][Cl] with high selectivity over H_2 and N_2. This indicated the benefits of aliphatic carboxylate anions for obtaining high CO_2 sorption in PILs.
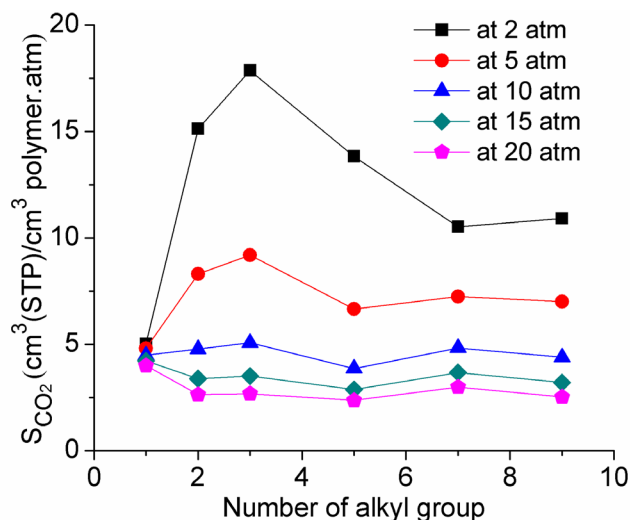
Figure 3.5 CO_2 solubility coefficient (S_{CO_2}) of PILs with increasing alkyl group in aliphatic carboxylate anion at different pressure.

3.3.4.4 Effect of aromatic carboxylate anion on gas sorption

It could be seen from Table 3.4 and 3.5 that PILs possessing aromatic carboxylate anion (viz., Bz^-, DMB^-, DHB^-, NB^-, DNB^-, DPA^-, BL^- and NA^-) showed lower CO_2 sorption than PILs possessing aliphatic carboxylate anions. The gas solubility in a polymer is affected by gas condensability, polymer free volume and polymer-gas interactions [Li (2011)]. Thus, lowering CO_2 sorption in these PILs, could be because of lower pKa of aromatic craboxylate anions than that of aliphatic carboxylate anions. Another reason for lowering CO_2 sorption in aromatic carboxylates could be the steric hindrance due to aromatic ring. Blath et al. (2012), have observed that in case of ILs, [EMIM][Benzoate] have four to five times higher Henry's law constants than acetate containing ILs. The pKb difference between benzoate and acetate of 0.56 can explain the absorption difference between [EMIM][Benzoate] and [EMIM][acetate] [Blath (2012)]. Simultaneously, steric hindrance due to the benzol ring was also responsible for lower CO_2 sorption [Blath (2012)]. Another possible reason for such low CO_2 sorption could be lower d_{sp} (one of the major of free volume) in PILs possessing aromatic carboxylates anions than that of PILs possessing aliphatic carboxylate anions.

It could be seen from Table 3.4 and 3.5 that even though P[DADMA][Bz] exhibited appreciable CO_2 sorption and selectivity over H_2 and N_2, other aromatic carboxylates containing PILs possess very low CO_2 sorption coefficient. It should be noted that the aromatic carboxylate anion possess rigid structure. Thus, it can be said that anion flexibility could also play a role for

governing CO_2 sorption in PILs. Among the PILs containing aromatic craboxylate anions, P[DADMA][DMB] exhibited appreciable CO_2 sorption, but still lower than the PILs containing aliphatic carboxylate anions.

3.3.4.5 Comparison of CO_2 sorption of these PILs with reported ILs and PILs

The remarkably high CO_2 sorption and selectivity over H_2 and N_2 of these PILs possessing aliphatic carboxylate anions shows promises for their applicability as a CO_2 separation media and thus worth to compare with reported ILs and PILs. CO_2 sorption of various PILs reported at 1-2 atm, which are < 10.5 cm^3(STP)/cm^3 polymer.atm (Appendix Table 1). Bara et al. (2009), have reviewed CO_2 sorption of some ionic liquids. They have noted that S_{CO_2} remains in the range of 1.44-2.40 cm^3(STP)/cm^3 polymer.atm, with S_{CO_2}/S_{N_2} in the range of 20-89 at 25 and 40 °C. In comparison to reported PILs and ILs, present PILs (possessing aliphatic carboxylate anions, viz., Pr^-, Bu^-, He^-, Oc^- and De^-) exhibited higher S_{CO_2} (10.4-17.9 cm^3 (STP)/cm^3 polymer.atm), with extraordinary high S_{CO_2}/S_{N_2} and S_{CO_2}/S_{H_2} of 109-296.5 and 65-128.8, respectively, at 2 atm and 35 °C (Table 3.4). This indicated the significance of carboxylate anion for possessing high CO_2 sorption. Wang et al. (2012), investigated CO_2 sorption of [N2224][carboxylate]-nH_2O with various carboxylate anion. It is noted that the CO_2 absorption in these ILs, varied between 20 -66 mol% (0.20-0.66 mol CO_2/mol compound) at 25 °C and 0.1 MPa, while in the present PILs these values are 12-26 mol% at 1 atm and 35 °C. Blath et al. (2012), also shown good CO_2 absorption in ILs possessing carboxylate anions (9-23.5 mol%) at 5.7 bar and 60 °C. Authors have noted that IL containing a carboxylic anion can be a promising alternative to common amine scrubbing processes to overcome their disadvantages [Blath (2012)]. The present PILs also exhibited similar or even higher CO_2 sorption than these ILs, indicating their potential for CO_2 separation. Even at high pressure of ~ 20 atm, S_{CO_2} of present PILs (esp. those possessing aliphatic carboxylate anions) remains high in comparison to the common polymers such as PC, PSF, Matrimid etc. [Hellums (1989)], McHattie (1992), Scholes (2010), Horn (2012)].

In spite of polymeric nature of these PILs, they could not be transformed in to good film form, due to their brittle nature. Thus, even though these PILs exhibited attractive CO_2 sorption and selectivity over H_2 and N_2, they could not be used as a membrane material for CO_2

separation application. This suggested that alternative strategies are required to use these PILs as a membrane material for CO_2 separation, which is elaborated in the following section.

3.3.4.6 Possible alternatives for applicability of PILs as a membrane material

To obtain a film (membrane), promising methodologies such as crosslinking, co-polymerization and support by porous polymer [Hu (2006), Bara (2007b, 2008a), Hudiono (2011), Li (2011, 2012), Carlisle (2013), Chi (2013)] could be practiced. It should be noted that all these PILs are based on flexible aliphatic backbone, which could be responsible for their brittle nature. Thus, by changing flexible aliphatic backbone to a rigid aromatic backbone can be used to tune their film forming nature. Higher CO_2 sorption capacity as well as its higher CO_2 solubility selectivity over H_2 and N_2 in some of the PILs can make them promising candidate for making blend membrane with mechanically strong film forming polymer for CO_2 separation.

3.4   Conclusions

Polymeric ionic liquids (PILs) based on poly(diallyldimethylammonium chloride), P[DADMA][Cl] and various aliphatic and aromatic carboxylate anions were prepared by a simple anion exchange method. Na salts of carboxylic acids were prepared by using equimolar aq. NaOH. All these PILs were water soluble. FTIR spectroscopy confirmed the formation of PILs with requisite anions. WAXD spectra of these PILs indicated their amorphous nature. Thermal stability of PILs decreased than the precursor PIL (P[DADMA][Cl]). This lowering was attributed to the decreased interchain interactions caused by increased size of the anion in comparison to Cl^- anion. In the series of PILs investigated, P[DADMA][Bu] exhibited highest S_{CO_2} at 2 atm coupled with excellent CO_2 based selectivities (CO_2/H_2 = 296.5 and CO_2/N_2 = 127.7). Even at high pressure (at 20 atm) CO_2 solubility and selectivity over H_2 and N_2 of these PILs was considerably higher than most of the earlier reported PILs, ILs and common polymers. In general, PILs with aliphatic carboxylate anions possessed a combination of high CO_2 sorption and high selectivity over H_2 and N_2. This indicated their promises as a next generation CO_2 sorbent materials. In spite of these attractive CO_2 sorption properties, they could not able to transform into good film form due to brittleness. Blending of these PILs with film forming polymer can be one of the option to use these high performance PILs as a membrane materials for CO_2 separation application.

Chapter 4

Investigations with PIL-PEBAX blend membranes

4.1 Introduction

PILs based on aliphatic backbone and possessing carboxylated anions exhibited high CO_2 sorption and selectivity over H_2 and N_2 as given in Chapter 2 and 3. These PILs are P[DADMA][Ac], P[DADMA][Bz], P[VBTMA][Ac], P[DADMA][Pr], P[DADMA][Bu], P[DADMA][He], P[DADMA][Oc] and P[DADMA][De]. Although their CO_2 sorption properties were attractive, they could not be used as a membrane material for investigating permeation properties due to their brittle nature and thus inability to form films. To obtain a film out of brittle PILs, other methodologies such as crosslinking, co-polymerization, coating on a porous polymer support were evaluated earlier [Hu (2006), Bara (2007b, 2008a, 2010), Hudiono (2011), Li (2011, 2012), Li (2010, 2013), Chi (2013)]. Blending of PILs with mechanically stable polymer could also be an another promising option, which is not really pursued in the literature.

Polymer blends are unique in nature because they provide a useful tool to combine advantages of each of the component and a continuous range of performance is predicted by changing the composition of the blend [Mannan (2013)]. This method offers a time and cost-effective combination of polymers with different separation and physicochemical properties to obtain desired superior properties, which are not otherwise possible with individual polymers. It is well known that mechanical and thermal properties can be improved by blending [Mannan (2013)]. Various types of polymer blend membranes were demonstrated for gas separation, e.g. PSF-PI, PEI-PAI, PU-PDMS, PVAm-PVA, SPEEK-Matrimid, PEI-PVP, PPO-PVP, PU-PVAc, etc. [Mushtaq (2013), Salleh (2011)]. The polymer possessing good mechanical strength, high processability and high gas permeability would be preferable for the blend membrane preparation.

Lin and Freeman (2005) have reported an overview about material selection for CO_2 separation. They noted that ethylene oxide (EO) units in the polymer appear to be the most useful groups to achieve high CO_2 permeability and high CO_2 base permselectivity. Homopoly(ethylene oxide) (PEO) consists of EO monomeric units, but its disadvantage is that it

has a strong tendency to crystallize and consequently, it presents low gas permeability [Car (2008)]. Block copolymers containing EO units as poly(amide-*b*-ether) has been shown as alternative material for this purpose [Car (2008), Liu (2013)]. Poly(ether-block-amide) copolymers (PEBAX) is a thermoplastic elastomer combining linear chains of rigid polyamide (PA) segments interspaced with flexible polyether (PE) segments. The hard amide block in PEBAX operates as an almost impermeable phase providing mechanical strength, whereas the soft flexible amorphous ether block is the locus for most of the gas transport [Tocci (2008)]. PEBAX copolymers have high polar or quadrupolar / nonpolar (e.g., CO_2/H_2 or CO_2/N_2) gas selectivity, making them interesting membrane materials for the removal of CO_2 from mixtures with light gases such as hydrogen or nitrogen [Bondar (2000)]. The large variety of PEBAX is available based on different proportion of ether and amide segment in the matrix. They have the following general chemical structure [Bondar (2000), Car (2008), Kim (2001), Schole (2012), Liu (2013)];

$$HO \left[\underset{O}{\overset{\parallel}{C}} - PA - \underset{O}{\overset{\parallel}{C}} - O - PE - O \right]_n H$$
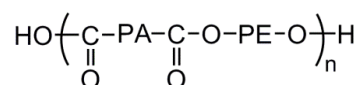
where, PA is an aliphatic polyamide "hard" block (i.e., nylon-6 [PA6], poly[imino(1-oxohexamethylene)], or nylon-12 [PA12]; poly[imino(1-oxododecamethylene)]) and PE is a polyether "soft" block, either poly(ethylene oxide) [PEO] or poly-(tetramethylene oxide) [PTMEO] [Bondar (2000)]. Crystalline amide block in PEBAX functions as an impermeable phase and provide mechanical strength, whereas ether block in PEBAX acts as the permeable phase due to its high chain mobility [Kim (2001)]. The physical and gas permeation properties of PEBAX known to be varied with the variation of PA and PE segments [Bondar (2000), Kim (2001), Barbi (2003), Armstrong (2012), Lara-Estévez (2012), Liu (2013)].

The blending of PEBAX and PEG (CO_2-philic material) was demonstrated earlier [Car (2008), Yave (2009, 2010a, 2010b), Mannan (2013), Liu (2013)]. It was observed that addition of PEG changed both, the structural and morphological properties of the polymer matrix. It was noted that the CO_2-philic nature and amorphous state of the PEG, contributed to its higher solubility and diffusivity [Liu (2013)]. Upon addition of PEG, CO_2 permeability increased without affecting P_{CO_2}/P_{N_2} and P_{CO_2}/P_{CH_4} selectivity with small increment in P_{CO_2}/P_{H_2} selectivity. This observation conveyed that the PEBAX could be a good material for blending with present PILs.

Among various PEBAX grades studied for CO_2 permeation and sorption, PEBAX-2533 exhibited higher performance than others [Bondar (2000), Barbi (2003), Armstrong (2012), Liu (2013)]. This suggests that PEBAX-2533 could be a better candidate for the preparation of blend membranes with PILs.

In this part of the work, PEBAX-2533 and P[DADMA][Ac] (a PIL possessing high CO_2 sorption and sorption selectivity over H_2 and N_2, but brittle in nature) were blended together. The blend membranes were prepared with varying proportions of PIL content in the blend. It was expected that incorporation of PIL in PEBAX would lead to improved CO_2 separation performance. The requisite physical properties of the blend membranes were examined. Pure gas permeability of the blend membranes was investigated.

4.2 Experimental

4.2.1 *Materials*

P[DADMA][Ac] was synthesized as given earlier [Chapter 2, Section 2.2.2.1]. PEBAX-2533 was gifted by Arkema. *n*-Propanol was procured from Merck. Pure gases (He, H_2, and N_2, min. purity: 99.9%)) were procured from Vadilal Chemical Ltd., while CH_4 and CO_2 with purity of 99.995% were procured from Air Liquide.

4.2.2 *PEBAX-PIL Blend membrane preparation*

PEBAX-PIL blend membranes were prepared in varying weight ratio (5, 10, 20 and 25 wt. %) and designated as PEBAX-PIL$_x$, where x represents the weight percent of PIL in the formed blend membrane. A 14 % (wt./v) solution of P[DADMA][Ac] was prepared in water. PEBAX was dissolved in *n*-propanol (3 % wt/v) at 70 °C for 2 h with continuous stirring. PEBAX-PIL blend membranes were prepared by adding appropriate amount of 14 wt. % PIL solution in the PEBAX solution and stirred for 2 h. The formed homogeneous blend solution was poured on to a flat teflon surface (Figure 4.1) at 70 °C and maintained for 12 h under dry atmosphere. Formed film was peeled off and dried in a vacuum oven at 60 °C for one week in order to remove the residual solvent. The average thickness of the membranes was around 60 ($\pm$5) μm. The schematic of blend membrane is given in Figure 4.2.
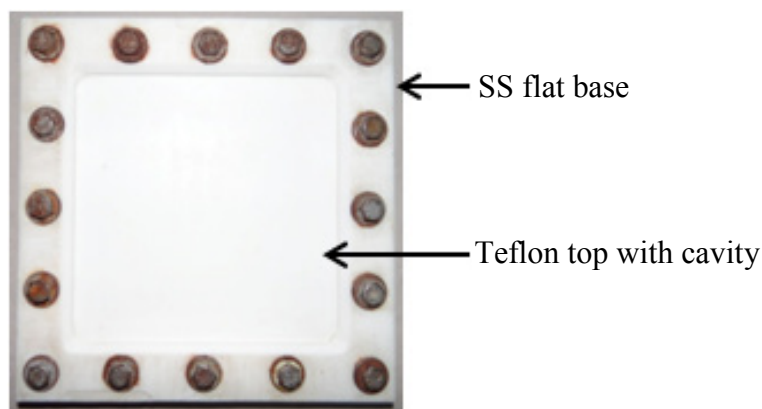
Figure 4.1 Teflon plate with SS base used for blend membrane preparation.
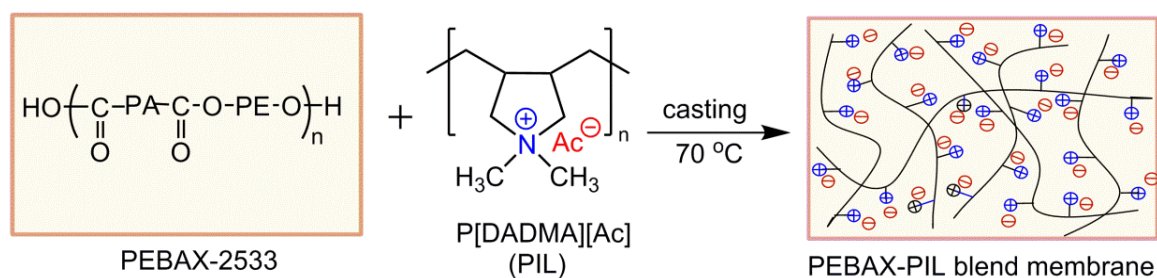
Figure 4.2 Schematic of blend membrane preparation.

4.2.3   Characterizations

The density (ρ) measurement of PEBAX-PIL blend membranes was performed using specific gravity bottle. For this purpose, organic solvent having adequate density and negligible sorption in PILs was selected. The maximum sorption of decalin in blends was ≤ 1.8 wt. % for the exposure of 2 h at 35 °C. Five samples of each PILs were analyzed and variation in the density was found to be $\pm$ 0.006 g/cm^3. The wide-angle X-ray diffraction (WAXD) spectra of all blend membranes were recorded using Rigaku X-ray diffractometer (D-max 2500) with Cu-K$_\alpha$ radiation in 2θ range of 5-40°. The d-spacing (d$_{sp}$) of major amorphous hollow was calculated by Bragg's equation (nλ = 2dsinθ; where, n =1 and λ is the wavelength of X-ray radiation =1.54 Å). The thermogravimetric analysis (TGA) was performed on Perkin Elmer TGA-7 under N$_2$ atmosphere with a heating rate of 10 °C/min. Physical properties of blend membranes thus obtained are summarized in Table 4.1.

4.2.4   Gas permeation

The variable volume method [Stern (1963)] was used for the determination of gas permeability. A schematic of the permeation equipment used is shown in the Figure 4.3, while the photograph of the permeation cell as shown in Figure 4.4. One end of the feed side of the cell was connected through valve V_1 to the feed gas cylinder outlet and a pressure gauge (0-550 psi range). The valve V_2 was vent and used to control the feed pressure. On the permeate side of the cell, a calibrated borosilicate glass capillary (I.D. = either 1.0 or 1.5 mm) containing a small mercury slug (~ 4-6 mm in length) was connected. The membrane cell assembly was kept in a thermostat. Displacement of the mercury slug was monitored against time.
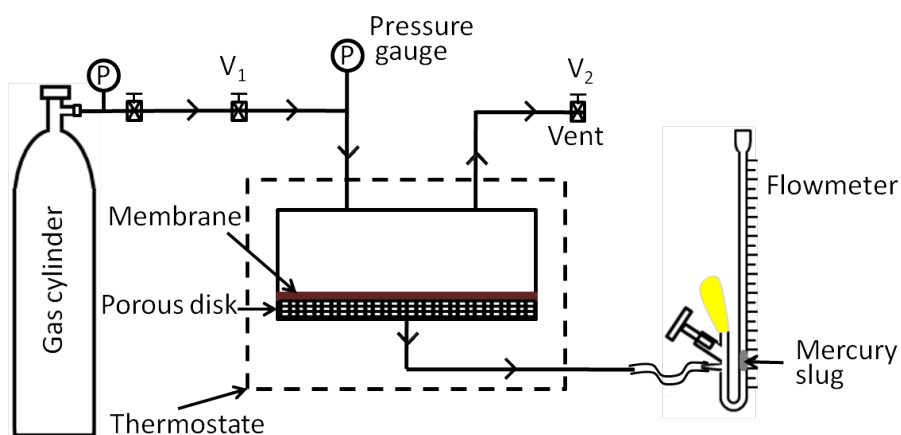
Figure 4.3 Schematic of gas permeation equipment.
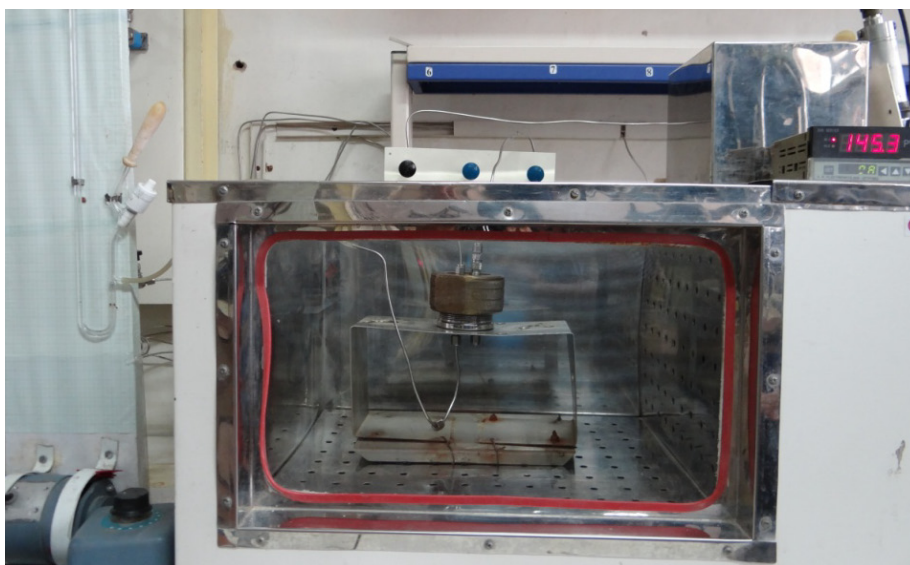
Figure 4.4 Photograph of gas permeation equipment.

The permeability measurement using pure gases (He, H_2, N_2, CH_4 and CO_2) was carried out at upstream gas pressure of 10 atm and at 35 °C; while maintaining the permeate side at the atmospheric pressure. Membrane samples (5 cm in diameter) after removing from the vacuum oven were immediately mounted in the permeation cell. The gas permeability was calculated using following equation:

$$P = \frac{N \cdot l}{(p_1 - p_2)}$$
(4.1)

where, 'P' is the permeability coefficient expressed in Barrer, 'N' is the steady-state penetrant flux ($cm^3/cm^2 \cdot sec$), 'p_1' and 'p_2' are the feed and permeate side pressures (cm Hg), while 'l' is the membrane thickness (cm). The permeability measurements were repeated with at least 3 different membrane samples prepared under identical conditions and the data averaged. Variation in the permeability was maximum 15 %, depending upon the gas analyzed. The permeability coefficient for various gases and ideal selectivity for gas pairs are given in Table 4.2 and 4.3, respectively.

4.3   Results and Discussion

4.3.1   PEBAX-PIL blend membrane preparation

For the membrane preparation, *n*-propanol was chosen as a solvent, since PEBAX was easily soluble upon heating at 70 °C. Moreover, it remained soluble after addition of small quantity of water in the solution. PIL was dissolved in water with maximum possible concentration (14 % wt./v) and appropriate amount of this stock solution was used for making blend membranes. This stock solution was used since P[DADMA][Ac] is highly hygroscopic and its weighing in polymer form would involve error. The blend membranes were prepared by solution casting on a teflon surface that allowed easy removal of membrane without any stretching. Blend membranes till 20 wt. % PIL content could be easily prepared. Beyond this concentration, blend membranes were sticky in nature due to their hygroscopic nature.

4.3.2   Physical properties

Optical images of blend membranes are shown in Figure 4.5. An increment in color intensity with increase in PIL content was observed. Except PEBAX-PIL$_{25}$, all other membranes showed good homogeneity.
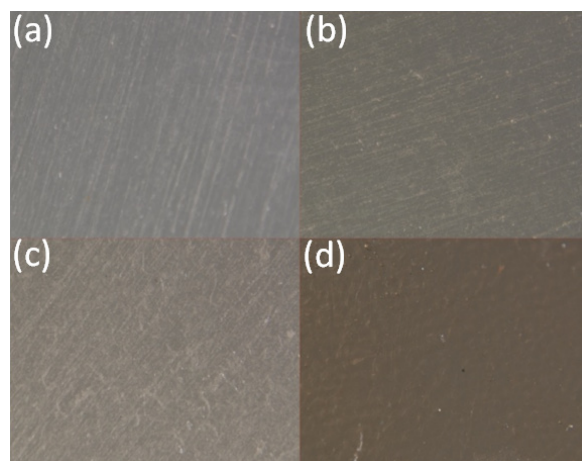
Figure 4.5 Optical images of blend membranes (a: PEBAX-2533, b: PEBAX-PIL$_{10}$, c: PEBAX-PIL$_{20}$, d: PEBAX-PIL$_{25}$).
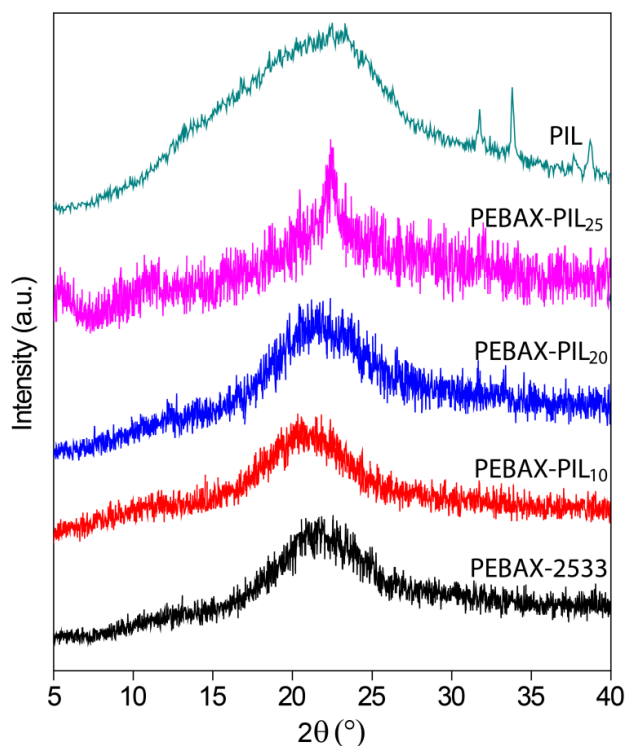
Figure 4.6 WAXD patterns of blends and pure polymers.

Wide angle X-ay diffraction (WAXD) pattern of these PILs is shown in Figure 4.6. The d-spacing (d$_{sp}$) calculated from WAXD spectra is given in Table 4.1. It can be seen that PEBAX-2533 exhibited amorphous hallow at 2θ ~ 21°, which is in good agreement with the reported

results [Bondar (1999), Tocci (2008)]. Blend membranes of 10 and 20 wt % PIL contents showed amorphous nature, while PEBAX-PIL$_{25}$ exhibited a sharp crystalline peak, even though PIL possessed amorphous nature.

Table 4.1 Physical properties of membranes.

Polymer	d_{sp}[a] (Å)	ρ[b] (gm/cm^3)	IDT[c] (°C)
PEBAX-2533	4.12	1.01[d]	380
PEBAX-PIL$_{10}$	4.23	1.04	394
PEBAX-PIL$_{20}$	4.07	1.07	394
P[DADMA][Ac] (PIL)	3.91	1.14	190

[a]: d-Spacing obtained from wide angle X-ray diffraction spectra, [b]: density measured at 35 °C, [c]: initial decomposition temperature determined by TGA, [d]: Ref [Kim (2001), Bondar (1999)].

It was observed that the density of blend membranes were lying in between the density of individual components (PEBAX-2533 and PIL), roughly following additivity rule (Table 4.1). It is known that in blend membranes that the density usually follows the additive model [Yave (2010b)].
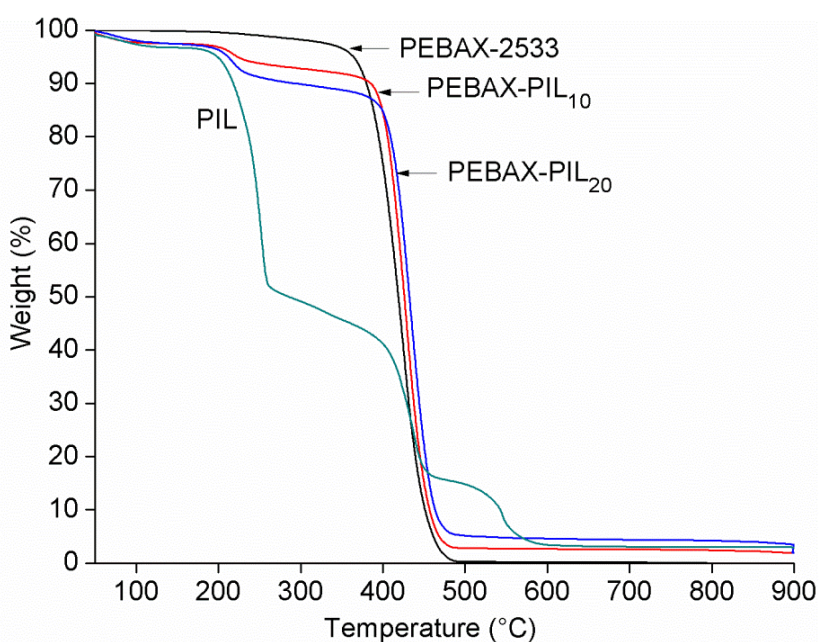
Figure 4.7 TGA curve of blends and pure polymers.

The TGA curves of blend membranes are given in Figure 4.7, while the IDT values are given in Table 4.1. It can be seen that thermal degradation of PEBAX starts at 380 °C, matching well with that of reported one [Lara-Estévez (2012)]. The TGA curve of PIL and blend membranes showed initial weight loss till 120 °C, which could be correlated to the loss of absorbed moisture. PIL used in the present study is known to be highly hygroscopic in nature (Chapter 2). Further weight loss of blend membrane starts at ~190 °C, which is similar to the degradation temperature of PIL.

4.3.3 *Gas permeation*

The gas permeability of blend membranes was studied at 10 atm upstream pressure and at 35 °C. The obtained data is summarized in Table 4.2. It was observed that the gas permeability of PEBAX-2533 match well with that of reported [Bondar (2000) and Barbi (2003)].

Table 4.2 Permeability coefficient (P)[a] of PEBAX and blend membranes.

Permeability coefficient	PEBAX-2533			PEBAX-PIL$_{10}$	PEBAX-PIL$_{20}$
	This work	Bondar et al. (2000)	Barbi et al. (2003)		
P_{He}	33.9	-	32	30.8	23.4
P_{H_2}	59.2	59.7	55	52.2	38.7
P_{N_2}	12.7	9.4	11.5	11.3	8.1
P_{CO_2}	287.0	221	276	269.0	202.0
P_{CH_4}	38.7	-	39	36.1	23.1

[a]: Expressed in Barrer (1 Barrer = 10^{-10} cm^3(STP).cm/cm^2.s.cm Hg).

It could be seen from Table 4.2 that the gas permeability of blend membranes decreased with increasing PIL content. This was in tune with the increasing density with the increase in the PIL content in blend membranes, conveying that the available free space is reduced after blend formation. It is known that the ether block in PEBAX acts as the permeable phase due to its high chain mobility [Kim (2001)]. In view of these, the lowering in gas permeation in the blend

membranes could be correlated to the restrictions in the PEBAX chain mobility brought by its interactions with PIL and formation of homogeneous blend. It is reported that compared to miscible ionic liquid based blends, where molecular level interactions may restrain chain flexibility and reduce gas permeability, heterogeneous PVDF/RTIL blend systems showed far superior gas transport properties [Chen (2012a)]. Liu et al. (2013) have noted that low molecular weight of PEG acts as a plasticizer and increased the permeability, as anticipated. In the present case, molecular weight of PIL is too high (average molecular weight is 100,000 - 200,000), which, due to interactions with PEBAX would restrict molecular motion and thus diffusivity. The decrease in gas permeability for He, H_2, N_2 and CH_4 was 31-40 %, while that of CO_2, it was slightly lower (29%). This could be due to the CO_2-philic nature of PIL, which possibly permeate CO_2 faster based on preferred solubility.

Table 4.3 Permselectivity (P_A/P_B)[a] of PEBAX and blend membranes.

Permselectivity	PEBAX-2533			PEBAX-PIL$_{10}$	PEBAX-PIL$_{20}$
	This work	Bondar et al. (2000)	Barbi et al. (2003)		
P_{He}/P_{H_2}	0.57	-	0.58	0.59	0.6
P_{He}/P_{N_2}	2.67	-	2.78	2.73	2.9
P_{He}/P_{CH_4}	0.88	-	0.82	0.85	1.01
P_{CO_2}/P_{N_2}	22.6	23.4	24.0	23.8	25.0
P_{CO_2}/P_{CH_4}	7.42	-	7.08	7.45	8.74
P_{CO_2}/P_{H_2}	4.85	3.7	5.02	5.15	5.22

[a]: Ratio of pure gas permeability.

It was interesting to note that the CO_2 based permselectivity (P_{CO_2}/P_{N_2}, P_{CO_2}/P_{CH_4} and P_{CO_2}/P_{H_2}) was increased with the addition of PIL in PEBAX (Table 4.3). This may not be just due to the overall reduction in the gas permeability of blend membranes. The presence of CO_2-philic nature of PIL possessing high CO_2 sorption might be responsible for this enhancement in CO_2 based selectivity. This assumption could be supported by comparatively lower increase in

helium (non-interactive gas) based permselectivity than that of CO_2 based permselectivity. In view of inert nature of helium, its permeability is governed by the diffusivity. In the case of CO_2, the permeability is governed by diffusivity as well as solubility due to interactions of this gas with the polymer. Although, CO_2 based selectivity were increased, the overall increase was very low. On the other hand, decrease in CO_2 permeability was ~ 30 %. This could be because of lower PIL content in blend membranes, which could not be able to increased CO_2 based permselectivity significantly. At higher levels of PIL in the blend, phase separation occurred. Car et al. (2008) and Yave et al. (2009), also demonstrated the CO_2 permeability of PEBAX-PEG blend membrane were increased significantly only at higher PEG content (> 20 wt. %). This indicated higher amount of PIL in blend membrane would be able to enhance solubility based gas permeability and selectivity over other gases. Thus, alternative polymer, which can form a well miscible blend with higher amount of PIL could be a beneficial. Alternatively, an appropriate PIL that has lower hydrophilicity could be used that can form miscible blend with PEBAX. This would involve tuning of anion, which would sacrifice CO_2 sorption capacity than P[DADMA][Ac] and thus was not pursued further.

4.4 Conclusions

PEBAX-PIL blend membranes were fabricated by using PEBAX-2533 and P[DADMA][Ac]. The homogeneous blend membrane could be prepared up 20 wt. % PIL content, above this PIL content, phase separation occurred. It was observed that all the membranes were amorphous in nature. The density was increased with increased PIL content in the blend membrane. These membranes easily sustained high upstream pressure of 10 atm with no physical change after the gas permeation analysis. Though permeability for all the gases decreased with increasing PIL content, the CO_2 based permselectivity (esp. P_{CO_2}/P_{N_2}, P_{CO_2}/P_{CH_4} and P_{CO_2}/P_{H_2}) increased only marginally. This small increase in CO_2 based selectivity was coupled with comparatively larger sacrifice on decrease in permeability.

Chapter 5

Film forming PILs based on rigid, fully aromatic polybenzimidazole: Synthesis, investigation of physical and gas permeation properties

5.1   Introduction

In earlier study of PILs based on P[DADMA] and P[VBTMA] [Chapter 2 and 3], some of the PILs exhibited good CO_2 sorption and CO_2 sorption based selectivity, but they could not be used as a membrane material due to their film forming inability (brittle nature). The alternative way to use these PILs as a CO_2 separation membrane by blending with PEBAX was opted [Chapter 4]. This approach shows insignificant improvement in permselectivity with a larger decreased in CO_2 permeability [Chapter 4]. Though efforts towards transforming brittle PILs into a membrane by employing methodologies such as crosslinking [Bara (2007b, 2008a, 2008b), Carlisle (2010, 2013), Li (2011, 2012)], copolymerization [Hu (2006), Chi (2013), Li (2010, 2013)] or support by porous polymer are demonstrated [Bara (2008a 2010), Hudino (2011), Li (2011)], these PIL seems to be associated with limitations such as low pressure-withstand ability, reduced IL group density per repeat unit and generally known lowering of permeability by crosslinking of a polymer. This dictates a need of alternate approach for synthesizing PILs so that above drawbacks could be successfully mitigated.

Intuitively, film forming ability in PILs can be induced if fully aromatic rigid backbone could be architectured. Recently our group has demonstrated an altogether different methodology of obtaining film forming PILs possessing rigid and fully aromatic backbone (polybenzimidazole) [Kumbharkar (2008)]. For this purpose, polybenzimidazole was specifically chosen due to couple of reasons. Film forming ability of polybenzimidazoles (PBIs) is being widely employed to make proton exchange membranes for fuel cell. Possibility of converting PBI's imidazole moiety into imidazolium cation (by *N*-quaternization using alkyl/aryl group) positions this family of polymers as promising candidates for transforming them into PILs. Moreover, PBIs possess excellent mechanical and thermal stability [Mader (2008), Li (2009a), Kumbharkar (2009a)]. Possibilities of PIL structural variations achievable while using PBI as a precursor are multidimensional. For example, a large choice is available for alkyl/aryl groups to

be used for the *N*-quaternization of PBI-imidazole. Moreover, choices of structural variations at the level of PBI backbone itself are numerous. Either or both monomers of PBI, viz., tetramine and/or dicarboxylic acid are known to offer wide structural (and thus property) variations in PBIs [Mader (2008), Li (2009a), Kumbharkar (2009a), Mustarelli (2012)]. One of the most imperative peculiarities of this approach is that all PBIs (except ABPBI) have two imidazole groups available per repeat unit that can be effectively *N*-quaternized. This would introduce two IL characters per repeat unit of PBI. This unique feature distinctly differentiates proposed methodology of synthesizing PILs from the known methodologies.

During earlier work [Kumbharkar (2008)] on this new methodology, methyl group was used as the *N*-substituent and obtained quaternized PBIs with iodide ion were exchanged with only two anions (BF_4^- and Tf_2N^-). Obtained PILs possessed excellent film forming ability. The permeation property investigation of these PILs revealed that they possess promising CO_2 permeability as well as selectivity. These encouraging results prompted further investigations on this methodology to generate structure – property relationship if this new family of materials.

This Chapter deals with investigating effect of anion on PILs obtained from PBI-BuI and methyl group as the *N*-substituent. The PBI-BuI (PBI based on *3,3'*-diaminobenzedene and *tert*-butyl isophthalic acid) was particularly chosen due to its higher permeability than that of common PBI-I, based on isophthalic acid. The methyl group was purposely retained same so that the effects of anion variation could be better evident. Formed PILs were thoroughly investigated for film forming ability, mechanical, thermal and requisite physical properties that would shed a light on basic material characteristics. Detailed gas permeation properties of PILs (permeation, sorption and diffusion) using pure gases (He, H_2, N_2, CH_4 and CO_2) were investigated.

5.2   Experimental

5.2.1 Materials

3,3'-Diaminobenzidine (DAB), *5-tert*-butylisophthalic acid (BuI), sodium hydride (60 % dispersion in mineral oil), dry dimethyl sulphoxide (DMSO, 0.01% H_2O), reagents for anion exchange, viz., silver tetrafluoroborate ($AgBF_4$), lithium bis(trifluoromethane) sulfonimide ($LiTf_2N$), silver acetate (CH_3COOAg), silver trifluoroacetate (CF_3COOAg), silver heptafluorobutyrate (C_3F_7COOAg), silver benzoate (C_6H_4COOAg), silver methanesulfonate (CF_3SO_3Ag), silver trifluoromethanesulfonate (CF_3SO_3Ag), silver *p*-toluenesulfonate

(C$_6$H$_4$CH$_3$SO$_3$Ag) and silver nitrate (AgNO$_3$) were procured from Aldrich Chemicals. Polyphosphoric acid (PPA) was procured from Alfa Aesar. Methyl iodide, potassium thiocyanate (KSCN, 98%) and sodium chloride (NaCl, 99%) were procured from S.D. Fine Chemicals. Pure gases, viz.; He, H$_2$, N$_2$, CH$_4$ and CO$_2$ were procured as per details given in Chapter 4.

5.2.2 Synthesis

5.2.2.1 Polybenzimidazole

Polybenzimidazole (PBI-BuI) was synthesized by polycondensation of DAB and *5-tert-*butyl isophthalic acid (BuI) as reported earlier (Scheme 5.1) [Kumbharkar (2009a)]. A three-necked round bottom flask equipped with a mechanical stirrer, N$_2$ inlet and CaCl$_2$ drying tube was charged with 1200 g of PPA and 40 g (0.1867 mol) of DAB. Temperature of the reaction mixture was elevated to 140 ºC. After the dissolution of DAB, 41.49 g of BuI (0.1867 mol) was added, temperature was raised to 170 ºC and maintained for 5 h under constant flow of N$_2$. The temperature was further raised to 200 ºC and maintained for 12 h. The polymer was obtained by precipitation of the reaction mixture in water. Obtained dark brown polymer threads were crushed, thoroughly washed with water, kept in 10% NaHCO$_3$ for 16 h and again washed with water, until the filtrate was neutral to pH. The collected polymer was immersed in acetone for 16 h, filtered and dried in vacuum oven at 100 ºC for 3 days. Its purification by dissolving in DMAc (3% w/v) and reprecipitation in water yielded a yellow colored fibrous polymer.
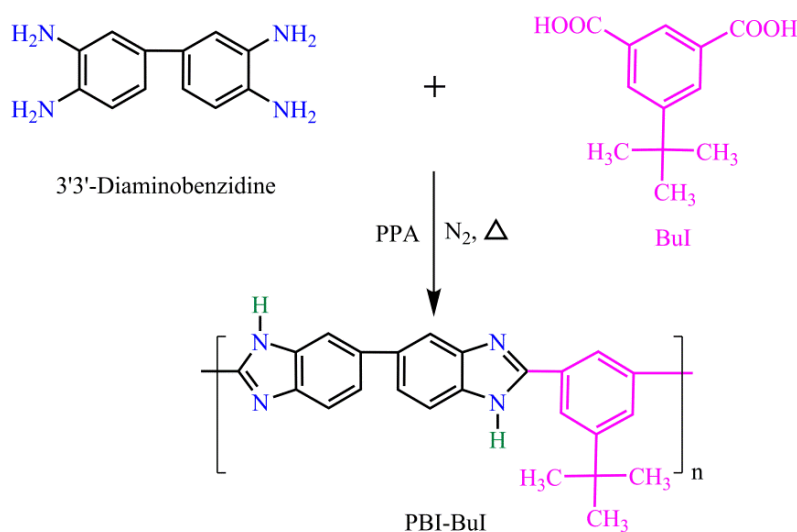
Scheme 5.1 Synthesis of PBI-BuI.

5.2.2.2 N-Quaternization of PBI-BuI

A 3-necked flask was charged with 600 ml of dry DMSO, 20 g of PBI-BuI, 4.62 g of NaH (60 % mineral oil dispersion form, 2.1 molar equivalents) and stirred under dry N_2 atmosphere at ambient temperature for 24 h. The reaction mixture was then heated at 80 ºC for an hour. A deep blood red color was developed after complete dissolution of PBI-BuI, indicating formation of its *N*-sodium salt. The reaction mixture was allowed to cool to the ambient and 32.76 g of methyl iodide (4.2 equivalents) was added slowly over a period of 15 minutes while stirring. A yellow precipitate was formed, which was dissolved as the reaction temperature was elevated to 80 ºC. The reaction mixture was stirred further for 24 h, temperature was lowered down to the ambient and then precipitated in a mixture of toluene:acetone (1:1). Obtained golden yellow fibrous precipitate was dried at 80 ºC for 24 h. It was further purified by dissolving in DMF and reprecipitation in the same nonsolvent. Obtained polymer was dried in vacuum oven at 80 ºC for 3 days and stored in desiccator until use. Obtained *N*-quaternized PBI (PIL) was designated as [TMPBI-BuI][I], based on the parent PBI and the anion it holds (Scheme 5.2).
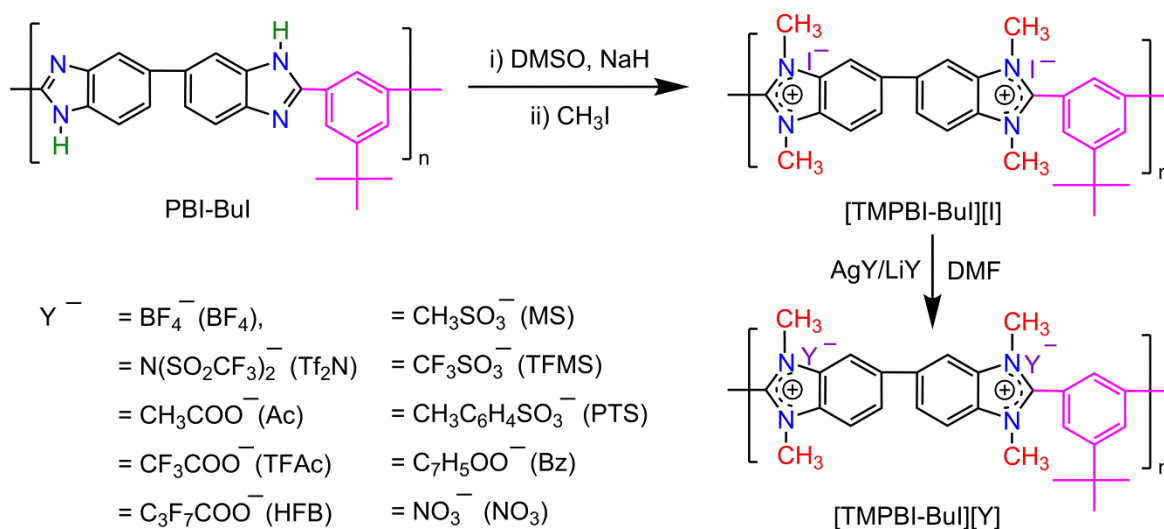
Scheme 5.2 Synthesis of PILs based on PBI-BuI.

5.2.2.3 Iodide exchange of N-quaternized PBI-BuI

Polymeric ionic liquids (PILs) with varying anions were obtained by exchanging the iodide of the *N*-quaternized PBI-BuI by anions of interest (BF_4^-, Tf_2N^-, Ac^-, $TFAc^-$, HFB^-, Bz^-, MS^-, $TFMS^-$, PTS^- and NO_3^-). Typically, a two necked flask equipped with a calcium chloride guard tube was charged with 5 g of a quaternized PBI-BuI (0.007396 mol) and 100 ml

of a DMF. After complete dissolution, 2 molar equivalent of the silver salt of an anion was added while stirring. Formation of AgI precipitate began with the addition of silver salt, while the anion exchanged polymer remained in dissolved state. The reaction mixture was further stirred at the ambient temperature for 24 h in order to ensure complete replacement of iodide by the requisite anion. The precipitated AgI was removed by repeated centrifugation at 12000 RPM. Formed PIL was recovered from the supernatant solution by solvent evaporation. It was further purified by dissolving in DMF (8% w/w), followed by precipitation using suitable nonsolvent (water in case of PILs with BF_4^- as an anion and acetone: toluene mixture (1:1) in case of PILs with other anions). Purified PIL was dried at 60 ºC in a vacuum oven for 3 days.

The iodide exchange by Tf_2N^- anion was performed using $LiTf_2N$. A 5 g of an *N*-quaternized PBI-BuI (0.007396 mol) was dissolved in a 100 ml of solvent, 4.25 g of $LiTf_2N$ (2 mol) was added and stirred for 24 h. The resulting homogeneous reaction mixture was precipitated in water and obtained PIL was thoroughly washed in order to remove LiI. It was subsequently dried at 60 °C. It's further purified by dissolving in DMF (8% w/w) and reprecipitating in water followed by drying at 60 ºC in the vacuum oven for 48 h yielded pale yellow colored PIL. An amount of iodide exchanged in all the PILs with different anions was estimated by Volhard's method [Jeffery (1989)], as given in Section 5.2.4.1.

5.2.3   Membrane preparation

The dense membranes (films) were prepared by solution casting method on a flat glass surface using 3% (w/v) PIL solution in DMAc at 80 °C for 18 h under dry conditions. After the solvent evaporation, formed membrane was peeled off and dried in a vacuum oven at 100 °C for a week in order to remove traces of the solvent.

5.2.4   Characterizations

5.2.4.1 Degree of PBI-BuI N-quaternization (DQ) and iodide exchange

The degree of *N*-quaternization (DQ) of PBI-BuI was determined by ^{1}H-NMR (recorded on Bruker AC-200 using DMSO-d$_6$ as the solvent) while comparing integration of methyl protons with that of aromatic ones. Percent of the iodide exchanged by a requisite anion was determined by Volhard's method [Jeffery (1989)], in which a 0.1 g of PIL powder was stirred in 25 ml of 0.01M AgNO$_3$ solution for 24 h. An excess of unreacted AgNO$_3$ was titrated against

0.01 M KSCN. From the amount of $AgNO_3$ consumed, iodide content in the PIL (and thus the percent of iodide exchange) was estimated.

5.2.4.2 FT-IR analysis

The FT-IR spectrum of polymers in thin film form (~10 μm) was recorded at the ambient temperature as well as at 150 °C using Perkin Elmer Spectrum GX spectrophotometer provided with a high temperature assembly of Mettler Toledo make with FP90 central processor.

5.2.4.3 Physical properties

The solubility of PILs was determined by stirring 0.1 g of PIL in 10 ml of a solvent at ambient for 24 h. In case of insolubility, heating at 80 °C (or near boiling point, in case of the low boiling solvents) for 24 h was employed. The inherent viscosity (η_{inh}) of PILs was determined at different concentrations (0.025 to 0.2 g/dL) in DMSO at 35 °C. The water sorption capacity of PILs was determined by immersing the dry membrane samples (in triplicate, size: 2x1 cm^2) in water at 35 °C for 72 h. The percent sorption was calculated using Eq. 5.1 (variation from the average: ±1.3 %).

$$\% \text{ Water sorption} = \frac{Ws - Wi}{Wi} \times 100 \qquad (5.1)$$

where, Ws is the weight of the membrane after water sorption and Wi is its initial weight in the dry state.

Water contact angle of the dry membrane surface was determined by the sessile drop method using Digidrop instrument (Kruss, Germany) while placing a water drop of 0.08 μl on the membrane surface. The measurement was repeated with five membrane samples and the data averaged (maximum variation from the average: ±2.4°).

The tensile tests were performed at the ambient temperature on Linkam TST-350 microtensile testing instrument using dumbbell shaped film samples (6 samples for each membrane of length: 2 cm, width: 0.3 cm and average thickness: 80 μm). Stress–strain curves were obtained with at a speed of 100 μm/s.

The wide angle X-ray diffraction (WAXD) pattern of PILs in the film form was recorded using Rigaku X-ray diffractometer (D-max 2500) with Cu-K$_\alpha$ radiation. The average intersegmental *d*-spacing (d$_{sp}$) for the amorphous peak maxima was calculated using Bragg's

equation ($n\lambda = 2d\sin\theta$). The density (ρ) of membranes was measured at 35 °C by using specific gravity bottle and decalin as the solvent that exhibited negligible sorption in PILs (< 2 %). This measurement was repeated with five samples and the deviation from average value was ≤ 0.005 g/cm^3.

The thermogravimetric analysis (TGA) was performed using Perkin Elmer TGA-7 in N_2 atmosphere with a heating rate of 10 °C/min. The glass transition temperature (T_g) was determined using DSC Q-10 (TA instruments, USA) under N_2 atmosphere with a heating rate of 10 °C/min.

5.2.5   *Gas permeation and sorption*

The permeability measurement using pure gases (He, H_2, N_2, CH_4 and CO_2) was carried out by standard variable volume method at upstream gas pressure of 20 atm and at 35 °C, as mentioned in Chapter 4 (Section 4.2.4). The permeability measurements were repeated with at least 4 different membrane samples prepared under identical conditions and the data averaged. The variations in permeability from the average maximum 15 %, depending upon the gas analyzed.

The pure gas sorption isotherms using H_2, N_2, CH_4 and CO_2 were obtained at 35 °C using equipment that consisted of the dual-volume, single-transducer set up based on pressure decay method, as mentioned in Chapter 2, Section 2.2.4. The solubility coefficient (S) and solubility selectivity (S_A/S_B), sorption parameters (k_D, C'_H and b) were determined at 20 atm. The permeability coefficient along with its solubility coefficient at 20 atm was used to estimate the diffusivity coefficient ($D_A = P_A/S_A$).

5.3   **Results and discussion**

5.3.1   *Synthesis*

5.3.1.1 *PBI-BuI synthesis*

In order to investigate effects of variation in anion on gas sorption and physical properties of PILs based on aromatic backbone, PBI-BuI was chosen for the *N*-quaternization. Its selection was based on higher known gas sorption and permeation of PBI-BuI than that of base PBI-I based on isophthalic acid (owing to the presence of bulkier *tert*-butyl group in PBI-BuI [Kumbharkar (2006)]). It was anticipated that PBI-BuI backbone would be advantageous in

offering high gas permeation properties of resulting PILs. Another reason in selecting PBI-BuI was high solvent solubility of [TMPBI-BuI][I] (precursor PIL) at the concentration used for metathesis (5 % wt/v in DMF) than that of other PILs based on PBI-I as a backbone [Kumbharkar (2008)].

PBI-BuI could be synthesized by solution polycondensation in PPA, which acts as both, condensation agent as well as polymerization solvent [Mader (2008)]. The ratio of DAB:PPA as 1:30 w/w and sequential rise in temperature after the addition of the 5-*tert*-butylisophthalic acid (170 °C and then 200 °C) was based on our previous investigations [Kumbharkar (2009a)]. The time of reaction at 200 °C was 12 h in order to achieve high enough inherent viscosity (~1.0 dL/g) that could form a mechanically stable film. The purified PBI-BuI was used further for PIL synthesis.

5.3.1.2 *N-Quaternization of PBI-BuI by methyl iodide*

Although imidazole group of a PBI can be substituted by a variety of alkyl/aryl groups, methyl iodide was chosen as a reagent for performing *N*-quaternization. With the smallest sized methyl group, effects of IL character in resulting PILs can be easily evident without much additional effects arising from the added *N*-substituent. The *N*-quaternization of PBI-BuI could be easily performed by an in-situ formation of their Na-salt, followed by the addition of a small excess of methyl iodide (4.2 molar equivalents). An immediate precipitate formation at the ambient temperature was indication of the *N*-substitution. The temperature was needed to elevate till 80 ºC in order to achieve complete dissolution (solution phase would assist completion of the *N*-quaternization reaction). The non-solvent needed for the polymer precipitation was toluene and acetone mixture (1:1), since partial solubility was observed in acetone, methanol and water (one of which could have been the obvious choice as the non-solvent). The yield after the purification was >90%. This was a primary indication of almost complete *N*-quaternization of the PBI-BuI. Quantitative estimation of the degree of quaternization (DQ) is discussed below.

5.3.1.3 *Estimation of the degree of N-quaternization (DQ)*

The ^{1}H-NMR spectra of *N*-quaternized PBI-BuI is given in Figure 5.1. An absence of a broad peak in the range of δ 13-14 (ascribed to imidazole N-H in the case of unsubstituted PBI-BuI) indicated that the *N*-substitution reaction has occurred. A quantitative estimation of the *N*-

quaternization was done by comparing integration of protons belonging to the methyl group (appearing in the range δ 4-4.5) with that of aromatic protons appearing in the range of δ 7.5-9.5. It was found that in case of [TMPBI-BuI][I], the degree of *N*-quaternization was > 96 %. Further improvement could be possible by optimization of time and temperature, which were not addressed.
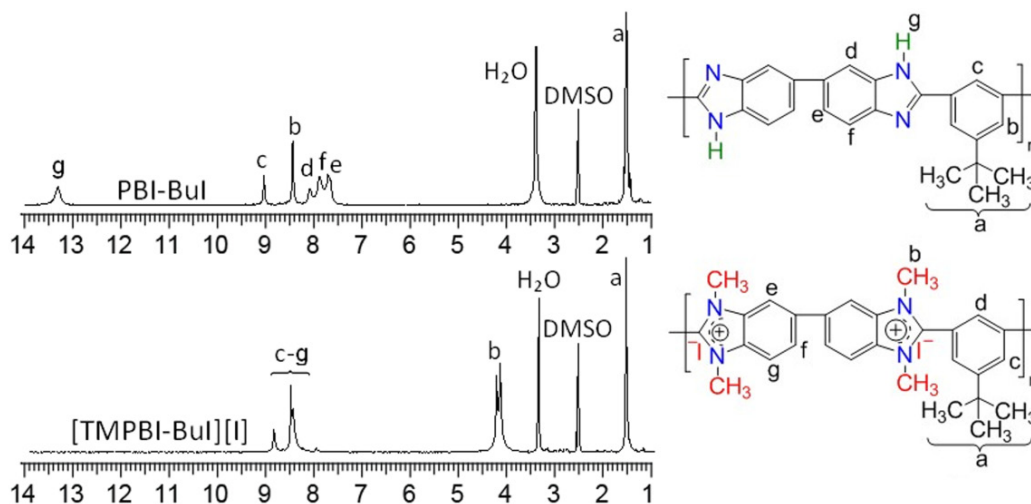
Figure 5.1 ^{1}H-NMR spectra of PBI-BuI and PILs.

5.3.1.4 *Exchange of iodide by other anions*

The iodide exchange of [TMPBI-BuI][I] was done with different anions, viz.; Tf$_2$N⁻, BF$_4$⁻, Ac⁻, TFAc⁻, HFB⁻, Bz⁻, MS⁻, TFMS⁻, PTS⁻ and NO$_3$⁻ in order to investigate effects of anion variation. The silver salt of an anion was purposely chosen for the iodide exchange. It was anticipated that the PIL obtained after iodide exchange would remain dissolved in the solvent, while the byproduct (AgI) would precipitate out. This would lead to irreversible nature of the exchange reaction and thus a high degree of iodide exchange can be obtained. During the exchange of iodide by the silver salt of BF$_4$⁻, Ac⁻, TFAc⁻, HFB⁻, Bz⁻, MS⁻, TFMS⁻, PTS⁻ and NO$_3$⁻; immediate precipitate formation of the AgI was indeed observed. This indicated that the exchange reaction is quite rapid, in spite of the polymeric nature of cation. In all cases, high yield of the AgI precipitate (> 90%) indicated completion of the iodide exchange and thus, success of selecting silver salt for the iodide exchange. The estimation of iodide in thus formed PIL by Volhard's method (given in Table 5.1) showed almost quantitative exchange of iodide by another anion. It is worth to mention that this was made possible without any need of parameter optimizations (e.g. solvents, salt quantity or duration of reaction). It is known that such exchange

reactions are usually performed using an excess of NaBF$_4$ while manipulating the solvent system, reaction time, etc. [Blasig (2007a), Chapter 2].

In the case of iodide exchange by Tf$_2$N$^-$, the salt needed to be used was LiTf$_2$N, owing to the commercial unavailability of Ag salt of this anion. The byproduct LiI remained dissolved in the solution. It was removed during the polymer precipitation in water. Obtained polymer needed thorough water wash for the complete removal of LiI. The iodide exchange by Tf$_2$N$^-$ was 86%. This was not as high as in the cases of metathesis performed using the Ag-salt of anions, as discussed above. This observation can be explained on the basis of dissolved state of byproduct LiI, which may remain in equilibrium with the PIL possessing Tf$_2$N$^-$ anion.

Table 5.1 Physical properties of PILs.

PILs	Iodide exchange (mol %)[a]	η_{inh}[b] (dL/g)	d_{sp}[c] (Å)	ρ[d] (gm/cm^3)	T_g[e]	TGA		Water sorption (wt %)	Water contact angle (°)
						IDT[f] (°C)	W$_{900}$[g] (%)		
[TMPBI-BuI][I]	0	3.1	3.71	1.469	ND	250	418	4.9	87
[TMPBI-BuI][BF$_4$]	~100	3.5	4.27	1.312	ND	374	42.9	9.9	82
[TMPBI-BuI][Tf$_2$N]	86.1	3.3	6.86	1.489	189	465	33.5	0.6	89
[TMPBI-BuI][Ac]	95.3	0.92	3.79	1.282	ND	195	50.6	WS	—
[TMPBI-BuI][TFAc]	98.2	4.4	3.76	1.423	ND	215	46.2	WS	—
[TMPBI-BuI][HFB]	99.1	3.8	5.14	1.457	ND	150	37.3	99.8	48
[TMPBI-BuI][MS]	96.2	4.4	4.03	1.392	254	370	49.7	WS	—
[TMPBI-BuI][TFMS]	98.3	6.3	4.52	1.436	308	451	37.4	0.6	97
[TMPBI-BuI][PTS]	99.1	4.4	4.03	1.334	ND	333	45.4	4.1	85
[TMPBI-BuI][Bz]	94.0	2.2	3.67	1.306	ND	136	35.5	WS	—
[TMPBI-BuI][NO$_3$]	~100	4.1	3.73	1.345	ND	236	44.7	15.3	79
PBI-BuI[h] (base case)	—	1.0	4.69	1.193	ND	525	67.9	12.3	83

[a]: Determined by Volhard's method, [b]: inherent viscosity determined using 0.2 g/dL solution at 35 ºC, [c]: d-spacing obtained from wide angle X-ray diffraction spectra, [d]: density measured at 35 ºC, [e]: glass transition temperature, [f]: initial decomposition temperature, [g]: char yield at 900 °C, [h]: Ref. [Kumbharkar (2009a)], ND: not detected, WS: water soluble.

5.3.2   *FTIR analysis*

FTIR spectra of PILs scanned at the ambient temperature showed a broad band in the range of ~3100-3700 cm^{-1} (Figure 5.2a), attributable to the sorbed moisture. When the scans were recorded at 150 ºC (Figure 5.2b), this band disappeared in almost all PILs.
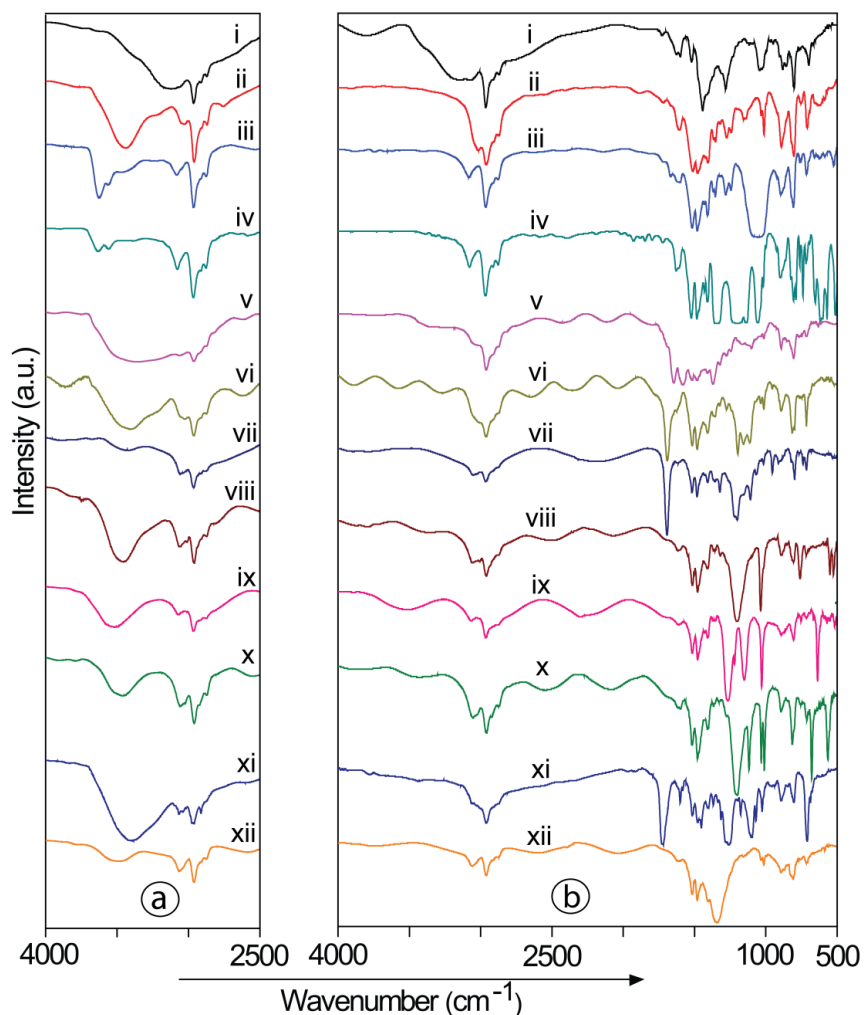
Figure 5.2 FT-IR spectra of PILs based recorded at (a) ambient and (b) 150 °C (i: PBI-BuI; ii: [TMPBI-BuI][I]; iii: [TMPBI-BuI][BF$_4$]; iv: [TMPBI-BuI][Tf$_2$N]; v: [TMPBI-BuI][Ac]; vi: [TMPBI-BuI][TFAC]; vii: [TMPBI-BuI][HFB]; viii: [TMPBI-BuI][MS]; ix: [TMPBI-BuI][TFMS]; x: [TMPBI-BuI][PTS]; xi: [TMPBI-BuI][Bz]; xii: [TMPBI-BuI][NO$_3$]).

In the case of unsubstituted PBI-BuI, a wide band appearing at ~2400-3400 cm^{-1} (responsible for N-H stretching) has vanished after the *N*-quaternization, as could be easily anticipated. In all PILs, characteristic bands for benzimidazole (1500-1650 cm^{-1}, attributable to C=C/C=N stretching vibrations and ring modes) [Musto (1993)] was originated from the cationic

PBI backbone. In the case of [TMPBI-BuI][BF$_4$], a band at ~1080 cm^{-1} is attributable to the B-F stretching vibrations, as was observed in RTIL, [BMI][BF$_4$] possessing this anion [Suarez (1996)]. In case of PIL possessing Tf$_2$N$^-$ anion, bands at ~1360 cm^{-1} and 618 cm^{-1} are attributable to the asymmetric stretching and bending vibrations of SO$_2$; respectively. In these spectra, a band at 1130-1240 cm^{-1} is attributable to the symmetric stretching vibrations of C-F bond. Similar band was seen in the spectra of LiTFSI [Pennarun (2005)]. In the spectra of [TMPBI-BuI][Ac] and [TMPBI-BuI][Bz], the C=O stretching (belonging to the ester group) was observed at 1652 and 1698 cm^{-1}, respectively. These stretching vibrations in the spectra of [TMPBI-BuI][TFAc] and [TMPBI-BuI][HFB] were noted at 1690 cm^{-1} and 1696 cm^{-1}, respectively. Bands in the range of 1100-1230 cm^{-1} are attributable to C-F stretching [Silverstein (1981)]. The [TMPBI-BuI][MS], [TMPBI-BuI][TFMS] and [TMPBI-BuI][PTS] showed strong absorption band in the region of 1010-1060 cm^{-1} due to alkyl/aryl sulfoxide, while the bands at 1120-1190 cm^{-1} are ascribed to the symmetric SO$_2$ stretching [Silverstein (1981)]. These bands due to [MS] and [PTS] anions were reported for ILs possessing these anions [Golding (2002)]. The bands attributable to N=O and N-O stretching in [TMPBI-BuI][NO$_3$] were noted at 1522 cm^{-1} and 816 cm^{-1}, respectively [Silverstein (1981)].

5.3.3   *Physical properties*

5.3.3.1 Solvent solubility

The solubility of PILs in various solvents is summarized in Table 5.2. The solubility was enhanced after the iodide exchange. PILs with Tf$_2$N$^-$ as an anion ([TMPBI-BuI][Tf$_2$N]) was freely soluble in polar aprotic solvents, viz., cyclohexanone, acetone and acetonitrile (in which the respective iodide counterpart was insoluble). Although, [TMPBI-BuI][BF$_4$] was insoluble in cyclohexanone and acetone, it was soluble in acetonitrile. Effect of anion on solvent solubility of PILs was also observed. Those possessing BF$_4$$^-$, TF$_2N^-$, MS$^-$, TFMS$^-$, PTS$^-$ and NO$_3$$^-$ anions were soluble in acetonitrile. Interestingly, PILs with Ac$^-$, TFAc$^-$, MS$^-$ and Bz$^-$ anion showed solubility even in water and alcohols, while those possessing fluorinated carboxylate anions, viz., HFB$^-$ and TFMS$^-$ were insoluble in water. Hydrophobic nature of these PILs is further supported by their water sorption and contact angle analysis (Section 5.3.3.2). All these PILs were insoluble in other volatile common solvents examined, viz.; chloroform, tetrachloroethane, toluene and ethyl acetate.

Table 5.2 Solvent solubility of PILs investigated.

PILs	DMF	DMAc	DMSO	Cyclo-hexanone	H_2O	Acetone	CH_3CN	CH_3OH	*1*-Propanol
[TMPBI-BuI][I]	++	+	++	−	−	−	−	−	−
[TMPBI-BuI][BF$_4$]	++	++	++	−	−	−	++	−	−
[TMPBI-BuI][Tf$_2$N]	++	++	++	++	−	++	++	±	±
[TMPBI-BuI][Ac]	++	++	++	−	++	−	±	++	++
[TMPBI-BuI][TFAc]	++	++	++	−	++	±	±	++	+
[TMPBI-BuI][HFB]	++	++	++	−	±	−	±	+	+
[TMPBI-BuI][MS]	++	+	+	−	++	±	++	++	++
[TMPBI-BuI][TFMS]	++	++	+	−	−	++	++	+	±
[TMPBI-BuI][PTS]	++	+	+	−	±	−	++	+	±
[TMPBI-BuI][Bz]	++	++	++	−	++	±	±	++	++
[TMPBI-BuI][NO$_3$]	++	+	++	−	−	−	+	++	+
PBI-BuI (base case)	++	++	++	−	−	−	−	−	−

++: Soluble at ambient, +: soluble after heating at 80 ºC / reflux for 24 h in case of low boiling solvent, ±: partially soluble or swelling after heating, −: insoluble.

5.3.3.2 Hydrophilicity of PILs

In view of observed deviations in water solubility of PILs possessing different carboxylate anions, water sorption and contact angle measurement shed further light on their bulk and surface properties, respectively. These properties as summarized in Table 5.1, convey that the anion of PIL indeed dictate these properties, although their polycation remained the same. PILs with Tf$_2$N¯ and TFMS¯ anions (viz., [TMPBI-BuI][Tf$_2$N] and [TMPBI-BuI][TFMS]) showed negligible water sorption. This was in line with their high water contact angle of 89° and 97°, respectively. The hydrophobic nature of PIL with Tf$_2$N¯ anion counterpart was also observed earlier [Dobbelin (2009)]. The PIL, [TMPBI-BuI][HFB] exhibited high water sorption (99.8%) and thus low contact angle of 48°. It was noted that [TMPBI-BuI][NO$_3$] showed appreciable water sorption, which was supported by its lower contact angle of 79°. Thus, the hydrophilicity of PILs can be tuned by exchanging their anion, as also observed by clicking the anion of polyelectrolyte brushes [Azzaroni (2007)] and while tuning the solvent solubility

[Marcilla (2004)]. A wide variation in wettability observed in present cases by a simple anion exchange methodology reveals that they can be used as hydrophobic/hydrophilic switchable surfaces in developing smart devices such as self-cleanness, discrete liquid droplet manipulators or tunable optical lenses [He (2008)].

5.3.3.3 Solution viscosity

The Table 5.2 shows that the inherent viscosity of PILs increased considerably than that of parent PBI-BuI. In order to gain further insights, inherent viscosity at varying concentrations (0.025 to 0.2 g/dL) was obtained.
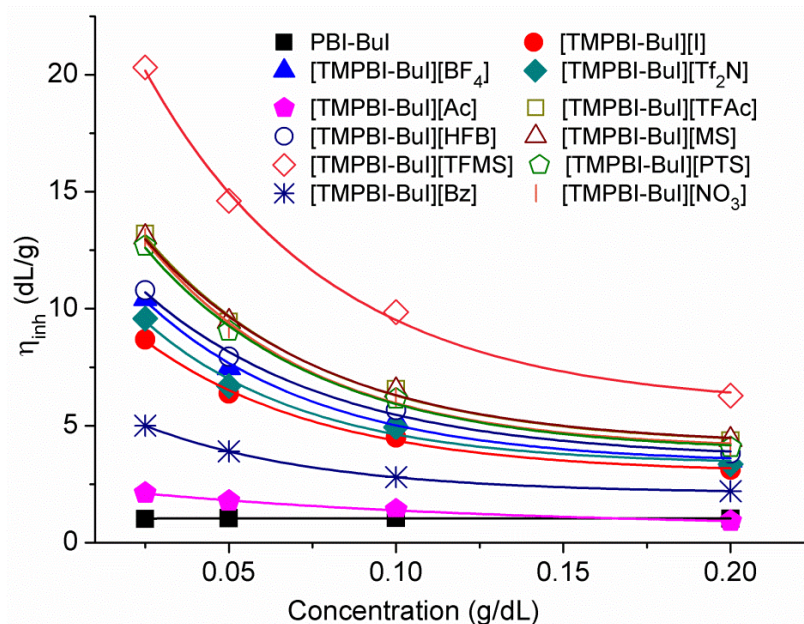
Figure 5.3 Viscosity of PILs as a function of PIL concentration determined at 35 °C.

Figure 5.3 shows that these PILs show a typical polyelectrolyte behavior; wherein viscosity decreased with an increase in the concentration. Such a behavior is known for polyelectrolytes possessing tetralkylammonium as the cation [Bhowmik (2008), Chen (2011), Ono (2012)]. This behavior is attributed to the chain extension at lower concentrations, offering high inherent viscosity than that with higher concentrations. This behavior was not observed for unsubstituted PBI-BuI, as it does not possess any charge in the backbone. The viscosity of PILs varied with variation in the anion. It was interesting to note that [TMPBI-BuI][TFMS] exhibited highest inherent viscosity, while two PILs, viz., [TMPBI-BuI][Ac] and [TMPBI-BuI][Bz]

showed considerably lower inherent viscosity than that of other PILs (Table 5.1). The extreme behavior of these PILs could be because of a large difference in the pKa of conjugate acid of anions (pKa of TFMS$^-$ =−13, Ac$^-$ =−4.76, Bz$^-$ = −4.2) [MacFarlene (2006), Hollingsworth (2002)]. Different behavior of these PILs was observed in case of water solubility, film forming ability, density and thermal stability, as discussed in following sections.

5.3.3.4 Film forming ability

Present PILs, except [TMPBI-BuI][Ac] and [TMPBI-BuI][Bz] exhibited excellent film forming ability as shown in Figure 5.4.
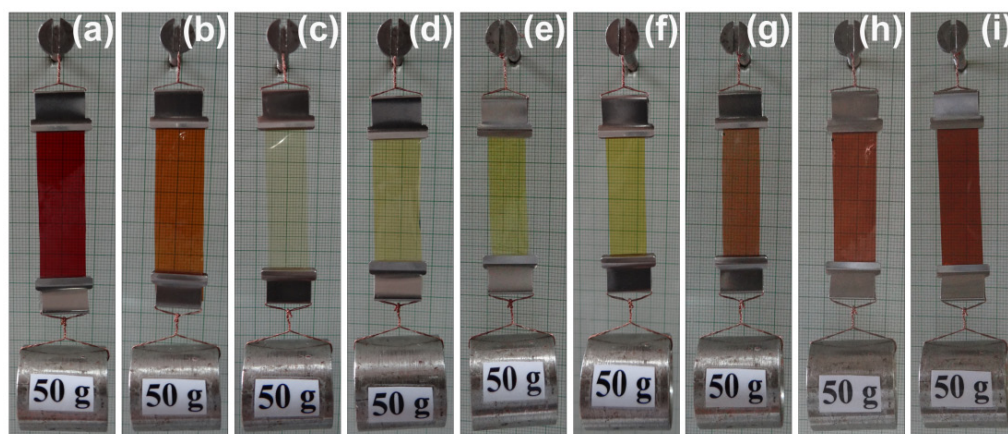

Figure 5.4 Photograph of film forming PILs (a: [TMPBI-BuI][I]; b: [TMPBI-BuI][BF$_4$]; c: [TMPBI-BuI][Tf$_2$N]; d: [TMPBI-BuI][TFAc]; e: [TMPBI-BuI][HFB]; f: [TMPBI-BuI][MS]; g: [TMPBI-BuI][TFMS]; h: [TMPBI-BuI][PTS]; i: [TMPBI-BuI][NO$_3$]).

PIL films (4 cm x 1 cm, prepared by solution casting method) sustained applied load of 50 g for 24 h without any break or tear. On the contrary, many of the PILs based on aliphatic backbone are known to be brittle in nature [Tang (2005e), Hu (2006), Bara (2007b, 2008a), Chapter 2]. This significantly different behavior of present PILs can be attributable to their rigid and fully aromatic backbone. They are synthesized by *N*-quaternization of a mechanically strong polymer, PBI-BuI; followed by the iodide exchange. During this process, even after inducing the IL character, the backbone of PBI remains the same. This rigid aromatic backbone retains its film forming ability even after chemical modification of PBI-BuI. This protocol does not need any external aid such as crosslinking, copolymerization, blending, polymer support, etc. (which are followed in the literature for gaining the film forming ability to PILs). Another aspect of these PILs is that the induced IL character (in the form of imidazolium cation) is located in the

chain backbone itself. On the contrary, most of the reported PILs possess IL character in the side chain grafted to main chain backbone [Green (2009), Mecerreyes (2011), Yaun (2011, 2013)].

It was observed that color of PIL films changes with the variation of backbone and anions they hold (Figure 5.4). The PIL possessing I^- anion was dark brown in color, while those with fluorinated anions are lighter in color. The UV-vis spectra of PILs with varying anions showed difference in their absorption pattern (Figure 5.5), which is in agreement with their observed color. Although variation in anion changes color of the PIL film, anion basicity seems to have no effect on governing the color of PIL. The pKa of conjugate acid of anion decreased in the order: HFB^- (0.4) > NO_3^- (-1.5) > Tf_2N^- (-4.0) > I^- (-7.0) > $TFMS^-$ (13) [MacFarlane (2006)]. The color intensity of PIL films does not follow this order. PILs possessing NO_3^-, I^- and $TFMS^-$ anion exhibited dark brown color, while PILs possessing HFB^- and Tf_2N^- anion are lighter in color (Fig 5.4.). It may be possible that conformation of the chain backbone changes with the anion variation, imparting variations in color. The bulk of anion could be one of the factors responsible for conformational variations.
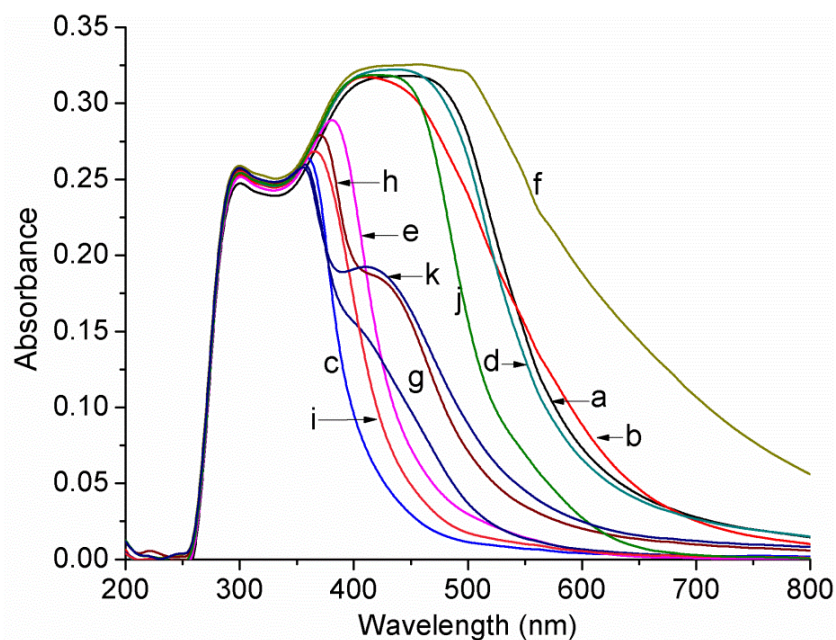
Figure 5.5 UV-vis spectra of PILs (a: [TMPBI-BuI][Ac]; b: [TMPBI-BuI][Bz]; c: [TMPBI-BuI][HFB]; d: [TMPBI-BuI][TFAc]; e: [TMPBI-BuI][BF$_4$]; f: [TMPBI-BuI][NO$_3$]; g: [TMPBI-BuI][MS]; h: [TMPBI-BuI][PTS]; i: [TMPBI-BuI][Tf$_2$N]; j: [TMPBI-BuI][I]; k: [TMPBI-BuI][TFMS]).

5.3.3.5 Mechanical property analysis

The film forming ability of present PILs prompted necessity of analyzing their mechanical properties. The tensile strength, modulus and percent elongation of PILs investigated at the ambient is summarized in Table 5.3, while respective stress-strain curves are given in Figure 5.6. It could be seen that PILs exhibited lower tensile strength and modulus than their parent PBI-BuI. This is mainly attributable to the difference in interchain interactions present within a PIL and PBI matrix. In PBI-BuI, presence of H-bonding provides strong interchain interactions and thus high mechanical strength [Li (2009a)]. During the formation of a PIL by *N*-quaternization, the H-bonding present in PBI-BuI is now eliminated; lowering interchain interactions in the formed polycation. This leads to lowering in mechanical properties of a PIL in comparison to its parent PBI-BuI. In spite of this, all PILs (except the two: [TMPBI-BuI][Ac] and [TMPBI-BuI][Bz]) formed strong films. This signifies present approach of PIL formation, wherein, the backbone of the parent rigid PBI-BuI remains the same after inducing IL character in it. On the contrary, most of the PILs known in the literature (including those based on single backbone and varying anions) do not exhibit film forming nature, owing aliphatic nature of their backbone.
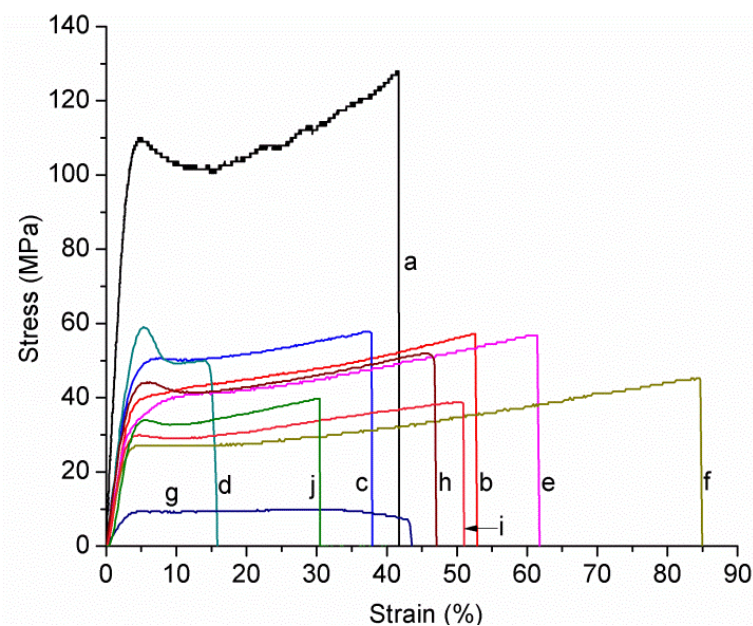
Figure 5.6 Stress-strain curve of PILs (a: PBI-BuI; b: [TMPBI-BuI][I]; c: [TMPBI-BuI][BF$_4$]; d: [TMPBI-BuI][Tf$_2$N]; e: [TMPBI-BuI][TFAC]; f: [TMPBI-BuI][HFB]; g: [TMPBI-BuI][MS]; h: [TMPBI-BuI][TFMS]; i: [TMPBI-BuI][PTS]; j: [TMPBI-BuI][NO$_3$]).

Table 5.3 Mechanical properties of PILs.

PILs	Tensile strength (MPa)	Modulus (MPa)	% Strain at break
[TMPBI-BuI][I]	55.6	1312	48.2
[TMPBI-BuI][BF$_4$]	59.6	1400	44.8
[TMPBI-BuI][Tf$_2$N]	56.4	1583	15.6
[TMPBI-BuI][TFAc]	60.7	1184	68.7
[TMPBI-BuI][HFB]	46.7	972	90.3
[TMPBI-BuI][MS]	8.6	287	39.1
[TMPBI-BuI][TFMS]	57.3	1353	57.9
[TMPBI-BuI][PTS]	40	1063	50.1
[TMPBI-BuI][NO$_3$]	55.6	1312	48.2
PBI-BuI (base case)	129	3625	41.6

Anions found to play a crucial role in governing mechanical properties of PILs. Among the PILs investigated, [TMPBI-BuI][Tf$_2$N] showed high modulus than that of PILs containing other anion. PILs with TFAc⁻ and HFB⁻ anion showed high elongation (Figure 5.6). This could be due to their highly hydrophilic nature, as assessed by water sorption and contact angle measurement. They might have absorbed moisture during the sample loading and / or testing. This study revealed that in general, PILs based on PBI backbone exhibited good mechanical strength, in which, anion play their role in governing these properties.

5.3.3.6 Chain packing: WAXD and density analysis

The WAXD patterns of present PILs are shown in Figure 5.7. It could be seen that in spite of introducing distinct ionic characters, PILs remained amorphous in nature. This could be due to the adopted methodology for their synthesis, where rigid aromatic PBI-BuI backbone would inhibit ordered packing arrangement. It may also be possible that good solvent solubility of these PILs restrict phase segregation. The *d*-spacing (d$_{sp}$) of PILs corresponding to the amorphous peak maxima in the respective WAXD patterns is given in Table 5.1.
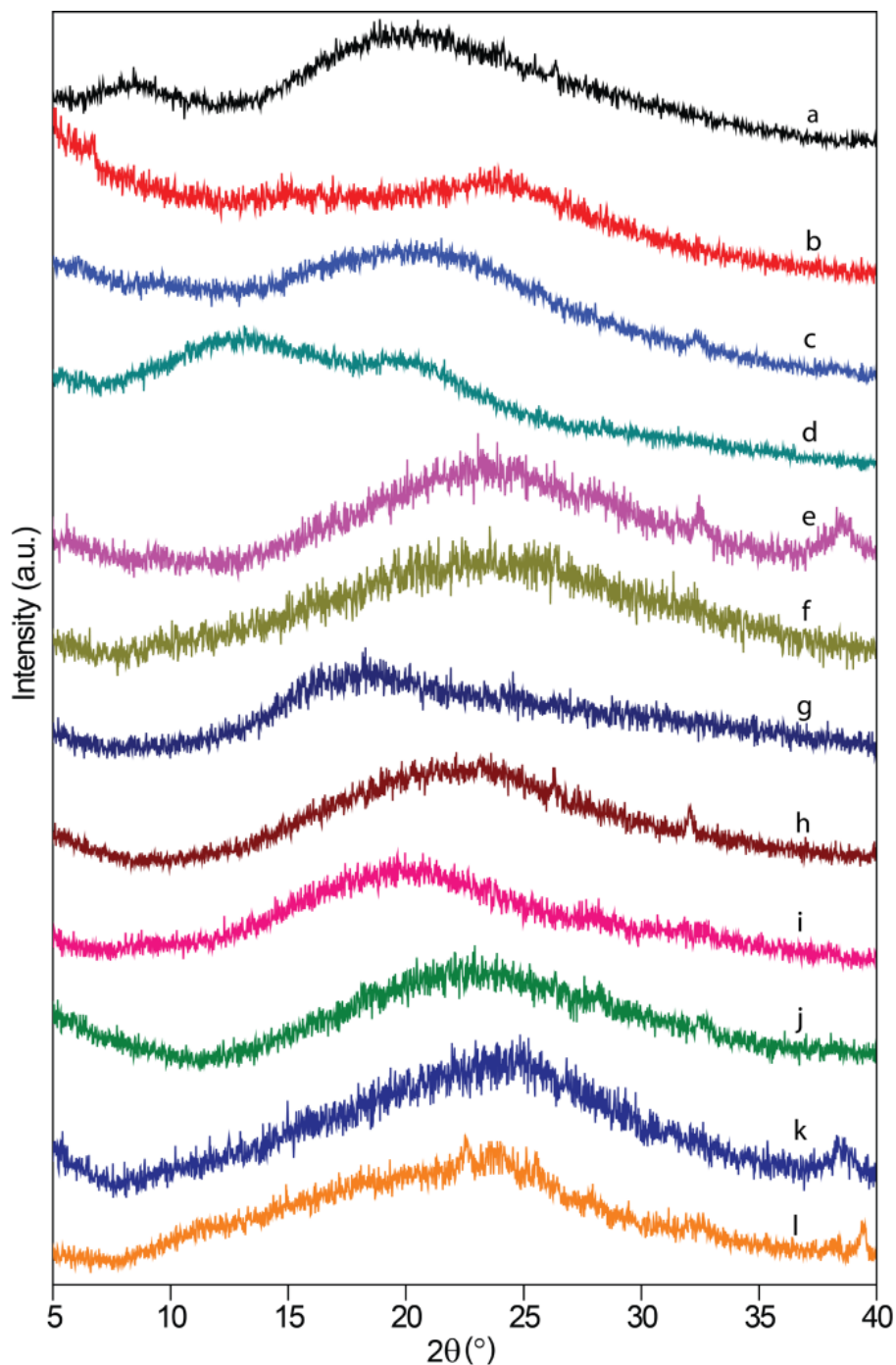
Figure 5.7 Wide angle X-ray diffraction patterns of PILs (a: PBI-BuI; b: [TMPBI-BuI][I];
c: [TMPBI-BuI][BF_4]; d: [TMPBI-BuI][Tf_2N]; e: [TMPBI-BuI][Ac]; f: [TMPBI-BuI][TFAC];
g: [TMPBI-BuI][HFB]; h: [TMPBI-BuI][MS]; i: [TMPBI-BuI][TFMS]; j: [TMPBI-BuI][PTS];
k: [TMPBI-BuI][Bz]; l: [TMPBI-BuI][NO_3]).

It is evident from Figure 5.7 that the nature of anion had its own effect on governing the

chain packing in PIL. The d_{sp} in PILs possessing $TFMS^-$, HFB^- and Tf_2N^- as an anion was

higher than those with other anions. This is attributable to the bulkier nature of fluorinated anions.

The density of PILs was generally higher than the respective unsubstituted PBI-BuI, indicating closer chain packing in their matrix. It is qualitatively supported by the WAXD analysis. In spite of added bulk of the anion, d_{sp} of PIL did not increase considerably than their parent PBI. Density of the PILs varied in the order of their anion as $Ac^- < Bz^- < BF_4^- < PTS^- < NO_3^- < MS^- < TFAc^- < TFMS^- < HFB^- < I^- < Tf_2N^-$ (Table 5.1). It was also noted that the density of PILs increased with increasing number of fluorine atoms in the anion belonging to carboxylate as well as sulfonate family ($Ac^- < TFAc^- < HFB^-$ and $MS^- < TFMS^-$). This behavior of higher density for PILs with fluorinated anion than their non-fluorinated analogue was also observed in P[DADMA] based PILs [Chapter 2]. Among all these PILs, [TMPBI-BuI][Ac] showed lowest density; as also observed earlier in the case of P[DADMA] based PILs [Chapter 2]. These observations suggest that the anion also plays a profound role in governing density of PIL, irrespective of the backbone being aliphatic or aromatic.

5.3.3.7 Thermal stability of PILs

TGA curves of these PILs are shown in Figure 5.8 and their initial decomposition temperature (IDT) is given in Table 5.1. It could be seen that PILs exhibited lower thermal stability than their parent PBI-BuI. This decreased thermal stability could be attributed to multiple reasons. Addition of an alkyl group in PIL eliminating H-bonding in PBI could be one of the primary reasons. Such lowering in IDT was also observed for disubstituted PBIs by couple of alkyl groups [Kumbharkar (2009a)] and previous work on PILs based on PBI [Kumbharkar (2008)]. Another reason could be the induced ionic character that could be vulnerable to thermo-oxidative conditions. Chen et al. (2012b), reported that the thermal stability of quaternized polymers is lower than their unquaternized counterparts. Not only these two, but the nature of anion was found to have a significant effect on governing the thermal stability of PILs. As could be seen from thermograms (Figure 5.8), thermal stability of PILs increased in the order of anion variation as: $Bz^- < HFB^- < Ac^- < TFAc^- < NO_3^- < I^- < MS^- < BF_4^- < PTS^- < TFMS^- < Tf_2N^-$. In the series, [TMPBI-BuI][Tf$_2$N] showed highest IDT (465 °C) and [TMPBI-BuI][Bz] showed lowest IDT (136 °C). The higher thermal stability of PIL with Tf_2N^- anion than that with halide anion is known [Hsieh (2010)]. In comparison to the present PIL with iodide anion,

thermal stability of PILs possessing carboxylated anions was lower. On the contrary, PILs with sulfonated anions showed higher thermal stability than the parent PIL. Our previous investigation on PILs based on P[DADMA] as a polycation shown similar variations in thermal stability by variation in their anion [Chapter 2]. A lower thermal stability of PILs with carboxylated anion could be because of higher basicity of these anions. Wang et al. (2011), reported that the thermal stability of IL decrease with increasing basicity of anion.

Glass transition temperature (T_g) of only few PILs could be detected in the DSC thermogram. The T_g of [TMPBI-BuI][Tf$_2$N], [TMPBI-BuI][MS] and [TMPBI-BuI][TFMS] was 189 °C, 254 °C and 308 °C, respectively; indicating glassy nature of these PILs (Table 5.1).
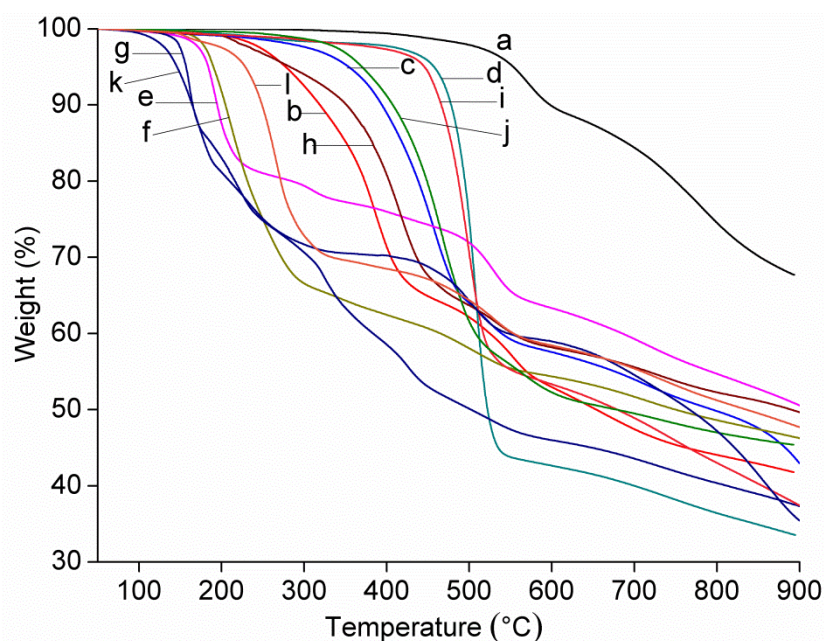

Figure 5.8 TGA curve of PILs (a: PBI-BuI; b: [TMPBI-BuI][I]; c: [TMPBI-BuI][BF$_4$]; d: [TMPBI-BuI][Tf$_2$N]; e: [TMPBI-BuI][Ac]; f: [TMPBI-BuI][TFAC]; g: [TMPBI-BuI][HFB]; h: [TMPBI-BuI][MS]; i: [TMPBI-BuI][TFMS]; j: [TMPBI-BuI][PTS]; k: [TMPBI-BuI][Bz]; l: [TMPBI-BuI][NO$_3$]).

5.3.4 Gas permeation properties

All PIL membranes investigated sustained high upstream pressure (20 atm) during their gas permeation analysis. Such high pressure sustainability without any failure is promising towards their practical applicability, since industrial scale gas separations (e.g. CO$_2$ separation from natural gas) are usually performed at high pressures [Li (2011)]. The rigid aromatic

backbone of this new family of PILs may be helpful in inducing observed pressure sustainability. The gas permeation data of these PILs obtained at 20 atm upstream pressur is given in Table 5.4.

With an increase in d_{sp} of present PILs, a general increase in P_{H_2} and P_{CO_2} was observed (Figure 5.9). This behavior is in accordance with the glassy nature of present PILs.
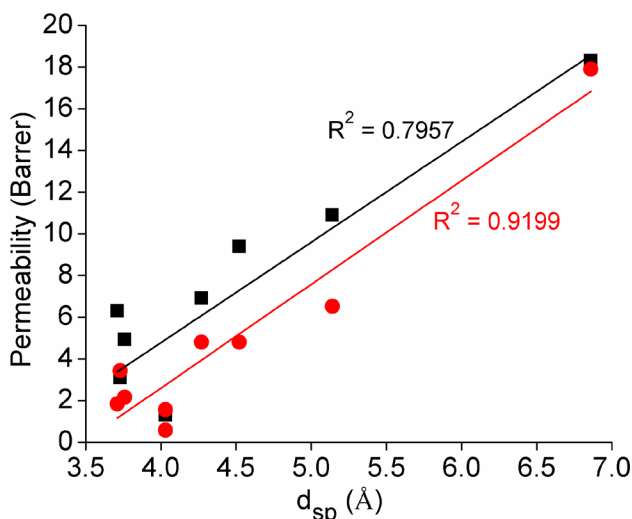
Figure 5.9 Variation in H_2 (■) and CO_2 (●) permeability with d_{sp} of PILs.

Table 5.4 Permeability coefficient (P)[a] and permselectivity (P_A/P_B) of PILs.

PILs	P_{He}	P_{H_2}	P_{N_2}	P_{CH_4}	P_{CO_2}	$\dfrac{P_{He}}{P_{H_2}}$	$\dfrac{P_{He}}{P_{CH_4}}$	$\dfrac{P_{H_2}}{P_{N_2}}$	$\dfrac{P_{H_2}}{P_{CH_4}}$	$\dfrac{P_{H_2}}{P_{CO_2}}$	$\dfrac{P_{CO_2}}{P_{N_2}}$	$\dfrac{P_{CO_2}}{P_{CH_4}}$	$\dfrac{P_{N_2}}{P_{CH_4}}$
[TMPBI-BuI][I]	5.0	6.3	0.06	0.05	1.84	0.79	100	105	126	3.4	31	37	1.2
[TMPBI-BuI][BF$_4$]	9.1	6.9	0.20	0.10	4.8	1.32	91	35	69	1.4	24	48	2.0
[TMPBI-BuI][Tf$_2$N]	26	18.3	0.78	0.42	17.9	1.42	62	23	44	1.0	23	43	1.9
[TMPBI-BuI][TFAc]	6.9	4.9	0.13	0.05	2.16	1.41	138	38	98	2.3	17	43	2.6
[TMPBI-BuI][HFB]	19.8	12.8	0.49	0.21	6.52	1.55	94	26	61	2.0	13	31	2.3
[TMPBI-BuI][MS]	2.1	1.4	0.03	0.016	1.56	1.50	131	47	88	0.9	52	98	1.9
[TMPBI-BuI][TFMS]	11.7	9.4	0.23	0.12	5.85	1.24	98	41	78	1.6	25	49	1.9
[TMPBI-BuI][PTS]	2.3	1.3	0.02	0.008	0.64	1.77	288	65	163	2.0	32	80	2.5
[TMPBI-BuI][NO$_3$]	3.3	3.1	0.09	0.05	3.43	1.06	66	34	62	0.9	38	69	1.8
PBI-BuI[b] (base case)	10.1	10.7	0.06	0.05	1.91	0.94	202	178	214	5.6	32	38	1.2

[a]: Determined at 20 atm upstream pressure, expressed in Barrer (1 Barrer = 10^{-10} cm^3(STP).cm/cm^2.s.cm Hg), [b]: Ref. [Kumbharkar (2006)].

A closer look at their permeation properties (Table 5.4) reveals that many of them possessed a good combination of permeability (P_{He}, P_{H_2} and P_{CO_2}) and selectivity (P_{H_2}/P_{CH_4}, P_{H_2}/P_{N_2}, P_{CO_2}/P_{CH_4}). One of the important peculiarities of present PILs is that many of them (esp. [TMPBI-BuI][Tf$_2$N], [TMPBI-BuI][MS] and [TMPBI-BuI][NO$_3$]) exhibited P_{H_2}/P_{CO_2} closer to ~ 1. This high P_{CO_2} seems to be an important outcome of inducing IL character in the present glassy PILs.

The role of IL character in governing CO_2 permeation of these PILs is seen in Figure 5.10, where CO_2 permeability is considerably elevated than that of the parent PBI, while selectivity is changed only marginally.
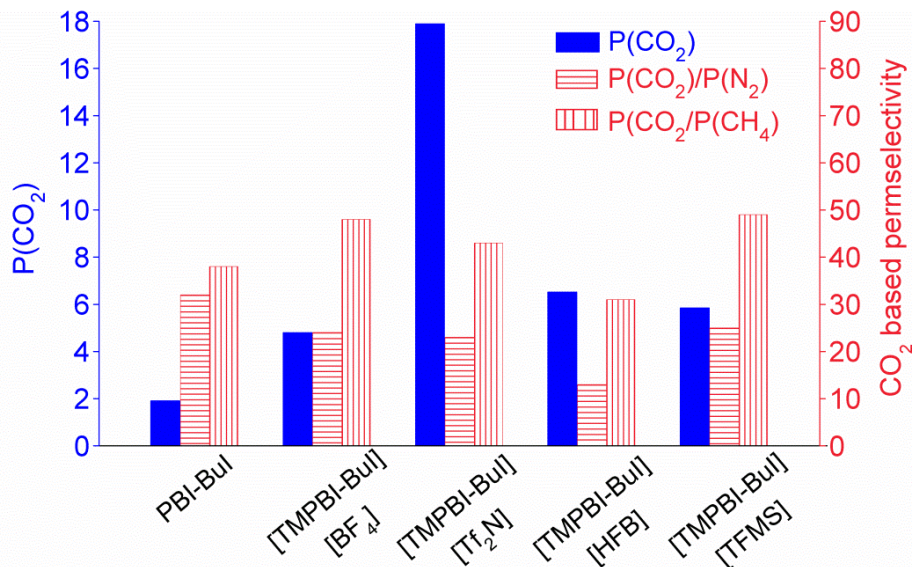
Figure 5.10 CO_2 permeability and permselectivity over N_2 and CH_4 of PILs based on PBI-BuI.

As a result of elevation in P_{CO_2}, the CO_2 based ideal selectivity (esp. P_{CO_2}/P_{CH_4}) of present PILs is generally higher than usual glassy polymers (e.g. Matrimid, PSF, PPO, PC [Sanders (2013)]) and most of the reported PILs; as could be seen from Figure 5.11. The data of PILs taken from the literature is given in Table 1.2 of the Chapter 1. It is evident that present PILs are placed at the left-upper corner of Robeson upper bound [Robeson (2008)] (Figure 5.11), possessing attractive P_{CO_2}/P_{CH_4} selectivity. Some of the present PILs exhibited higher CO_2 permeability as well as selectivity than that of Matrimid, PC and PSF. Their lower permeability

in comparison to the reported PILs [Hu (2006), Bara (2007b), Bara (2008a), Hudiono (2011), Li (2011, 2012), Hao (2013), Carlisle (2013), Chi (2013)] could be attributed to couple of reasons. Present PILs possess rigid PBI-based backbone than the aliphatic (and flexible) backbone of known PILs. Secondly, the permeability of known PILs is reported at lower pressure (of ~ 2 atm), while present PILs are investigated at 20 atm. It is well known that CO_2 permeability reduced with the applied pressure [Hu (2003), Ghosal (1996)].
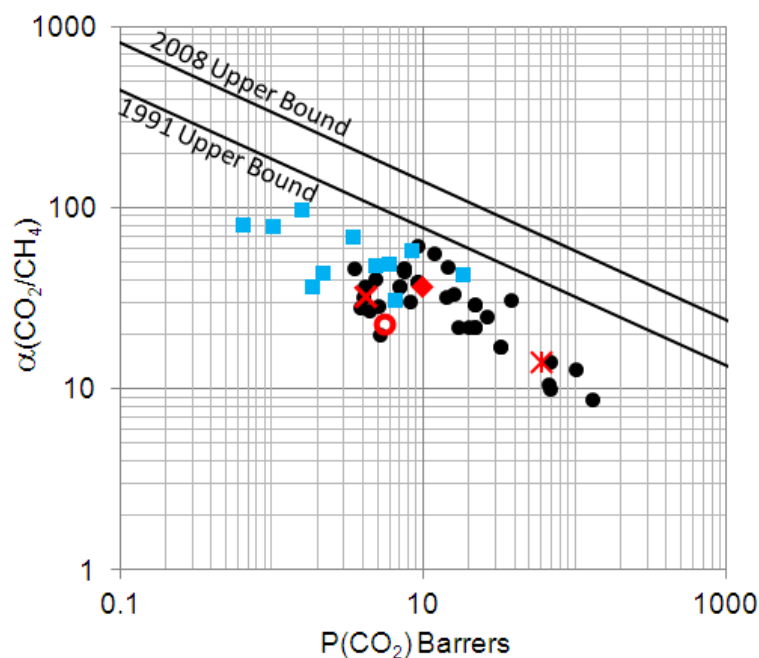
Figure 5.11 Comparison of CO_2 permeability and CO_2/CH_4 permselectivity of present PILs (■) with that of reported PILs (●) and commercially relevant polymers [Matrimid (◆), PC (○), PSF (✖), PPO (✳)].

Another peculiarity of present PILs is that many of them exhibited higher helium permeability than that of H_2. The P_{He}/P_{H_2} of ~ 1.5-1.77 for [TMPBI-BuI][HFB], [TMPBI-BuI][MS] and [TMPBI-BuI][PTS] is remarkably higher than for the common glassy polymers for which P_{He}/P_{H_2} selectivity lies between 0.9 to 1.1. Present PILs possessed a large variation in their gas permeation properties with the variation in backbone polycation as well as variation in anion, as discussed below.

5.3.4.1 Effects of polycation backbone on gas permeation

In order to compare the effect of backbone variation, present PILs were compared with the earlier reported PILs based on PBI-I and ABPBI [Kumbharkar (2008)]. It was observed that for PILs with a particular anion and methyl substituent, gas permeability increased in the order of variation in polycation backbone as: [DMABPBI] < [TMPBI-I] < [TMPBI-BuI]. This follows the same order of increasing gas permeability of their parent PBIs. It should be noted that PBI-BuI has comparatively open matrix than that of PBI-I and ABPBI owing to the presence of bulky *tert*-butyl group in its backbone. The overall higher CO_2 permeation in PILs based on PBI-BuI than PILs based on other two PBIs indicated structural variations in PBI has significant role in governing CO_2 permeation in PILs and can serve as an effective tool in PIL structure architecture.

In the present case of [TMPBI-BuI] as a polycation backbone, although permeability of other gases varied based on the anion they hold, P_{CO_2} and P_{CO_2}/P_{CH_4} are generally higher than that of parent PBI-BuI. Within this series of PILs, those with BF_4^-, Tf_2N^-, HFB^- and $TFMS^-$ anion possessed good combination of P_{CO_2} and CO_2 based selectivity; while those with MS^-, PTS^- and NO_3^- possessed highly attractive P_{CO_2}/P_{CH_4} selectivity.

5.3.4.2 Effect of anion variation on gas permeation

It could be seen from Table 5.4 that PILs possessing bulkier anion (Tf_2N^- or HFB^-) exhibited higher gas permeability. The looser chain packing caused by these bulky anions is supported by the higher d_{sp} of these PILs (Table 5.1). PILs possessing I^-, MS^-, PTS^- and NO_3^- anion exhibited lower permeability than the parent PBI-BuI (as a result of lowering in their d_{sp}). Although observed variation in the gas permeability can be roughly correlated with the variation in the d_{sp} of PILs (Figure 5.9), effects of anion and cation properties and gas sorption in these PILs would have their own effect.

Table 5.4 shows that [TMPBI-BuI][TFMS] possessing fluorinated anion exhibited higher gas permeability than its non-fluorinated analog, [TMPBI-BuI][MS]. The role of fluorinated groups in enhancing permeability is well known in various types of polymers, e.g. polysulfone, polycarbonate and polyimide [McHattie (1992), Hellums (1989), Calle (2010)]. The aspect of P_{H_2}/P_{CO_2} approaching to ~1 is not only obeyed by PILs possessing Tf_2N^- anion (higher

permeability), but also by PILs possessing MS^- and NO_3^- anions, which have low permeability. Generally, improved CO_2 permeability of present PILs than their parent PBI-BuI, high P_{CO_2}/P_{CH_4} selectivity (than reported PILs and conventional glassy polymers) and P_{H_2}/P_{CO_2} of ~ 1 for some of them necessitated the need to investigate gas sorption in them, as discussed below.

5.3.5 *Gas sorption*

The sorption isotherms for present PILs using pure gases (H_2, N_2, CH_4 and CO_2) obtained at 35 °C showed a typical dual-mode nature (Figure 5.12), as usually observed for glassy polymers [Karadkar (2007), Li (2013)]. The DSC analysis of these PILs could detect a high glass transition temperature (T_g) for only some of them, allowing to speculate their glassy nature, since they hold the rigid PBI backbone (Table 5.1).
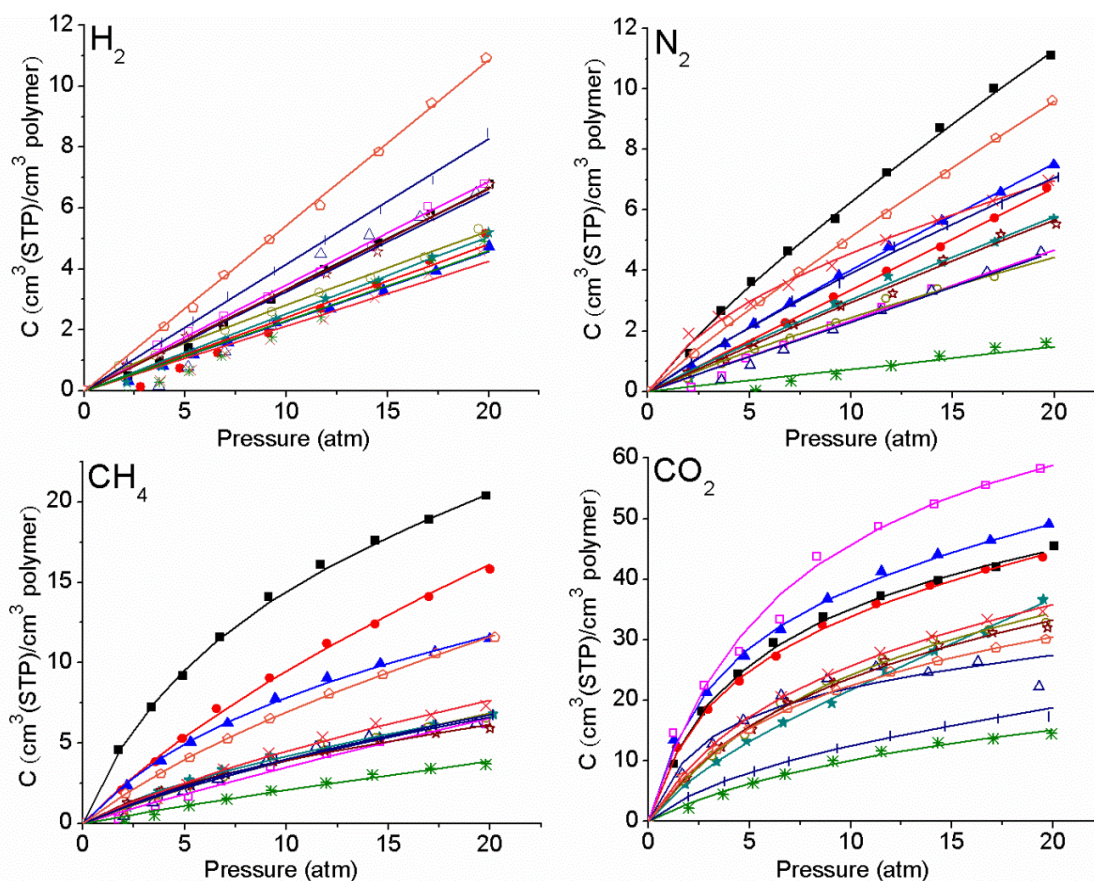
Figure 5.12 Gas sorption isotherm of PILs based on PBI-BuI at 35 °C (●: [TMPBI-BuI][I], ▲: [TMPBI-BuI][BF₄], ★: [TMPBI-BuI][Tf₂N], □: [TMPBI-BuI][Ac], ○: [TMPBI-BuI][TFAc], △: [TMPBI-BuI][HFB], ☆: [TMPBI-BuI][MS], ×: [TMPBI-BuI][TFMS], ✳: [TMPBI-BuI][PTS], ∣: [TMPBI-BuI][Bz], ⬠: [TMPBI-BuI][NO₃], while the solid lines represent the best fit obtained using the dual-mode model).

The sorption of different gases in present PILs is increased in the order: $H_2 < N_2 < CH_4 < CO_2$. This followed the order of increasing inherent condensabilities of these gases (critical temperature, T_c, of H_2, N_2, CH_4 and CO_2 increases in the order: 32.98 K < 126.20 K < 190.56 K < 304.12 K [Li (2009b)], respectively). This observation was common for all the PILs. Figure 5.12 shows that for present PILs, there is a large variation in the sorption of a particular gas.

Table 5.5 Solubility coefficient (S)[a] and solubility selectivity (S_A/S_B) of PILs at 20 atm.

| PILs	S_{H_2}	S_{N_2}	S_{CH_4}	S_{CO_2}	S_{N_2}/S_{CH_4}	S_{CO_2}/S_{H_2}	S_{CO_2}/S_{N_2}	S_{CO_2}/S_{CH_4}
[TMPBI-BuI][I]	0.40	0.34	0.81	2.22	0.42	5.55	6.53	2.74
[TMPBI-BuI][BF$_4$]	0.23	0.38	0.58	2.46	0.66	10.7	6.47	4.24
[TMPBI-BuI][Tf$_2$N]	0.25	0.29	0.34	1.84	0.85	7.36	6.34	5.41
[TMPBI-BuI][Ac]	0.34	0.23	0.33	2.95	0.71	8.68	12.60	8.98
[TMPBI-BuI][TFAc]	0.26	0.22	0.34	1.72	0.65	6.62	7.78	5.03
[TMPBI-BuI][HFB]	0.33	0.23	0.33	1.37	0.69	4.15	5.96	4.14
[TMPBI-BuI][MS]	0.33	0.28	0.31	1.66	0.92	5.03	5.88	5.41
[TMPBI-BuI][TFMS]	0.21	0.35	0.38	1.79	0.91	8.52	5.14	4.68
[TMPBI-BuI][PTS]	0.23	0.07	0.19	0.75	0.38	3.26	10.17	3.88
[TMPBI-BuI][Bz]	0.41	0.35	0.34	0.94	1.04	2.29	2.66	2.77
[TMPBI-BuI][NO$_3$]	0.54	0.48	0.58	1.53	0.83	2.83	3.18	2.63
PBI-BuI[b] (base case)	0.33	0.57	1.04	2.24	0.55	6.79	3.93	2.15

[a]: Expressed in $cm^3(STP)/cm^3polymer.atm$, [b]: Ref. [Kumbharkar 2006].

5.3.5.1 Effect of polycation backbone on the gas sorption in PILs

Table 5.5 presents the solubility coefficient (S) and solubility selectivity (S_A/S_B) for different PILs at 20 atm. It could be seen that the solubility coefficient (S) of PBI-BuI based PILs exhibited general lowering in the sorption coefficient of gases (except for a couple of H_2 and CO_2 cases). It was reported that solubility coefficient of ABPBI based PILs was higher than that of parent ABPBI, while in case of PBI-I based PILs, variations in the sorption coefficient of different gases in comparison to their parent PBI-I were marginal [Kumbharkar (2008)]. Observed variations from a PBI to PIL could be explained on the basis of variations in the chain packing density of PBIs, which increases in the order: PBI-BuI < PBI-I < ABPBI. This is

assessed by their d_{sp} or fractional free volume (v_f of ABPBI, PBI-I and PBI-BuI are: 0.279, 0.309 and 0.339; respectively [Kumbharkar (2008)]). After the *N*-quaternization, although chain packing density is anticipated to decrease in case of ABPBI and PBI-I, this may not be necessarily obeyed by PBI-BuI. In case of PBI-BuI based PILs, bulk of the added methyl group and that of anion could be accommodated in the initially available free space of PBI-BuI. This could be possible due to the looser chain packing of PBI-BuI as evidenced by its higher d_{sp} or v_f than that of PBI-I or ABPBI.

Irrespective of variations observed in the gas sorption, CO_2 based sorption selectivities (Table 5.5) are generally increased in all PILs, than that of parent PBI. In other words, incorporation of IL character in a PBI has improved its CO_2 sorption specificity, a niche property of IL character. This was also supported by the improvement in the CO_2 sorption expressed in mol % for most of the PILs than their precursor PBI-BuI (Figure 5.13).
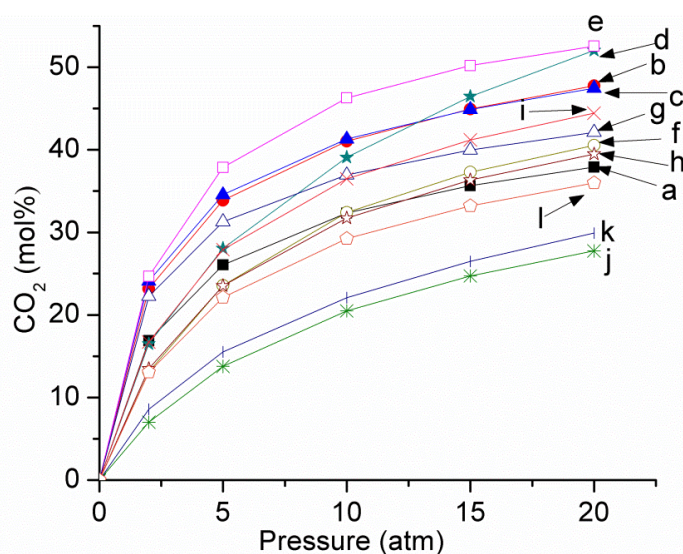
Figure 5.13 CO_2 sorption isotherms of PILs at 35 °C represented in mol %; w.r.t. the molecular weight of PIL repeat unit (a: PBI-BuI, b: [TMPBI-BuI][I], c: [TMPBI-BuI][BF$_4$], d: [TMPBI-BuI][Tf$_2$N], e: [TMPBI-BuI][Ac], f: [TMPBI-BuI][TFAc], g: [TMPBI-BuI][HFB], h: [TMPBI-BuI][MS], i: [TMPBI-BuI][TFMS], j: [TMPBI-BuI][PTS], k: [TMPBI-BuI][Bz], l: [TMPBI-BuI][NO$_3$]).

5.3.5.2 *Effect of variation of anion on CO$_2$ sorption*

It was observed that PILs possessing Tf$_2$N$^-$, TFAc$^-$, HFB$^-$, MS$^-$, TFMS$^-$, PTS$^-$, Bz$^-$ and NO$_3^-$ anion showed general decrease in the gas sorption than that of the precursor PBI-BuI (Table 5.5). This could be correlated to the accommodation of anion in the available free space

as well as to the reduction in 'microvoids' or the unrelaxed volume as a result of inducing ionic character in the PIL backbone. As seen from Table 5.1, d_{sp} of PILs was reduced than their parent PBI-BuI (with an exception of [TMPBI-BuI][Tf$_2$N]). Li et al. (2013), have observed a similar decrease in the CO_2 sorption with an increase in IL group concentration ([C$_{12}$(DAPIM)$_2$][NTf$_2$]$_2$) in co-polyimides. The reduction in free volume was said to be responsible for the decrease in gas sorption and it was more dominant factor than the polymer-gas interactions. In the present study, although S_{CO_2} in PILs was decreased, the CO_2 based sorption selectivities, viz., S_{CO_2}/S_{N_2} and S_{CO_2}/S_{CH_4} were increased in almost all the cases, than their precursor PBI-BuI. This increase was made possible even after inducing ionic liquid character (that is reducing 'microvoids' or the unrelaxed volume in the PBI-BuI matrix as shown by lowering in d_{sp}). Thus, in comparison to the common glassy polymers, PILs can favorably sorb CO_2.

In cases of PILs with carboxylate anion, CO_2 solubility decreased (Figure 5.12) in the order of their anion as Ac$^-$ > TFAc$^-$ > HFB$^-$; while in case of PILs with sulfonated anions (and MS$^-$ and TFMS$^-$), the CO_2 sorption was almost similar. From these examples, it would be too early to conclude on the effect of fluorine content in the anion and more work would be necessary. In view of the polymeric nature of present PILs, unlike ionic liquids, nature of anions or cations may not be the only controlling parameters for governing the CO_2 sorption. It would have been worth to estimate the fractional free volume (v_f) of present PILs, but could not be attempted due to unavailability of Van der waal's volume of anions used and any speculation made on 'microvoids' or the unrelaxed volume in the present PILs is based on observed d_{sp}. It would be prudent to have a close look at gas sorption parameters, as discussed below.

5.3.5.3 Gas sorption parameters

The gas sorption parameters (k_D, b and C$'_H$) for present PILs are given in Table 5.6. It could be seen that Henry's solubility coefficient, k_D (ascribed to the gas dissolution in rubbery state) was lower for all the gases. It could be attributable to the glassy nature of these PILs. For present PILs, k_D did not vary significantly than that of parent PBI. This parameter is also known to be dependent on the gas-polymer interaction [Barbari (1988)]. The C$'_H$ is considered as the hole-filling constant, which represents maximum amount of the penetrant sorbed into

'microvoids' or the unrelaxed volume of the polymer matrix [Barbari (1988), Kanehashi (2005)]. It is worth to note its remarkably high value for CO_2.

Table 5.6 Dual-mode sorption parameters[a] obtained during gas sorption in PILs.

PILs	H_2			N_2			CH_4			CO_2		
	k_D	C'_H	B	k_D	C'_H	B	k_D	C'_H	b	k_D	C'_H	b
[TMPBI-BuI][I]	0.240	0.63	3×10^{-5}	0.335	0.71	0.001	0.473	11.2	0.074	0.645	37.2	0.282
[TMPBI-BuI][BF$_4$]	0.228	0.18	4.8×10^{-4}	0.295	3.30	0.048	0.200	11.3	0.108	0.633	42.6	0.302
[TMPBI-BuI][Tf$_2$N]	0.253	0.18	3×10^{-4}	0.244	1.62	0.060	0.210	3.5	0.148	1.386	10.6	0.295
[TMPBI-BuI][Ac]	0.321	1.17	0.029	0.233	0.84	0.0001	0.233	5.0	0.031	0.261	70.9	0.16
[TMPBI-BuI][TFAc]	0.242	0.43	0.999	0.163	2.01	0.068	0.215	4.6	0.062	0.306	42.8	0.098
[TMPBI-BuI][HFB]	0.326	2.67	1.8×10^{-5}	0.230	1.99	5.4×10^{-5}	0.164	6.2	0.059	0.300	24.4	0.357
[TMPBI-BuI][MS]	0.328	1.97	0.0015	0.227	3.29	0.026	0.162	3.9	0.142	0.405	35.0	0.128
[TMPBI-BuI][TFMS]	0.212	3.0	3.5×10^{-5}	0.185	4.10	0.199	0.194	7.2	0.054	0.479	34.9	0.149
[TMPBI-BuI][PTS]	0.228	6.0	0.0002	0.073	1.45	9.4×10^{-5}	0.118	4.9	0.222	0.182	18.3	0.083
[TMPBI-BuI][Bz]	0.396	1.41	0.016	0.265	2.93	0.074	0.209	3.9	0.095	0.452	12.5	0.174
[TMPBI-BuI][NO$_3$]	0.542	1.14	0.0006	0.414	1.99	0.098	0.309	9.2	0.071	0.361	30.5	0.161
PBI-BuI[b] (base case)	0.333	0.42	0.0002	0.456	3.01	0.132	0.327	18.8	0.146	0.438	43.7	0.237

[a]: k_D is expressed in $cm^3(STP)/cm^3 polymer.atm$, C'_H is expressed in $cm^3(STP)/cm^3 polymer$, while b is expressed in atm^{-1}, [b]: Ref. [Kumbharkar (2006)].

For all PILs, C'_H was favourably higher for CO_2 than that of other gases. This is in accordance with the gas sorption behaviour observed for most of the common glassy polymers [Kumbharkar (2006), Karadkar (2007), McHattie (1992), Barbari (1988)], possessing high C'_H for CO_2 than for other gases. The Langmuir affinity constant 'b' is the ratio of rate constants of sorption and desorption processes and characterizes the sorption affinity for particular gas-polymer system [Pixton (1995b)]. This parameter is negligible for H_2 and N_2 than that for CH_4. It is considerably higher in case of CO_2. For a particular PIL, both, C'_H and b were increased with increasing the order of gas condensability.

### 5.3.6 *Analysis of diffusivity*

The diffusion coefficient of gases for the present PILs estimated based on permeability and solubility coefficient are given in Table 5.7. Among present PILs, those with fluorinated anions possessed high diffusivity, as anticipated. As could be seen from the Figure 5.14, the diffusivity coefficient was found to correlate well with the kinetic diameter of gases [Kumbharkar (2006), Karadkar (2007)]. Similarly, it could be seen from Figure 5.15 that the diffusivity of gases can be roughly correlated with the d_{sp} of PILs.

Table 5.7 Diffusivity coefficient (D)[a] of gases in PILs and diffusivity selectivity (D_A/D_B) estimated at 20 atm.

PILs	D_{H_2}	D_{N_2}	D_{CH_4}	D_{CO_2}	$\dfrac{D_{H_2}}{D_{N_2}}$	$\dfrac{D_{H_2}}{D_{CO_2}}$	$\dfrac{D_{N_2}}{D_{CH_4}}$	$\dfrac{D_{CO_2}}{D_{N_2}}$	$\dfrac{D_{CO_2}}{D_{CH_4}}$
[TMPBI-BuI][I]	11.9	0.13	0.05	0.63	92.1	19.0	2.6	4.8	12.6
[TMPBI-BuI][BF$_4$]	22.8	0.40	0.13	1.48	57.0	15.4	3.1	3.7	11.4
[TMPBI-BuI][Tf$_2$N]	55.6	2.04	0.94	7.39	27.3	7.5	2.2	3.6	7.9
[TMPBI-BuI][TFAc]	14.3	0.45	0.11	0.95	31.8	15.1	4.1	2.1	8.6
[TMPBI-BuI][HFB]	29.5	1.62	0.48	3.62	18.2	8.1	3.4	2.2	7.5
[TMPBI-BuI][MS]	3.2	0.08	0.04	0.71	40.3	4.5	2.0	8.9	17.8
[TMPBI-BuI][TFMS]	34.0	0.50	0.24	2.48	68.0	13.7	2.1	5.0	10.3
[TMPBI-BuI][PTS]	4.3	0.22	0.03	0.65	19.5	6.6	7.3	3.0	21.7
[TMPBI-BuI][NO$_3$]	4.4	0.14	0.07	1.7	31.1	2.6	2.0	12.1	24.3
PBI-BuI[b](base case)	24.6	0.08	0.04	0.65	308.0	37.9	2.0	8.1	16.3

[a]: Expressed in 10^{-8} cm^2/s, [b]: Ref. [Kumbharkar (2006)].

It could be seen from Table 5.7 that in these PILs, the D_{H_2}/D_{CO_2} consistently decreased than that of the parent PBI-BuI, irrespective of the anion they hold. This conveyed that the initial openness of the PBI backbone could be helpful in reducing D_{H_2}/D_{CO_2}. Its further lowering could be made possible by choosing bulky alkyl/aryl group to be used as the *N*-substituent, so that the benefits of the ionic liquid character in PILs towards enhancing CO_2 permeation characteristics can be drawn in a better way. This aspect will be addressed in the next Chapter.
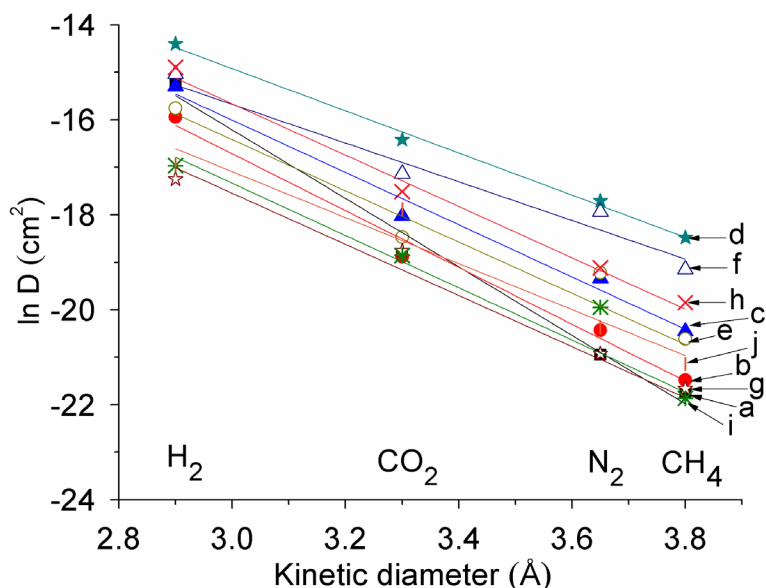
Figure 5.14 Correlation of diffusion coefficient with kinetic diameter (Å) of gases for PILs based on PBI-BuI (a: PBI-BuI; b: [TMPBI-BuI][I]; c: [TMPBI-BuI][BF$_4$]; d: [TMPBI-BuI][Tf$_2$N]; e: [TMPBI-BuI][TFAC]; f: [TMPBI-BuI][HFB]; g: [TMPBI-BuI][MS]; h: [TMPBI-BuI][TFMS]; i: [TMPBI-BuI][PTS]; j: [TMPBI-BuI][NO$_3$]).
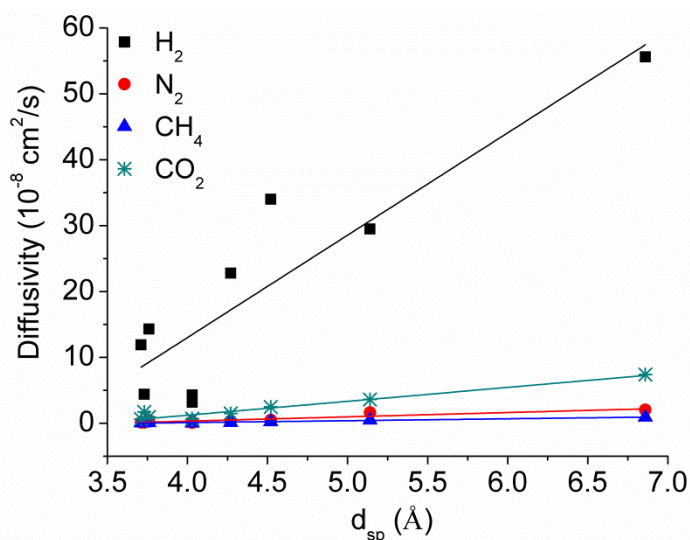
Figure 5.15 Correlation of diffusion coefficient with d$_{sp}$ of PILs based on PBI-BuI.

5.4   Conclusions

We have developed a series of film forming polymeric ionic liquids (PILs) based on rigid PBI-BuI backbone via *N*-quaternization by a methyl group followed by anion exchange with variety of anions. Their structural elucidation by ^{1}H NMR and FT-IR provided support for

quantitative PBI quaternization by the methyl group. The iodide anion of a polycation was exchanged with chosen anions by metathesis, leading to appreciable anion exchange. This approach of PIL synthesis provides two IL characters per repeat unit of PILs. All PILs, except [TMPBI-BuI][Ac] and [TMPBI-BuI][Bz] have shown excellent film forming ability with good mechanical strength. This conveyed the benefits of adopted methodology of choosing rigid aromatic backbone for PIL preparation. Although PBI as a family of polymers is known for poor solvent solubility, their conversion into PIL improved the solvent solubility. Some of the PILs are soluble in cyclohexanone, acetone, acetonitrile and alcohols; while some of them (viz., [TMPBI-BuI][Ac], [TMPBI-BuI][TFAc], [TMPBI-BuI][MS] and [TMPBI-BuI][Bz]) are even water soluble. This excellent solvent solubility would be helpful in their easy processability to useful forms such as film, gels, coating solution, etc. for various applications. By changing the anion, water sorption and contact angle of these PILs showed diverse variation, from water soluble to highly hydrophobic nature. This tunability of PIL hydrophilicity by merely changing the anion could be highly advantageous towards their applicability as hydrophobic/hydrophilic switchable surfaces. The viscosity investigations of these PILs suggested their typical polyelectrolyte behavior. The d_{sp} and density of these PILs varied with the variation of anions. It was found that PILs with fluorinated anions showed higher d_{sp} and density than their non-fluorinated analogue. The thermal stability of these PIL reduced than that of precursor PBI-BuI. Anion associated with a PIL showed its own effect on governing the thermal stability. The glass transition temperature of some of the PILs conveyed their glassy nature.

All film forming PILs could withstand high pressure (20 atm) during their gas permeation analysis, which is highly advantageous towards their practical applicability. In spite of their rigid aromatic backbone, many of them exhibited high CO_2 based permselectivity (esp. P_{CO_2}/P_{CH_4} of ~ 69-98) than reported PILs and conventional polymers used as the gas separation membrane materials. The anion was found to have profound role on governing CO_2 sorption and permeation properties. Among PILs investigated, those with Tf_2N^-, BF_4^-, HFB^- and $TFMS^-$ anions showed high gas permeation, signifying the role of bulky anions to loosen the chain packing density efficiently than of other anions. The synergistic effect of inducing IL characters in PBI backbone was seen by a larger improvement in CO_2 permeability than that for other gases. In comparison to the parent PBI-BuI, P_{CO_2} was increased without much compromise on its permselectivity over N_2 and CH_4. The induced IL character in PBI-BuI backbone improved CO_2

sorption selectivity over N_2 and CH_4 than their precursor PBI-BuI, indicating further tuning of PIL structure can bring beneficial effects. The [TMPBI-BuI][Ac] exhibited highest CO_2 sorption and CO_2 based selectivity, indicating potentials of this anion, inspite of its PIL being brittle. Though the CO_2 permeability of present PILs seems to be lower than some of the reported PILs, their excellent pressure withstand capacity and mechanical strength, coupled with high thermal stability and possibility of tuning their structure further makes this family of PILs as a promising candidates for CO_2 separation.

Chapter 6

Structural tuning while varying *N*-substituent of PBI for enhancing permeation properties of PILs

6.1 Introduction

In earlier Chapter, an altogether different approach of obtaining film forming PILs by *N*-quaternization of rigid aromatic polybenzimidazoles (PBIs) with alkyl halide was validated by choosing various anions. PILs possessing halide as counter anion exhibited lower gas permeability than their precursor PBI. The exchange of halide by chosen anions yielded PILs with excellent film formation ability, which could withstand high applied pressure (20 atm) during their gas permeability analysis (except PILs based on Ac^- and Bz^-). Though PILs possessing bulky anions (viz., Tf_2N^-, BF_4^-, HFB^-, $TFMS^-$) showed enhanced gas permeability than their parent PBIs, it was lower than some of the reported PILs (based on aliphatic backbone evaluated at lower pressures) [Hu (2006), Bara (2007, 2008a, 2008b), Hudino (2011), Carlisle (2012, 2013), Hao (2013)]. There is a scope of improving gas permeability of this new series of PILs by the variation in the bulk of '*N*-substituent' used for the PBI-quaternization.

Sanders et al. (2013), have noted that polymers offering the best combinations of gas selectivity and permeability are generally glassy and have rigid structures that exhibit poor chain packing. In essence, these polymers offer the size distribution of free volume elements required for approaching molecular sieving characteristics. Since transport in polymers occurs through a solution-diffusion mechanism, diffusivity of a penetrant can be tuned by modifying the polymer chain and subgroup flexibility, as well as free volume present in the polymer structure [Li (2013)]. In the case of PILs based on PBIs, the same methodology needs to be applied for the elevation of their gas permeability. Glassy nature of PBI and possibility to tune structure through *N*-substitution can be easily performed. This would lead to the enhancement primarily in gas diffusivity. PIL's ability to possess high CO_2 sorption [Mecerreyes (2011), Yaun (2013)] is anticipated to additively enhance CO_2 separation properties of this new family of PILs based on PBIs.

This Chapter deals with PILs obtained by *N*-quaternization of PBI-I and PBI-BuI using bulky alkyl halide (*n*-butyl iodide, *4-tert*-butylbenzyl bromide). It was anticipated that these bulky *N*-substituents would disrupt the chain packing of a rigid aromatic PBI more effectively than the

methyl group used in earlier cases [Chapter 5] and would ultimately enhance gas permeation characteristics of resulting PILs. The halide exchange of obtained precursor PILs were performed by two promising anions (Tf_2N^- and BF_4^-). Obtained PILs were characterized by requisite physical properties. Investigations with pure gas permeation and sorption are presented.

6.2   Experimental

6.2.1   *Materials*

3,3′-Diaminobenzidine (DAB), isophthalic acid (I), *5-tert*-butylisophthalic acid (BuI), sodium hydride (60 % dispersion in mineral oil), dry dimethyl sulphoxide (DMSO, 0.01% H_2O), *N,N*-dimethylacetamide (DMAc), *n*-butyl iodide (BI), *4-tert*-butylbenzyl bromide (BzBr), silver tetrafluoroborate ($AgBF_4$) and lithium bis(trifluoromethane)sulfonimide ($LiTf_2N$) were procured from Aldrich Chemicals. Polyphosphoric acid (PPA) was procured from Alfa Aesar. Potassium thiocyanate (KSCN), silver nitrate ($AgNO_3$), *N,N*-dimethylformamide (DMF), *N*-methyl-*2*-pyrrolidone (NMP), acetonitrile, methanol, ethanol, *1*-propanol and acetone were purocured from Merck. Pure gases, viz.; He, H_2, N_2, CH_4 and CO_2 were procured as given in Chapter 4.

6.2.2   *Synthesis*

Two polybenzimidazoles, viz.; PBI-I and PBI-BuI were synthesized by polycondensation reaction of DAB with either isophthalic or *5-tert*-butylisophthalic acid, respectively, as given in Chapter 5 (Scheme 6.1).
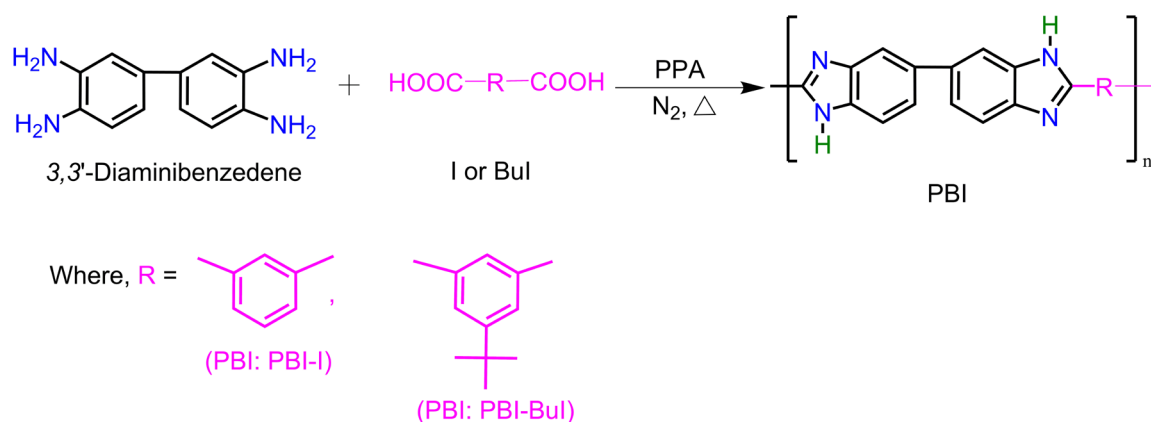
Scheme 6.1 Synthesis of PBI.

The *N*-quaternization of PBI-I and PBI-BuI was performed in dry DMSO by preparing Na salt of PBI followed by addition of the alkyl halide (Scheme 1). A 3-necked flask was charged

with 300 ml of Dry DMSO, 10 g of PBI (PBI-I or PBI-BuI) and 2.1 molar equivalents of NaH while stirring under dry N_2 atmosphere at the ambient temperature. After 3 h, the reaction mixture was heated at 80 ºC for 2 h. It was then cooled to the ambient and 4.2 equivalent of alkyl halide (BI or BzBr) was added slowly over a period of 15 min while stirring. A yellow precipitate was formed, which was dissolved after the reaction temperature was elevated to 80 ºC (20 h). The polymer was obtained by precipitation in a non-solvent (acetone in case of quaternization with BzB*r*, while a mixture of toluene:acetone (1:1) was used in case of quaternization with BI). The polymer was further purified by dissolving in DMF and reprecipitation in the respective nonsolvent. Obtained polymer was dried in vacuum oven at 80 ºC for 3 days and stored in desiccator until use.
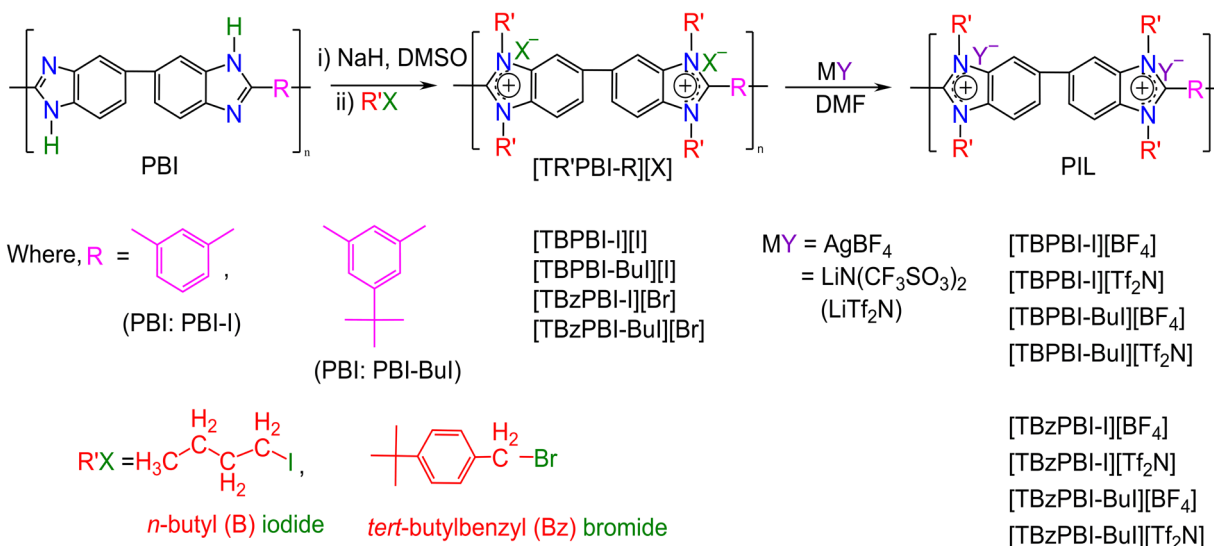
Scheme 6.2 Synthesis of PILs based on PBI-I and PBI-BuI

Anion exchange of *N*-quaternized PBI was performed by simple metathesis reaction with either BF_4^- or Tf_2N^- salt. Typically, a two necked flask equipped with a calcium chloride guard tube was charged with 5 g of a quaternized PBI and 100 ml of DMF. After the complete dissolution, 2 molar equivalent of $AgBF_4$ was added while stirring. Formation of the AgI or AgBr precipitate began after the addition of $AgBF_4$, while the anion exchanged polymer remained in dissolved state. The reaction mixture was further stirred at the ambient temperature for 24 h in order to ensure the complete replacement of anion. The precipitated AgI or AgBr was removed by repeated centrifugation at 12000 RPM. Formed PIL was recovered from the supernatant solution

by solvent evaporation. It was further purified by dissolving in DMF (8% w/w) followed by reprecipitating in water. Purified PIL was dried at 80 ºC in a vacuum oven for 3 days.

The exchange of iodide or bromide by Tf_2N^- was performed using $LiTf_2N$ at the ambient temperature. A 5 g of *N*-quaternized PBI was dissolved in 100 ml of solvent, 2 mol of $LiTf_2N$ was added and stirred for 24 h. A homogeneous reaction mixture was precipitated in water. Obtained PIL was thoroughly washed with water in order to remove LiI or LiBr and then dried at 80 °C. It was further purified by dissolving in DMF (8% w/w), reprecipitating in water, followed by drying at 80 ºC in the vacuum oven for 3 days. The designation of PILs (Quaternized PBIs) is based on their parent PBI, alkyl halide used for the quaternization and the anion they hold (Scheme 6.2).

6.2.3 Degree of PBI N-quaternization (DQ) and halide exchange

The degree of *N*-quaternization (DQ) of a PBI was determined by ^{1}H-NMR (recorded on Bruker AC-200 using DMSO-d_6 as the solvent). The extent of iodide or bromide anion exchanged by BF_4^- or Tf_2N^- was determined by Volhard's method [Jeffery (1980)]. For this, 0.1 g of PIL powder was stirred in 30 ml of 0.01 M $AgNO_3$ solution for 24 h. An excess of unreacted $AgNO_3$ was titrated against 0.01 M KSCN. From the amount of $AgNO_3$ consumed, iodide or bromide content in the PIL (and thus the percent of anion exchanged) was estimated.

6.2.4 Membrane preparation

Dense membranes of PILs were prepared by solution casting method on a flat glass surface (using their 3% w/v solution in DMAc) at 80 °C for 18 h under dry atmosphere. After the solvent evaporation, formed membrane was peeled off and dried in a vacuum oven at 80 °C for a week in order to remove traces of the solvent.

6.2.5 Characterizations

The solubility of PILs in common organic solvents was determined by adding 0.1 g of PIL in 10 ml of a solvent while stirring at the ambient temperature for 24 h. In case of insolubility, heating at 80 °C (or near boiling point, in case of the low boiling solvents) for 24 h was employed. The inherent viscosity (η_{inh}) of PILs was determined at 0.2 g/dL concentration in DMSO at 35 °C.

FT-IR spectrum of PILs in thin film form (~10 μm) was recorded at the ambient temperature using Perkin Elmer Spectrum GX spectrophotometer. The wide angle X-ray

diffraction (WAXD) pattern of PILs in the film form was recorded using Rigaku X-ray diffractometer (D-max 2500) with Cu-K$_\alpha$ radiation. The average intersegmental d-spacing (d$_{sp}$) for the amorphous peak maxima was calculated using Bragg's equation (nλ = 2dsinθ). The density (ρ) of PIL films was measured at 35 °C by using specific gravity bottle and decalin as the solvent that exhibited negligible sorption in PILs (< 1.2 %). This measurement was repeated with three samples and deviation from the average value was $\leq$ 0.004 g/cm^3.

Thermogravimetric analysis (TGA) was performed using Perkin Elmer TGA-7 in N$_2$ atmosphere with a heating rate of 10 °C/min. The glass transition temperature (T$_g$) was determined using DSC Q-10 (TA instruments, USA) under N$_2$ atmosphere with a heating rate of 10 °C/min.

6.2.6 *Gas sorption and permeation*

The pure gas sorption isotherms using H$_2$, N$_2$, CH$_4$ and CO$_2$ were obtained at 35 °C using equipment that consisted of the dual-volume, single-transducer set up based on pressure decay method, as mentioned in Chapter 2 (Section 2.2.4). The solubility coefficient (S) and solubility selectivity (S$_A$/S$_B$), sorption parameters (k$_D$, C'$_H$ and b) were determined at 20 atm.

The permeability measurement using pure gases (He, H$_2$, N$_2$, CH$_4$ and CO$_2$) was carried out by standard variable volume method at upstream gas pressure of 20 atm and at 35 °C, as mentioned in Chapter 4 (Section 4.2.4). The permeability measurements were repeated with at least 3 different membrane samples prepared under identical conditions and the data averaged. Variation in permeability from the average was maximum < 10 %, depending upon the gas analyzed. The permeability coefficient for a particular gas along with its solubility coefficient at 20 atm was used to estimate the diffusivity coefficient (D$_A$ = P$_A$/S$_A$).

6.3 Results and discussion

6.3.1 *Synthesis*

6.3.1.1 N-quaternization of PBIs

PBI-I and PBI-BuI was successfully synthesized by polycondensation reaction having inherent viscosity of 0.8 and 1.0 dL/g in DMSO, respectively. The *N*-quaternization of PBI-I and PBI-BuI could be successfully achieved by in-situ formation of their Na-salt, followed by addition of a alkyl halide. For the formation of Na salt of PBI, the reaction mixture (PBI and NaH in DMSO) was kept at room temperature for 3 h. In order to ensure completion of Na-salt formation,

this homogeneous solution was further heated at 80 °C for 2 h. At this stage, a deep blood red color was developed, as also was observed earlier [Kumbharkar (2009b), Chapter 5], indicating formation of *N*-sodium salt. The addition of BI or BzBr in the reaction mixture showed distinctly different behaviour. The addition of BzBr showed an immediate precipitate formation, while in case of BI; precipitate formation started after 10-15 min. This indicated a sluggish nature with BI towards *N*-substitution of PBI. In both the cases, formed precipitate was dissolved slowly after the temperature was elevated to 80 ºC. This temperature elevation was performed in order to achieve complete dissolution and thus to aid substitution reaction in the solution phase. Formed solution remained clear and homogeneous even after the temperature was lowered to the ambient, indicating formation of *N*-quaternized PBI. The yield of resulting PIL after purification was > 85 %. This high yield was a primary indication of almost complete *N*-quaternization of the PBI, which was further quantified as given below.

6.3.1.2 *Estimation of the degree of N-quaternization (DQ)*

The ^{1}H-NMR spectra of unsubstituted and quaternized PBIs are given in Figure 6.1. In the spectra of unsubstituted PBI-I and PBI-BuI, a broad peak at δ 13–14 ppm corresponds to protons belonging to 'N-H' of imidazole. In the spectra of quaternized PBIs, this peak disappeared completely (Figure 6.1). This indicates that almost complete *N*-quaternization of PBI had taken place. The quantitative estimation of *N*-quaternization by BI was done by comparing integration of *N*-substituted $-CH_2-$ protons appearing at δ 3.7–5 ppm to the integration of aromatic protons of precursor PBI appearing at δ 7.5–9.5 ppm. In the case of *N*-quaternization by BzBr, quantitative estimation of *N*-quaternization was done by comparing integration of aromatic proton belonging to *tert*-butylbenzyl group appeared at δ 6.5–7.5 ppm to the aromatic protons of precursor PBI appearing at δ 7.5–9.5 ppm. The degree of *N*-quaternization for [TBPBI-I][I] and [TBPBI-BuI][I] was ~85.6 % and 85.3 %, respectively; while for [TBzPBI-I][Br] and [TBzPBI-BuI][Br], it was 93.4 and 88.4 %, respectively. A slightly lower DQ of *n*-butyl substituted PBIs could be related to the sluggishness of this reaction as discussed above. It may be worth to recall that the degree of *N*-quaternization obtained recently using -CH_3 group as a substituent was > 96% [Chapter 5]. This high DQ could be related to the smaller size of substituent (-CH_3) than the present cases of bulky (B or Bz) substituents.
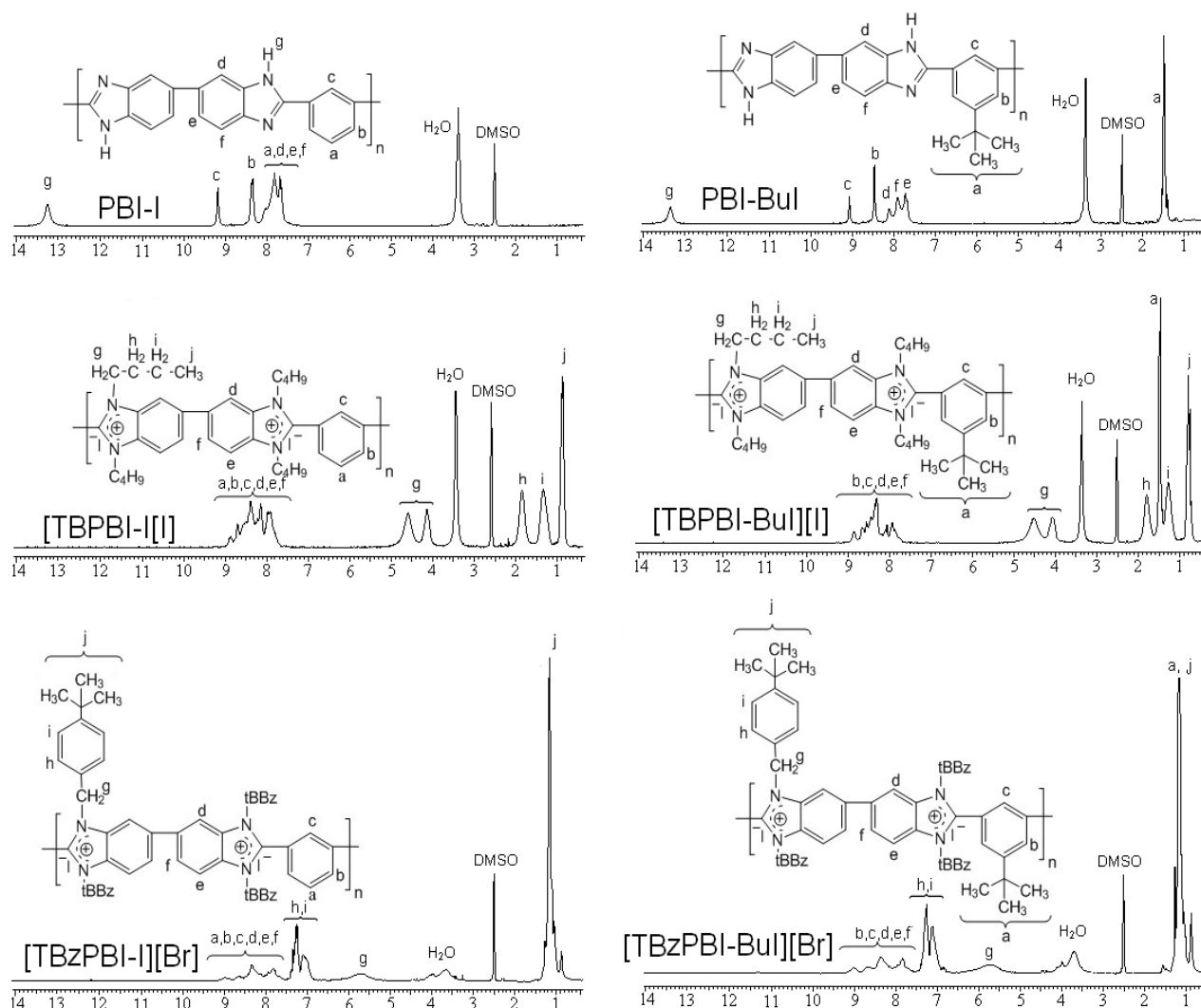
Figure 6.1 ^{1}H NMR spectra of PILs based on PBI-I and PBI-BuI.

6.3.1.3 Anion exchange

Anion exchange in all four *N*-quaternized PBIs was performed using BF_4^- and Tf_2N^- anions. These two anions were specifically chosen based on earlier study [Chapter 5]. PILs based on these anions exhibited easy processability, strong film forming ability, good mechanical strength, high thermal stability, high CO_2 permeability as well as appreciable CO_2 based permselectivity over N_2 and CH_4, than that of PILs based on other anion. The percent anion exchange was determined by Volhard's method [Jeffery (1989)] and the data is given in Table 6.1. Anion exchange in case of PILs possessing BF_4^- anion was slightly higher than that of PILs possessing Tf_2N^- anion. Similar results were observed in earlier work of PBI based PILs [Chapter 5].

Table 6.1 Physical properties of PILs.

PILs	Anion exchange[a] (%)	η_{inh}[b] (dL/g)	d_{sp}[c] (Å)	ρ[d] (gm/cm^3)	T_g[e] (°C)	TGA	
						IDT[f] (°C)	W$_{900}$[g] (%)
PILs based on PBI-I							
[TBPBI-I][I]	-	3.5	4.09	1.402	ND	256	39.0
[TBPBI-I][BF$_4$]	90.0	3.4	4.18	1.364	ND	379	52.6
[TBPBI-I][Tf$_2$N]	86.3	3.5	4.40	1.405	179	418	37.3
[TBzPBI-I][Br]	-	3.1	4.97	1.236	ND	219	35.1
[TBzPBI-I][BF$_4$]	~100	3.7	5.17	1.209	171	328	46.6
[TBzPBI-I][Tf$_2$N]	86.0	3.8	5.27	1.312	185	359	30.1
PBI-I[h] (base case 1)	-	0.9	4.05	1.331	416	600	71.8
PILs based on PBI-BuI							
[TBPBI-BuI][I]	-	3.2	4.26	1.326	ND	261	44.8
[TBPBI-BuI][BF$_4$]	91.0	3.5	4.36	1.280	ND	384	53.2
[TBPBI-BuI][Tf$_2$N]	87.0	3.6	4.45	1.338	180	430	41.2
[TBzPBI-BuI][Br]	-	3.5	5.12	1.175	ND	213	27.0
[TBzPBI-BuI][BF$_4$]	~100	3.3	5.21	1.172	174	335	46.8
[TBzPBI-BuI][Tf$_2$N]	87.0	3.4	5.21	1.284	191	373	32.1
PBI-BuI[h] (base case 2)	-	1.0	4.69	1.193	ND	525	66.9

[a]: Determined by Volhard's method, [b]: inherent viscosity determined using 0.2 g/dL solution at 35 °C, [c]: d-spacing obtained from wide angle X-ray diffraction spectra, [d]: density measured at 35 °C, [e]: glass transition temperature, [f]: initial decomposition temperature, [g]: char yield at 900 °C, [h]: Ref. [Kumbharkar (2009a)], ND: Not detectable.

6.3.2 *FT-IR analysis*

FTIR spectra of PILs scanned at the ambient temperature are given in Figure 6.2. In all the PILs, characteristic bands for benzimidazole (1500-1650 cm^{-1}, attributable to C=C/C=N stretching vibrations and ring modes) [Musto (1993)] is originated from the cationic PBI backbone. In PILs possessing BF$_4^-$ anion, a band at ~1080 cm^{-1} is attributable to the B-F stretching vibrations, as was observed in RTIL, [BMI][BF$_4$] possessing this anion [Suarez (1996)]. In case of PILs possessing Tf$_2$N$^-$ anion, bands at ~1360 cm^{-1} and 618 cm^{-1} are attributable to the asymmetric stretching and bending vibrations of SO$_2$; respectively. In these spectra, a band at 1130-1240 cm^{-1}

is attributable to the symmetric stretching vibrations of C-F bond. Similar band was seen in the spectra of LiTFSI [Pennarun (2005)]. All the PILs exhibited a broad band in the range of ~3100-3700 cm^{-1}, attributable to the sorbed moisture, as also observed in earlier work [Chapter 5].
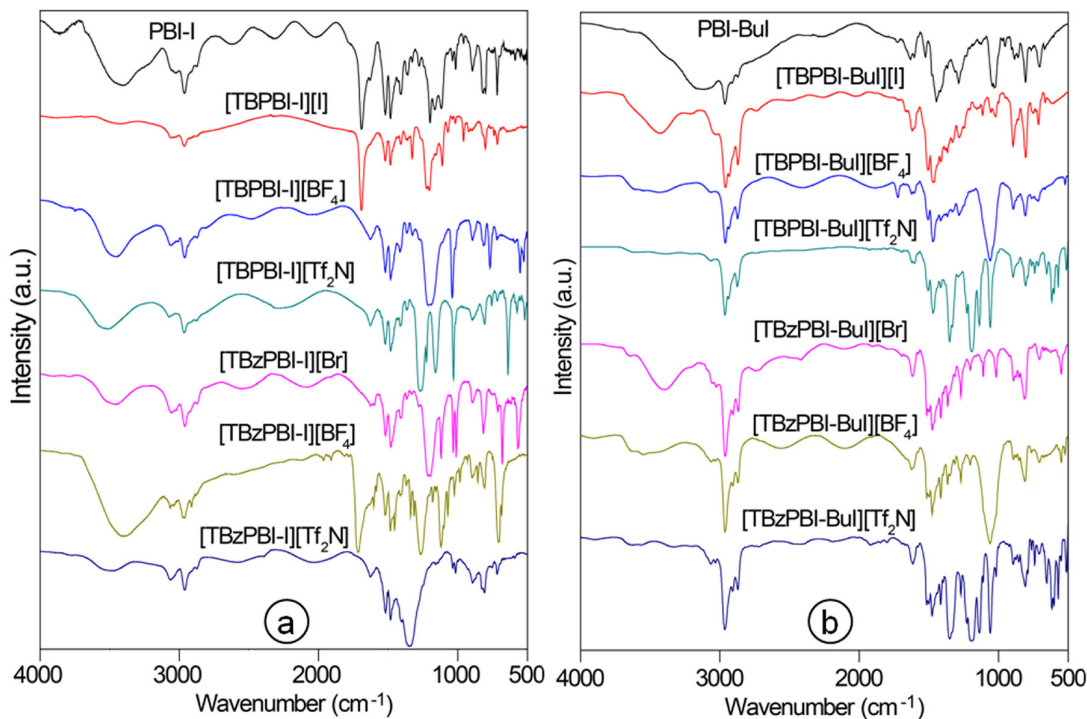
Figure 6.2 FT-IR spectra of PILs based on a) PBI-I and b) PBI-BuI.

6.3.3 *Physical properties*

6.3.3.1 Solvent solubility and solution viscosity

The solubility of PILs in various solvents is summarized in Table 6.2. All these PILs were freely soluble in polar solvent such as DMF, DMAc, DMSO and NMP. PILs with BF$_4^-$ as an anion were soluble in acetonitrile, while those with Tf$_2$N$^-$ as an anion were easily soluble in acetone at the ambient temperature. It may be recalled that unsubstituted PBI [Kumbharkar (2009a)] and disubstituted PBI [Kumbharkar (2009b)] are insoluble in these solvents. Such enhanced solubility of PILs containing BF$_4^-$ and Tf$_2$N$^-$ as an anion was also observed in earlier study of methylated PBI based PILs [Chapter 5]. All these PILs were insoluble in water and alcohols examined (Table 6.2). The inherent viscosity of PILs is given in Table 6.1. It was observed that viscosity of PILs increased considerably than that of respective parent PBI (η_{inh} of PBI-I = 0.8 and PBI-BuI = 1.0 dL/g). The increased viscosity is mainly due to the polyelectrolyte behavior induced by quaternization of PBI [Chapter 5].

Table 6.2 Solvent solubility of PILs.

PILs	DMF	DMAc	DMSO	NMP	Acetone	CH$_3$CN	Methanol	Ethanol	*1*-Propanol
Based on PBI-I									
[TBPBI-I][I]	++	++	++	++	–	–	–	–	–
[TBPBI-I][BF$_4$]	++	++	++	++	–	++	–	–	–
[TBPBI-I][Tf$_2$N]	++	++	++	++	++	–	–	–	–
[TBzPBI-I][Br]	++	++	++	++	–	–	–	–	–
[TBzPBI-I][BF$_4$]	++	++	++	++	–	++	–	–	–
[TBzPBI-I][Tf$_2$N]	++	++	++	++	++	–	–	–	–
PBI-I (base case 1)	+	+	+	+	–	–	–	–	–
Based on PBI-BuI									
[TBPBI-BuI][I]	++	++	++	++	–	–	–	–	–
[TBPBI-BuI][BF$_4$]	++	++	++	++	–	++	–	–	–
[TBPBI-BuI][Tf$_2$N]	++	++	++	++	++	–	–	–	–
[TBzPBI-BuI][Br]	++	++	++	++	–	–	–	–	–
[TBzPBI-BuI][BF$_4$]	++	++	++	++	–	++	–	–	–
[TBzPBI-BuI][Tf$_2$N]	++	++	++	++	++	–	–	–	–
PBI-BuI (base case 2)	++	++	++	++	–	–	–	–	–

++: Soluble at ambient, +: soluble after heating at 80 ºC / reflux for 24 h in case of low boiling solvent , −: insoluble even after heating at 80 ºC.

6.3.3.2 Film forming ability

Film forming nature exhibited by all these PILs indicated promises of their applicability as a membrane material. Bara et al. (2007b), have observed that the styrene-based PILs with smaller alkyl substituents (methyl, butyl or hexyl) were able to form films, while those with a longer alkyl substituents (*n*-octyl or *n*-decyl) showed lack of sufficient mechanical stability and could not be used for gas permeation analysis. It may be noted that, present PILs with bulkier substituents (*n*-butyl and *tert*-butylbenzyl) exhibited excellent film forming ability. This could be attributed to the selection of rigid backbone of present PILs, which offers the mechanical strength to the present PILs, while reported PILs are mostly based on aliphatic backbone. This shows a benefit of used approach of PIL synthesis, which supports our earlier finding that rigid PBI backbone renders film forming nature to PILs.

6.3.3.3 Chain packing: WAXD and density analysis

WAXD patterns of these PILs (Figure 6.3 and 6.4) indicated their amorphous nature. The average intersegmental *d*-spacing (d_{sp}) of PILs are given in Table 6.1. It was observed that *tert*-butylbenzyl substituted PILs showed higher d_{sp} than that of *n*-butyl substituted PILs. This could be attributed to the bulkier nature of *tert*-butylbenzyl group (V_w = 97.89 cm^3/mol), which loosen PBI chain packing more effectively than by *n*-butyl group (V_w = 44.36 cm^3/mol). Similar effects of these substituent on governing d_{sp} of disubstituted PBI was observed [Kumbharkar (2009b)]. It could be seen from Table 6.1 that a PIL based on PBI-BuI exhibited higher d_{sp} than that of PIL based on PBI-I, possessing same substituent and anion. This could be attributed to initial open structure of PBI-BuI due to presence of *tert*-butyl group in its backbone, than that of PBI-I (d_{sp}: PBI-BuI = 4.69 Å and PBI-I = 4.04 Å) [Kumbharkar (2006)]. The d_{sp} in all four polycations (viz., [TBPBI-I], [TBzPBI-I], [TBPBI-BuI], [TBzPBI-BuI]) increased in the order of their anion variation as I^- / Br^- < BF_4^- < Tf_2N^-, indicating bulk of the anion could also be governing the chain packing density. Such a variation in d_{sp} was also observed in methyl substituted PBI based PILs [Chapter 5].
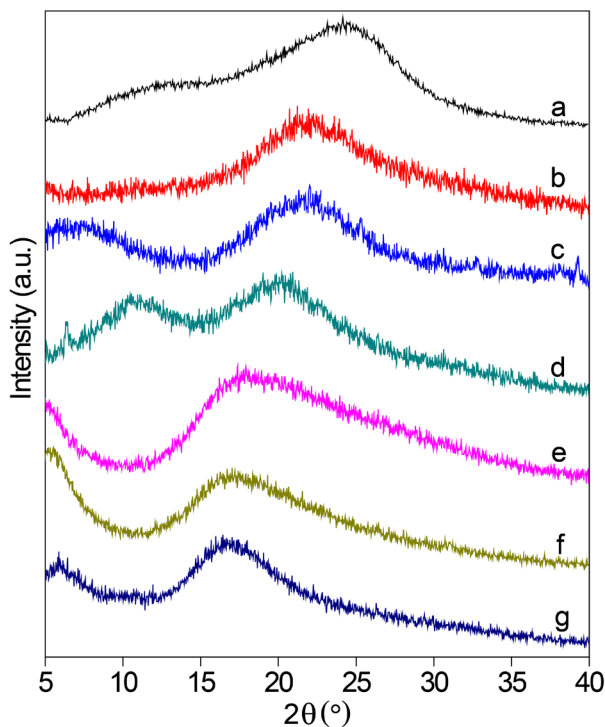
Figure 6.3 Wide angle X-ray diffraction pattern of PILs based on PBI-I (a: PBI-I; b: [TBPBI-I][I]; c: [TBPBI-I][BF$_4$]; d: [TBPBI-I][Tf$_2$N]; e: [TBzPBI-I][Br]; f: [TBzPBI-I][BF$_4$]; g: [TBzPBI-I][Tf$_2$N]).
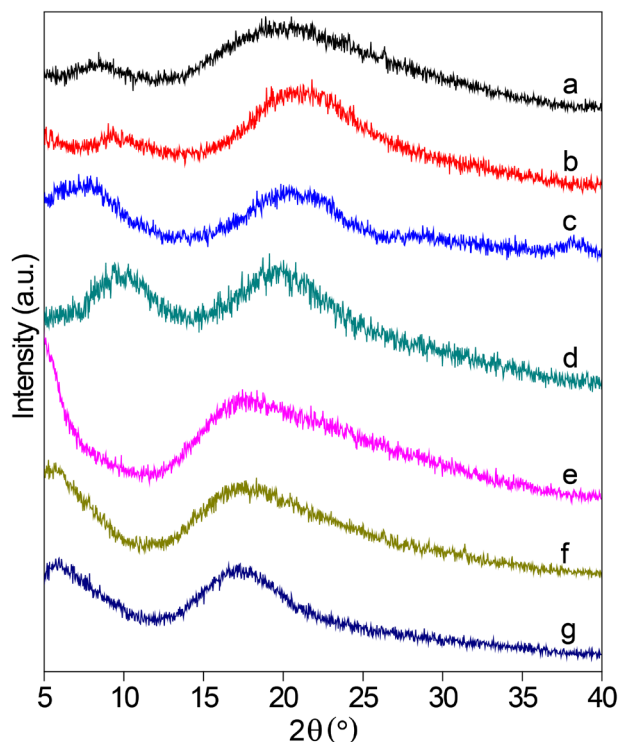
Figure 6.4 Wide angle X-ray diffraction patterns of PILs based on PBI-BuI (a: PBI-BuI; b: [TBPBI-BuI][I]; c: [TBPBI-BuI][BF$_4$]; d: [TBPBI-BuI][Tf$_2$N]; e: [TBzPBI-BuI][Br]; f: [TBzPBI-BuI][BF$_4$]; g: [TBzPBI-BuI][Tf$_2$N]).

It can be seen that the density of a PIL based on PBI-I was higher than that of PIL based on PBI-BuI (possessing same substituent and anion). It is known that precursor PBI-I has more closely packed structure than that of PBI-BuI (density of PBI-I = 1.33 g/cm^3 while for PBI-BuI = 1.19 g/cm^3) [Kumbharkar (2006)]. Similar results were obtained earlier in case of methyl substituted PBI based PILs [Chapter 5]. The effect of bulkier substituent towards loosening the chain packing was also reflected in the measured density of PILs. It was observed that PILs with *tert*-butylbenzyl substitution has lower density than those possessing *n*-butyl substitution. This is in line with the WAXD analysis as discussed above. In case of disubstituted PBI also, such lowering in density was noted with increasing the bulk of substituent [Kumbharkar (2009b)]. The density in a series of PILs possessing same polycation backbone increased in the order of their anion variation as, BF$_4^-$ < I$^-$ or Br$^-$ < Tf$_2$N$^-$ (Table 6.1). This indicates that substituent as well as anion played a major role in governing the packing density of PILs.

6.3.3.4 Thermal stability of PILs

The initial decomposition temperature (IDT) of PILs is given in Table 6.1. The IDT of PBI-I and PBI-BuI was found to be 600 and 524 °C, respectively (Supporting information). After conversion of a PBI to PIL, thermal stability was found to be decreased, as evident from the lowering in IDT of different PILs (Table 6.1). This decrease in thermal stability could be attributed to several reasons, viz., the elimination of H-bonding (leading to lowering in intermolecular attractions), addition of flexible alkyl group and presence of the anion. As could be seen from thermograms (Figure 6.5 and 6.6), the *n*-butyl substituted PIL showed higher thermal stability than *tert*-butylbenzyl substituted PILs. This could be due to the presence of thermally susceptible benzylic linkage in this substituent. Similar effects were caused by these substituent groups in case of disubstituted PBI [Kumbharkar (2009b)]. In cases of PILs with similar polycation but varying anion, the thermal stability increased by anions variation as, I^- / Br^- < BF_4^- < Tf_2N^-. Tang et al. (2009), have observed that PIL with Tf_2N^- anion exhibited higher thermal stability than its halide counterpart. This study indicated that the nature of substituent and anion play a profound role in governing thermal stability of a PIL.
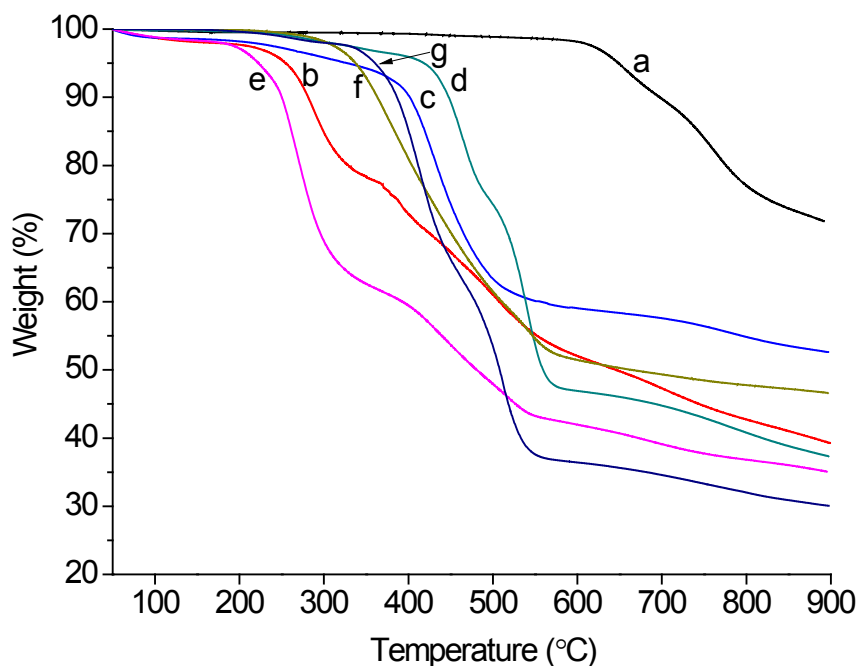
Figure 6.5 TGA curves of PILs based on PBI-I (a: PBI-I; b: [TBPBI-I][I];
c: [TBPBI-I][BF_4]; d: [TBPBI-I][Tf_2N]; e: [TBzPBI-I][Br]; f: [TBzPBI-I][BF_4];
g: [TBzPBI-I][Tf_2N]).
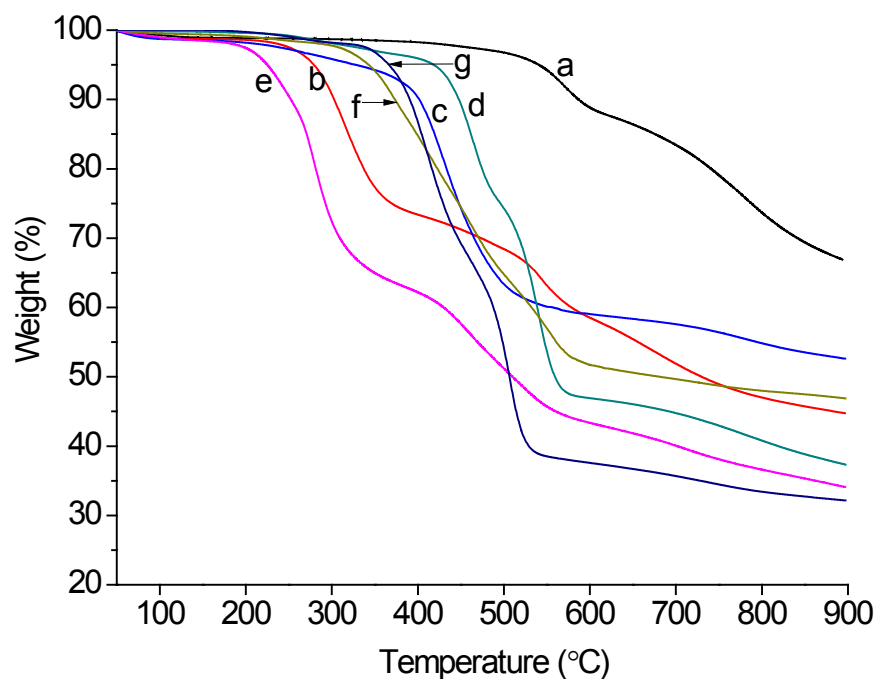
Figure 6.6 TGA curves of PILs based on PBI-BuI (a: PBI-BuI; b: [TBPBI-BuI][I];
c: [TBPBI-BuI][BF$_4$]; d: [TBPBI-BuI][Tf$_2$N]; e: [TBzPBI-BuI][Br];
f: [TBzPBI-BuI][BF$_4$]; g: [TBzPBI-BuI][Tf$_2$N]).

Glass transition temperature (T$_g$) of only few PILs could be detected in the DSC thermogram. As as given in Table 6.1, the T$_g$ of these PILs was found to be > 170 °C, indicating their glassy nature. Present PILs exhibited lower T$_g$ in comparison to the disubstituted PBI with similar substituent and backbone [Kumbharkar (2009b)]. Thus, the lowering in T$_g$ of PILs could be attributed to the presence of cation and anion in them. Although, their T$_g$ was decreased in comparison to PBI, it was higher than most of the reported PILs owing to the difference in backbone structure [Tang (2005b), Hu (2006), Li (2011, 2012), Carlisle (2013), Chi (2013)].

6.3.4   *Gas sorption*

The sorption isotherms for present PILs obtained at 35 °C using pure gases (H$_2$, N$_2$, CH$_4$ and CO$_2$) showed a typical dual-mode nature (Figure 6.7 and 6.8) as usually observed for the glassy polymers [Kumbharkar (2006), Li (2013)]. The sorption of different gases increased in the order: H$_2$ < N$_2$ < CH$_4$ < CO$_2$. This follows the trend of increasing order of inherent condensabilities of these gases (critical temperature (T$_c$) increases in the order -239.85 °C < -146.95 °C < -82.45 °C < 31.05 °C for H$_2$, N$_2$, CH$_4$ and CO$_2$, respectively) [Li (2009b)].
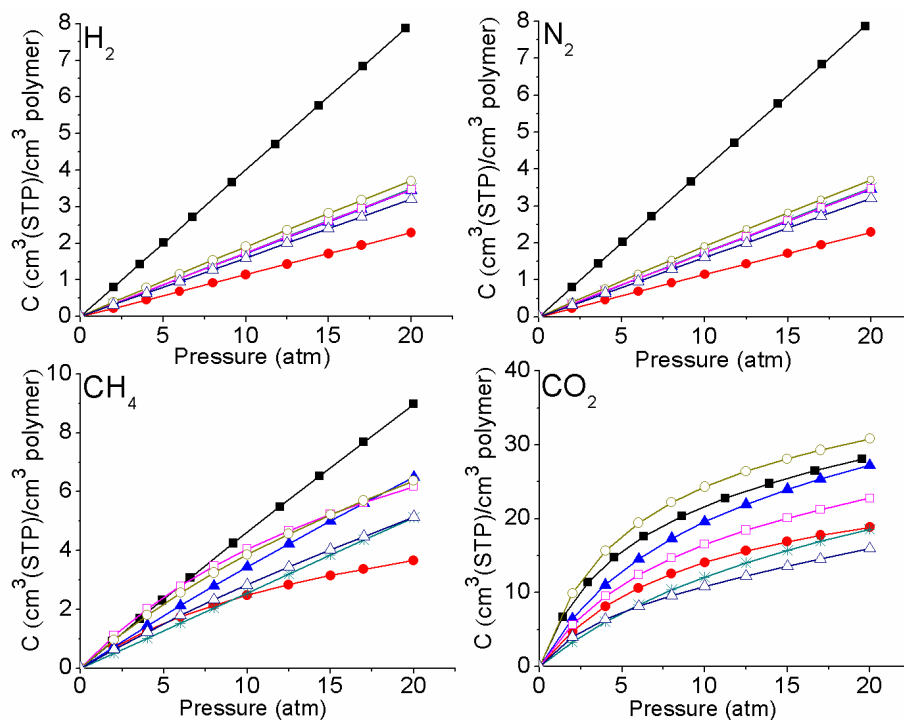
Figure 6.7 Gas sorption isotherm for PILs based on PBI-I at 35 ºC (■: PBI-I, ●: [TBPBI-I][I]; ▲: [TBPBI-I][BF$_4$]; ✳: [TBPBI-I][Tf$_2$N]; □: [TBzPBI-I][Br]; ○: [TBzPBI-I][BF$_4$]; △: [TBzPBI-I][Tf$_2$N]).
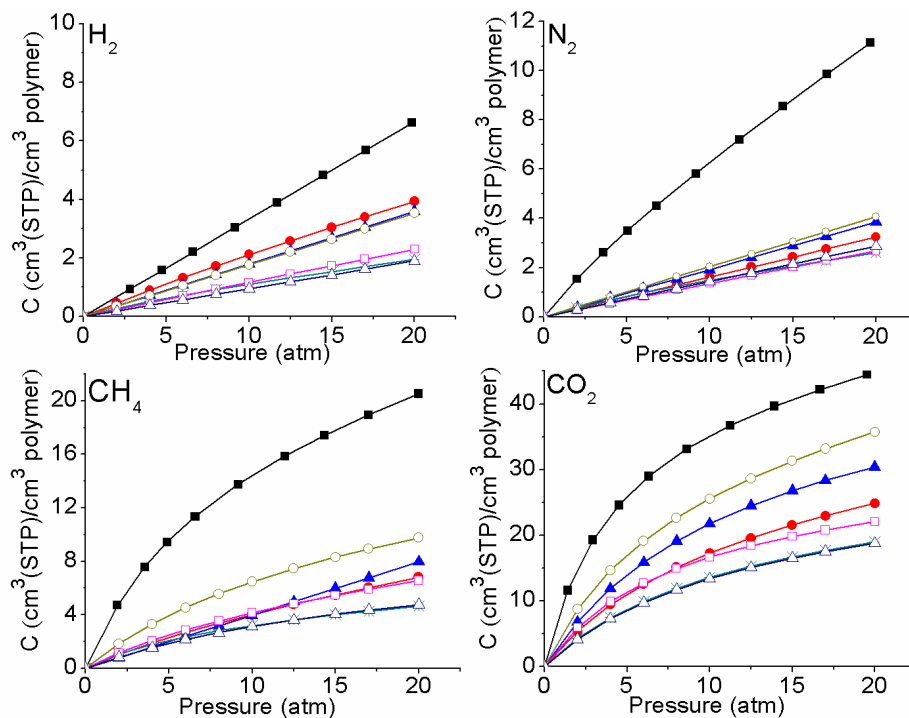
Figure 6.8 Gas sorption isotherm for PILs based on PBI-BuI at 35 ºC (■: PBI-BuI, ●: [TBPBI-BuI][I]; ▲: [TBPBI-BuI][BF$_4$]; ✳: [TBPBI-BuI][Tf$_2$N]; □: [TBzPBI-BuI][Br]; ○: [TBzPBI-BuI][BF$_4$]; △: [TBzPBI-BuI][Tf$_2$N]).

It can be seen from Figure 6.7 and 6.8 that variations in PBI backbone, *N*-substituents and anions of PILs had a considerable effect on PILs gas sorption. It would be worth to compare the CO_2 sorption behavior of these PILs based on these variations, as given below.

6.3.4.1 Effects of PBI backbone, N-substituent and anion variations on gas sorption

Table 6.3 presents the solubility coefficient (S) and solubility selectivity (S_A/S_B) for different PILs at 20 atm.

Table 6.3 Solubility coefficient (S)[a] and solubility selectivity (S_A/S_B) of PILs at 20 atm.

PILs	S_{H_2}	S_{N_2}	S_{CH_4}	S_{CO_2}	$\dfrac{S_{N_2}}{S_{CH_4}}$	$\dfrac{S_{CO_2}}{S_{H_2}}$	$\dfrac{S_{CO_2}}{S_{N_2}}$	$\dfrac{S_{CO_2}}{S_{CH_4}}$
PILs based on PBI-I								
[TBPBI-I][I]	0.11	0.11	0.18	0.94	0.63	8.95	8.24	5.15
[TBPBI-I][BF$_4$]	0.15	0.17	0.32	1.36	0.53	9.19	7.89	4.19
[TBPBI-I][Tf$_2$N]	0.11	0.17	0.26	0.93	0.68	8.26	5.33	3.63
[TBzPBI-I][Br]	0.11	0.17	0.31	1.14	0.56	10.25	6.56	3.69
[TBzPBI-I][BF$_4$]	0.16	0.19	0.32	1.54	0.58	9.61	8.31	4.84
[TBzPBI-I][Tf$_2$N]	0.10	0.16	0.26	0.80	0.62	8.27	4.98	3.11
PBI-I[b] (base case 1)	0.37	0.40	0.45	1.42	0.89	3.84	3.55	3.16
PILs based on PBI-BuI								
[TBPBI-BuI][I]	0.20	0.16	0.34	1.24	0.47	6.32	7.68	3.65
[TBPBI-BuI][BF$_4$]	0.18	0.19	0.40	1.52	0.48	8.46	7.91	3.82
[TBPBI-BuI][Tf$_2$N]	0.10	0.13	0.23	0.95	0.57	9.73	7.31	4.08
[TBzPBI-BuI][Br]	0.14	0.25	0.37	1.38	0.67	9.84	5.60	3.75
[TBzPBI-BuI][BF$_4$]	0.20	0.20	0.49	1.79	0.42	9.11	8.77	3.66
[TBzPBI-BuI][Tf$_2$N]	0.10	0.14	0.24	0.94	0.60	9.87	6.54	3.94
PBI-BuI[b] (base case 2)	0.33	0.57	1.04	2.24	0.55	6.79	3.93	2.15

[a]: Expressed in cm^3 (STP)/cm^{3}polymer.atm, [b]: Ref. [Kumbharkar (2006)].

It was observed that solubility coefficient for a gas was generally higher for PBI-BuI based PILs than that of PBI-I based PILs for a common substituent and anion. This is attributable to the higher d_{sp} (and lower density) in earlier cases, which is indicative parameters for higher fractional free volume present in them (FFV of present PILs could not be estimated due to unavailability of group contribution parameters). As a result, S_{N_2}/S_{CH_4} followed the reverse order, which is as

anticipated based on the glassy nature of these PILs. On the other hand, CO_2 based sorption selectivity does not show any such systematic variation. Thus, the ionic liquid character in these PILs could be dominating towards governing CO_2 sorption (and selectivity) than their glassy nature. It is known that the gas sorption in polymer is a function of polymer–gas interaction as well as available fractional free volume [Barbari (1988), Kanehashi (2005)]. For PILs possessing *tert*-butyl benzyl group, solubility coefficient for all gases was higher than for those possessing *n*-butyl group. This was more evident in PBI-I based PILs than that of PBI-BuI based PILs and for those possessing either halide or BF_4^- as an anion. In case of PILs with Tf_2N^- as an anion, effect of backbone or substituent variation was not really evident.

It was observed that for a particular backbone and *N*-substituent case, CO_2 sorption generally increased in the order of anion variation as, $Tf_2N^- < I^- / Br^- < BF_4^-$. The similar order was observed in earlier study of methyl substituted PBI based PILs [Chapter 5] and P[DADMA] based PILs [Chapter 2]. The higher CO_2 sorption of PILs possessing BF_4^- anion than that of PILs with halide or Tf_2N^- anions is known [Tang (2009), Mecerreyes (2011), Yaun (2013)]. This indicated that even after bulky substitution in PILs, anion played a significant role in governing their CO_2 sorption.

6.3.4.2 Effect of IL nature on gas sorption

When compared with the sorption properties of parent PBI, it was observed that the formation of PILs by bulky substitution of PBI led to decrease in S_{CO_2}. In spite of this, CO_2 based sorption selectivity (S_{CO_2}/S_{H_2}, S_{CO_2}/S_{N_2} and S_{CO_2}/S_{CH_4}) for PILs was increased in comparison to parent unsubstituted PBI. This could be due to preferential CO_2 sorption in PILs than other gases and thus depicting the presence of IL character in them.

It was interesting to note that methyl substituted PBI based PILs exhibited higher CO_2 sorption [Chapter 5] than the present PILs possessing bulky *N*-substituent (than methyl). This could be attributed to the high IL density (number of IL groups in repeat unit/molecular weight of the repeat unit) in the methyl substituted PBI based PILs than in present PILs. The CO_2 sorption expressed in mol% of the present PILs is given in Figure 6.9 and 6.10. It is comparable with the earlier reported methyl substituted PBI based PILs [Chapter 5]. The comparison of sorption expressed in cc/cc shows that it was lower in present case than that of methyl-substituted PILs, as given in Chapter 5. It was also observed that present PILs exhibited higher CO_2 based sorption

selectivity (viz., S_{CO_2}/S_{N_2} and S_{CO_2}/S_{CH_4}) than their disubstituted analogue (viz., DBPBI-I, DBzPBI-I, DBPBI-BuI and DBzPBI-BuI) [Kumbharkar (2010)]. This supports our proposition of introducing IL character in the PILs can preferably sorb CO_2 than other gases, which can improve the CO_2 sorption selectivity and hence CO_2 separation performance.
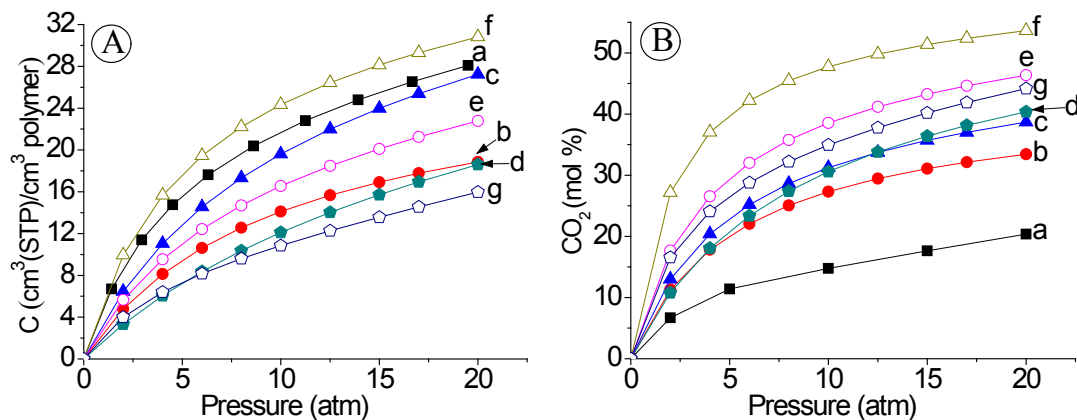
Figure 6.9 CO_2 sorption isotherms for PILs based on PBI-I at 35 ºC represented in A) volumetric term and B) mol %; w.r.t. the molecular weight of PIL repeat unit (a: PBI-I; b: [TBPBI-I][I]; c: [TBPBI-I][BF$_4$]; d: [TBPBI-I][Tf$_2$N]; e: [TBzPBI-I][Br]; f: [TBzPBI-I][BF$_4$]; g: [TBzPBI-I][Tf$_2$N]).
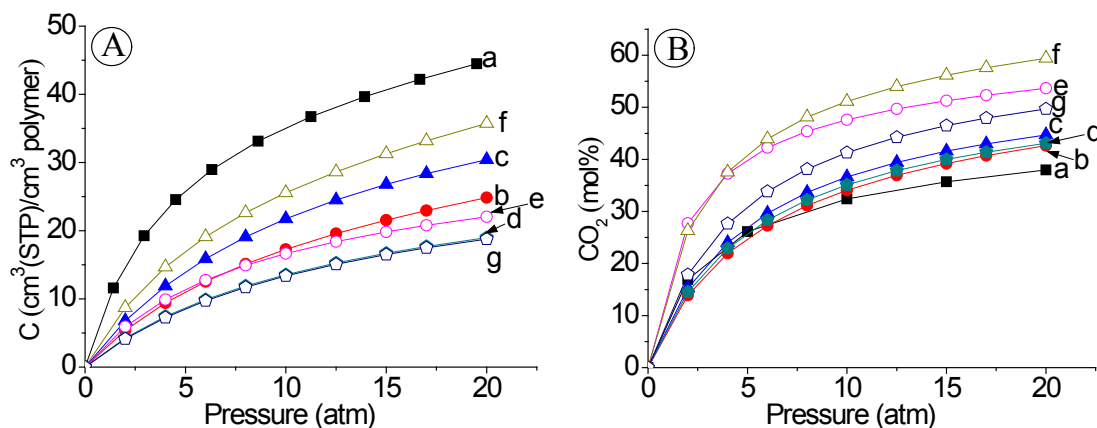
Figure 6.10 CO_2 sorption isotherms for PILs based on PBI-BuI at 35 ºC represented in A) volumetric term and B) mol %; w.r.t. the molecular weight of PIL repeat unit (a: PBI-BuI; b: [TBPBI-BuI][I]; c: [TBPBI-BuI][BF$_4$]; d: [TBPBI-BuI][Tf$_2$N]; e: [TBzPBI-BuI][Br]; f: [TBzPBI-BuI][BF$_4$]; g: [TBzPBI-BuI][Tf$_2$N]).

6.3.4.3 Gas sorption parameters

The gas sorption parameters (k_D, b and $\mathbb{C}_H$) for present PILs obtained using Eq. 1 are given in Table 6.4. It could be seen that Henry's solubility coefficient, k_D (ascribed to the gas

dissolution in rubbery state) was lower for all the gases. It could be attributable to the glassy nature of these PILs as observed in DSC analysis (Table 6.1). For present PILs, k_D did not vary significantly than that of respective parent PBI, owing to their glassy nature. The Henry's law coefficient, k_D has the same physical meaning for glassy polymers as it does for rubbery polymers and liquids [Barbari (1988)].

Table 6.4 Dual-mode sorption parameters[a] obtained during gas sorption in PILs.

PILs	H_2			N_2			CH_4			CO_2		
	k_D	C'_H	b	k_D	C'_H	b	k_D	C'_H	b	k_D	C'_H	b
Based on PBI-I												
[TBPBI-I][I]	0.105	0.58	7.3×10^{-5}	0.114	2.88	2.8×10^{-5}	0.020	5.74	0.066	0.051	25.9	0.110
[TBPBI-I][BF$_4$]	0.148	1.56	4.5×10^{-6}	0.173	2.44	3.5×10^{-5}	0.243	4.22	0.032	0.226	32.9	0.112
[TBPBI-I][Tf$_2$N]	0.109	0.16	0.043	0.174	2.24	1.5×10^{-5}	0.256	4.83	2.4×10^{-5}	0.196	26.5	0.062
[TBzPBI-I][Br]	0.111	1.58	3.9×10^{-5}	0.173	3.29	2.2×10^{-5}	0.043	9.95	0.057	0.225	25.4	0.129
[TBzPBI-I][BF$_4$]	0.157	1.04	0.004	0.163	1.12	0.032	0.105	8.83	0.047	0.199	33.6	0.198
[TBzPBI-I][Tf$_2$N]	0.097	0.12	3.7×10^{-5}	0.160	0.24	1.1×10^{-5}	0.158	4.69	0.037	0.398	9.6	0.250
PBI-I[b] (base case 1)	0.398	1.89	0.011	0.397	3.56	0.011	0.405	1.93	0.042	0.293	27.97	0.205
Based on PBI-BuI												
[TBPBI-BuI][I]	0.149	2.03	0.045	0.162	1.65	1.8×10^{-5}	0.207	4.31	0.082	0.269	29.3	0.099
[TBPBI-BuI][BF$_4$]	0.180	1.55	1.2×10^{-5}	0.192	2.51	1.7×10^{-5}	0.398	4.58	2.7×10^{-5}	0.112	44.4	0.087
[TBPBI-BuI][Tf$_2$N]	0.078	0.50	0.171	0.092	1.22	0.408	0.086	3.91	0.148	0.098	26.3	0.091
[TBzPBI-BuI][Br]	0.139	1.32	7×10^{-4}	0.212	1.03	0.1	0.135	7.22	0.092	0.246	27.6	0.227
[TBzPBI-BuI][BF$_4$]	0.176	0.93	2.8×10^{-5}	0.204	1.06	1.7×10^{-4}	0.107	12.95	0.071	0.460	36.2	0.137
[TBzPBI-BuI][Tf$_2$N]	0.095	0.82	9.2×10^{-6}	0.143	1.66	1.1×10^{-4}	0.015	8.97	0.050	0.066	27.8	0.084
PBI-BuI[b] (base case 2)	0.333	0.42	0.0002	0.456	3.01	0.132	0.327	18.78	0.146	0.438	43.72	0.237

[a]: k_D is expressed in cm^3(STP)/cm^3polymer.atm, C'_H is expressed in cm^3(STP)/cm^3polymer, while b is expressed in atm^{-1}, [b]: Ref. [Kumbharkar (2006)].

The C'_H is considered as the hole-filling constant, which represents maximum amount of the penetrant sorbed into 'microvoids' or the unrelaxed volume of the polymer matrix [Barbari (1988), Kanehashi (2005)]. In present cases, this parameter was lower for all gases in comparison to their parent PBI (Table 6.4), in turn, indicating a need to introduce structural features that would improve fractional free volume. For all PILs, C'_H was higher for CO_2 than other gases, indicating favorable interactions between PIL and CO_2. It was interesting to note that the PILs containing

BF_4^- anion exhibited higher C'_H than that of other anions, indicated CO_2 can preferably be sorbed in BF_4^- containing PILs. The Langmuir affinity constant 'b' is the ratio of rate constants of sorption and desorption processes and characterizes the sorption affinity for particular gas-polymer system [Pixton (1995b)]. This parameter is negligible for H_2 and N_2 than that for CH_4. It is considerably higher in case of CO_2. For a particular PIL, both, C'_H and b were increased with increasing the order of gas condensability.

6.3.5 *Gas permeation properties*

The pure gas permeability for He, H_2, N_2, CH_4 and CO_2 and ideal selectivity for various gas pairs were determined at 20 atm and are given in Table 6.5. It could be seen that the gas permeability of PILs varied with the variation of PBI, substituents used (either *n*-butyl or *tert*-butylbenzyl) and anions, which is discussed in following sections.

Table 6.5 Permeability coefficient (P)[a] and permselectivity (A/B) of PILs.

PILs	P_{He}	P_{H_2}	P_{N_2}	P_{CH_4}	P_{CO_2}	$\dfrac{P_{He}}{P_{H_2}}$	$\dfrac{P_{He}}{P_{CH_4}}$	$\dfrac{P_{H_2}}{P_{N_2}}$	$\dfrac{P_{H_2}}{P_{CH_4}}$	$\dfrac{P_{H_2}}{P_{CO_2}}$	$\dfrac{P_{CO_2}}{P_{N_2}}$	$\dfrac{P_{CO_2}}{P_{CH_4}}$	$\dfrac{P_{N_2}}{P_{CH_4}}$
PILs based on PBI-I													
[TBPBI-I][I]	4.1	3.6	0.05	0.05	1.9	82	82.0	72	72	1.9	38	38	1.0
[TBPBI-I][BF$_4$]	7.2	7.4	0.25	0.17	6.5	29	42.4	30	44	1.1	26	38	1.5
[TBPBI-I][Tf$_2$N]	18.4	16.9	0.82	0.41	12.7	22	44.9	21	41	1.3	15	31	2.0
[TBzPBI-I][Br]	12.5	13.9	0.36	0.21	8.0	35	59.5	39	66	1.7	22	38	1.7
[TBzPBI-I][BF$_4$]	25.3	35.3	1.08	0.85	18.8	23	29.8	33	42	1.9	17	22	1.3
[TBzPBI-I][Tf$_2$N]	37.7	39.8	2.00	1.53	28.6	19	24.6	20	26	1.4	14	19	1.3
PBI-I[b] (base case 1)	1.05	0.6	0.0048	0.0018	0.16	219	583	125	333	3.8	33	89	2.7
PILs based on PBI-BuI													
[TBPBI-BuI][I]	10.4	13.0	0.34	0.29	6.5	31	35.9	38	45	2.0	19	22	1.2
[TBPBI-BuI][BF$_4$]	14.8	17.7	0.64	0.50	15.6	23	29.6	28	35	1.1	24	31	1.3
[TBPBI-BuI][Tf$_2$N]	23.9	22.8	1.05	0.85	16.9	23	28.1	22	27	1.3	16	20	1.2
[TBzPBI-BuI][Br]	17.3	22.2	0.69	0.49	9.6	25	35.3	32	45	2.3	14	20	1.4
[TBzPBI-BuI][BF$_4$]	37.1	51.7	2.03	1.76	39.4	18	21.1	25	29	1.3	19	22	1.2
[TBzPBI-BuI][Tf$_2$N]	47.1	49.9	2.82	2.30	38.9	17	20.5	18	22	1.3	14	17	1.2
PBI-BuI[b] (base case)	10.1	10.7	0.06	0.05	1.91	0.94	202	178	214	5.6	32	38	1.2

[a]: Determined at 20 atm upstream pressure, expressed in Barrer (1 Barrer = 10^{-10} cm^3(STP).cm/cm^2.s.cm Hg), [b]: Ref. [Kumbharkar (2006)].

6.3.5.1 Effects of PBI backbone, N-substituent and anion variations on gas permeation

It could be seen from Table 6.5 that the formation of PILs with bulky substituents led to large increase in CO_2 permeability than that of precursor PBI. It was observed that CO_2 permeability in PBI-I based PILs increased up to 178 times than their parent PBI-I ($P_{CO_2} = 0.16$ Barrer) and up to 20.6 times in PBI-BuI based PILs than their parent PBI-BuI ($P_{CO_2} = 1.91$ Barrer). This indicated that *N*-quaternization by bulky substituent was more efficient in creating additional free space in initially closed packed structure of PBI-I than that of comparatively loosely packed PBI-BuI.

In a particular PBI based PILs, the gas permeability increased in the order of substituent variation as, methyl [Chapter 5] < *n*-butyl < *tert*-butylbenzyl. This variation in permeability could be correlated to the size of substituent, which would increase the free spacing in PILs in the same order. The enhancement in the CO_2 permeability in present PILs than that of methyl substituted PILs is upto 10 folds. This indicated the benefits of PILs formation by bulky group substitution. The increase in gas permeability with increasing side alkyl chain in PILs was reported earlier [Bara (2007b), Li (2012)].

Effect of bulky group substitution on gas permeability would be clearly understand by correlating fractional free volume (FFV) of these PILs with gas permeability. The same could not be determined due to unavailability of Van der waal's volume of anions used. Thus, the correlation of density of PILs (with common anion and varying polycation) with CO_2 permeability and CO_2 based permselectivity is presented in Figure 6.11. It can be seen that the CO_2 permeability was decreased with increasing the density of PILs possessing common anion (BF_4^- and Tf_2N^-). The general trade-off relation of CO_2 permeability and CO_2 based permselectivity was observed also noted in these PILs. This ascertains that the loosening in chain packing density was responsible for improving gas permeability of these PILs. The similar trade-off relation in gas permeability and selectivity was observed in styrene and acrylate based PILs [Bara (2007b)]. Li et al. (2012) also observed similar increase in gas permeability with decreasing P_{CO_2}/P_{N_2} selectivity by increasing alkyl chain length in the polycation. It was interesting to note that the CO_2 permeability of PILs increased almost two folds when substituents changed from *n*-butyl to *tert*-butylbenzyl, while P_{CO_2}/P_{N_2} and P_{CO_2}/P_{CH_4} affected only marginally. This suggested that the size and shape of the substituents is also important for governing CO_2 permeability and permselectivity in PILs.
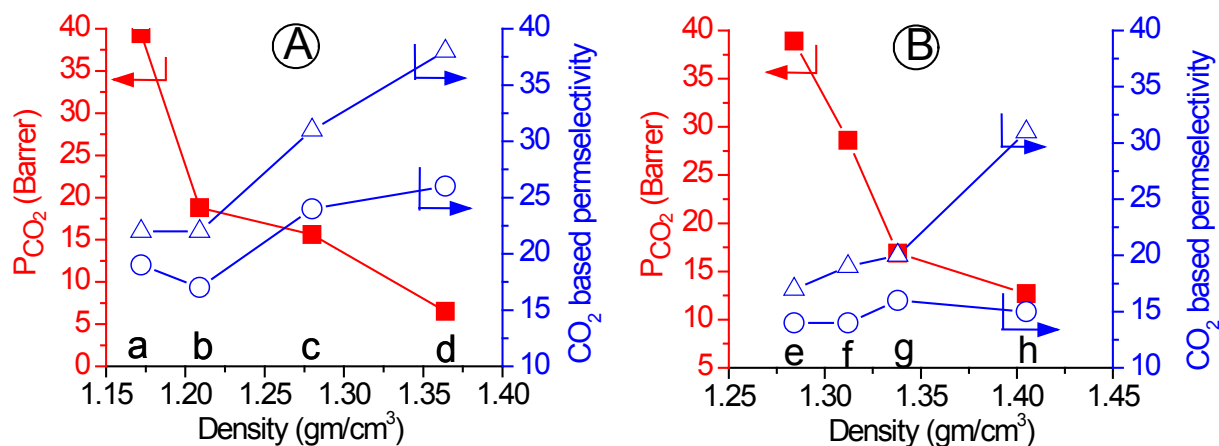
Figure 6.11 Variation in permeability P_{CO_2} (■) and selectivity (P_{CO_2}/P_{N_2} :○ and P_{CO_2}/P_{CH_4} : △) with density of (A) PILs possessing BF_4^- anion (viz., a: [TBzPBI-BuI][BF$_4$], b: [TBzPBI-I][BF$_4$], c: [TBPBI-BuI][BF$_4$], d: [TBPBI-I][BF$_4$]) and (B) PILs possessing Tf_2N^- anion (viz., e: [TBzPBI-BuI][Tf$_2$N], f: [TBzPBI-I][Tf$_2$N], g: [TBPBI-BuI][Tf$_2$N], h: [TBPBI-I][Tf$_2$N]).

It can be seen from Table 6.5 that the nature of anion had a considerable effect on the gas permeability. In PILs with four polycation (viz., [TBPBI-I], [TBzPBI-I], [TBPBI-BuI] and [TBzPBI-BuI]), gas permeability increased in the order of anion variation as I^- / $Br^- < BF_4^- < Tf_2N^-$; following the order of increasing bulk of the anion. As a results, He and H_2 based selectivity (P_{He}/P_{N_2}, P_{He}/P_{CH_4}, P_{H_2}/P_{N_2} and P_{H_2}/P_{CH_4}) decreased in the same order. These results are also in accordance with the earlier observed results in case of methyl substituted PBI based PILs [Chapter 5]. Interestingly, CO_2 based permselectivity behaved differently. It was observed that PILs based on PBI-BuI and possessing BF_4^- anions exhibited higher CO_2 based permselectivity than for PILs possessing other anions. It was made possible due to higher CO_2 sorption in earlier case (PIL with BF_4^- anion) than those with other anions (Section 6.3.4.1), since gas permeability is a product of gas diffusivity and solubility. It was interesting to note that in cases of [TBPBI-BuI] and [TBzPBI-BuI], even though its anion, Tf_2N^- is bulkier, the CO_2 permeability for PILs possessing BF_4^- and Tf_2N^- anion was almost similar, while P_{CO_2}/P_{N_2} and P_{CO_2}/P_{CH_4} selectivity was higher for PILs containing BF_4^- anion. This indicated that BF_4^- is a better CO_2 selective anion in governing separation performance of PILs.

6.3.5.2 Effects of IL density in the PBI backbone

The role of IL character in governing CO_2 permeation and CO_2 based selectivity of these PILs is clearly seen while comparing with the base PBI cases. The CO_2 permeability in PILs increased significantly, as mentioned in Section 6.3.5.1, while selectivity was decreased marginally. The bulky group substitution in PILs was responsible to increase gas permeability, while presence of IL character maintained their CO_2 based permselectivity. This can be clearly seen in Figure 6.12, which shows CO_2 permeability of the present PILs is considerably higher with slight lowering in CO_2 based permselectivity (esp. P_{CO_2}/P_{N_2} and P_{CO_2}/P_{CH_4}) than usual glassy polymers (Matrimid and PSF) [Sanders (2013)]. This effect is more pronounced in PILs based on PBI-BuI than that of PBI-I. It can be seen that [TBzPBI-BuI][BF$_4$] and [TBzPBI-BuI][Tf$_2$N] exhibited higher CO_2 permeability than that of Matrimid (~ 4 times) and PSF (~ 8 times), with only marginal lowering in P_{CO_2}/P_{N_2} and P_{CO_2}/P_{CH_4} permselectivity.
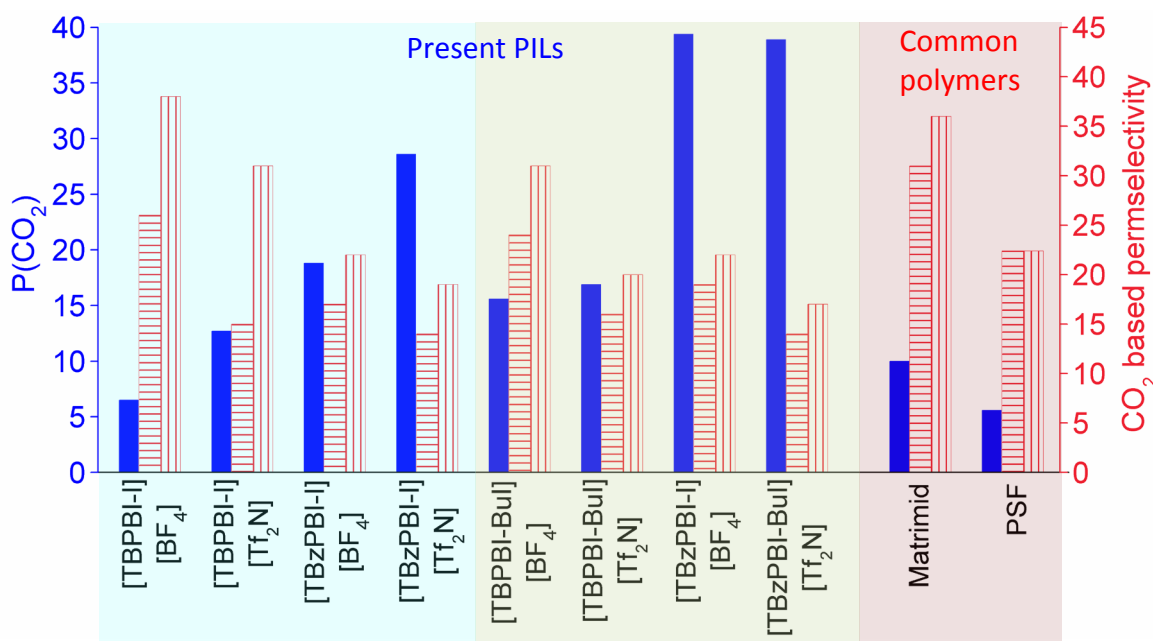
Figure 6.12 CO_2 permeability and CO_2 based permselectivity of PILs based on PBI-I, Matrimid and PSF (where, ▬: P_{CO_2}, ▭: P_{CO_2}/P_{N_2}, ▥: P_{CO_2}/P_{CH_4}).

The effect of IL density in governing CO_2 permeation performance could be seen in Figure 6.13. The effect on CO_2 permeability (Figure 6.13a) was not conclusive enough since this parameter is also governed by diffusivity that is solely a function of chain openness. On the other

hand, effect of IL density is clearly visible on governing the selectivity in PILs. This indicated that presence of high IL character is beneficial for improving CO_2 based permselectivity.
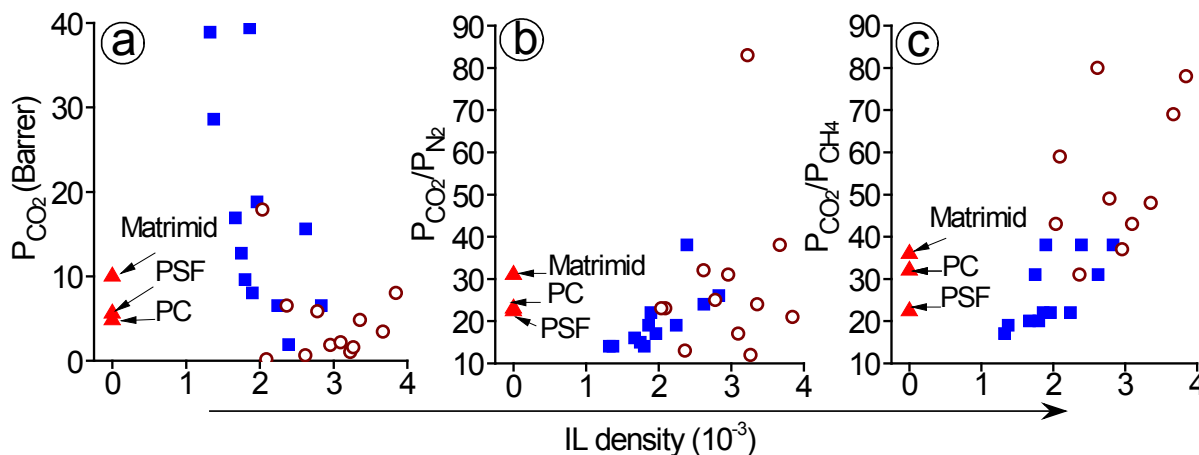
Figure 6.13 Variation in a) P_{CO_2}, b) P_{CO_2}/P_{CH_4} and c) P_{CO_2}/P_{N_2} with IL density of PILs based on PBI (■: Present PILs, o: [Chapter 5] and ▲: common polymers [Ref: Sanders (2013)].

6.3.6 *Analysis of gas diffusivity*

The diffusion coefficient of gases for the present PILs is estimated based on measured solubility and permeability coefficient at 20 atm. The obtained diffusion coefficient of all the gases is given in Table 6.6. It can be seen that for PILs possessing common anion and PBI backbone, but different substituent, gas diffusion decreased in the order of substituent size as, *tert*-butylbenzyl > *n*-butyl > methyl [Chapter 5]. The increase in diffusivity was reflected in enhancing gas permeability as discussed above. It was observed that for same substituents and anions, gas diffusivity in PILs based on PBI-BuI is higher than in PILs based on PBI-I. This could be due to initial open structure of PBI-BuI than PBI-I. This suggested that even after bulky group substitution, the precursor PBI used for PIL preparation played a role in governing gas diffusivity.

For a particular polycation, the diffusivity coefficient for a gas was found to be increased in the variation of anion as, $I^- / Br^- < BF_4^- < Tf_2N^-$, indicating bulk of the anion also contributed in enhancing gas diffusivity and hence gas permeability. It is worth to note that for PILs possessing PBI-BuI backbone ([TBPBI-BuI] and [TBzPBI-BuI]), even though the BF_4^- anion resulted in lowering gas diffusivity than that of Tf_2N^- anion; the CO_2 permeability of [TBPBI-BuI][BF_4] and [TBzPBI-BuI][BF_4] are almost comparable to the [TBPBI-BuI][Tf_2N] and [TBPBI-BuI][Tf_2N]. This could be because of the higher CO_2 sorption in cases of PILs containing BF_4^- anion than Tf_2N^- anion. This high sorption in PILs with BF_4^- anion would counter balance its lower diffusivity and hence it exhibit comparable CO_2 permeability. This supports that not only

increased free space, but presence of CO_2 selective anion also could improve gas separation performance. This observation prompts that the presence of flexible segments might increase the permeation performance with a small compromise on the selectivity.

Table 6.6 Diffusivity coefficient (D)[a] of gases in PILs and diffusivity selectivity (D_A/D_B) estimated at 20 atm.

PILs	D_{H_2}	D_{N_2}	D_{CH_4}	D_{CO_2}	$\dfrac{D_{H_2}}{D_{N_2}}$	$\dfrac{D_{H_2}}{D_{CO_2}}$	$\dfrac{D_{N_2}}{D_{CH_4}}$	$\dfrac{D_{CO_2}}{D_{N_2}}$	$\dfrac{D_{CO_2}}{D_{CH_4}}$
PILs based on PBI-I									
[TBPBI-I][I]	24.7	0.4	0.2	1.5	70.7	16.1	1.7	4.4	7.3
[TBPBI-I][BF$_4$]	37.7	1.1	0.4	3.6	33.6	10.5	2.8	3.2	9.0
[TBPBI-I][Tf$_2$N]	117.0	3.7	1.2	10.4	31.9	11.2	3.1	2.8	8.7
[TBzPBI-I][Br]	96.1	1.6	0.5	5.3	59.7	18.0	3.1	3.3	10.3
[TBzPBI-I][BF$_4$]	167.5	4.3	2.0	9.3	38.8	18.1	2.1	2.1	4.6
[TBzPBI-I][Tf$_2$N]	302.3	9.5	4.5	27.1	31.8	11.1	2.1	2.9	6.1
PBI-I[b] (base case 1)	1.2	0.009	0.003	0.09	136.7	14.3	3.0	9.6	28.7
PILs based on PBI-BuI									
[TBPBI-BuI][I]	49.6	1.6	0.7	4.0	30.6	12.4	2.5	2.5	6.1
[TBPBI-BuI][BF$_4$]	74.7	2.6	1.0	7.8	29.1	9.6	2.7	3.0	8.2
[TBPBI-BuI][Tf$_2$N]	173.4	7.3	2.8	13.6	23.9	12.8	2.6	1.9	4.8
[TBzPBI-BuI][Br]	120.2	2.1	1.0	5.3	57.3	22.9	2.1	2.5	5.2
[TBzPBI-BuI][BF$_4$]	196.5	7.7	2.7	16.7	25.5	11.8	2.8	2.2	6.1
[TBzPBI-BuI][Tf$_2$N]	379.3	15.3	7.3	31.5	24.8	12.0	2.1	2.1	4.3
PBI-BuI[b] (base case 2)	24.6	0.08	0.04	0.7	308.0	37.9	2.2	8.1	17.6

[a]: Expressed in cm^3 (STP)/cm^{3}polymer.atm, [b]: [Kumbharkar (2006)].

As could be seen from the Figure 6.14 and 6.15, the diffusivity coefficient was well correlated with the kinetic diameter of gases, as observed for common glassy polymers [Kumbharkar (2006), Karadkar (2007)]. It was observed that all present PILs exhibited higher diffusivity than that of precursor PBI, as a result of loose chain packing due to bulky substituents

and presence of anions. A trade-off relation in gas permeability and selectivity was observed in all the PILs, in tune with their typical glassy nature.
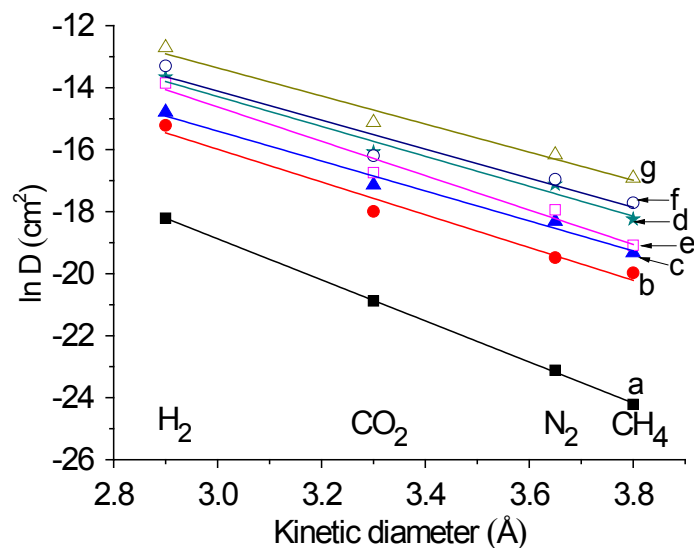
Figure 6.14 Correlation of diffusion coefficient with kinetic diameter (Å) of gases for PILs based on PBI-I (a: PBI-I; b: [TBPBI-I][Br]; c: [TBPBI-I][BF$_4$]; d: [TBPBI-I][Tf$_2$N]; e: [TBzPBI-I][I]; f: [TBzPBI-I][BF$_4$]; g: [TBzPBI-I][Tf$_2$N]).
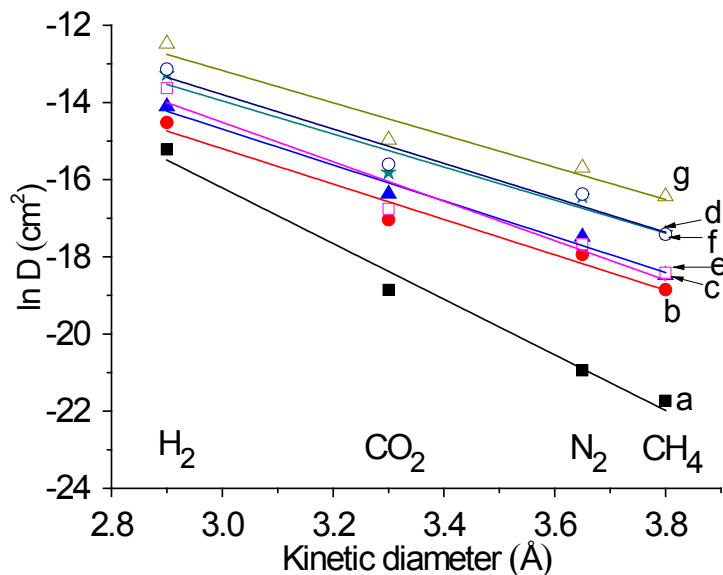
Figure 6.15 Correlation of diffusion coefficient with kinetic diameter (Å) of gases for PILs based on PBI-BuI (a: PBI-BuI; b: [TBPBI-BuI][Br]; c: [TBPBI-BuI][BF$_4$]; d: [TBPBI-BuI][Tf$_2$N]; e: [TBzPBI-BuI][I]; f: [TBzPBI-BuI][BF$_4$]; g: [TBzPBI-BuI][Tf$_2$N]).

6.3.7   Comparison with literature PILs and further work needed

This study attempted the enhancement in gas permeability of PBI based PILs. Although, CO_2 permeability of PBI based PILs was increased by bulky group substitution than methyl substituted PBI based PILs, it was still lower than some of the reported PILs. The CO_2 permeability of literature-PILs is reported upto 130 Barrer, but with much lower CO_2 based permselectivity (P_{CO_2}/P_{N_2} = 14 and P_{CO_2}/P_{CH_4} = 8.7) than that of present PILs [Carlisle (2013)]. The high CO_2 permeability of reported PILs is attributable to the rubbery nature (and thus easy diffusion of gases), while the present PILs are glassy in nature (T_g of some of the PILs are > 170 °C). It is said that the glassy polymeric membranes dominate industrial membrane separations because of their high permselectivity along with good mechanical properties [Shekhawat (2003)]. One another advantage of the present PILs is their good film forming ability. These PILs could easily sustain 20 atm upstream pressures in gas permeation cell, while the gas permeation of most of the reported PILs was taken at only ~1-2 atm. This work distinctly brings out the benefits of selecting aromatic backbone for PILs formation. For practical application, even though their permeability may remain lower, the selectivity, an important parameter for the practical significance is considerably high. The permeate flux in practical cases can be increased by increasing membrane area to cater the need.

These results conveyed that further work is needed for efficient improvement in gas permeability while maintaining their permselectivity. This could be possible by systematic structural architecture on PILs backbone that would improve CO_2 permeability preferably. Such efforts would include asymmetric alkyl substitution to disturb the chain packing further, introduction of aliphatic linkage in the backbone to increase diffusivity, etc.

6.4   Conclusions

PILs with bulky substituents (*tert*-butylbenzyl and *n*-butyl) for enhancement in gas permeability were synthesized successfully by *N*-quaternization of PBI-I and PBI-BuI followed by anion exchange with BF_4^- and Tf_2N^- anions. The ^{1}H NMR and Volhard's method confirms the formation of PILs in a quantitative manner. Solvent solubility of these PILs increased than that of parent PBIs. This is particularly advantageous for transforming them into the required membrane form (flat sheet or hollow fibre). WAXD patterns of PILs indicated their amorphous nature. Although the thermal stability of the bulky substituted PILs decreased than their parent PBIs, it is

high enough to operate these PILs for high temperature gas separation applications. These PILs also form strong and tough films (can easily sustained 20 atm upstream pressures in gas permeation cell). This further supports our earlier finding that rigid aromatic backbone in PILs renders film forming nature. The CO_2 sorption in these PILs increased in the order of anion variation as, $Tf_2N^- < I^- / Br^- < BF_4^-$. Though CO_2 sorption coefficient slightly decreased in all the PILs than that of parent PBI, sorption selectivity of CO_2 over H_2, N_2 and CH_4 increased significantly, indicating the CO_2 specificity of these PILs. Gas permeability of these PILs increased with increasing size of the substituent, which was the main objective of using bulky substituents. PIL with Tf_2N^- as an anion showed higher gas permeability than that of others. This indicated bulk of the substituent as well as anion contributed for enhancing the gas permeability. The combination of CO_2 specific anion coupled with high free volume in PILs offered higher CO_2 permeability and comparable permselectivity than the common glassy polymer used for CO_2 separation (Matrimid, PSF, PC, etc.). Film forming nature and improved permeability of bulky group substituted PILs though are attractive, investigations of PIL to possess higher permselectivity during practical gas separation condition is necessitated to employ them as a membrane materials for gas separation application, especially CO_2.

Chapter 7

Physical and CO$_2$ sorption properties of PILs possessing flexible linkage in PBI backbone

7.1   Introduction

In earlier work [Chapter 2 and 3], it was observed that PILs with aliphatic backbone were unable to form strong film due to their brittle nature; while PILs based on rigid aromatic PBI exhibited film forming ability with high mechanical strength. These films were able to sustain high upstream pressure (20 atm) during their gas permeation analysis [Chapter 5 and 6]. The gas permeability of PILs based on PBI and with bulky alkyl substitution was higher than that of methyl substituted PILs [Chapter 6]. Though the gas permeability was increased with bulky substitution, it was lower than some of the known PILs [Chapter 6]. Most of these PILs possessing high gas permeability are rubbery in nature. The higher chain flexibility due to rubbery nature seems to be responsible for higher gas diffusion and thus high permeability. Owing to their rubbery nature, these PILs possessed low selectivity. It is known that, the diffusion coefficients are sensitive to polymer chain flexibility and the free volume in the polymer [Sanders (2013)].

One of the most common approaches to enhance gas permeation in glassy polymer is to use of block-copolymers [Tena (2013)]. The promising block-copolymers include both hard and soft blocks. The hard block can have a well-packed and rigid structure, providing mechanical stability. As a result, it forms a glassy segment of the copolymer chain with usually low free volume [Tena (2013)] and thus permeability. The soft block consists of more flexible chains that can form rubbery segments in the copolymer with habitually high free volume (and thus better diffusivity than glassy segment). Thus formed copolymer would have enough strength as well as high permeability.

It is reported that in aromatic–aliphatic copoly(ether-imide)s, gas permeability was increased with increasing chain length of the PEO [Tena (2013)]. It is also known that in combination with flexible soft polymers like silicone rubber or polyethylene glycol, copolymerized polycarbonates exhibit gas permeabilities that are high enough (P_{CO_2} = 970 Barrer) to make the membrane separation process economically viable [Sridhar (2007)]. These

results suggested that incorporation of additional flexibility in the rigid aromatic PILs would enhance its gas permeability, while the presence of rigid aromatic structure would maintain its mechanical strength. With this background information, it was thought to investigate gas permeation properties of PILs based on aromatic-aliphatic backbone.

The objective of this part of the work was to introduce flexibility in PILs via structural modification of PBI while choosing its one of the monomer (dicarboxylic acid) that contains flexible linkage. To evaluate proposed concept, suberic acid (HOOC(CH$_2$)$_6$—COOH) was reacted with *3,3'*-diaminobenzedene (DAB) to offer a PBI containing flexibility. The obtained PBI was converted to PIL by *N*-quaternization using *4-tert*-butylbenzyl bromide as an alkylating agent. Its selection was based on results obtained during earlier work [Chapter 6], wherein PILs based on *tert*-butylbenzyl substitution exhibited higher gas permeation than methyl substituted PILs. It was anticipated that, in present PILs with aliphatic-aromatic backbone, the gas permeability will be governed by improved diffusion due to bulky substitution and aliphatic nature, while the gas selectivity will also be controlled by the backbone rigidity. The halide exchange was done with BF$_4^-$ and Tf$_2$N$^-$ anions.

7.2   Experimental

7.2.1   Materials

3,3'-Diaminobenzidine (DAB), suberic acid, sodium hydride (60 % dispersion in mineral oil), dry dimethyl sulphoxide (DMSO, 0.01% H$_2$O), *4-tert*-butylbenzyl bromide, silver tetrafluoroborate (AgBF$_4$) and lithium bis(trifluoromethane) sulfonimide (LiTf$_2$N) were procured from Aldrich Chemicals. Polyphosphoric acid (PPA) was procured from Alfa Aesar. Potassium thiocyanate (KSCN, 98%) and sodium chloride (NaCl, 99%) were procured from S.D. Fine Chemicals. Formic acid was obtained from Thomos Beaker. All these chemicals and solvents were used without further purification.Pure gases, viz.; He, H$_2$ and N$_2$ (minimum purity of 99.9%) were procured from Vadilal Chemicals Ltd., while CH$_4$ and CO$_2$ (99.995% purity) were procured from Air Liquide.

7.2.2   Synthesis of Polybenzimidazole (PBI$_6$)

A three-necked round bottom flask equipped with a mechanical stirrer, N$_2$ inlet and CaCl$_2$ drying tube was charged with 1200 g of PPA and 40 g (0.18668 mol) of DAB.

Temperature of the reaction mixture was elevated to 140 ºC. After dissolution of DAB, 0.18668 mol of a suberic acid was added; temperature was raised to 170 ºC and maintained for 1 h under constant flow of N_2. The temperature was further raised to 200 ºC and maintained for 1 h 40 min. The polymer was obtained by precipitation of the reaction mixture in water. Obtained dark brown polymer threads were crushed, thoroughly washed with water, kept in 10% NaHCO$_3$ for 16 h and again washed with water, until the filtrate was neutral to pH. The collected polymer was immersed in acetone for 16 h, filtered and dried in vacuum oven at 100 ºC for 3 days. Formed PBI was designated as PBI$_6$, where '6' denotes the number of -CH$_2$- groups present in the aliphatic dicarboxylic acid used for the PBI synthesis (Scheme 7.1).
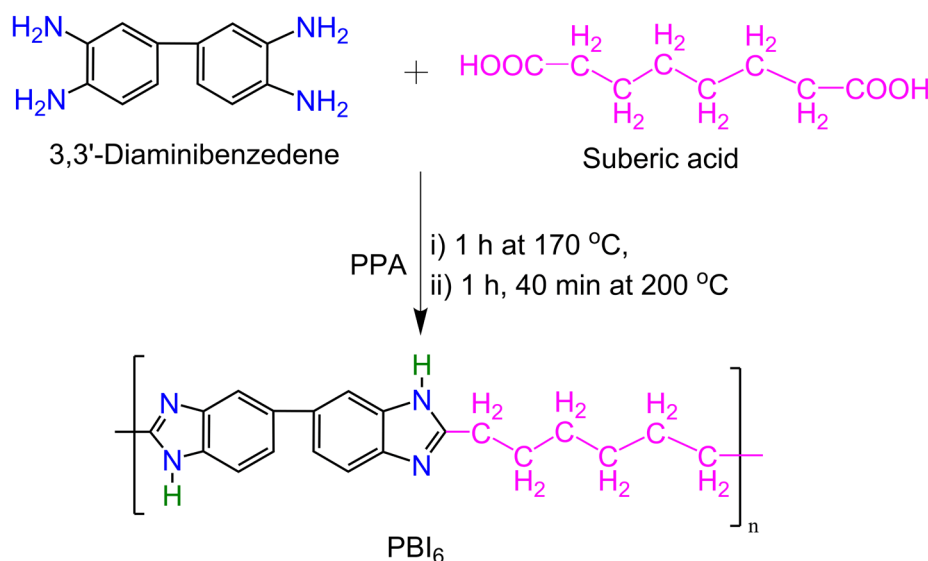
Scheme 7.1 Synthesis of PBI$_6$.

7.2.3   N-Quaternization of PBI$_6$

A 3-necked flask was charged with 400 ml of dry DMSO, 10 g of PBI$_6$, 2.1 molar equivalents of NaH and stirred under dry N_2 atmosphere at 170 ºC for 3 h. The high temperature for the *N*-sodium salt formation was necessitated due to the sluggish dissolution of PBI$_6$. After complete dissolution was occurred, temperature of the red colored reaction mixture was lowered to the ambient and 4.2 equivalent of *4-tert*-butylbenzyl bromide was added slowly over a period of 15 min while stirring. A yellow precipitate was formed, which was dissolved subsequently as the reaction temperature was elevated to 80 ºC. The reaction mixture was stirred further for 20 h, temperature was lowered down to the ambient and precipitated in acetone. Obtained polymer

was further purified by dissolving in DMSO and reprecipitation in acetone. The obtained PIL was designated as [TBzPBI$_6$][Br] (Scheme 7.2).
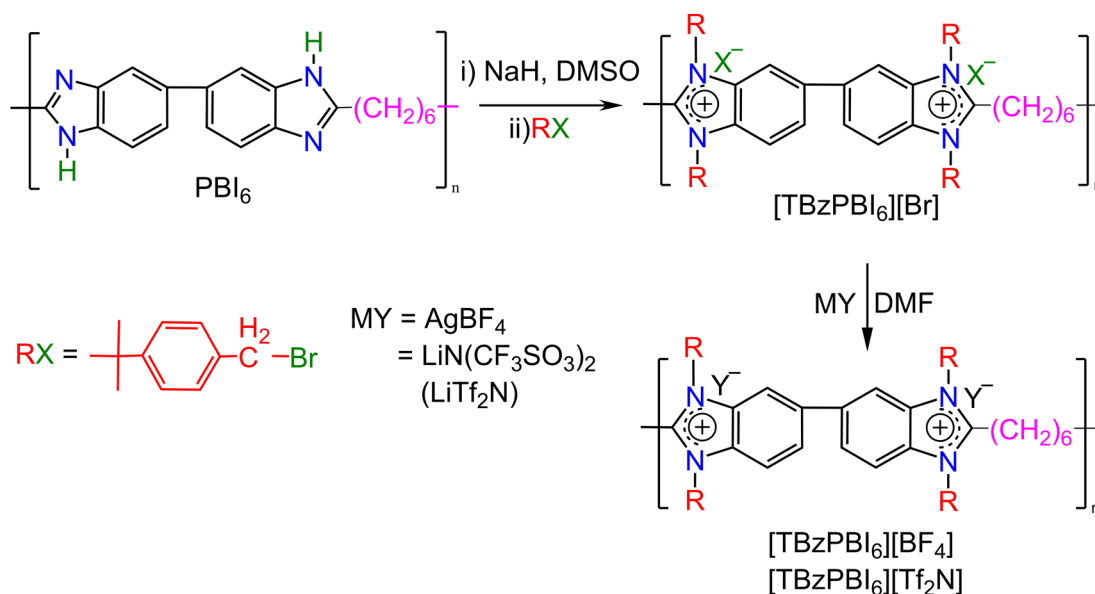
Scheme 7.2 Synthesis of PILs based on PBI$_6$.

7.2.4 *Anion exchange*

A two necked flask equipped with a calcium chloride guard tube was charged with 5 g of a quaternized PBI$_6$ and 100 ml of DMF. After the complete dissolution, 2 molar equivalent of AgBF$_4$ was added while stirring. Formation of the AgBr precipitate began with the addition of AgBF$_4$, while the anion exchanged polymer remained in the dissolved state. The reaction mixture was further stirred at ambient for 24 h in order to ensure complete replacement of the anion. The precipitated AgBr was removed by repeated centrifugation at 12000 RPM. Formed PIL was recovered from the supernatant solution by solvent evaporation. It was purified further by dissolving in DMF (8% w/w), followed by reprecipitating in water. Purified PIL ([TBzPBI$_6$][BF$_4$]) was dried at 80 ºC in a vacuum oven for 3 days.

The bromide exchange by Tf$_2$N$^-$ anion was performed using LiTf$_2$N. A 5 g of [TBzPBI$_6$][Br] was dissolved in a 100 ml of DMF, 2 mol of LiTf$_2$N was added and stirred for 24 h. A resulting homogeneous reaction mixture was precipitated in water; obtained PIL was thoroughly washed with water in order to remove LiBr and then dried at 80 °C. It was further purified by dissolving in DMF (8% w/w), reprecipitating in water, followed by drying at 80 ºC in

the vacuum oven for 3 days. An amount of Br¯ exchanged in both the PILs was estimated by Volhard's method as given below in Section 7.2.6.1.

7.2.5   Membrane preparation

The dense membranes (films) were prepared by solution casting method on a flat glass surface using 3% (w/v) PIL solution in DMAc at 80 °C for 18 h under dry conditions. After solvent evaporation, formed membrane was found to be brittle that cracked while handling. It was dried in a vacuum oven at 80 °C for a week in order to remove traces of the solvent.

7.2.6   Characterizations

7.2.6.1 Degree of N-quaternization (DQ) and bromide exchange

The degree of *N*-quaternization of PBI_6 (DQ) was determined by ^{1}H-NMR (recorded on Bruker AC-200 using DMSO-d_6 as the solvent). These spectra are shown in Figure 7.1. The percent of bromide exchanged by a requisite anion was determined by Volhard's method [Jeffery (1989)], in which, 0.1 g of PIL powder was stirred in 30 ml of 0.01M $AgNO_3$ solution for 24 h. An excess of unreacted $AgNO_3$ was titrated against 0.01 M KSCN. From the amount of $AgNO_3$ consumed by PIL, its bromide content (and thus the percent of anion exchange) was estimated.

7.2.6.2 Physical properties

The solubility of PILs in common organic solvents was determined by stirring 0.1 g of PIL in 10 ml of a solvent at the ambient for 24 h. In case of insolubility, heating at 80 °C (or near boiling point, in case of the low boiling solvents) for 24 h was employed. Observations are given in Table 7.1. The inherent viscosity (η_{inh}) of PILs was determined at 0.2 g/dL concentration in DMSO at 35 °C and given in Table 7.2.

The wide angle X-ray diffraction (WAXD) pattern of PILs in the film form was recorded using Rigaku X-ray diffractometer (D-max 2500) with Cu-K_α radiation. The average intersegmental *d*-spacing (d_{sp}) for the amorphous peak maxima was calculated using Bragg's equation. The density (ρ) of membranes was measured at 35 °C by using specific gravity bottle and decalin as the solvent that exhibited negligible sorption in PILs (< 2 %). This measurement was repeated with five samples and the deviation from average value was ≤ 0.005 g/cm^3.

Thermogravimetric analysis (TGA) of polymers was performed using Perkin Elmer

TGA-7 in N_2 atmosphere with a heating rate of 10 °C/min. The glass transition temperature (T_g) was determined using DSC Q-10 (TA instruments, USA) under N_2 atmosphere with a heating rate of 10 °C/min.

7.2.7 *Gas sorption*

Pure gas sorption isotherms for H_2, N_2, CH_4 and CO_2 were determined at 35 °C as given in Chapter 2, Section 2.2.4. The solubility coefficient (S) and solubility selectivity (S_A/S_B) at 20 atm are given in Table 7.3. The dual mode sorption parameters (k_D, b and C_H) obtained for present PILs are given in Table 7.4.

7.3   Results and discussion

7.3.1 *Synthesis, degree of quaternization and anion exchange*

The chosen ratio of DAB:PPA (1:30, w/w) and the time of reaction at 200 °C as 1 h 40 min offered high enough inherent viscosity of ~1.7 dL/g. The purified PBI_6 was used for PILs synthesis. The *N*-quaternization of PBI_6 by bulky substituent could be successfully achieved by in-situ formation of Na-salt of PBI_6, followed by the addition of a small excess of *tert*-butylbenzyl bromide (4.2 molar equivalents). The Na-salt formation of PBI_6 required heating of reaction mixture at 170 ºC for 3 h. Such a harsh condition was needed due to the insolubility of PBI_6 in DMSO. The same observation was reported for *N*-quaternization of ABPBI due to its insolubility in DMSO [Kumbharkar (2008)]. The formed solution remained homogeneous after cooling it to the ambient temperature. During *N*-quaternization of PBI_6, an immediate precipitate formation indicated the progress of reaction. Formed precipitate was slowly dissolved after the temperature was elevated to 80 ºC. This temperature elevation was performed in order to achieve the complete dissolution, which would aid the substitution reaction in the solution phase. Formed solution remained clear and homogeneous even after temperature was lowered to the ambient. The formed [TBzPBI$_6$][Br] was precipitated in acetone, yielding a yellow fibrous polymer. Obtained polymer after vacuum drying at 80 °C was purified by dissolving in DMF and reprecipitation while stirring in acetone. The yield of PIL after its purification was > 85 %.

The ^{1}H-NMR spectra of *N*-quaternized PBI_6 are given in Figure 7.1. In the spectra of PBI_6, broad peak appeared in the range of δ 13-14 correspond to the proton belonging to N-H of imidazole. In the cases of *N*-quaternized PBIs, this peak was disappeared completely. This

indicates almost complete *N*-quaternization was occurred. The quantitative estimation of [TBzPBI$_6$][Br] was done based on the comparison of integration of aromatic proton belonging to *tert*-butylbenzyl group appeared in the range of δ 6.5 – 7.5 to the aromatic protons of precursor PBI$_6$ appearing in the range of δ 7.5 – 9.5. It was found that the degree of *N*-quaternization for [TBzPBI$_6$][Br] was 85 %.
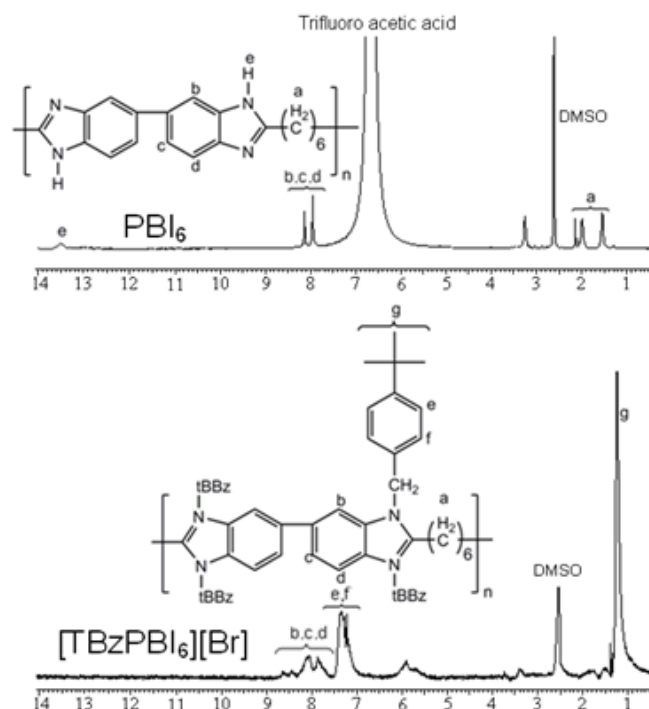
Figure 7.1 ^{1}H NMR spectra of [TBzPBI$_6$][Br] and PBI$_6$.

Anion exchange of [TBzPBI$_6$][Br] was performed using BF$_4$$^-$ and Tf$_2$N$^-$ anion. These two anions were chosen based on better physical and gas separation properties observed with these anions in earlier cases of PBI based PILs [Chapter 5 and 6]. The percent anion exchange was determined by Volhard's method [Jeffery (1989)]. This analysis showed that the anion exchange in case of PILs possessing BF$_4$$^-$ anion was higher (92 %) than that of PILs possessing Tf$_2$N$^-$ anion (84 %). This higher exchange with BF$_4$$^-$ anion could be attributed to the use of silver salt for anion exchange reaction. Such a difference was also observed in earlier cases of exchange with [TMPBI-BuI], [TBPBI-I], [TBPBI-BuI], [TBzPBI-I] and [TBzPBI-BuI] based PILs [Chapter 5 and 6].

7.3.2 Physical properties

7.3.2.1 Solvent solubility

Conversion of PBI into a PIL improved the solvent solubility. This is evidenced by the solubility of all PILs in DMF, DMAc, DMSO and NMP; in which, PBI_6 is insoluble (Table 7.1). The solubility was further enhanced after the bromide exchange. The $[TMPBI_6][BF_4]$ and $[TMPBI_6][Tf_2N]$ were freely soluble in polar aprotic solvents, viz., acetonitrile and acetone, respectively (in which the bromide counterpart was insoluble). The similar behaviour for PILs containing BF_4^- and Tf_2N^- as an anion was observed in earlier study of PILs based on PBI-I and PBI-BuI [Chapter 5 and 6]. All these PILs were insoluble in water and alcohols examined.

Table 7.1 Solvent solubility of PILs based on PBI_6.

PILs	DMF	DMAc	DMSO	NMP	Acetone	CH_3CN	Methanol	Ethanol	*1*-Propanol
$[TBzPBI_6][Br]$	+	++	++	++	−	−	−	−	−
$[TBzPBI_6][BF_4]$	++	++	++	++	−	++	−	−	−
$[TBzPBI_6][Tf_2N]$	++	++	++	++	++	−	±	−	−
PBI_6 (base case)	−	−	±	±	−	−	−	−	−

++: Soluble at ambient, +: soluble after heating at 80 ℃ / reflux in case of acetone and acetonitrile for 24 h, ±: partially soluble or swelling after heating, −: insoluble

7.3.2.2 Film forming ability

Present PILs were brittle in nature and unable to form film. In comparison to PBI-I and PBI-BuI based PILs (with the same substituent and anion), the only difference in these PILs is the presence of flexible aliphatic linkage. Though the PBI_6 exhibited good film forming ability, its PIL formation reduced the mechanical strength. It was observed in earlier cases that, formation of PILs decreased the mechanical strength of PBI-I and PBI-BuI [Chapter 5]. In view of higher inherent viscosity of PBI_6 than that of PBI-I or PBI-BuI, presence of aliphatic linkage in the PIL backbone seems to be the major responsible factor for film forming inability of present PILs. A brittle nature of PILs based on aliphatic backbone is well reported [Tang (2005e), Hu (2006), Bara (2007b, 2008a)]. Present results conveyed that the rigid aromatic backbone may be essential for gaining film forming nature and any induced flexibility in the backbone may compromise on film forming ability.

7.3.2.3 Solution viscosity

Table 7.2 shows that inherent viscosity of PILs increased than that of parent PBI$_6$. This increase in viscosity is mainly due to the presence of cation and anion in the polymer matrix. It is known that PBI based PILs exhibited polyelectrolyte effect and possess higher inherent viscosity than their precursor PBI [Chapter 5 and 6]. The observed viscosity for these PILs was lower than that of PILs based on PBI-I and PBI-BuI possessing same substituent and anion. This could be attributed to the presence of flexible alkyl group in the PBI backbone.

Table 7.2 Physical properties of PILs based on PBI$_6$.

PILs	% Anion exchange[a]	η_{inh}[b] (dL/g)	d_{sp}[c] (Å)	ρ[d] (gm/cm^3)	T_g[e] (°C)	TGA	
						IDT[f] (°C)	W$_{900}$[g] (%)
[TBzPBI$_6$][Br]	–	2.3	4.43	1.340	195	253	15.2
[TBzPBI$_6$][BF$_4$]	92.0	2.3	4.50	1.364	164	300	8.4
[TBzPBI$_6$][Tf$_2$N]	86.0	2.6	4.79	1.430	153	405	5.0
PBI$_6$ (base case)	–	1.7	4.48	1.289	266	459	23.1

[a]: Determined by Volhards method, [b]: inherent viscosity determined using 0.2 g/dL solution at 35 ºC, [c]: d-spacing obtained from wide angle X-ray diffraction spectra, [d]: density measured at 35 ºC, [e]: glass transition temperature, [f]: initial decomposition temperature, [g]: char yield at 900 °C.

7.3.2.4 Packing density parameters

WAXD patterns of these PILs (Figure 7.2) indicated their amorphous nature. The average *d*-spacing (d_{sp}) of PILs corresponding to the amorphous peak maxima is given in Table 7.2. The d_{sp} in theses PILs increased in the order of their anion variation as: Br$^-$ < BF$_4^-$ < Tf$_2$N$^-$. This shows that bulk of the anion is responsible for the increase in d_{sp}. Higher d_{sp} for PILs with Tf$_2$N$^-$ as an anion was also observed in earlier PILs based on PBI [Chapter 5 and 6] and P[DADMA] based PILs [Chapter 2].

The PIL density increased in the order of their anion variation as BF$_4^-$ < Br$^-$ < Tf$_2$N$^-$ (Table 7.2). The similar results of variation in density with the variation in anion were observed PBI-I and PBI-BuI based PILs [Chapter 5 and 6]. This shows that nature of the anion also play a role in governing density.
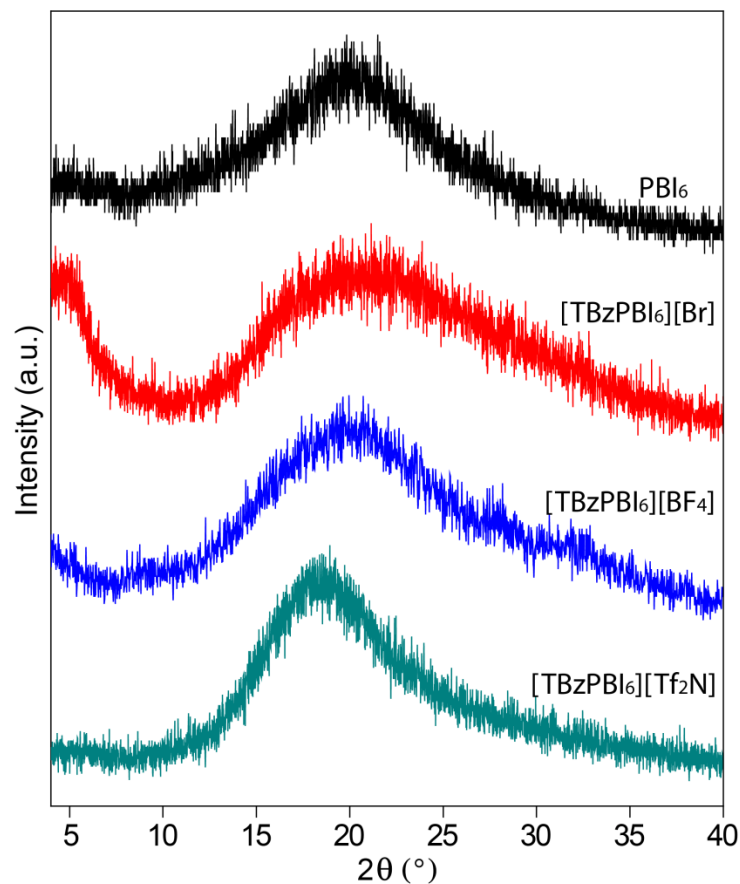
Figure 7.2 Wide angle X-ray diffraction patterns of PILs based on PBI_6.

7.3.2.5 Thermal stability of PILs

The TGA of present PILs along with their parent PBI_6 are given in Figure 7.3, while initial decomposition temperature (IDT) is given in Table 7.2. Thermal stability of these PILs decreased than their parent PBI_6, as also observed in earlier cases. This decrease in thermal stability could be attributed to the elimination of H-bonding, substitution by alkyl group and presence of anion.

The IDT values of present PILs (based on PBI_6) are similar to the PILs based on PBI-I and PBI-BuI (with similar substituent and anion) [Chapter 6], indicating that even the backbone was changed from aromatic to aliphatic, thermal stability of the PILs was almost similar and the aliphatic linkage in PIL has insignificant role in determining TGA pattern. As also could be seen from thermograms (Figure 7.3), the nature of anions was found to have a significant effect on thermal stability of the PILs (Table 7.2). PILs with the varying anion, thermal stability of PILs increase with the order of anions as $Br^- < BF_4^- < Tf_2N^-$, showing the similar effect of anion on

governing thermal stability as seen in earlier study [Chapter 2, 5 and 6]. Glass transition temperature of the present PILs could be detected easily (which was difficult in earlier cases). In spite of aliphatic linkage in the backbone, T_g of these PILs (Table 7.2) indicated their glassy in nature.
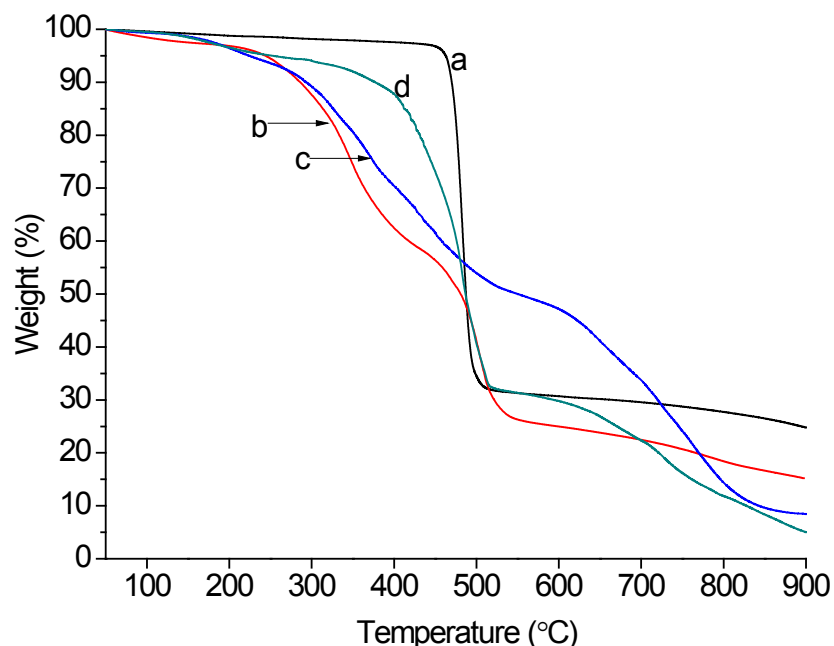
Figure 7.3 TGA curves of PILs based on PBI_6 (a: PBI_6; b: $[TBzPBI_6][Br]$; c: $[TBzPBI_6][BF_4]$; d: $[TBzPBI_6][Tf_2N]$.

7.3.3 *Gas sorption*

The sorption isotherms for present PILs obtained at 35 °C using pure gases (H_2, N_2, CH_4 and CO_2) showed a typical dual-mode nature (Figure 7.4) as usually observed for glassy polymers [Kumbharkar (2006), Li (2013)]. The sorption of different gases increased in the order: $H_2 < N_2 < CH_4 < CO_2$. This follows the trend of increasing order of inherent condensabilities of these gases (for example, critical temperature (T_c) increases in the order -239.85 °C < -146.95 °C < -82.45 °C < 31.05 °C for H_2, N_2, CH_4 and CO_2 respectively) [Li (2009b)]. It can be seen from Fig. 7.4 that variation in anions of PILs had a considerable effect on gas sorption. It would be interesting to compare the CO_2 sorption behaviour for these PILs with the earlier investigated PBI based PILs, as discussed in following sections.
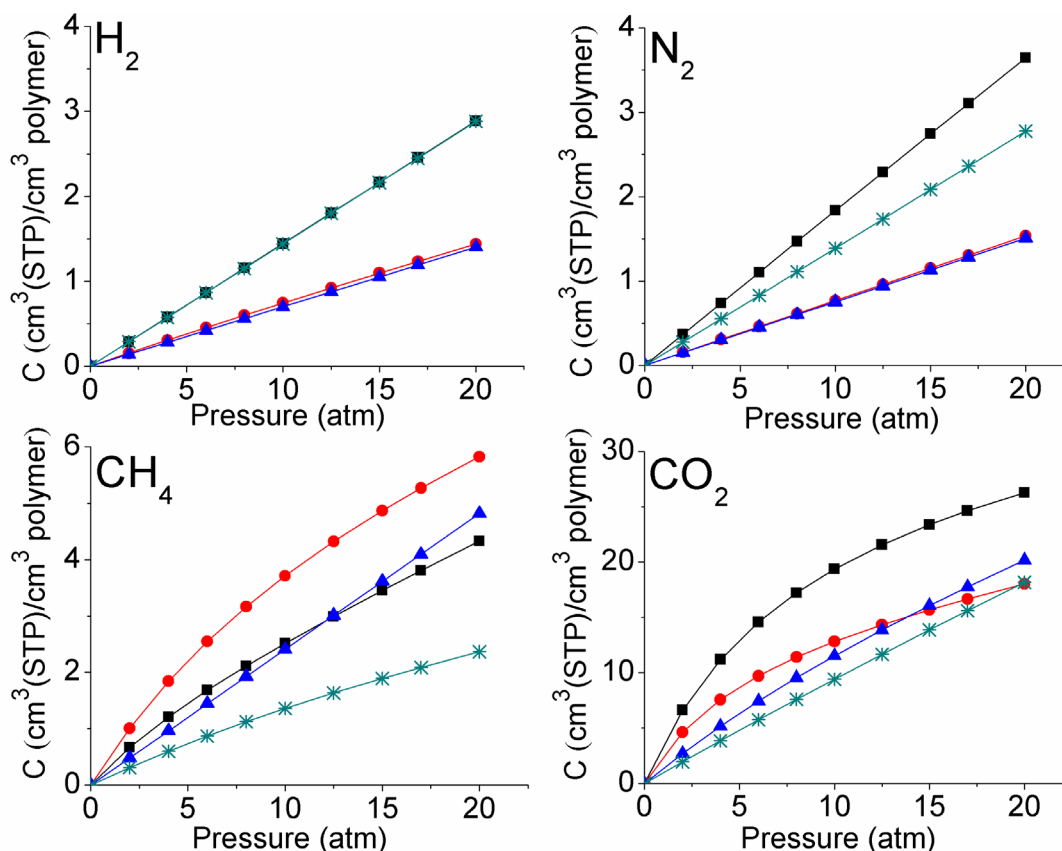
Figure 7.4 Gas sorption isotherms for PILs based on PBI_6 at 35 ºC (■: PBI_6; ●: $[TBzPBI_6][Br]$; ▲: $[TBzPBI_6][BF_4]$; ✳: $[TBzPBI_6][Tf_2N]$).

Table 7.3 Solubility coefficient $(S)^a$ and solubility selectivity (S_A/S_B) of PILs at 20 atm.

PILs	S_{H_2}	S_{N_2}	S_{CH_4}	S_{CO_2}	S_{N_2}/S_{CH_4}	S_{CO_2}/S_{H_2}	S_{CO_2}/S_{N_2}	S_{CO_2}/S_{CH_4}
$[TBzPBI_6][Br]$	0.07	0.08	0.29	0.90	0.26	12.52	11.73	3.09
$[TBzPBI_6][BF_4]$	0.07	0.08	0.24	1.01	0.31	14.39	13.39	4.18
$[TBzPBI_6][Tf_2N]$	0.14	0.14	0.12	0.91	1.17	6.31	6.55	7.68
PBI_6 (base case)	0.14	0.18	0.22	1.32	0.84	9.15	7.24	6.09

^{a}: Expressed in cm^3 (STP)/cm^3polymer.atm.

7.3.3.1 *Effect of aliphatic linkage in the backbone*

Gas solubility coefficient (S) and solubility selectivity (S_A/S_B) for present PILs at 20 atm is summarized in Table 7.3. It was observed that S_{CO_2} of PILs based on PBI_6 was lower than that of PILs based on PBI-BuI and PBI-I possessing same substituent and anion [Chapter 6]. This

could be because of the fact that the precursor PBI_6 has lower CO_2 sorption than PBI-I and PBI-BuI. It was observed that precursor PBI used for PIL preparation had its own effect on governing their gas sorption [Chapter 6]. It could be seen from Table 7.3 that present PILs showed lower CO_2 sorption than that of parent PBI_6. Such behaviour was observed in PILs based on PBI-BuI with the same substituent and anion. It is known that, gas sorption in polymer is mainly governed by available free volume and gas-polymer interaction [Barbari (1988), Tang (2009)]. In PILs, gas-polymer interaction is anticipated to be governed by its IL character [Mecerreyes (2011), Yaun (2013)]. The bulky substituent in the present PILs increased the repeat unit molecular weight, which led to lowering in IL character in PILs matrix. Moreover, formation of PILs by bulky substituent decreased the T_g than that of precursor PBI_6. This would lead to decrease in microvoids or the unrelaxed volume. Both these parameters could be responsible for reducing CO_2 sorption in present PILs than their parent PBI_6. The effect of IL character in polymer on governing the CO_2 sorption can also be seen in Figure 7.5. It shows that CO_2 sorption expressed in mol% of the present PILs is higher than that of precursor PBI_6. This implies that IL character indeed helps in elevating CO_2 sorption in PILs.
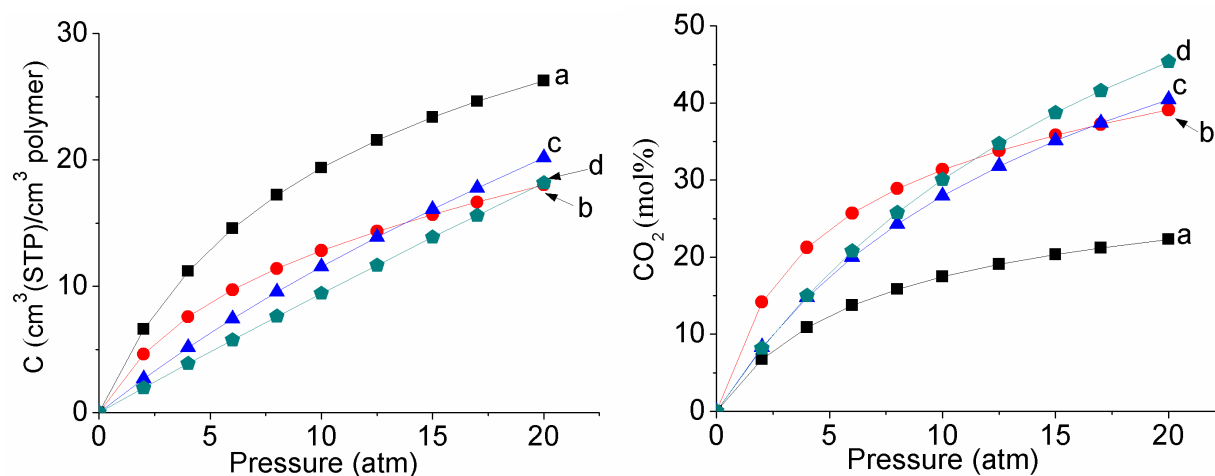
Figure 7.5 CO_2 sorption isotherms for PILs based on PBI_6 at 35 ºC (a: PBI_6; b: $[TBzPBI_6][Br]$; c: $[TBzPBI_6][BF_4]$; d: $[TBzPBI_6][Tf_2N]$).

The CO_2 sorption specificity of present PILs was also supported by increase in their CO_2 based sorption selectivities, viz., S_{CO_2}/S_{H_2} and S_{CO_2}/S_{N_2} than their parent PBI_6. This also

suggests that presence of IL character in the polymer lead to preferential sorption of CO_2, which can ultimately improve the CO_2 separation characteristics.

7.3.3.2 Effect of variation of anion on gas sorption

Effect of anion variation on the gas sorption could be seen from Figure 7.4. It was observed that the CO_2 sorption in present PILs increased in the order: $Tf_2N^- < Br^- < BF_4^-$. The similar trend was observed in PILs based on PBI-I and PBI-BuI [Chapter 5 and 6]. This indicated that even though after backbone variation from completely rigid aromatic backbone to flexible aliphatic-aromatic backbone, anion holds a profound role in governing CO_2 sorption in PILs. Present observations of gas sorption suggest that CO_2 sorption is governed by available free volume as well as gas-PIL interactions. Hence it would be worth to pay attention to gas sorption parameters, as discussed below.

7.3.3.3 Gas sorption parameters

The gas sorption parameters for present PILs obtained from sorption isotherms are given in Table 7.4.

Table 7.4 Dual-mode sorption parameters[a] obtained during gas sorption in PILs.

PILs	H_2			N_2			CH_4			CO_2		
	k_D	C'_H	b	k_D	C'_H	b	k_D	C'_H	b	k_D	C'_H	b
[TBzPBI$_6$][Br]	0.06	0.60	0.03	0.08	1.93	4.58×10^{-6}	0.09	6.88	0.0	0.31	15.2	0.18
[TBzPBI$_6$][BF$_4$]	0.07	2.12	3.8×10^{-5}	0.08	1.61	4.22×10^{-5}	0.24	4.92	2.8×10^{-5}	0.50	22.6	0.04
[TBzPBI$_6$][Tf$_2$N]	0.14	1.04	3.6×10^{-5}	0.14	1.75	0.001	0.04	4.35	0.0	0.69	16.8	0.09
PBI$_6$ (base case)	0.14	0.65	4.3×10^{-4}	0.17	1.58	0.01	0.16	1.63	0.14	0.179	32.4	0.12

[a]: k_D is expressed in $cm^3(STP)/cm^3$polymer.atm, C'_H is expressed in $cm^3(STP)/cm^3$polymer, while b is expressed in atm^{-1}.

It could be seen that Henry's solubility coefficient, k_D (ascribed to the gas dissolution in rubbery state) was lower for all the gases, owing to the glassy nature of PILs. The C'_H (hole-filling constant) which represents maximum amount of the penetrant sorbed into 'microvoids' or the unrelaxed volume of the polymer matrix [Barbari (1988), Kanehashi (2005)]. In all cases,

this parameter was lower for all gases in comparison to their parent PBI_6 (Table 7.4). This could be due to the lower T_g of PILs than their parent PBI_6 (Table 7.2), indicating lower microvoids or unreleaxed volume in PILs than in parent PBI_6. For all the PILs, C'_H was higher for CO_2 than for other gases. This is in accordance with the gas sorption behavior observed for most of the common glassy polymers [Kumbharkar (2006), Karadkar (2007), McHattie (1992), Barbari (1988)], possessing high C'_H for CO_2 than for other gases. The Langmuir affinity constant 'b' is negligible for H_2 and N_2 than that for CH_4, while it is considerably higher in case of CO_2. For a particular PIL, both, C'_H and b were increased with increasing the order of gas condensability as observed in prior cases of PILs based on PBI-I and PBI-BuI.

7.3.3.4 Alternatives approach for membrane preparation of aliphatic-aromatic PBI based PILs

In view of brittle nature of present PILs, alternative strategies for membrane preparation need to be investigated. It is known that brittle PILs could be transformed into film form by following different methodologies, viz., crosslinking, copolymerization or supporting on a porous polymer film [Hu (2006), Bara (2007b, 2008a), Li (2011, 2012), Hudino (2011), Chi (2013)]. The systematic crosslinking of PILs by using dialkyl halide for *N*-quaternization could improve its mechanical strength. Another approach could be partial *N*-quaternization of aliphatic-aromatic PBI. By these approaches the film forming ability could be regained without much sacrifice on anticipated benefits of flexibility in the backbone (ease in diffusivity and CO_2 sorption specificity).

7.4   Conclusions

PILs with flexible linkage in the backbone were successfully synthesized by *N*-quaternization of aliphatic-aromatic PBI (PBI_6). The ^{1}H NMR and Volhard's method confirmed the formation of PILs in a quantitative manner. The *N*-quaternization with *tert*-butylbenzyl bromide could be successfully performed with > 85% degree of quaternization. PILs were developed by bromide exchange with BF_4^- and Tf_2N^- anions. Conversion of PBI_6 into PIL improved its solvent solubility. The physical properties viz., d_{sp}, density, thermal stability and T_g of PILs followed the similar trend as observed in PILs based on PBI-I and PBI-BuI, indicating anion play a profound role for governing these properties. This is especially important in the event that the backbone of PILs changed from rigid to flexible. The introduction of aliphatic

linkage in the backbone of these PILs lowered the T_g to a larger extent as compared to the PILs based on PBI-I and PBI-BuI. Although CO_2 sorption of these PIL was lower than PILs based on PBI-I and PBI-BuI, it was counterbalanced by improved CO_2 based sorption selectivity over H_2, N_2 and CH_4. Unfortunately, the obtained PILs could not form strong films, indicating necessity of fully aromatic backbone for film formation or need for following alternate methodology to make film out of these PILs.

Chapter 8
Conclusions

This work deals with investigations of new families of polymeric ionic liquids (PILs) based on aliphatic and aromatic backbone. Effects of structural variation in their backbone, anion and *N*-substitution using various alkyl groups on physical and gas permeation properties were analyzed. Initially, PILs based on aliphatic backbone were synthesized by metathesis (anion exchange reaction) of commercially available precursor, P[DADMA][Cl]. Promising anions belonging to carboxylates, sulfonates and inorganic types were employed for this purpose. Use of silver salt of anions for metathesis reaction offered almost quantitative replacement of halide anion than that in the cases of Na or Li salt of anions. PILs containing fluorinated anions were more effective in chain loosening (judged by d_{sp} and density variations) than that of non-fluorinated ones. PILs possessing sulfonated anions generally exhibited higher IDT than that of carboxylated anions. PILs possessing carboxylated anion exhibited attractive CO_2 sorption capacity as well as sorption selectivity over H_2 and N_2, in comparison to other two families of anions. Selectivity in case of PILs containing Ac^- and Bz^- anion was highly attractive (S_{CO_2}/S_{N_2} of 114.3 and 41.5, respectively). Anion-basicity was found to have profound effect on governing CO_2 sorption in these PILs.

Based on encouraging results with Ac^- and Bz^- anions, more understanding with PILs possessing various carboxylated anions of higher basicity and bulkier nature was gathered. For this study, PILs based on P[DADMA] as a backbone and aliphatic carboxylate anion with increasing alkyl chain length as well as substituted aromatic carboxylate anions were employed while obtaining high anion exchange (> 87 %). Assertive effect of varying alkyl chain length of carboxylated anions on improving CO_2 sorption in PILs could only be seen at lower pressures (2-5 atm). PILs based on aromatic carboxylate anions exhibited lower CO_2 sorption than that of aliphatic carboxylate anions. A lower basicity of aromatic carboxylate anions than that of aliphatic carboxylated anions and close PIL chain packing (decreased d_{sp}) seems to be responsible for such a lowering. Nonetheless, these PILs exhibited considerably higher CO_2 sorption and its selectivity over other gases, than for most of the reported PILs, ionic liquids and common polymers. This observation showed promises for their application as CO_2 absorbent

164

materials. In spite of such attractive properties, they could not be investigated as membrane materials due to their brittleness. Thus, an alternative technique was necessitated for extracting their benefits.

One of the promising PILs from above study, viz., P[DADMA][Ac] was blended with PEBAX-2533 possessing good permeability. Formed membranes were capable of sustaining high upstream pressure (10 atm) without any physical damage during gas permeation analysis. Incorporation of PILs in PEBAX-2533 reduced the gas permeation, as anticipated. Unfortunately, enhancement in CO_2 based selectivity was insignificant. This was thought to be the result of rubbery nature of PEBAX, in which PIL would be acting as impermeable filler. Although bending with other polymers could have been explored, it was thought to move away from aliphatic backbone of PILs. Another reason for arriving at this decision was appearance of literature conveying inability of such PILs to form films (membranes).

PILs possessing aromatic backbone were obtained by following an altogether different methodology of postmodification (*N*-quaternization using methyl group, followed by iodide exchange with various promising anions) of polybenzimidazole (PBI-BuI). This new methodology offered PILs possessing excellent film formation ability. Salient features of this methodology include wide structural tunability via structural variations in monomers of PBI, alkyl/aryl group used for *N*-substituion and available anion diversity. Another significant advantage of this methodology is that it leads to two IL characters per repeat unit of a PIL.

Initially, PILs based on PBI-BuI were successfully synthesized with > 96 % *N*-quaternization and almost quantitative iodide exchange by another anion of interest. These new series of PILs was thoroughly characterized for physical properties that are known to affect gas permeation (d_{sp}, density, thermal and mechanical properties, water sorption, contact angle, etc.). Glass transition temperature could be detected only for some of the PILs conveying their glassy nature. Anion variation offered wide diversity in some of these properties, esp. water sorption, conveying property tuning is easily possible. All PILs (except those based on acetate and benzoate as an anions) offered mechanically strong films with high enough tensile strength, indicating role of rigid aromatic backbone in governing film forming ability. Some of these PILs exhibited higher CO_2 permeability coupled with better permselectivity as compared to the established gas separation membrane materials (PC, PSF and Matrimid). One of the PILs,

[TMPBI-BuI][Ac] exhibited highest CO_2 sorption. This further endorsed the role of Ac^- anion in improving CO_2 sorption (as also observed in PILs with aliphatic backbone).

Efforts towards enhancing gas permeability of above PILs were attempted by choosing bulkier *N*-substituent than methyl. These PILs synthesized using bulky *n*-butyl and *tert*-butylbenzyl group and two PBIs (PBI-I and PBI-BuI) as backbone retained peculiarities as observed in above series of methylated PILs. Their anion exchange with BF_4^- and Tf_2N^- anions was high enough (> 85%), they offered tough films and possessed adequate physical properties. Variation of backbone, substituent nature and anion were found to have their own role in governing gas sorption and permeation properties. The gas permeability enhancement with the substituent bulk was more evident in case of PBI based PILs, than for PBI-BuI based PILs, since the latter parent PBI possessed higher initial chain separation due to presence of *tert*-butyl group. Enhancement in the CO_2 permeability of PILs by bulky group substitution was upto ~ 2.5-10 times than their respective methylated PBI based analogs, conveying successes of adopted methodology. These PILs being glassy in nature, followed a conventional trade-off relationship and their permselectivity were lower.

All these new PILs based on PBI possessed polyelectrolyte behavior, a typical peculiarity of *N*-quaternized polymers known in the literature. Improvements achieved in their solvent solubility in comparison to their parent PBI is highly beneficial for their processing them into a desired membrane form. Such membranes could easily sustain high upstream pressure (20 atm) during their gas permeation analysis. This is particularly advantageous towards their practical applicability for gas separation.

It was thought that benefits of IL character could be better brought if the flexible linkages is introduced in the parent PBI. PILs based on such PBI would govern the permeation through soft segments whereas, the rigid backbone would render mechanical strength. PILs were prepared using aliphatic-aromatic PBI (PBI_6). The *N*-quaternization was performed with *tert*-butylbenzyl group while anion exchange was carried out using chosen anions, viz., BF_4^- and Tf_2N^-. Even though the backbone of PILs varied from rigid aromatic to flexible aliphatic-aromatic, the physical properties viz., solvent solubility, d_{sp}, density, thermal stability and T_g of these PILs were in tune with that of earlier PBI based PILs. Although CO_2 sorption of these PILs was lower than their precursor PBI_6, CO_2 based sorption selectivity over H_2, N_2 and CH_4 were higher. Although this was promising, unfortunately obtained PILs could not be transformed into

good film form and were brittle in nature. This indicated that fully aromatic backbone is probably essential in obtaining film forming ability to PILs.

This work initially established an understanding towards effects of anion variation on physical and gas sorption properties of PILs. Gained information was later utilized in better understanding peculiarities of PILs possessing bulky *N*-substituent and flexible linkage (soft segments) in the backbone. The most significant outcome of the work is the validation on proposition that the fully aromatic backbone is necessary in obtaining film forming PILs. Applicability of PILs as membrane material for CO_2 separation is highly dependent on this crucial property. Few PILs demonstrated considerably high CO_2 separation properties than that of established membrane materials. For practical applicability, they need to be converted to either asymmetric or thin film composite (TFC) form. This work thus opens up an entirely new approach of membrane material development, especially for CO_2.

References

Aaron D., Tsouris C., *Sep. Sci. Technol.*, **2005**, 40, 321–348.

Agular-Vega M., Paul D.R., *J. Polym. Sci., Part B: Polym. Phys.,* **1993**, 31, 1599–1610.

Abedini R., Nezhadmoghadam A., *Petroleum & Coal,* **2010**, 52(2) 69–80.

Aitken B.S., Lee M., Hunley M. T., Gibson H.W., Wagener K.B., *Macromolecules*, **2010,** 43, 1699–1701,

Aki S.N.V.K., Mellein B.R., Saurer E.M., Brennecke J.F., *J. Phys. Chem. B.,* **2004,** *108,* 20355–20365.

Amarasekara A.S., Shanbhag P., *Polym. Bull.,* **2011**, 67, 623–629.

Anderson J.L., Dixon J.K., Brennecke J.F., *Acc. Chem. Res.*, **2007**, 40, 1208–1216.

Anthony J.L., Maginn E.J., Brennecke J.F., *J. Phys. Chem. B.,* **2002,** 106, 7315–7320.

Anthony J.L., Anderson J.L., Maginn E.J., Brennecke J.F., *J. Phys. Chem. B.,* **2005,** 109, 6366–6374.

Armstrong S., Freeman B., Hiltner A., Baer E., *Polymer*, **2012**, 53 1383–1392.

Azzaroni O., Brown A.A., Huck W.T.S., *Adv. Mater.,* **2007**, 19, 151–154.

Bara J.E., Gabriel C.J., Lessmann S., Carlisle T.K., Finotello A., Gin D.L., Noble R.D., *Ind. Eng. Chem Res.*, **2007a**, 46, 5380–5386.

Bara J.E., Lessmann S., Gabriel C.J., Hatakeyama E.S., Noble R.D., Gin D.L., *Ind. Eng. Chem. Res.* **2007b,** 46, 5397–5404.

Bara J.E., Hatakeyama E.S., Gabriel C.J., Zeng X., Lessmann S., Gin D.L., Noble R.D., *J. Membr. Sci.*, **2008a**, 316, 186–191.

Bara J.E., Gabriel C.J., Hatakeyama E.S., Carlisle T.K., Lessmann S., Noble R.D., Gin D.L., *J. Membr. Sci.*, **2008b**, 321, 3–7.

Bara J.E., Hatakeyama E.S., Gin D.L., Noble R.D., *Polym. Adv. Technol,.* **2008c**, 19, 1415–1420.

Bara J.E., Gin D.L., Noble R.D., *Ind. Eng. Chem. Res.,* **2008d,** 47, 9919–9924.

Bara J.E., Carlisle T.K., Gabriel C.J., Camper D., Finotello A., Gin D.L., Noble R.D., *Ind. Eng. Chem. Res.,* **2009a,** 48, 2739–2751.

Bara J.E., Noble R.D., Gin D.L., *Ind. Eng. Chem. Res.,* **2009b,** 48, 4607–4610.

Bara J.E., Camper D.E.,Gin D.L., Noble R.D., *Accounts Chem. Res.,* **2010,** 43, 1, 152–159.

Barbari T.A., Confort R.M., *Polym. Adv. Technol.*, **1994**, 5, 698–707.

Barbari T.A., Koros W.J., Paul D.R., *J. Polym. Sci., Part B: Polym. Phys.,* **1988**, 26, 729–744.

Barbari T.A., Koros W.J., Paul D.R., *J. Membr. Sci.*, **1989**, 42, 69–86.

Barbi V., Funari S.S., Gehrke R., Scharnagl N., Stribeck N., *Macromolecules* **2003,** 36, 749–758.

Barrer R.M., *Trans Faraday Sci.*, **1939**, 35, 628–643.

Barrer R.M., Chio H.T., *J. Polym. Sci. C.*, **1965**, 10, 111–138.

Bates E.D., Mayton R.D., Ntai I., Davis J.H., *J. Am. Chem.* Soc., **2002**, 124, 926–927.

Bernardo P., Drioli E., Golemme G., *Ind. Eng. Chem. Res.* **2009,** 48, 4638–4663.

Bernardo P., Clarizia G., *Chem. Eng. Trans*., **2013**, 32, 1999–2004.

BholeY.S., "Investigations on gas permeation and related physical properties of structurally architectured aromatic polymers (polyphenylene oxides and polyarylates), polyarylate-clay nanocomposites and poly(ionic liquid)" *Ph.D. dissertation*, **2007**, University of Pune, India.

Bhowmik P.K., Kamatam S., Han H., Nedeltchev A.K., *Polymer*, **2008**, 49, 1748–1760.

Blanchard L.A., Hancu D., Beckman E.J., Brennecke J.F., *Nature*, **1999**, 399, 28–29.

Blasig A., Tang J., Hu X., Tan S.P., Shen Y., Radosz M., *Ind. Eng. Chem. Res.*, **2007a**, 46, 5542–5547.

Blasig A., Tang J., Hu X., Shen Y., Radosz M., *Fluid Phase Equilib.* **2007b**, 256, 75–80.

Blath J., Deubler N., Hirth T., Schiestel T., *Chem. Eng. J.*, **2012**, 181–182, 152–158.

Bondar V.I., Freeman B.D., Pinnau I., *J. Polym. Sci., Part B: Polym. Phys.,* **1999**, 37, 2463–2475.

Bondar V.I., Freeman B.D., Pinnau I., *J. Polym. Sci., Part B: Polym. Phys.,* **2000**, 38, 2051–2062.

Bondi A., *J. Phys. Chem.*, **1964**, 68, 441–451.

Brunetti A.,, Scura F., Barbieri G., Drioli E., *J. Membr. Sci.*, **2010**, 359, 115–125.

Cabusas M.E.Y., *Ph.D. dissertation*, 1998, Virginia Polytechnic Institute and State University, Blacksburg, Virginia.

Cadena C., Anthony J.L., Shah J.K., Morrow T.I., Brennecke J.F., Maginn E.J., *J. Am. Chem. Soc.*, **2004**, 126, 5300–5308.

Calle M., Lozano A.E., Abajo J.D., Campa J.D.L., Alvarez C., *J. Membr. Sci.*, **2010**, 365, 145–153.

Car A., Stropnik C., Yave W., Peinemann K.V., *J. Membr. Sci.*, **2008**, 307, 88–95.

Cardiano P., Mineo P.G., Neri F., Schiavo S.L., Piraino P., *J. Mater. Chem.*, **2008**, 18, 1253–1260.

Carlisle T.K., Bara J.E., Lafrate A.L., Gin D.L., Noble R.D., *J. Membr. Sci.*, **2010**, 359, 37–43.

Carlisle T.K., Nicodemus G.D., Gin D.L., Noble R.D., *J. Membr. Sci.*, **2012**, 397–398, 24–37.

Carlisle T.K., Wiesenauer E.F., Nicodemus G.D., Gin D.L., Noble R.D., *Ind. Eng. Chem. Res.,* **2013**, 52, 1023−1032.

Chen J.Q., Shao Y.F., Yang Z., Yang H., Cheng R.S., *Chinese J. Polym. Sci.,* 2011, **29**, 750–756.

Chen H.Z., Li P., Chung T.S., *Int. J. Hydrogen Eng.*, **2012a**, 37, 11796–11804.

Chen C., Hess A.R., Jones A.R., Liu X., Barber G.D., Mallouk T.E., Allcock H.R., *Macromolecules*, **2012b**, 45, 1182−1189

Chern R.T., Provan C.N., *Macromolecules*, **1991**, 24, 2203–2207.

Chi W.S., Hong S.U., Jung B, Kang S.W., Kang Y.S., Kim J.H., *J. Membr. Sci.*, **2013**, 443, 54–61.

Chung T.S., Ren J., Wang R., Li D.F., Liu Y., Pramoda K.P., Cao C., Loh W.W., *J. Membr. Sci.*, **2003**, 214, 57−69.

Coates J., Interpretation of Infrared Spectra, A Practical Approach, *Encyclopedia of Analytical Chemistry,* **2006**, John Wiley & Sons, Ltd.

Coleman M.R., Koros W.J., *J. Membr. Sci.*, **1990**, 50, 285–297.

Coleman M.R., Koros W.J., *J. Polym. Sci., Part B: Polym. Phys.,* **1994**, 32, 1915–1926.

Costello L.M., Koros W.J., *J. Polym. Sci.; Part B: Polym. Phys.*, **1994**, 32, 701–713.

D'Alessandro D.M., Smit B., Long J.R., *Angew. Chem. Int. Ed.*, **2010**, 49, 6058–6082.

Do¨bbelin M., Tena-Zaera R., Marcilla R., Iturri J., Moya S., Pomposo J.E., Mecerreyes D., *Adv. Funct. Mater.*, **2009**, 19, 3326–3333.

Dortmundt, D., K. Doshi, "Recent Developments in CO_2 Removal Membrane Technology," *UOP LLC*, Des Plaines, Illinois, **1999**.

Dudley C.N., Schöberl B., Sturgill G.K., Beckham H.W., Rezac M.E., *J. Membr. Sci.*, **2001**, 191, 1–11.

Fang W., Luo Z., Jiang J., *Phys. Chem. Chem. Phys.,***2013**, 15, 651–658.

Freeman B.D., Bokobza l., Sergot P., Monnerie L., *Macromolecules,* **1990,** 23, 2566–2573.

George S.C., Thomos S., Prog. Polym. Sci., 2001, 26, 985–1017.

Ghosal K., Chern R.T., J. *Membr. Sci.,* **1992**, 72, 91–97.

Ghosal K., Freeman B.D., *Polym. Adv. Technol.*, **1994**, 5, 673–697.

Ghosal K., Chern R.T., Freeman B.D., Savarikar R., *J. Polym. Sci. Polym. Phys,* **1995,** 33, 657–666.

Ghosal K., Chern R.T., Freeman B.D., Daly W.H., Negulescu I.I., *Macromolecules,* **1996,** 29, 4360–4369.

Golding J., Forsyth S., MacFarlane D. R., Forsyth M., Deacon G. B.., *Green Chemistry*, **2002**, 4, 223–229.

Goodrich B.F., de la Fuente J.C., Gurkan B.E., Zadigian D.J., Price E.A., Huang Y., Brennecke J.F., *Ind. Eng. Chem. Res.* **2011a,** 50, 111–118.

Goodrich B.F., de la Fuente J.C., Gurkan B.E., Lopez Z.K., Price E.A., Huang Y., Brennecke J.F., *J. Phys. Chem. B*, **2011b**, 115, 9140–9150.

Green O., Grubjesic S., Lee S., Firestone M.A., *J. Macromol. Sci. C. Polym. Reviews*, **2009**, 49 339–360.

Gülmüs S.A., Yilmaz L., *J. Polym. Sci.; Part B: Polym. Phys.*, **2007**, 45, 3025–3033.

Gurkan B.E., de la Fuente J.C., Mindrup E.M., Ficke l.E., Goodrich B.F., Price E.A., Schneider W.F., Brennecke J.F., *J. Am. Chem.* Soc., **2010**, 132, 2116–2117.

Hacarlioglu P., Toppare L., Yilmaz L., *J Appl. Polym. Sci.*, **2003**, 90, 776–785.

Hao L., Li P., Yang T., Chung T.S., *J. Membr. Sci.*, **2013**, 436, 221–231.

He Y., Inoue Y., *Polym. Int.*, **2000**, 49, 623–626.

He X., Yang W., Pei X., *Macromolecules,* **2008**, 41, 4615–4621

Hellums M.W., Koros W.J., Husk G.R., Paul D.R., *J. Membr. Sci.*, **1989**, 46, 93–112.

Hern´andez-Fern´andez F.J., de los R´ıos A.P., Rubio M., Tom´as-Alonso F., G´omez D., V´ıllora G., *J. Membr. Sci.*, **2007,** 293, 73–80.

Hirayama Y., Kase Y., Tanihara N., Sumiyama Y., Kusukia Y., Haraya K., *J. Membr. Sci.*, **1999**, 160, 87–99.

Hollingsworth C.A., Seybold P.G., Hadad C.M., *Int. J. Quant. Chem*.,, **2002**, 90, 1396–1403.

Horn N.R., Paul D.R., *Macromolecules*, **2012**, 45, 2820−2834.

Houde A.Y., Kulkarni S.S., Kharul U.K., Charati S.G., Kulkarni M.G., *J. Membr. Sci.*, **1995**, 103, 167–174.

Hsieh Y.N., Kuei C.H., Chou Y.K., Liu C.C., Leu K.L., Yang T.H., Wang M.Y., Ho W.Y., *Tetrahedron Letters*, **2010**, 51, 3666–3669.

Hu C.C., Chang C.S., Ruaan R.C., Lai J.Y., *J. Membr. Sci.*, **2003**, 226, 51–61.

Hu X., Tang J., Blasig A., Shen Y., Radosz M., *J. Membr. Sci.*, **2006**, 281, 130–138.

Hudiono Y.C., Carlisle T.K., LaFrate A.L., Gin D.L., Noble R.D., *J. Membr. Sci.*, **2011**, 370, 141–148.

Ismail A.F., Lorna W., *Sep. Pur. Technol*., **2002**, 27, 173–194.

Javaid A., *Chem. Eng. J.* **2005**, 112, 219–226.

Jeffery G.H., Bassett J., MendhamJ., Denney R.C., Vogel's Textbook of Quantitative Chemical Analysis, *British Library Cataloguing in Publication Data*, 5th edn, **1989**.

Kanehashi S., Nagai K., *J. Membr. Sci.*, **2005**, 253, 117–138.

Karadas F., Atilhan M., Aparicio S., *Energy Fuels*, **2010**, 24, 5817–5828.

Karadkar P.B., Kharul U.K., Bhole Y.S., Badhe Y.B., Tambe S.S., Kulkarni B.D., *J. Membr. Sci.*, **2007**, 303, 244–251.

Kesting R.E., Fritzsche A.K., *Polymeric gas separation membranes*, Wiley, New York **1993**.

Khulbe K.C., Matsuura T., Lamarche G., Kim H.J., *J. Membr. Sci.*, **1997**, 135, 211–223.

Khulbe K.C., Hamad F., Feng C., Matsuura T., Gumi T., Palet C., *Sep. Pur. Technol.*, **2004**, 36, 53–62.

Kim T. H., Koros W.J., Husk G.R., *J. Membr. Sci.*, **1989**, 46, 43–56.

Koros W. J., Paul D. R., *J. Polym. Sci., Polym. Phys.,* **1976**, 14, 1903–1907.

Koros W.J., Fleming G.K., *J. Membr. Sci.*, **1993**, 83, 1–80.

Koros W.J., Mahajan R., *J. Membr. Sci.*, **2000**, 175, 181–196.

Kumar V., Bhardwaj K.V., Jamdar S.N., Goel N. K., Sabharwal S., *J. Appl. Polym. Sci.*, **2006**, 102, 5512–5521.

Kumbharkar S.C., Karadkar P.B., Kharul U.K., *J. Membr. Sci.*, **2006**, 286, 161–169.

Kumbharkar S.C., "Structure - gas permeation property correlations in polybenzimidazoles and related polymers", *Ph.D. dissertation*, **2008**, University of Pune, India.

Kumbharkar S.C., Islam Md.N., Potrekar R.A., Kharul U.K., *Polymer*, **2009a**, 50, 1403–1413.

Kumbharkar S.C., Kharul U.K., *Eur. Polym. J.,* **2009b**, 45, 3363–3371.

Kumbharkar S.C., Kharul U.K., *J. Membr. Sci.*, **2010**, 357, 134–142.

Lara-Estévez J.C.I., Prado L.A.C.D.A., Schulte K., Bucio E., *Open J. . Polym. Chem.*, **2012**, 2, 63–69.

Lee K.J., Jho J.Y., Kang Y.S., Dai Y., Robertson G.P., Guiver M.D., Won J., *J. Membr. Sci.*, **2003**, 212, 147–155.

Li J.L., Chen B.H., *Sepn. Purif. Technol.*, **2005**, 41, 109–122.

Li F., Cheng F., Shi J., Cai F., Liang M., Chen J., *J. Power Sources*, **2007**, 165, 911–915.

Li Q., Jensen J.O., Savinell R.F., Bjerrum N.J., *Prog. Polym. Sci.,* **2009a**, 34, 449–477.

Li J.R., Kuppler R.J., Zhou H.C., *Chem. Soc. Rev.*, **2009b**, 38, 1477–1504.

Li P., Zhao Q., Anderson J.L., Varanasi S., Coleman M.R., *J. Polym. Sci. A. Polym. Chem.*, **2010**, 48, 4036–4046.

Li P., Pramoda K.P., Chung T.S., *Ind. Eng. Chem. Res.*, **2011**, 50, 9344–9353.

Li P., Paul D.R., Chung T.S., *Green Chem.*, **2012**, 14, 1052–1063.

Li p., Coleman M.R., *Eur. Polym. J.*, **2013**, 49, 482–491.

Lin W.H, Chung T.S., *J. Membr. Sci.*, **2001**, 186, 183–193.

Lin H., Freeman B.D., *J. Membr. Sci.*, **2005**, 739, 57–74.

Liu Y., Pan C.Y., Ding M.X., Xu J.P., *J. Appl. Polym. Sci.*, **1999**, 73, 521–526.

Liu Y., Wang Z.U., Zhou H.C., *Greenhouse Gas Sci. Technol.,* **2012***, 2, 239–259.

Liu S.L., Shao L., Chua M.L., Lau C.H., Wang H., Quan S., *Prog. Polym. Sci.,* **2013**, 38, 1089–1120.

Lu J., Yan F., Texter J., *Prog. Polym. Sci*., **2009**, 34, 431–448.

MacFarlane D.R., Pringle J.M., Johansson K.M., Forsyth S.A., Forsyth M., *Chem. Commun*., **2006**, 1905–1917.

MacFarlane D.R., Tachikawa N., Forsyth M., Pringle J.M., Howlett P.C., Elliott G.D., Davis J.M., Watanabe M., Simon P., Angell C.A., *Energy Environ. Sci*., **2014**, 7, 232–250.

Mader J., Xiao L., Schmidt T.J., Benicewicz B.C., *Adv. Polym. Sci.* **2008**, 216, 63–124.

Mannan H.A., Mukhtar H., Murugesan T., Nasir R., Mohshim D.F., Mushtaq A., *Chem. Eng. Technol.,* **2013**, 36, 11, 1838–1846.

Marcilla R., Blazquez J.A., Rodriguez J., Pomposo J.A., Mecerreyes D., *J. Polym. Sci.; Part A: Polym. Chem.,* **2004**, 42, 208–212.

Marcilla R., Blazquez J.A., Fernandez R., Grande H., Pomposo J.A., Mecerreyes D., *Macromol. Chem. Phys.,* **2005**, 206, 299–304.

Matsumi N., Sugai K., Miyake M., Ohno H., *Macromolecules,* **2006,** *39,* 6924–6927.

McCaig M.S., Paul D.R., *Polymer*, **1999**, 40, 7209–7225.

McCaig M.S., Paul D.R., *Polymer*, **2000**, 41, 629–637.

McGonigle E.-A., Liggat J.J., Pethrick R.A., Jenkins S.D., Daly J.H., Hayward D., *J. Polym. Sci.; Part B: Polym. Phys.*, **2004**, 42, 2916–2929.

McHattie J.S., Koros W.J., Paul D.R., *Polymer*, **1992**, 33, 1701–1711.

Mecerreyes D., *Prog. Polym. Sci*. **2011**, 36, 1629–1648.

Metz B., Davidson O., Coninck H.D., Loos m., Meyer L., IPCC Special Report on Carbon Dioxide Capture and Storage, Cambridge University Press, Cambridge, **2005**.

Michaels A.S., Bixler H.J., *J. Polym. Sci.*, **1961**, 50, 393–412.

Mori H., Yahagi M., Endo T., *Macromolecules,* **2009**, 42, 8082–8092.

Mulder M., *Basic principles of membrane technology*, Kluwer Academic Publisher, Dordrecht, **1996**.

Muldoon M.J., Aki S.N.V.K., Anderson J.L., Dixon J.K., Brennecke J.F., *J. Phys. Chem. B,* **2007,** 111, 9001–9009.

Mushtaq A., Mukhtar H.B., Shariff A.M., Mannan H.A., *Int. J. Eng. Technol.* **2013**, 13, 53–60.

Mustarelli P., Quartarone E., Grandi S., Angioni S., Magistris A., *Solid State Ionics*, **2012**, 225, 228–231

Musto P., Karaszt F.E., MacKnight W.J., *Polymer*, **1993**, 34, 14, 2934–2945.

Ngo H.L., LeCompte K., Hargens L., McEwen A.B., Thermochimica Acta, 2000, 357–358, 97–102.

Ono T., Ohta M., Sada K., *ACS Macro. Lett*., **2012**, 1, 1270−1273.

Pennarun P.Y., Jannasch P., *Solid State Ionics*, **2005**, 176, 1849–1859.

Petkovic M., Seddon K.R., Rebeloa L.P.N., Pereira C. S., *Chem. Soc. Rev.,* **2011**, 40, 1383–1403

Pixton M.R., Paul D.R., *Macromolecules*, **1995a**, 28, 8277–8286.

Pixton M.R., Paul D.R., *Polymer,* **1995b**, 36, 3165–3172.

Plasynski S.I., Chen Z.Y., US DOE National Energy Technology Laboratory, **2000**.

Powell C.E., Qiao G.G., *J. Membr. Sci.*, **2006,** 279, 1–49.

Privalova E.I., Karjalainen E., Nurmi M., Arvela P.M., Ernen K., Tenhu H., Murzin D.Y., Mikkola J.P., *Chem Sus Chem*, **2013**, 6, 1500–1509.

Raeissi S., Peters C.J., *Green Chem.*, **2009**, 11, 185–192.

Rey I., Johansson P., Lindgren J., Lasse`gues J. C., Grondin J., Servant L., *J. Phys. Chem. A,* **1998,** *102,* 3249–3258

Robeson L.M., *J. Membr. Sci.*, **1991**, 62, 165–185.

Robeson L.M., *J. Membr. Sci.*, **2008**, 320, 390–400.

Robeson L.M., Smith Z.P., Freeman B.D., Paul D.R., *J. Membr. Sci.*, **2014**, 453, 71–83.

Sadeghi M., Semsarzadeh M.A.., Moadel H., *J. Membr. Sci.,* **2009**, 331, 21–30.

Sales de J.A., Patr´ıcio P.S.O., Machado J.C., Silva G.G., Windm¨oller D., *J. Membr. Sci.*, **2008**, 310, 129−140.

Salleh W.N.W., Ismail A. F., Matsuura T., Abdullah M.S., *Sep. Pur. Reviews*, **2011**, 40, 261–311.

Sanders D.F., Smith Z.P., Guo R., Robeson L.M., McGrath J.E., Paul D.R., Freeman B.D., *Polymer*, **2013**, 54, 4729–4761.

Santos E., Albo J., Irabien A., *J. Membr. Sci.*, **2014**, 452, 277–283.

Scholes C.A., Kentish S.E., Stevens G.W., *Recent Patents on Chem. Eng.,* **2008**, 1, 52–66.

Scholes C.A., Tao W.X., Stevens G.W., Kentish S.E., *J. Appl. Polym. Sci.*, **2010**, 117, 2284–2289.

Scholes C.A., Bacus J., Chen G.Q., Tao W.X., Li G., Qader A., Stevens G.W., Kentish S.E., *J. Membr. Sci.*, **2012**, 389, 470–477.

Scovazzo P., Kieft, J., Finan D.A., Koval C., DuBois D., Noble R., *J. Membr. Sci.*, **2004**, 238, 57–63.

Shao L., Low B.T., Chung T.S., Greenberg A.R., *J. Membr. Sci.*, **2009,** 327. 18–31.

Shekhawat D., Luebke D.R., Pennline H.W., A Topical Report, United States Department of Energy, DOE/NETL-2003/1200, **2003**.

Shiflett M.B., Kasprzak D.J., Junk C.J., Yokozeki A., *J. Chem. Thermodynamics*, **2008**, 40, 25–31.

Shiflett M.B., Yokozeki A., *J. Chem. Eng. Data,* **2009,** 54, 108–114.

Shiflett M.B., Drew D.W., Cantini R.A., Yokozeki A., *Energy Fuels*, **2010**, 24, 5781–5789.

Shimekit B., Mukhtar H., Adv. Natural Gas Technol., InTech, ISBN 978-953-51-0507-7, **2012**.

Silverstein R.M., Spectrometric Identification of Organic Compounds, *John Wiley and Sons Inc.,* New York, 4th edn, **1981**.

Sridhar S., Smitha B., Aminabhavi T. M., *Sep. Pur. Reviews*, **2007**, 36, 2, 113–174,

Stern S.A., Gareis P.J., Sinclair T.F., Mohr P.H., *J. Appl. Polym. Sci.*, **1963**, 7, 2035–2051.

Stern S.A., Saxena V., *J. Membr. Sci.,* **1980**, 7, 47–59.

Stern S.A., Mauze G.R., Frisch H.L., *J. Polym. Sci.: Polym. Phys. Ed.*, **1983**, 21, 1275–1298.

Stern S.A., Mi Y., Yamamoto H., St. Clair A.K., *J. Polym. Sci. Polym. Phys. Ed.*, **1989**, 27, 1887–1909.

Stern S.A., *J. Membr. Sci.,* **1994,** 94, l–65.

Suarez P.A.Z., Dullius J.E.L., Einloft S., De Souza R.F., Dupont J., *Polyhedron*, **1996**, 15, 7, 1217–1219.

Supasitmongkol S., Styring P., *Energy Environ. Sci*., **2010**, 3, 1961–1972.

Suzuki K., Yamaguchi M., Hotta H., Tanabe N., Yanagida S., *J. Photochemistry Photobiology A. Chem*., **2004**, 164, 81–85.

Tang J., Tang H., Sun W., Plancher H., Radosz M., Shen Y., *Chem. Commun.*, **2005a**, 3325–3327.

Tang J., Tang H., Sun W., Radosz M., Shen Y., *J. Polym. Sci. A. Polym. Chem*., **2005b**, 43, 5477–5489.

Tang H., Tang J., Ding S., Radosz M., Shen Y., *J. Polym. Sci. A. Polym. Chem*., **2005c**, 43, 1432–1443.

Tang J., Tang H., Sun W., Radosz M., Shen Y., *Polymer*, **2005d**, 46, 12460–12467.

Tang J., Sun W., Tang H., Radosz M., Shen Y., *Macromolecules*, **2005e**, 38, 2037–2039.

Tang J., Shen Y., Radosz M., Sun W., *Ind. Eng. Chem. Res.,* **2009,** 48*,* 9113–9118.

Tena A., Marcos-Fernández A., Lozano A.E., deAbajo J., Palacio L., Prádanos P., Hernández A., *Chem. Eng. Sci*., **2013**, 104, 574–585.

Thomas W., *Chem Rev.*, **1999**, 99, 2071–2083.

Tome´ L.C., Patinha D.J.S., Freire C.S.R., Rebelo L.P.N., Marrucho I.M., *RSC Adv*., **2013a**, 3, 12220–12229.

Tome´ L.C., Mecerreyes D., Freire C.S.R., Rebelo L.P.N., Marrucho I.M., *J. Membr. Sci.,* **2013b**, 428, 260–266.

Tsujita Y., *Prog. Polym. Sci.*, **2003**, 28, 1377–1401.

Victor J.G., Torkelson J.M., *Macromolecules,* **1987,** 20, 2241–2250.

Vieth W.R., Howell J.M., Hsieh J.H., *J. Membr. Sci.,* **1976**, 1, 177–220.

Vijayakrishna k., Jewrajka S.J., Ruiz A., Marcilla R., Pomposo J.A., Mecerreyes D., Taton D., Gnanou Y., *Macromolecules,* **2008**, 41, 6299–6308.

Vimala J.F., Lawrence M., Prakash J.T.J., *Elixir Crystal Growth,* **2011**, 41, 5664–5667.

Vygodskii Y.S., Shaplov A.S., Lozinskaya E.I., Lyssenko K.A., Golovanov D.J., Malyshkina I.A., Gavrilova N.D., Buchmeiser M.R., *Macromol. Chem. Phys.* **2008**, 209, 40–51.

Wade L.G.Jr., *Organic Chemistry*, 5th Edition, Prentice-Hall, Upper Saddle River, NJ, **2003**.

Wandrey C., Hernández-Barajas J., Hunkeler D., *Adv. Polym. Sci*., **1999**, 145, 123–183.

Wang J.S., Naito Y., Kamiya Y., *J. Polym. Sci. B. Polym. Phys.***1996,** 34, 2027–2033.

Wang R., Cao C., Chung T.S., *J. Membr. Sci.,* **2002**, 198, 259–271.

Wang C., Luo H., Jiang D., Li H., Dai S., *Angew. Chem.* **2010**, 122, 6114–6117.

Wang C., Luo X., Luo H., Jiang D., Li H., Dai S., *Angew. Chem. Int. Ed.,* **2011**, 50, 4918–4922.

Wang G.N., Dai Y., Lu J.F., Xiao F., Wu Y.T., Zhang Z.B., Zhou Z., *J. Molecular Liquids*, **2012**, 168, 17–20.

Wilke A., Yuan J., Antonietti M., Weber J., *ACS Macro Lett.,* **2012**, 1, 1028–1031.

Xiong Y.B., Wang H., Wang Y.J., Wang R.M., *Polym. Adv. Technol*., **2012**, 23, 835–840.

Yuan J., Antonietti M., *Polymer*, **2011**, 52, 1469–1482.

Yuan J., Mecerreyes D., Antonietti M., *Prog. Polym. Sci.* **2013**, 38, 1009–1036.

Yave W., Car A., Peinemann K.V., Shaikh M.Q., Rätzke K., Faupel F., *J. Membr. Sci.,* **2009,** 339, 177–183.

Yave W., Car A., Funari S.S., Nunes S.P., Peinemann K.V., *Macromolecules*, **2010**, 43, 326–333.

Yave W., Car A., Peinemann K.V., *J. Membr. Sci.,* **2010,** 350, 124–129.

Yokozeki A., Shiflett M.B., Junk C.P., Grieco l.M., Foo T., *J. Phys. Chem. B,* **2008,** 112, 16654–16663.
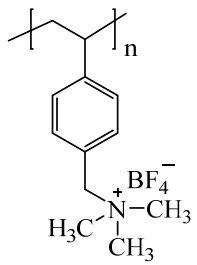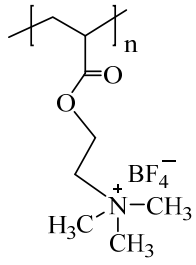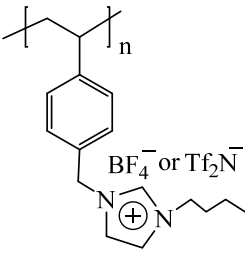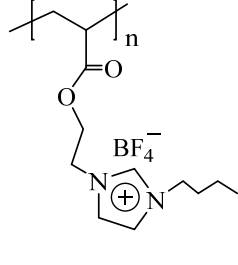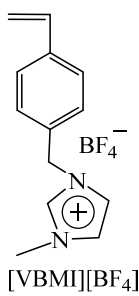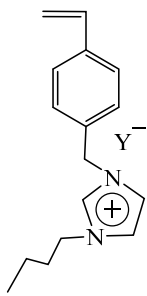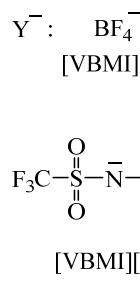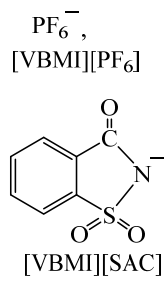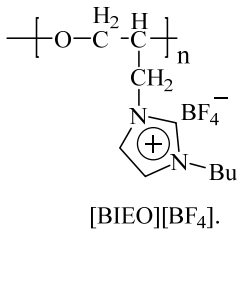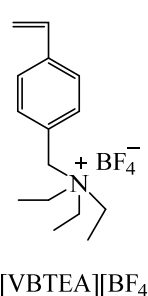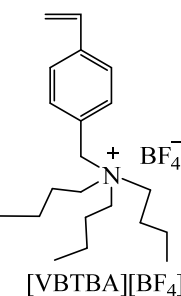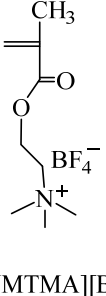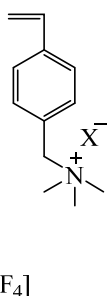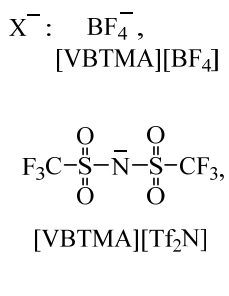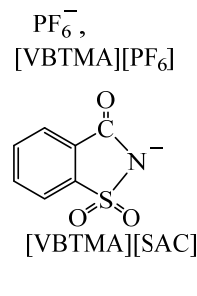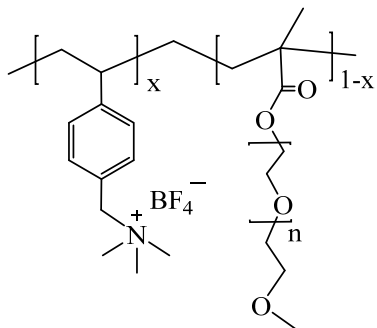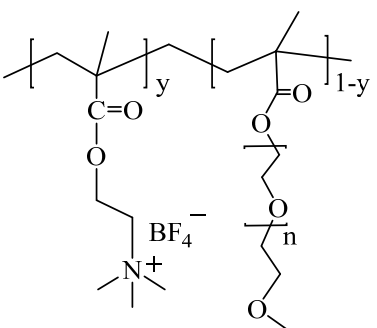
Zhang J., Zhang S., Dong K., Zhang Y., Shen Y., Lv X., *Chem. Eur. J*., **2006**, 12, 4021–4026.

Zhang Y., Zhang S., Lu X., Zhou Q., Fan W., Zhang X.P., *Chem. Eur. J,* **2009**, 15, 3003–3011.
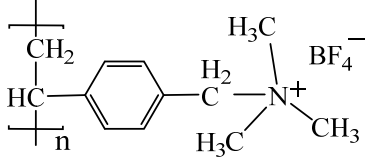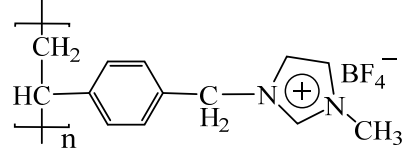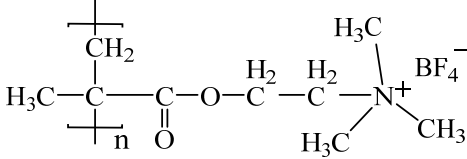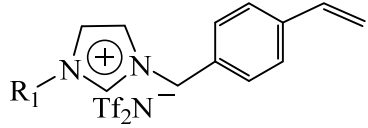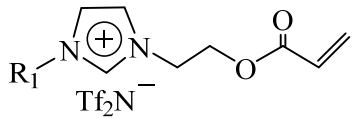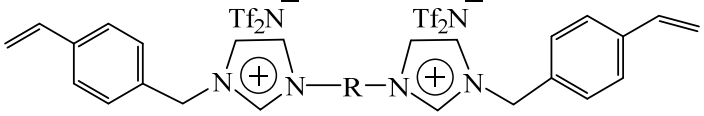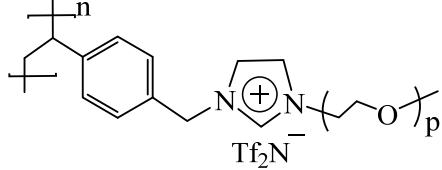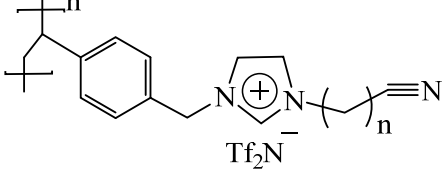
Zhang X., Zhang X., Dong H., Zhao Z., Zhang S., Huang Y., *Energy Environ. Sci*., **2012**, 5, 6668–6681.

Zhao H.Y., Cao Y.M., Ding X.L., Zhou M.Q., Yuan Q., *J. Membr. Sci.,* **2008**, 323, 176–184.
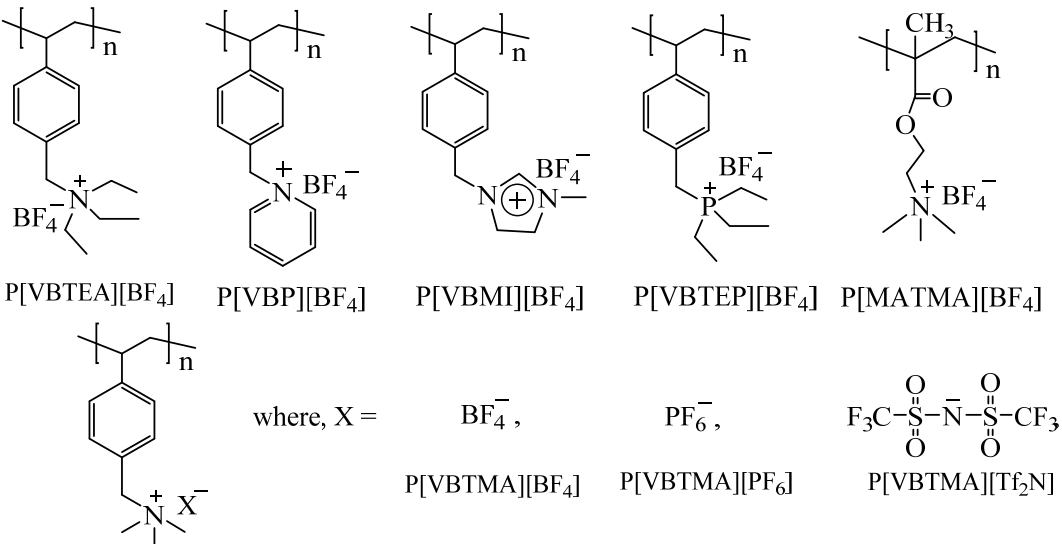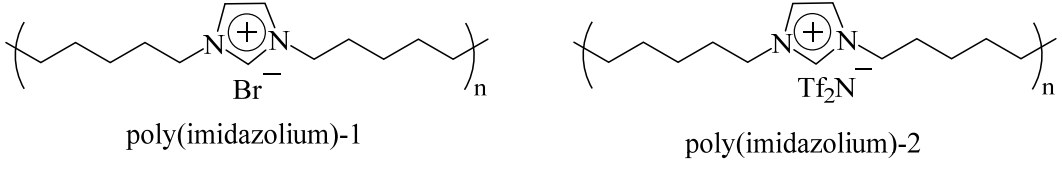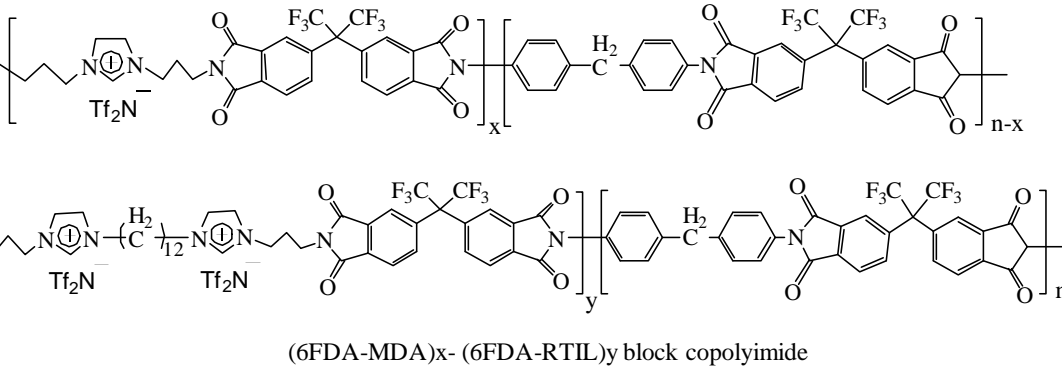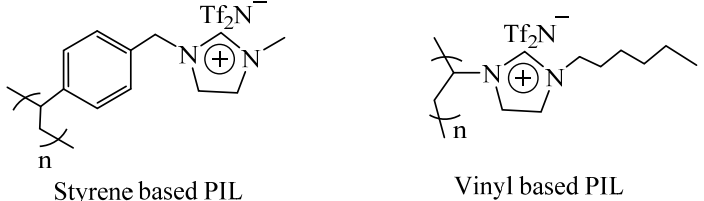
Appendix I
Chemical structure of PILs demonstrated for CO$_2$ permeation properties

Chemical structure of PILs or ILs	Ref.
P[VBTMA][BF$_4$] P[MATMA][BF$_4$] BF$_4^-$: P[VBBI]BF$_4$ Tf$_2$N$^-$: P[VBBI][Tf$_2$N] P[MABI][BF$_4$]	Tang (2005a, 2005c)
[VBMI][BF$_4$] [VBMI][Tf$_2$N] [VBMI][SAC] [BIEO][BF$_4$].	Tang (2005b)
[VBTEA][BF$_4$] [VBTBA][BF$_4$] [MTMA][BF$_4$] [VBTMA][Tf$_2$N] [VBTMA][SAC]	Tang (2005d)
P[VBTMA][BF$_4$]-g-PEG P[MTMA][BF$_4$]-g-PEG	Hu (2006)
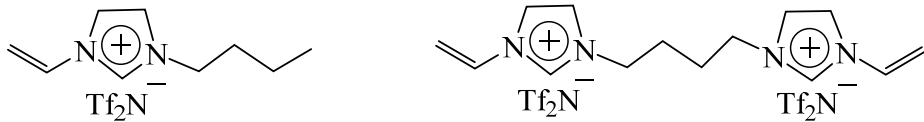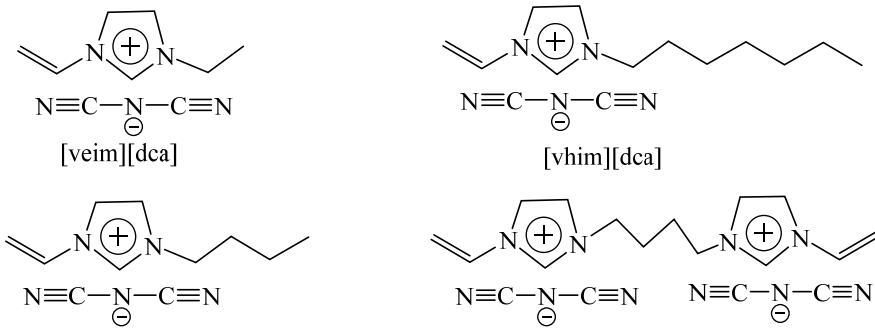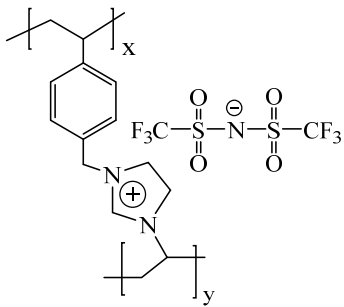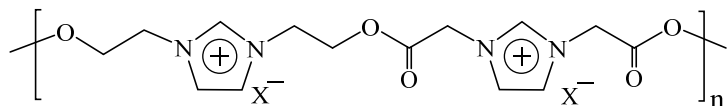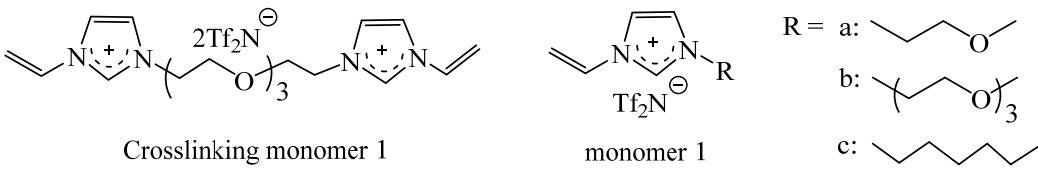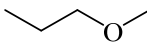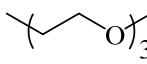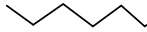
179

Chemical structure of PILs or ILs	Ref.
P[VBTMA][BF$_4$] P[VBMI][BF$_4$] P[MATMA][BF$_4$]	Blasig (2007a, 2007b)
where, R$_1$ = Me, *n*-Bu, *n*-Hex where, R$_1$ = Me, *n*-Bu RTIL monomers	Bara (2007b)
where, R= = -(CH$_2$)$_6$- = -(CH$_2$)$_2$O(CH$_2$)$_2$- = -((CH$_2$)$_2$O)$_2$(CH$_2$)$_2$)- GRTIL cross-linkable monomers	Bara (2008a)
where, p= 1, 2 where, p= 3,5 RTIL monomers functionalized with polar substituents	Bara (2008b)
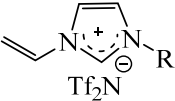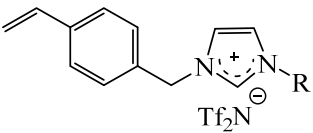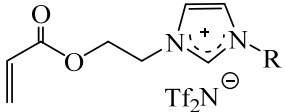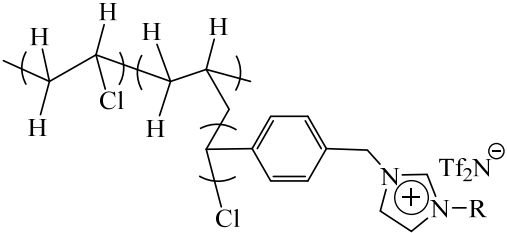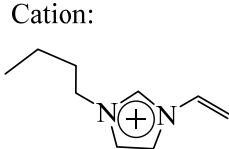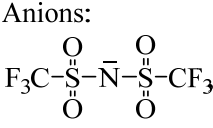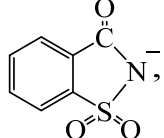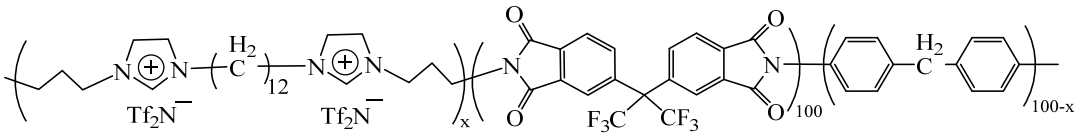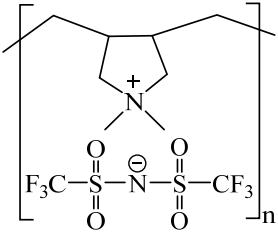
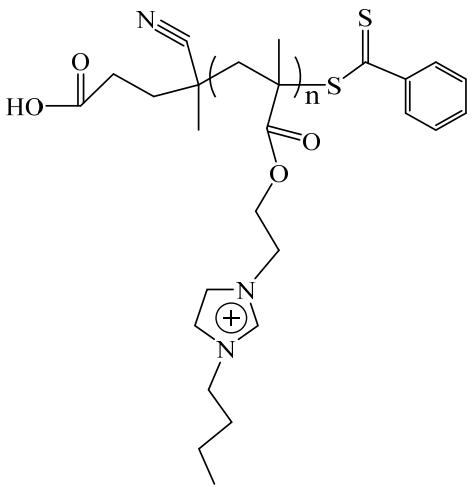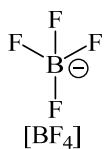| Chemical structure of PILs or ILs	Ref.
P[VBTEA][BF4] P[VBP][BF4] P[VBMI][BF4] P[VBTEP][BF4] P[MATMA][BF4] where, X = BF4⁻, PF6⁻, F3C-S(O)(O)-N-S(O)(O)-CF3, P[VBTMA][BF4] P[VBTMA][PF6] P[VBTMA][Tf2N]	Tang (2009), Supasit mongkol (2010)
poly(imidazolium)-1 Br⁻ poly(imidazolium)-2 Tf2N⁻	Carlisle (2010)
(6FDA-MDA)x- (6FDA-RTIL)y block copolyimide	Li (2010)
Styrene based PIL Vinyl based PIL	Hudino (2011)

Chemical structure of PILs or ILs	Ref.
Continued Appendix I. Chemical structure -------	
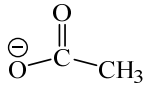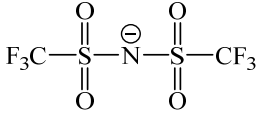
Chemical structure of PILs or ILs	Ref.
[vbim][Tf₂N] (RTIL monomer) [C₄(dvim)₂][Tf₂N](RTIL based crosslinker)	Li (2011a)
[veim][dca] [vhim][dca] [vbim][dca] crosslinker	Li (2012)
[3-(4-vinylbenzyl)-1-vinylimidazolium][Tf₂N]	Wilke (2012)
X= BF₄ or PF₆ PIL-BF₄ or PIL-PF₆	Xiong (2012)
Crosslinking monomer 1 monomer 1 R = a: b: c:	Carlisle (2012)

<table>
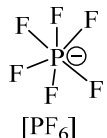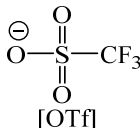<tr><td colspan="2">Continued Appendix I. Chemical structure -------</td></tr>
</table>

182

Chemical structure of PILs or ILs	Ref.
R = a: -(CH_3)$ b: -(CH_2)_5CH_3$ c: -(CH_2CH_2O)_2CH_3$ d: -(CH_2CH_2O)_3CH_3$ e: -(CH_2)_2(CF_2)_3CF$ f: -CH_2Si(CH_3)_2OSi(CH_3)_3$ R = a: -(CH_3)$ b: -(CH_2)_5CH_3$ c: -(CH_2CH_2O)_2CH_3$ R = a: -(CH_3)$ b: -(CH_2)_3CH_3$ RTIL monomers	Carlisle (2013)
PVC-g-PIL	Chi (2013)
Cation: [VBIM] Anions: [Tf_2N] [SCN] PF_6^-, [PF_6] Cl^- [Cl]	Fang (2013)
6FDA-(MDA/RTIL) backbone	Li (2013)
Poly([pyr_{11}][NTf_2])	Tome (2013b)

Continued Appendix I. Chemical structure -------	
Chemical structure of PILs or ILs	**Ref.**

Chemical structure of PILs or ILs	Ref.
Cation: ... Anions: ... Br⁻ [Br] ... [BF₄] ... [PF₆] ... [OTf] ... [acetate] ... [Tf₂N] ... P[BIEMA]	Privalova (2013)

Cation:

Anions:

Br $^{\ominus}$

[Br]

[BF₄]

[PF₆]

[OTf]

[acetate]

[Tf₂N]

P[BIEMA]

Appendix II
CO_2 sorption of reported PILs

PIL	Operating conditions		CO₂ concentration			Ref.
	Temperature (°C)	Pressure (atm)	mol %	wt. %	cm³/ (cm³.PIL.atm)	
P[VBTMA][BF₄]	22	0.78	10.22	–	–	Tang (2005a)
P[MATMA][BF₄]	22	0.78	7.99	–	–	
P[VBBI][BF₄]	22	0.78	2.27	–	–	
P[MABI][BF₄]	22	0.78	1.80	–	–	
P[VBTMA][BF₄]	22	12	44.8	–	–	
P[VBBI][PF₆]	22	0.78	2.8			Tang (2005b)
P[VBBI][BF₄]	22	0.78	2.27	–	–	
P[VBBI][Sac]	22	0.78	1.55	–	–	
P[VBBI][Tf₂N]	22	0.78	2.23	–	–	
P[VBMI][BF₄]	22	0.78	3.05			
P[MABI][BF₄]	22	0.78	1.78	–	–	
P[EIBO][BF₄]	22	0.78	1.06	–	–	
P[VBTMA][PF₆]	22	0.78	10.66	–	–	
PVBIT	RT	0.78	2.22	0.305	–	Tang (2005c)
P[VBTEA][BF₄]	22	0.78	4.85	–	–	Tang (2005d)
P[VBTBA][BF₄]	22	0.78	3.1	–	–	
P[VBTMA][PF₆]	22	0.78	10.66	–	–	
P[VBTMA][BF₄]	22	0.78	10.22	–	–	
P[VBTMA][Tf₂N]	22	0.78	2.85	–	–	
P[VBTMA][Sac]	22	0.78	2.67	–	–	
PVBIH	22	0.78	2.75	0.322	–	Tang (2005e)
PVBIT	22	0.78	2.22	0.305	–	
PBIMT	22	0.78	1.77	0.241	–	
P[VBTMA][BF₄]-g-PEG2000	35	2.81	–	–	4.41	Hu (2006)
P[MTMA][BF₄]-g-PEG2000	35	2.81	–	–	5.25	

185

PIL	Operating conditions		CO₂ concentration			Ref.
	Temperature (°C)	Pressure (atm)	mol %	wt. %	cm³/ (cm³.PIL.atm)	
P[VBTMA][BF₄]	35	10	–	–	2.68[a]	Blasig (2007a)
P[VBMI][BF₄]	35	10	–	–	1.45[a]	
P[VBTMA][BF₄]	25	15	–	–	2.67	Blasig (2007b)
	50	15	–	–	1.69	
	75	15	–	–	1.11	
P[MTMA][BF₄]	25	15	–	–	2.33	
	50	15	–	–	1.57	
	75	15	–	–	1.01	
Styrene-Based Poly(RTILS)-methyl	20	2	–	–	4.00	Bara (2007b)
Styrene-Based Poly(RTILS)-butyl	20	2	–	–	4.40	
Styrene-Based Poly(RTILS)-hexyl	20	2	–	–	3.90	
Acrylate-Based Poly(RTILS)-methyl	20	2	–	–	3.60	
Acrylate-Based Poly(RTILS)-butyl	20	2	–	–	4.50	
Poly(GRTIL) -(CH₂)₆-spacer	20	2	–	–	2.8	Bara (2008a)
Poly(GRTIL) -(CH₂)₂O(CH₂)₂- spacer	20	2	–	–	3.8	
Poly(GRTIL) -(CH₂)₂O)₂(CH₂)₂- spacer	20	2	–	–	3.5	
Styrene-Based Poly(RTILS)-(CH₂)₂OCH₃	22	2	–	–	3.37	Bara (2009b)
P[VBTEA][BF₄]	22	1	–	–	5.86[a]	Tang (2009)
P[VBP][BF₄]	22	1	–	–	5.51[a]	
P[VBTEP][BF₄]	22	1	–	–	4.68[a]	
P[VBMI][BF₄]	22	1	–	–	3.94[a]	
P[VBTMA][BF₄]	22	1	–	–	10.5[a]	
P[VBTMA][PF₆]	22	1	–	–	8.8[a]	
P[VBTMA][Tf₂N]	22	1	–	–	2.5[a]	

Continued Appendix II. CO₂ sorption ----------

PIL	Operating conditions		CO$_2$ concentration			Ref.
	Temperature (°C)	Pressure (atm)	mol %	wt. %	cm^3/ (cm^3.PIL.atm)	
Poly[imidazolium][Br]	RT	2	–	–	0.45	Carlisle (2010)
Poly[imidazolium][Tf$_2$N]	RT	2	–	–	0.79	
6.5% block [DAPIM][NTf$_2$]$_2$ copolyimide	35	10	–	–	4.0	Li (2010)
14.8% block[DAPIM][NTf$_2$]$_2$ copolyimide	35	10	–	–	3.64	
25.8% [DAPIM$_2$][NTf$_2$]$_2$ copolyimide	35	10	–	–	3.68	
P[VBTMA][PF$_6$]	20	1	–	77	–	Supasitmo-ngkol (2010)
PILs-PF$_6$	25	0.85	4.2	–	–	Xiong (2012)
PILs-BF$_4$	25	0.85	4.5	–	–	
P[vbim][Tf$_2$N]	35	10	–	–	1.14[a]	Li (2011a)
Poly([veim][dca])	35	1	–	–	0.488[a]	Li (2012)
Poly([vbim][dca])	35	1	–	–	0.728[a]	
Poly([vhim][dca])	35	1	–	–	1.082[a]	
Mesoporous PIL	0	1	–	2.02[a]	–	Wilke (2012)
Bulk PIL	0	1	–	0.57[a]	–	
10 mol% random [C$_{12}$(DAPIM)$_2$] [NTf$_2$]$_2$ copolyimides	35	10	–	–	2.43	Li (2013)
20 mol% random [C$_{12}$(DAPIM)$_2$] [NTf$_2$]$_2$ copolyimides	35	10	–	–	2.01	
poly([pyr11][NTf$_2$]	20	1	–	–	1.44	Tome (2013b)
Poly(VBIM)Tf$_2$N	35	10	–	–	1.13	Fang (2013)

Continued Appendix II. CO$_2$ sorption ----------

***Continued Appendix II.* CO$_2$ sorption ----------**

PIL	**Operating conditions**		**CO$_2$ concentration PIL**			**Ref.**
	Temperature (°C)	**Pressure (atm)**	**mol %**	**wt. %**	**cm^3/(cm^3.PIL.atm)**	**Pressure (atm)**
Vinyl-based, imidazolium poly(RTIL) [Poly(1)]-methyl	RT	2	–	–	3.3	Carlisle (2013)
Poly(1)-Hexyl	RT	2	–	–	3.8	
Poly(1)-$(CH_2CH_2O)_2CH_3$	RT	2	–	–	3.2	
Poly(1)-$(CH_2CH_2O)_3CH_3$	RT	2	–	–	3.9	
Poly(1)-$(CH_2)_2(CF_2)_3CF_3$	RT	2	–	–	3.9	
Poly(1)-$(CH_2)_2Si(CH_3)_2OSi(CH_3)$	RT	2	–	–	3.5	
P5[BIEMA][NTf_2]	25	1	–	0.153[a]	–	Privalova (2013)
P5[BIEMA][OTf]	25	1	–	0.205[a]	–	
P5[BIEMA][Br]	25	1	–	0.288[a]	–	
P5[BIEMA][BF_4]	25	1	–	0.299[a]	–	
P5[BIEMA][PF_6]	25	1	–	0.331[a]	–	
P6[BIEMA][acetate]	25	1	–	1.2[a]	–	

[a]: CO$_2$ solubility of the reported PILs is converted into given unit

Appendix III
CO$_2$ permeation and selectivity over N$_2$ and CH$_4$ of reported PILs

PILs	T$_g$ (°C)	Temperature (°C)	Pressure (atm)	P$_{CO_2}$ (Barrer)	$\frac{P_{CO_2}}{P_{N_2}}$	$\frac{P_{CO_2}}{P_{CH_4}}$	Ref.
P[VBTMA][BF$_4$]-g-PEG2000	158	35	2.81	17	60	22	Hu (2006)
P[VBTMA][BF$_4$]-g-PEG475	156	35	2.81	6	—	—	
P[MTMA][BF$_4$]-g-PEG2000	NA	35	2.81	38	70	31	
P[MTMA][BF$_4$]-g-PEG475	NA	35	2.81	3	—	—	
Styrene-Based Poly(RTILS)-methyl	NA	20	2	9.2	32	39	Bara (2007b)
Styrene-Based Poly(RTILS)-butyl	NA	20	2	20	30	22	
Styrene-Based Poly(RTILS)-hexyl	NA	20	2	32	28	17	
Acrylate-Based Poly(RTILS)-methyl	NA	20	2	7	31	37	
Acrylate-Based Poly(RTILS)-butyl	NA	20	2	22	30	22	
Poly(GRTIL) -(CH$_2$)$_6$-spacer	NA	20	2	4.4	22	27	Bara (2008a)
Poly(GRTIL) -(CH$_2$)$_2$O(CH$_2$)$_2$-spacer	NA	20	2	4	28	32	
Poly(GRTIL) -(CH$_2$)$_2$O)$_2$(CH$_2$)$_2$-spacer	NA	20	2	3.8	23	28	
Poly(RTIL) OEG$_1$ substituents	NA	22	2	16	41	33	Bara (2008b)
Poly(RTIL) OEG$_2$ substituents	NA	22	2	22	44	29	
Poly(RTIL) C$_3$CN substituents	NA	22	2	4.1	37	37	
Poly(RTIL) C$_5$CN substituents	NA	22	2	8.2	40	30	
Poly[imidazolium][Br]	NA	RT	2	0.13	-	-	Carlisle (2010)
Poly[imidazolium][Tf$_2$N]	NA	RT	2	5.2	24	20	
6.5% block [DAPIM][NTf$_2$]$_2$ copolyimide	286	35	10	14.4	23.2	46.7	Li (2010)
14.8% block [DAPIM][NTf$_2$]$_2$ copolyimide	281	35	10	11.7	24.9	55.6	
25.8% [DAPIM$_2$][NTf$_2$]$_2$ copolyimide	276	35	10	9.2	22.2	61.5	
8% [C$_{12}$(DAPIM)$_2$] [NTf$_2$]$_2$ copolyimide	276	35	10	7.4	23.5	46.4	

PILs	T_g (°C)	Temperature (°C)	Pressure (atm)	P_{CO_2} (Barrer)	$\dfrac{P_{CO_2}}{P_{N_2}}$	$\dfrac{P_{CO_2}}{P_{CH_4}}$	Ref.
Styrene based PIL	NA	23	1-1.5	9.2	32	39	Hudino
Vinyl based PIL	NA	23	1-1.5	67.3	14.5	10.6	(2011)
P[vbim][Tf$_2$N]	-39	35	10	101.4	22.3	—	Li (2011a)
Poly([veim][dca]	29	35	10	0.09	—	—	
Poly([vbim][dca]	-27	35	1	4.24	26.5	—	Li (2012)
Poly([vhim][dca]	-37	35	1	33.5	20.9	—	
P(vbim)Tf$_2$N	-60	35	3.5	101	20.6	12.9	Hao (2013)
8mol% block [C$_{12}$(DAPIM)$_2$] [NTf$_2$]$_2$ copolyimides	276	35	10	7.4	23.5	46.4	
10 mol% random [C$_{12}$(DAPIM)$_2$] [NTf$_2$]$_2$ copolyimides	257	35	10	7.5	25.8	44.2	Li (2013)
20 mol% random [C$_{12}$(DAPIM)$_2$] [NTf$_2$]$_2$ copolyimides	239	35	10	3.5	29.3	46	
Poly[pyr$_{11}$][NTf$_2$]	NA	21	1	5.09	22.2	28.6	Tome (2013b)
Vinyl-based, imidazolium poly(RTIL) [Poly(1)]-methyl	48	RT	2	4.8	29	40	
Poly(1)-Hexyl	40	RT	2	69	17	9.9	
Poly(1)-(CH$_2$CH$_2$O)$_2$CH$_3$	-10	RT	2	14	32	32	Carlisle
Poly(1)-(CH$_2$CH$_2$O)$_3$CH$_3$	-15	RT	2	26	34	25	(2013)
Poly(1)-(CH$_2$)$_2$(CF$_2$)$_3$CF$_3$	52	RT	2	69	11	14	
Poly(1)-(CH$_2$)$_2$Si(CH$_3$)$_2$OSi(CH$_3$)$_3$	-10	RT	2	130	14	8.7	
PVC-g-PIL 33 wt%	50-90	35	2	7.5	25	—	Chi
PVC-g-PIL 65 wt%	50-90	35	2	17.9	24.7	—	(2013)

NA: Not available

	Synopsis of the Thesis to be submitted to the Academy of Scientific and Innovative Research for Award of the Degree of Doctor of Philosophy in Chemistry	
Name of the Candidate	Mr. Rupesh Sudhakar Bhavsar	
Degree Enrolment No. & Date	Ph. D in Chemical Sciences (10CC11J26106); January 2011	
Title of the Thesis	Polymeric Ionic Liquids (PILs): Synthetic Approaches and Gas Permeation Studies with an Emphasis on CO₂ Separation	
Research Supervisor	Dr. Ulhas K. Kharul (AcSIR, CSIR-NCL, Pune)	

Introduction

Polymeric gas separation membranes are being increasingly used for variety of industrial gas separations applications due to their advantages over conventional processes (absorption, adsorption and cryogenics) such as lower capital and operating costs, operational simplicity, high reliability, light weight, modular nature (thus easy scale-up), ideal for remote locations and most importantly, environment friendly nature [Sanders (2013)]. Separation of CO_2 from flue gas, natural gas, enhanced oil recovery, biogas, water gas shift reaction, etc. is an important application of polymeric membranes in view of its industrial and environmental relevance. Development of economically viable CO_2 capture processes is becoming increasingly important as concerns over greenhouse gas emissions leading to global warming are being widely expressed [Tang (2005), Bara (2008), Xiong (2011)]. The CO_2 separation through membranes is largely governed by its interactions with the membrane material. Glassy polymeric materials have high selectivity and low permeability, while reverse is true for rubbery materials. Thus, more attention is paid towards development of glassy polymeric materials.

Statement of Problem

The performance (especially selectivity) of glassy polymeric membranes deteriorates due to the plasticization induced by interaction with CO_2. To overcome this barrier, materials with high inherent CO_2 sorption and temperature withstand capacity are preferred. In recent literature, ionic liquids (ILs) are shown to possess high CO_2 sorption and are being proposed as CO_2-selective separation media [Bara (2008), Xiong (2011)]. Although IL based supported membranes have been demonstrated, they possess poor stability (due to IL drain) leading to inadequate long-term performance and operation possible only at low pressures [Bara (2008)]. In

order to overcome these drawbacks, 'polymeric ionic liquids' (PILs) are emerging as a promising option. This class of new generation materials exhibits high CO_2 sorption, faster adsorption-desorption rates than ionic liquids and appreciable thermal stability [Xiong (2011), Mecerreyes (2011)]. Although they look to be promising in overcoming barriers faced by usual glassy polymers, most of the PILs are brittle in nature, unable to form film [Hu (2006), Bara (2008), Li (2011)] and thus cannot be converted into a membrane for practical separation. In order to bring potentials of PILs to practice, there is a need of better understanding of structure-property relationship, which would offer insight towards new material development that would address present drawbacks.

Aims and objectives

The overall aim of this work was to enhance an understanding towards gas sorption and permeation in polymeric ionic liquids (PILs). It was addressed through following objectives.

1) To investigate effects of anion variation on gas sorption properties of PILs based on commercially available precursor.

2) To explore an altogether different approach of synthesizing PILs: Post modification of a rigid polymer family (polybenzimidazoles).

    (i) Investigate film forming ability and physical properties while varying anions

    (ii) Investigate gas sorption, permeation properties and correlate them with physical properties.

Methodology used

1. Using commercially available PIL precursor, viz., P[DADMA][Cl], establish a metathesis protocol using salts of promising anions, investigate effects of anion variation on physical and gas sorption properties of resulting PILs.

2. With chosen polybenzimidazole backbone and methyl group as the *N*-substituent, develop a family of PILs and investigate effects of anion variations on gas sorption and transport properties.

3. Investigate effects of bulky group as the *N*-substituent, variation in PBI backbone to investigate effects of polycation variation.

Sample Results

Scheme 1: *Polymeric ionic liquids (PILs) based on aliphatic backbone: Effects of anion variation on CO_2 sorption*

PILs based on poly(diallyldimethylammonium chloride), P[DADMA][Cl] as a precursor were investigated by varying anions categorized into carboxylates, sulfonates and inorganic types. Variation in anion was found to have a large effect of physical as well as gas sorption properties of resulting PILs. Among the PILs investigated, those possessing carboxylate (especially acetate and benzoate) anions exhibited attractive CO_2 sorption coupled with sorption selectivity over N_2 and H_2 ($S_{CO_2}/S_{N_2} = 114.3$ and 41.5, for P[DADMA][Ac] and P[DADMA][Bz], respectively).

Scheme 2: *Effect of PIL structural variations through carboxylate anions on gas sorption*

The exciting results of high CO_2 sorption in PILs possessing acetate anion prompted an analysis of a family of PILs with carboxylate anions of varying structures. P[DADMA][Cl] was chosen as the common backbone. Effects of variation in alkyl chain length of carboxylated anion on physical and gas sorption properties were investigated. In the series of PILs investigated, P[DADMA][Bu] exhibited highest CO_2 sorption coupled with excellent sorption selectivity ($S_{CO_2}/S_{H_2} = 297$ and $S_{CO_2}/S_{N_2} = 127.7$ at 2 atm).

Scheme 3: *Investigations with PIL-PEBAX blends membranes*

The film forming inability of above PILs can be overcome by blending them with a film forming polymer. With this as an objective, one of the promising PIL from above study, viz., (P[DADMA][Ac]) exhibiting high CO_2 sorption and CO_2 based sorption selectivity was blended with PEBAX (known for excellent film forming ability as well as high gas permeability). It was anticipated that CO_2 permeation properties of the resulting blend could be higher than that of pristine PEBAX. The lowering in gas permeation of blend membranes was coupled with only slight improvement in CO_2 based permselectivity. Owing to this observation, this segment of work was discontinued.

Scheme 4: *Film forming PILs based on rigid, fully aromatic polybenzimidazole: Synthesis, investigation of physical and gas permeation properties*

In view of film forming inability of PILs based on aliphatic backbone, an altogether different approach of PIL synthesis was explored. A series of PILs was synthesized based on a

rigid polybenzimidazole (PBI-BuI) by its *N*-quaternization using the methyl group. Metathesis was performed with anions of interest. This approach was found to be highly successful towards offering film forming characteristic to resulting PILs. Physical properties of this new type of materials were examined. Most of the resulting PILs offered mechanically strong films with appreciable strength that easily sustained 20 atm upstream pressure during their gas permeation analysis. In comparison to the parent PBI-BuI, enhancement in the permeability of CO_2 was highly promising (upto ~ 9 times) for PILs with varying anion, without much compromise on the CO_2 permselectivity over N_2 and CH_4.

Scheme 5: *Structural tuning while varying N-substituent of PBI for enhancing permeation properties of PILs*

In order to further enhance CO_2 permeability, two PBIs were *N*-quaternized by bulky alkyl groups (*n*-butyl and *tert*-butylbenzyl) followed by metathesis with only chosen anions (BF_4^- and Tf_2N^-). After incorporation of large bulky groups also, formed PILs retained film forming ability and easily sustained 20 atm upstream during the gas permeability analysis. The effects of attempted structural variations on physical, gas sorption and permeation properties were investigated. CO_2 permeability in bulky group substituted PILs increased by ~ 2.5-10 times than their respective methylated PBI based PIL analogs.

References

[1] D. F. Sanders, *et al.*, *Polymer* **54** (2013) 4729–4761.

[2] J. Tang, *et al.*, *Macromolecules* **38** (2005) 2037–2039.

[3] J. E. Bara, *et al.*, *Ind. Eng. Chem. Res.* **316** (2008) 186–191.

[4] Y. B. Xiong, *et al.*, *Polym. Adv. Technol.* **23** (2012) 835–840.

[5] D. Mecerreyes, *et al.*, *Progr. Polym. Sci.* **36** (2011) 1629–1648.

[6] C. Hu*, et al.*, *J. Membr. Sci.* **226** (2003) 51–61.

[7] P. Li, *et al.*, *Ind. Eng. Chem. Res.* **50** (2011) 9344–9353.

Signature of the Candidate   Signature of the Ph.D. supervisor

(Mr. Rupesh Sudhakar Bhavsar)   (Dr. Ulhas. K. Kharul)

List of Publications:

1) **R. S. Bhavsar**, S. B. Nahire, M. S. Kale, S. G. Patil, P. P. Aher, R. A. Bhavsar and U. K. Kharul, *J. Appl. Polym. Sci.,* **120** (2011) 1090–1099.

2) **R. S. Bhavsar**, S. C. Kumbharkar and U. K. Kharul, *J. membr. Sci.* **389** (2012) 305–315

3) **R. S. Bhavsar**, S. C. Kumbharkar, A. S. Rewar and U. K. Kharul, *Poly. Chem.* **5** (2014) 4086-4096.

4) **R. S. Bhavsar**, S. C. Kumbharkar and U. K. Kharul, *J. Membr. Sci.,* **470** (2014) 494–503.

5) S. C. Kumbharkar, **R. S. Bhavsar** and U. K. Kharul, *RSC Adv.* **4** (2014) 4500-4503.

6) **R. S. Bhavsar**, and U. K. Kharul, Film forming polymeric ionic liquids (PILs) based on PBI: Effects of bulky *N*-substitution on their physical and gas permeation properties, *To be submitted.*

7) **R. S. Bhavsar**, and U. K. Kharul, Effect on structural variations in carboxylates as anion on gas sorption properties of PILs, *Under preparation.*

Patent:

- U. K. Kharul, S. C. Kumbharkar and **R. S. Bhavsar**, Quaternised polybenzimidazole, *WO2012/035556 A1* (2012) and *US2013/0184412 A1 (2013).*

Presentations in Conferences:

- **R. S. Bhavsar** and U. K.Kharul, Analysis of mechanical properties of polybenzimidazoles (PBI); Presented at international conference, *APA-2009*, held at IIT, Delhi; 17–20 December 2009.

- **R. S. Bhavsar,** R. H. Shevate, and U. K. Kharul, Synthesis and Investigation of Polymeric Forms of Ionic Liquids (PFILs) Based on Polybenzimidazole for CO_2 Separation; *Best Poster Award* at international conference, *PSE 2010*, held at Panjab university, Chandigarh, India; 26-27 November 2010.

- **R. S. Bhavsar** and U. K. Kharul, Film Forming Polymeric Ionic Liquids (PILs): Effect of Bulky Substitution on Physical and CO_2 Separation Properties; Presented at '3rd International Symposium, *FAPS Polymer Congress and MACRO 2013*, held at IISc, Bangalore**;** 15–18 May 2013.

- **R. S. Bhavsar** and U. K. Kharul, Polymeric Ionic Liquids (PILs): Effect of Backbone on their Physical and CO_2 Separation Properties; *Best Poster Award* at '2nd International Conference on Membrane (*ICM-2013*), held at Mahatma Gandhi University, Kottayam; 3–6 October 2013.